

Table of Contents

1. Methods & Materials	4
1.1. Experimental Considerations	4
1.2. Analytical Considerations	4
1.3. Single Crystal X-ray Diffraction Considerations	5
1.4. Computational Considerations	6
2. Synthesis	7
2.1. Synthesis of (CH₂CHSiMe₂)₃P₇ (1)	7
2.2. Synthesis of ({9-BBN}CH₂CH₂SiMe₂)₃P₇ (2)	10
2.3. Synthesis of ClSiMe₂CH₂CH₂(9-BBN) (3)	14
2.4. Solution Stability of ({9-BBN}CH₂CH₂SiMe₂)₃(P₇) (2)	15
3. Lewis Acidity Examination	19
3.1. Gutmann-Beckett Test of 2 and 3	19
3.2. Fluoride Ion Affinity (FIA)	20
4. General Procedure for Hydroboration	22
5. Screening Catalytic Conditions	23
5.1. Temperature and Solvent Screening	23
5.2. HB(pin) equivalents	24
5.3. Role of the Cluster in Catalysis	26
6. Characterization Data	29
6.1. Carbodiimides	29
6.1.1. 4b – N,N'-diisopropyl-N-(4,4,5,5-tetramethyl-1,3,2-dioxaborolan-2-yl)formimidamide.....	29
6.1.2. 10b – N,N'-dicyclohexyl-N-(4,4,5,5-tetramethyl-1,3,2-dioxaborolan-2-yl)formimidamide.....	31
6.1.3. 11b – N,N'-di-tert-butyl-N-(4,4,5,5-tetramethyl-1,3,2-dioxaborolan-2-yl)formimidamide.....	32
6.1.4. 12b – N'-tert-butyl-N-ethyl-N-(4,4,5,5-tetramethyl-1,3,2-dioxaborolan-2-yl)formimidamide.....	34
6.1.5. 13b – N-(4,4,5,5-tetramethyl-1,3,2-dioxaborolan-2-yl)-N,N'-bis(trimethylsilyl)formimidamide.....	36
6.1.6. 14b – N,N'-bis(2,6-diisopropylphenyl)-N-(4,4,5,5-tetramethyl-1,3,2-dioxaborolan-2-yl)formimidamide	37
6.2. Isocyanates	39
6.2.1. 5b - N-phenyl-N-(4,4,5,5-tetramethyl-1,3,2-dioxaborolan-2-yl)formamide	39
6.2.2. 15b – N-(4,4,5,5-tetramethyl-1,3,2-dioxaborolan-2-yl)-N-(p-tolyl)formamide ...	40
6.2.3. 16b - N-(4,4,5,5-tetramethyl-1,3,2-dioxaborolan-2-yl)-N-(4-(trifluoromethyl)phenyl)formamide.....	42
6.2.4. 17b – N-(4-fluorophenyl)-N-(4,4,5,5-tetramethyl-1,3,2-dioxaborolan-2-yl)formamide.....	44

6.2.5.	18b – N-(4-bromophenyl)-N-(4,4,5,5-tetramethyl-1,3,2-dioxaborolan-2-yl)formamide.....	46
6.2.6.	19b – N-cyclohexyl-N-(4,4,5,5-tetramethyl-1,3,2-dioxaborolan-2-yl)formamide 47	
6.2.7.	20b – N-tert-butyl-N-(4,4,5,5-tetramethyl-1,3,2-dioxaborolan-2-yl)formamide.	48
6.2.8.	21b – N-benzyl-N-(4,4,5,5-tetramethyl-1,3,2-dioxaborolan-2-yl)formamide.....	50
6.3.	Ketones	51
6.3.1.	6b – 4,4,5,5-tetramethyl-2-(1-phenylethoxy)-1,3,2-dioxaborolane	51
6.3.2.	22b – 2-(benzhydryloxy)-4,4,5,5-tetramethyl-1,3,2-dioxaborolane	53
6.3.3.	23b – 2-(phenyl((4,4,5,5-tetramethyl-1,3,2-dioxaborolan-2-yl)oxy)methyl)pyridine.....	54
6.3.4.	24b – 4,4,5,5-tetramethyl-2-(1-(thiophen-2-yl)ethoxy)-1,3,2-dioxaborolane	55
6.3.5.	25b – 4,4,5,5-tetramethyl-2-(1-(perfluorophenyl)ethoxy)-1,3,2-dioxaborolane	57
6.3.6.	26b - trimethyl(1-((4,4,5,5-tetramethyl-1,3,2-dioxaborolan-2-yl)oxy)ethyl)silane 58	
6.4.	Alkenes	60
6.4.1.	7b – 4,4,5,5-tetramethyl-2-phenethyl-1,3,2-dioxaborolane.....	60
6.4.2.	27b - 2-(4-bromophenethyl)-4,4,5,5-tetramethyl-1,3,2-dioxaborolane.....	61
6.4.3.	28b – 2-(4-methoxyphenethyl)-4,4,5,5-tetramethyl-1,3,2-dioxaborolane	63
6.4.4.	29b – 4,4,5,5-tetramethyl-2-(2-(naphthalen-2-yl)ethyl)-1,3,2-dioxaborolane ...	64
6.4.5.	30b – 2-(2-(4,4,5,5-tetramethyl-1,3,2-dioxaborolan-2-yl)ethyl)pyridine	65
6.4.6.	31b – 9-(2-(4,4,5,5-tetramethyl-1,3,2-dioxaborolan-2-yl)ethyl)-9H-carbazole..	67
6.5.	Alkynes	68
6.5.1.	8b – (E)-4,4,5,5-tetramethyl-2-styryl-1,3,2-dioxaborolane	68
6.5.2.	32b – (E)-2-(4-fluorostyryl)-4,4,5,5-tetramethyl-1,3,2-dioxaborolane.....	70
6.5.3.	33b – (E)-2-(4-chlorostyryl)-4,4,5,5-tetramethyl-1,3,2-dioxaborolane.....	71
6.5.4.	34b – (E)-2-(4-bromostyryl)-4,4,5,5-tetramethyl-1,3,2-dioxaborolane	73
6.5.5.	35b – (E)-4,4,5,5-tetramethyl-2-(4-(trifluoromethyl)styryl)-1,3,2-dioxaborolane 74	
6.5.6.	36b – (E)-2-(4-methoxystyryl)-4,4,5,5-tetramethyl-1,3,2-dioxaborolane.....	76
6.5.7.	37b – (E)-4,4,5,5-tetramethyl-2-(4-methylstyryl)-1,3,2-dioxaborolane.....	77
6.5.8.	38b – (E)-4,4,5,5-tetramethyl-2-(3-methylstyryl)-1,3,2-dioxaborolane.....	78
6.6.	Nitriles	80
6.6.1.	9b – N-benzyl-4,4,5,5-tetramethyl-N-(4,4,5,5-tetramethyl-1,3,2-dioxaborolan-2-yl)-1,3,2-dioxaborolan-2-amine	80
6.6.2.	39b – N-(4-bromobenzyl)-4,4,5,5-tetramethyl-N-(4,4,5,5-tetramethyl-1,3,2-dioxaborolan-2-yl)-1,3,2-dioxaborolan-2-amine	81
6.6.3.	40b – N-(4-methoxybenzyl)-4,4,5,5-tetramethyl-N-(4,4,5,5-tetramethyl-1,3,2-dioxaborolan-2-yl)-1,3,2-dioxaborolan-2-amine	83

6.6.4.	41b – N-(cyclohexylmethyl)-4,4,5,5-tetramethyl-N-(4,4,5,5-tetramethyl-1,3,2-dioxaborolan-2-yl)-1,3,2-dioxaborolan-2-amine	84
6.6.5.	42b – N-butyl-4,4,5,5-tetramethyl-N-(4,4,5,5-tetramethyl-1,3,2-dioxaborolan-2-yl)-1,3,2-dioxaborolan-2-amine	86
6.6.6.	43b - 4,4,5,5-tetramethyl-N-(pyridin-4-ylmethyl)-N-(4,4,5,5-tetramethyl-1,3,2-dioxaborolan-2-yl)-1,3,2-dioxaborolan-2-amine	87
6.6.7.	44b – 4,4,5,5-tetramethyl-N-(pyridin-2-ylmethyl)-N-(4,4,5,5-tetramethyl-1,3,2-dioxaborolan-2-yl)-1,3,2-dioxaborolan-2-amine	89
7.	Studies into Catalyst-Product Interactions	90
8.	Studies into Catalyst-Substrate Interactions	93
9.	Testing for Hidden Catalysis	94
10.	Catalyst Recycling	96
11.	Crystallographic Data	99
12.	Geometry Optimized Structures	100
13.	References	114

1. Methods & Materials

1.1. Experimental Considerations

All manipulations were performed under an inert atmosphere using standard Schlenk-line, and glovebox techniques. Glassware was flame dried prior to use.

Dry THF, Et₂O, toluene, and pentane were obtained using Innovative Technologies anhydrous engineering solvent purification systems and subsequently degassed. DME was dried over Na and purified by distillation. C₆D₆, and toluene-d₈, were dried over activated 3 Å molecular sieves. All solvents were stored over activated 3 Å molecular sieves.

Elemental phosphorus (Merck), Naphthalene (Fluorochem), chloro(dimethyl)vinylsilane (ClSiMe₂CHCH₂, Merck), 9-Borabicyclo[3.3.1]nonane dimer (9-BBN dimer, Merck) and all organic substrates (**4a** to **44a**) used in this study were purchased from commercial sources and used without any further purification. [Na(DME)_x]₃P₇ and (Me₃Si)₃P₇ were synthesized according to previously reported synthetic procedures.¹

1.2. Analytical Considerations

NMR Spectroscopy. ¹H, ¹¹B, ¹¹B{¹H}, ¹³C{¹H}, ¹⁹F, ²⁹Si DEPT90, ³¹P NMR spectra were recorded on a Bruker AVIII 400 spectrometer (operating frequencies: 399.78 MHz, 128.36 MHz, 100.53 MHz, 376.17 MHz, 79.48 MHz and 161.83 MHz for ¹H, ¹¹B, ¹³C, ¹⁹F, ²⁹Si and ³¹P, respectively). ¹H and ¹³C{¹H} NMR chemical shifts were internally referenced to the residual solvent resonances (C₆D₆ (benzene-d₆): ¹H δ = 7.16 ppm, ¹³C{¹H} δ = 128.02 ppm, C₇D₈ (toluene-d₈): ¹H δ = 7.09, 7.00, 6.98, 2.09 ppm, ¹³C{¹H} δ = 137.86, 129.24, 128.33, 125.49, 20.4 ppm). ¹¹B, ¹⁹F, ²⁹Si, ³¹P chemical shifts were externally referenced to BF₃·Et₂O, CFCl₃, Me₄Si, H₃PO₄, respectively. NMR samples were prepared under an inert atmosphere in 5 mm J Young NMR tubes. Data was analysed using MestReNova V14.0.0 software. The ¹¹B{¹H} NMR spectra of hydroborated alkenes (**7b**, **27b** – **31b**) was collected on a Bruker AVIII 400 spectrometer with a higher background signal of borosilicate.

Elemental Analysis. Elemental analysis was carried out by Mr. Martin Jennings and Mrs. Anne Davies at the Microanalytical Service, School of Chemistry, the University of Manchester using a Flash 2000 elemental analyser.

Mass spectrometry. Mass spectrometry samples were measured the Mass Spectrometry Service, School of Chemistry, the University of Manchester using an electrospray ionization or atmospheric pressure chemical ionization equipped Thermo Orbitrap Executive Plus Extended Mass Range mass spectrometer. Samples were prepared under a nitrogen atmosphere and injected into the ionization source of the mass spectrometer. For products **5b – 7b, 16b, 18b – 21b, 23b – 25b, 27b – 31b, 37b, 43b** and **44b** significant decomposition of the sample was observed, we attributed this to sample wait times in the autosampler. For these samples, they were self-injected immediately after preparation into a low-resolution electrospray ionization equipped Thermo Fischer LCQ Fleet mass spectrometer.

1.3. Single Crystal X-ray Diffraction Considerations

Data collection: X-ray diffraction data for compound **1** were collected using a Rigaku Oxford Diffraction Supernova diffractometer, equipped with a 4-circle kappa goniometer, a MoK α ($\lambda = 0.71073 \text{ \AA}$) microfocus source, an Eos CCD detector and an Oxford cryosystems Cryostream 700 nitrogen gas flow system, at a temperature of 100K. X-ray diffraction data for compound **2** were collected using a dual wavelength Rigaku FR-X rotating anode diffractometer using CuK α ($\lambda = 1.54146 \text{ \AA}$) radiation, equipped with an AFC-11 4-circle kappa goniometer, VariMAXTM microfocus optics, a Hypix-6000HE detector and an Oxford Cryosystems 800 plus nitrogen flow gas system, at a temperature of 100K. Data were collected and reduced using CrysAlisPro v42. Absorption correction was performed using empirical methods (SCALE3 ABSPACK) based upon symmetry-equivalent reflections combined with measurements at different azimuthal angles.

Crystal structure determination and refinements: The crystal structure was solved and refined against all F^2 values using the SHELX and Olex2 suite of programmes.²
³ All atoms were refined anisotropically. Hydrogen atoms were placed in calculated positions and refined using idealized geometries and assigned fixed isotropic displacement parameters. Data for compound **2** were poor, as the crystals of the

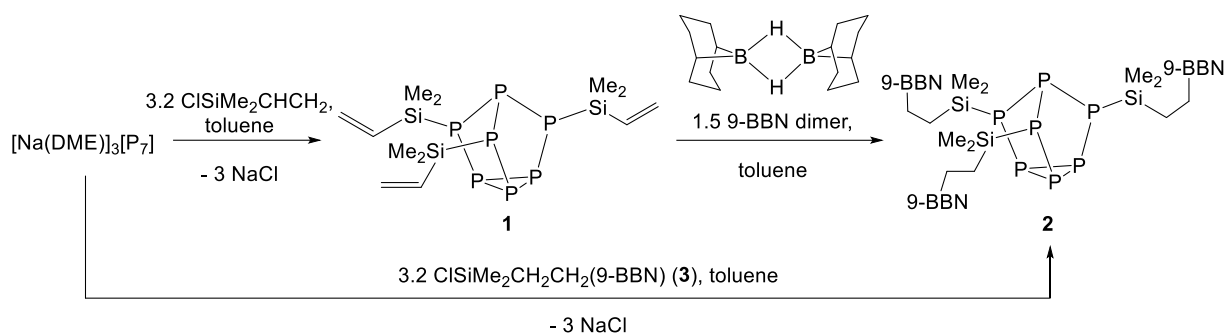
sample form as polycrystalline aggregates. As a result, there is a large contribution to the observed intensities from other diffracting components. This intensity contribution could not be accounted for by treating the data-set as a multi-component twin. As such, during the data reduction only reflections with good profiles were kept in order to strip out those with the worst other-component contribution. This results in low (95%) completeness for the data-set, in addition to the inclusion of some reflections with poorly fitting intensities that happened to have good reflection profiles. A consequence of this is a poor fit to weak reflections (high wR_2) and low bond precision (due to additional residual noise in the electron density map). However, the overall validity of the structural model is not impinged by this.

For compound **1**, the disordered $\text{SiMe}_2\text{CHCH}_2$ groups were refined with relatively strong similar neighbouring atomic displacement parameters and rigid bond restraints applied. For compound **2**, 9-BBN moieties were refined to have similar 1,2- and 1,3-bond distances, all carbon and boron atoms were refined with similar neighbouring atomic displacement parameters and rigid bond restraints applied. The disordered solvent pentane was refined to have idealized 1,2- and 1,3- fixed distance restraints. Crystallographic data have been deposited with the CCDC (CCDC 2192816 and 2192817).

1.4. Computational Considerations

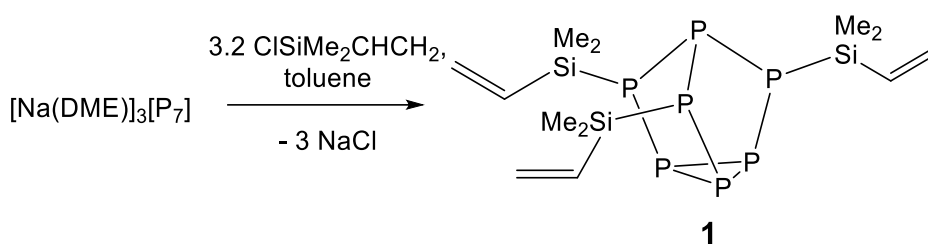
Density Functional Theory (DFT) calculations were performed with the Gaussian09 program package³ (version g09, rev.d01).⁴⁻⁸ Geometry optimizations and frequency calculations were conducted at the BP86/SV(p) level of theory. No symmetry constraints were applied during optimization. All minima were confirmed by the absence of imaginary frequencies. Initial geometries were prepared using X-ray diffraction coordinates where possible and Facio V22.1.1.64 software. Gibbs free reaction energies and enthalpies were calculated for standard conditions ($p = 1 \text{ atm}$, $T = 298 \text{ K}$) and are unscaled. HOMO and LUMO images were prepared using Avogadro V1.2.0 software.

2. Synthesis



Scheme S1. Synthetic routes to $(\{9\text{-BBN}\}\text{CH}_2\text{CH}_2\text{SiMe}_2)_3\text{P}_7$ (**2**).

2.1. Synthesis of $(\text{CH}_2\text{CHSiMe}_2)_3\text{P}_7$ (**1**)



Scheme S2. Synthesis of $(\text{CH}_2\text{CHSiMe}_2)_3\text{P}_7$ (**1**).

To a Schlenk flask charged with a stir bar and $[\text{Na}(\text{DME})_x]_3[\text{P}_7]$ (1.000 g, ~ 2 mmol), toluene (13 mL) was added and the suspension cooled to $-78\text{ }^\circ\text{C}$. $\text{ClSiMe}_2\text{CHCH}_2$ (0.9 mL, 6.52 mmol) was added dropwise. The suspension was warmed to room temperature and the resulting black solution was stirred for three days. The mixture was filtered yielding a clear orange solution. The solvent was removed under reduced pressure resulting in a yellow/orange powder of $(\text{CH}_2\text{CHSiMe}_2)_3\text{P}_7$ (**1**) which was dried under reduced pressure for five hours. Single crystals suitable of single crystal XRD analysis were obtained through cooling down a concentrated toluene solution.

Isolated Yield: 0.816 g, 1.73 mmol, 86 %.

^1H NMR (400 MHz, 298 K, C_6D_6): δ = 6.18 (dd, $^3J_{\text{HH}} = 20.1$ Hz, $^3J_{\text{HH}} = 14.4$ Hz, 3H, CH), 5.83 (dd, $^3J_{\text{HH}} = 14.4$ Hz, $^2J_{\text{HH}} = 3.2$ Hz, 3H, *cis*- CH_2), 5.63 (dd, $^3J_{\text{HH}} = 20.1$ Hz, $^2J_{\text{HH}} = 3.2$ Hz, 3H, *trans*- CH_2), 0.30 (s, 18H, SiCH_3) ppm.

$^{13}\text{C}\{^1\text{H}\}$ NMR (101 MHz, 298 K, C_6D_6): δ = 138.36 (s, CH), 133.32 (s, CH_2), 1.57 (s, SiCH_3) ppm.

$^{29}\text{Si}\{^1\text{H}\}$ NMR (79 MHz, 298 K, C_6D_6): δ = -2.36 (d, $^1J_{\text{SiP}} = 42.5$ Hz) ppm.

^{31}P NMR (162 MHz, 298 K, C_6D_6): $\delta = -152.69 - -159.38$ (m, 3P, *basal*), $-95.78 - -103.24$ (qq, $^1J_{\text{PP}} = 324.2$ Hz, $^2J_{\text{PP}} = 45.92$ Hz, 1P, *apical*), $6.22 - -2.42$ (m, 3P, *linking*) ppm.

Elemental analysis: Expected/Found: C = 30.51/ 30.58; H = 5.76/ 5.57; N = 0/ 0.

Mass spectrometry (APCI): $\text{C}_{12}\text{H}_{27}\text{P}_7\text{Si}_3 + \text{H}$ ($[\text{M} + \text{H}]^+$); Calcd. = 472.9657, Found = 472.9666.

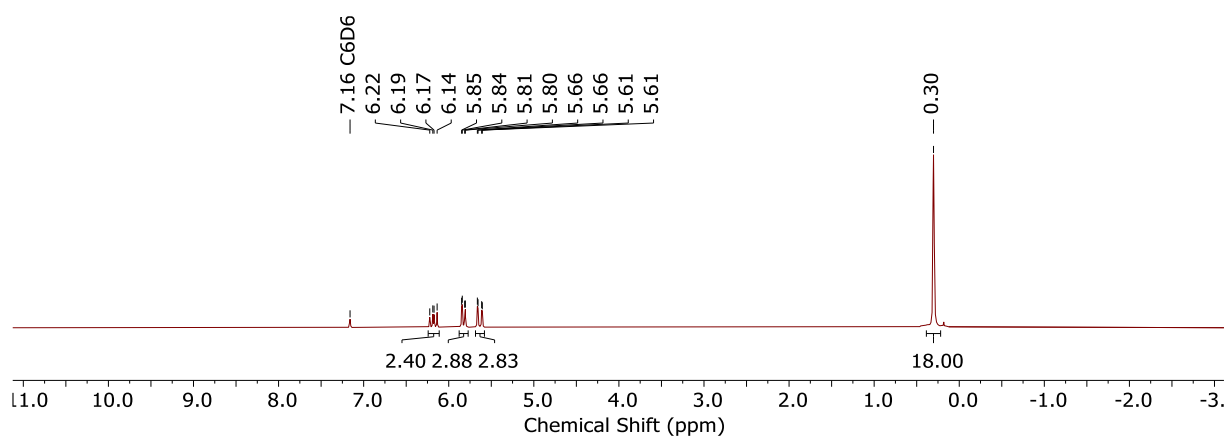


Figure S1. ^1H NMR spectrum (C_6D_6) of **1**.

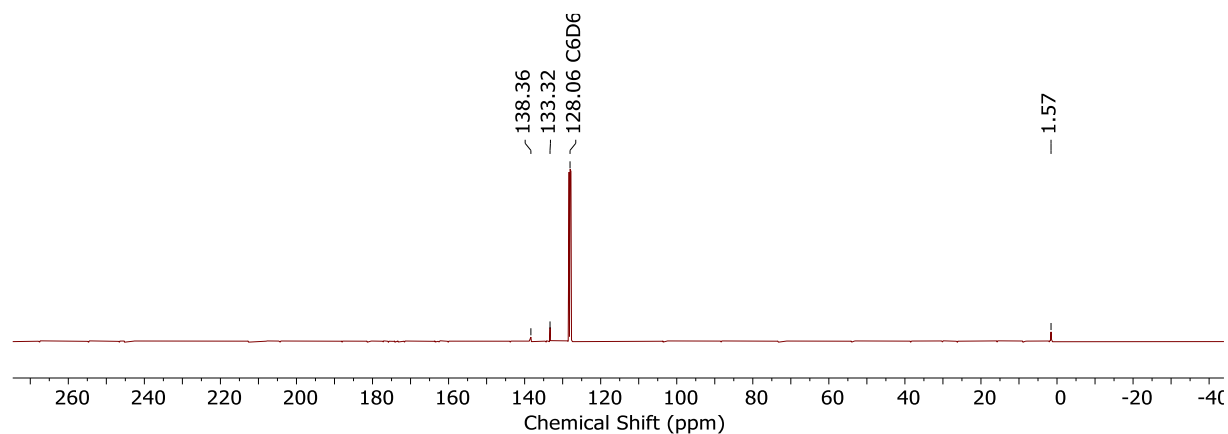


Figure S2. $^{13}\text{C}\{^1\text{H}\}$ NMR spectrum (C_6D_6) of **1**.

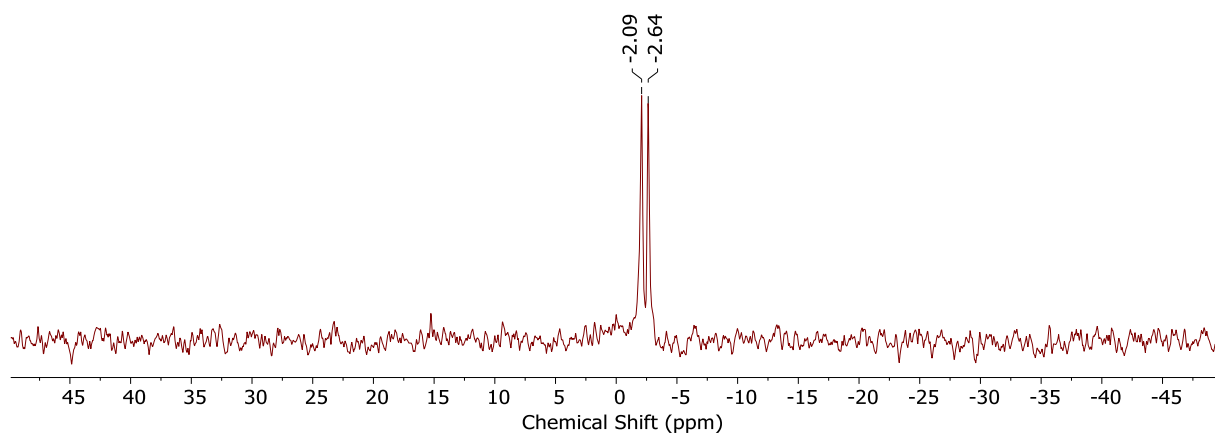


Figure S3. $^{29}\text{Si}\{^1\text{H}\}$ NMR spectrum (C_6D_6) of **1**.

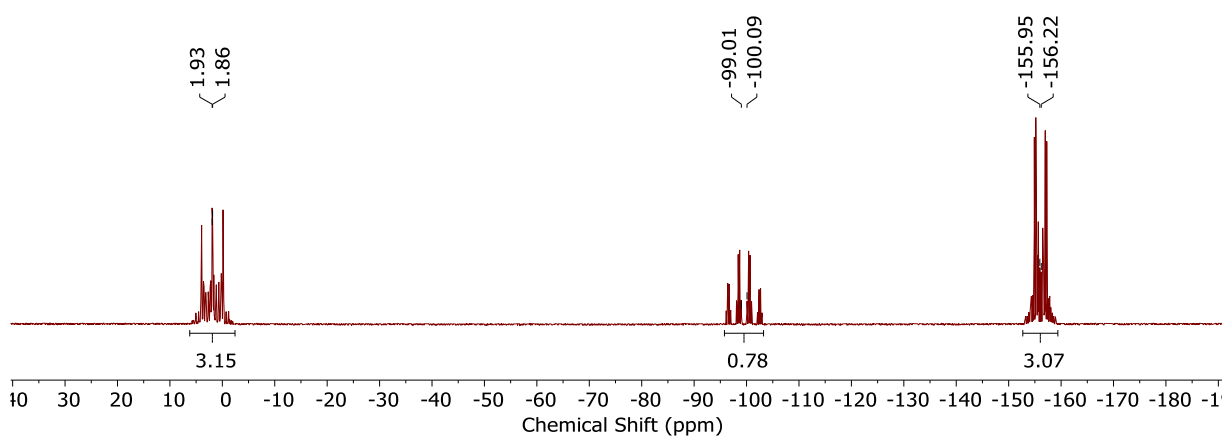


Figure S4. ^{31}P NMR spectrum (C_6D_6) of **1**.

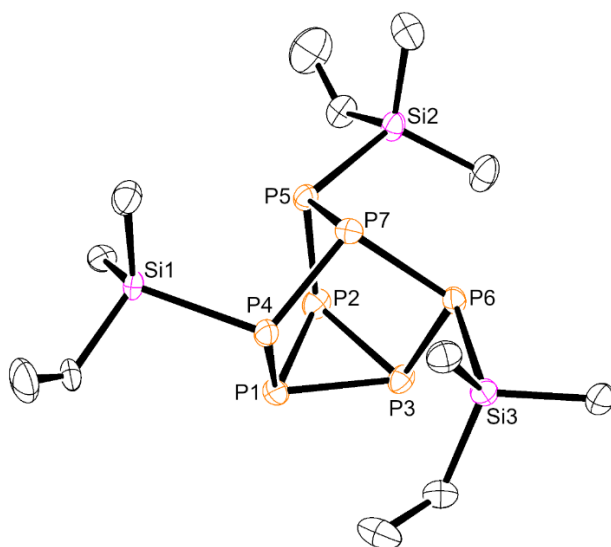
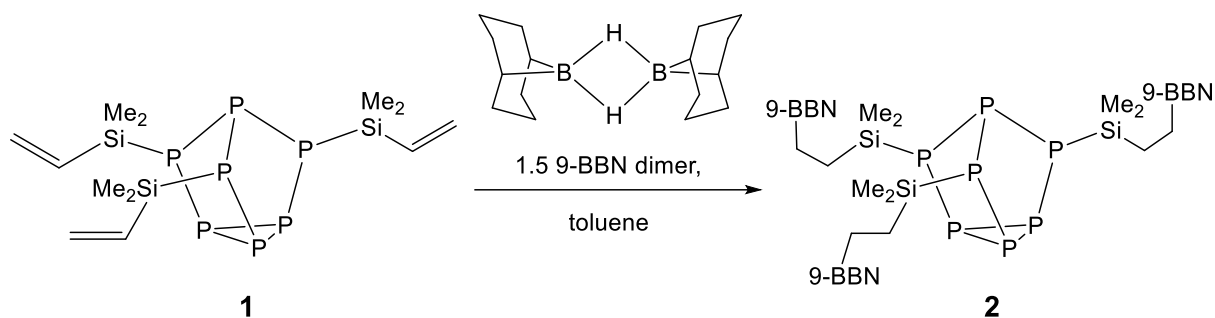


Figure S5. Molecular structure of **1**. Anisotropic displacement ellipsoids pictured at 50% probability. Hydrogen atoms omitted for clarity. Phosphorus: Orange; Silicon: Pink; Carbon: Black.

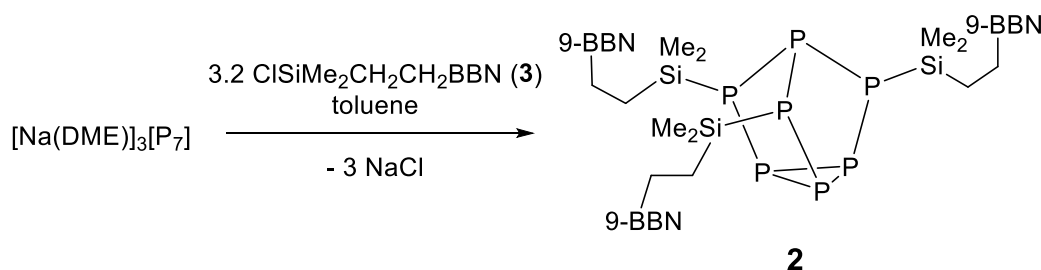
2.2. Synthesis of $(\{9\text{-BBN}\}\text{CH}_2\text{CH}_2\text{SiMe}_2)_3\text{P}_7$ (**2**)



Scheme S3. Synthesis of $(\{9\text{-BBN}\}\text{CH}_2\text{CH}_2\text{SiMe}_2)_3\text{P}_7$ (**2**).

To a Schlenk flask charged with a stir bar, $(\text{CH}_2\text{CHSiMe}_2)_3\text{P}_7$ (**1**, 1.000 g, 2.12 mmol) and 9-BBN dimer (0.775 g, 3.17 mmol), toluene (10 mL) was added at room temperature. The suspension was stirred for three days, volatiles were removed under reduced pressure and the residue was washed with Et_2O (4 mL). The resulting pale yellow powder was dried under reduced pressure for five hours yielding $(\{9\text{-BBN}\}\text{CH}_2\text{CH}_2\text{SiMe}_2)_3\text{P}_7$ (**2**).

Isolated Yield: 1.350 g, 1.61 mmol, 76 %



Scheme S4. Alternate synthesis of $(\{9\text{-BBN}\}\text{CH}_2\text{CH}_2\text{SiMe}_2)_3\text{P}_7$ (**2**).

2 can alternatively be prepared directly from $[\text{Na}(\text{DME})]_3[\text{P}_7]$: A Schlenk flask was charged with a stir bar and $[\text{Na}(\text{DME})]_3[\text{P}_7]$ (0.500 g, ~ 1 mmol) and toluene (10 mL). $\text{ClSiMe}_2\text{CH}_2\text{CH}_2(9\text{-BBN})$ (**3**, 0.791 g, 3.26 mmol) in toluene (5 mL) was added dropwise at room temperature and the suspension stirred for five days. The suspension was settled and filtered yielding a clear yellow solution. Volatiles were removed under reduced pressure and the residue was washed with pentane (5 mL) and Et_2O (5 mL) The resulting pale yellow powder was dried under reduced pressure for five hours yielding $(\{9\text{-BBN}\}\text{CH}_2\text{CH}_2\text{SiMe}_2)_3\text{P}_7$ (**2**). Crystals suitable for single crystal XRD analysis were obtained either concentrated pentane or Et_2O solutions at room temperature for several days.

Isolated Yield: 0.803 g, 0.96 mmol, 94 %.

^1H NMR (400 MHz, 298 K, C_6D_6): δ = 1.66 – 1.95 (m, 36H, CH_2), 1.46 (m, 6H, CH_2), 1.24 (m, 6H, CH), 0.90 (m, 6H, CH_2), 0.33 (s, 18H, SiCH_3) ppm.

^{11}B NMR (128 MHz, 298 K, C_6D_6): δ = 86.48 (s) ppm.

$^{13}\text{C}\{^1\text{H}\}$ NMR (101 MHz, 298 K, C_6D_6): δ = 33.69 (s, 9-BBN), 31.51 (s, 9-BBN), 23.70 (s, 9-BBN), 21.23 (s, CH_2), 12.27 (s, CH_2), 1.63 (s, SiCH_3) ppm.

$^{29}\text{Si}\{^1\text{H}\}$ NMR (79 MHz, 298 K, C_6D_6): δ = 11.75 (d, $^1J_{\text{SiP}}$ = 49.2 Hz) ppm.

^{31}P NMR (162 MHz, 298 K, C_6D_6): δ = -153.49 – -160.46 (m, 3P, *basal*), -96.41 – -105.05 (qq, $^1J_{\text{PP}}$ = 325.1 Hz, $^2J_{\text{PP}}$ = 45.5 Hz, 1P, *apical*), -0.12 – -8.47 (m, 3P, *linking*) ppm.

Elemental analysis: Expected/Found: C = 51.57/ 51.66; H = 8.66/ 8.67; N = 0/ 0.

Mass spectrometry (APCI): $\text{C}_{36}\text{H}_{72}\text{B}_3\text{P}_7\text{Si}_3+\text{Na}$ ($[\text{M}+\text{Na}]^+$); Calcd. = 861.3282, Found = 861.3307.

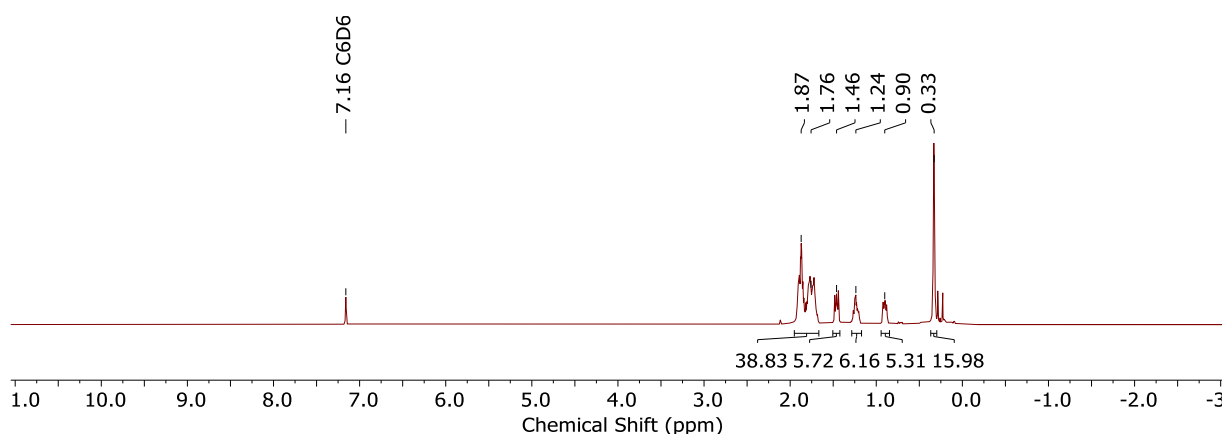


Figure S6. ^1H NMR spectrum (C_6D_6) of **2**.

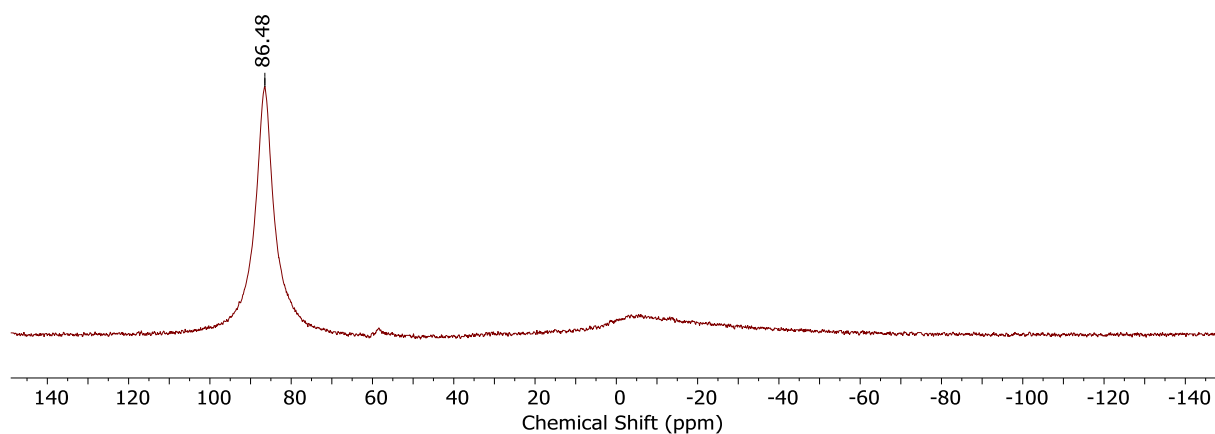


Figure S7. ^{11}B NMR spectrum (C_6D_6) of **2**.

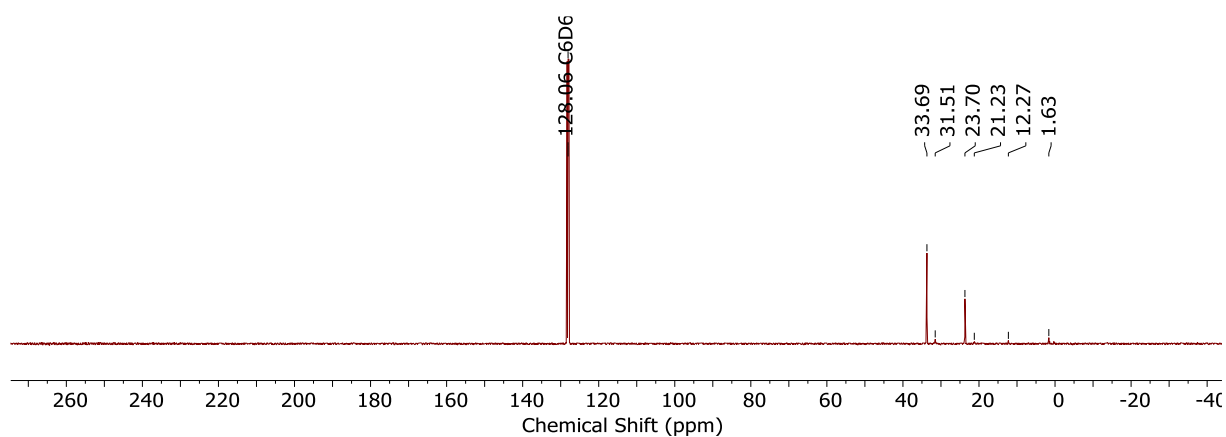


Figure S8. $^{13}\text{C}\{^1\text{H}\}$ NMR spectrum (C_6D_6) of **2**.

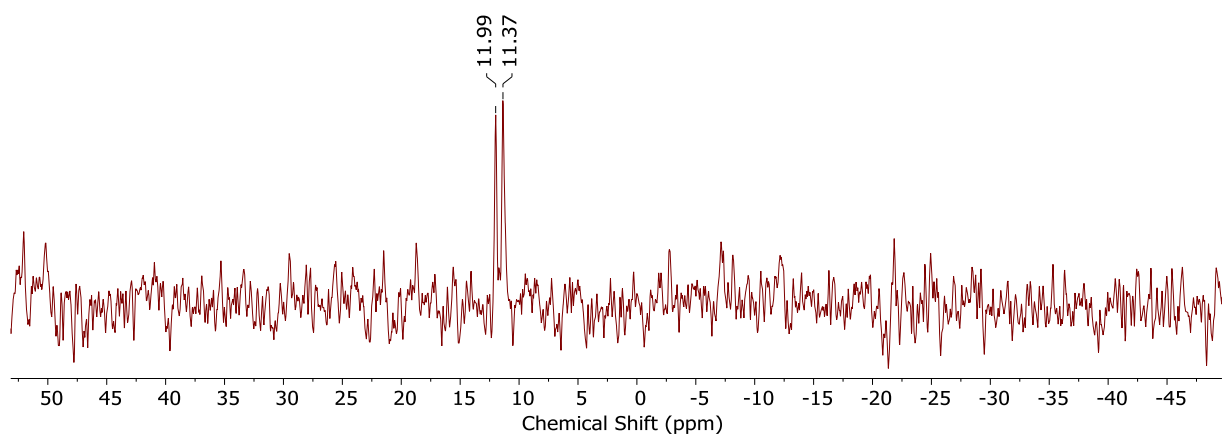


Figure S9. $^{29}\text{Si}\{^1\text{H}\}$ NMR spectrum (C_6D_6) of **2**.

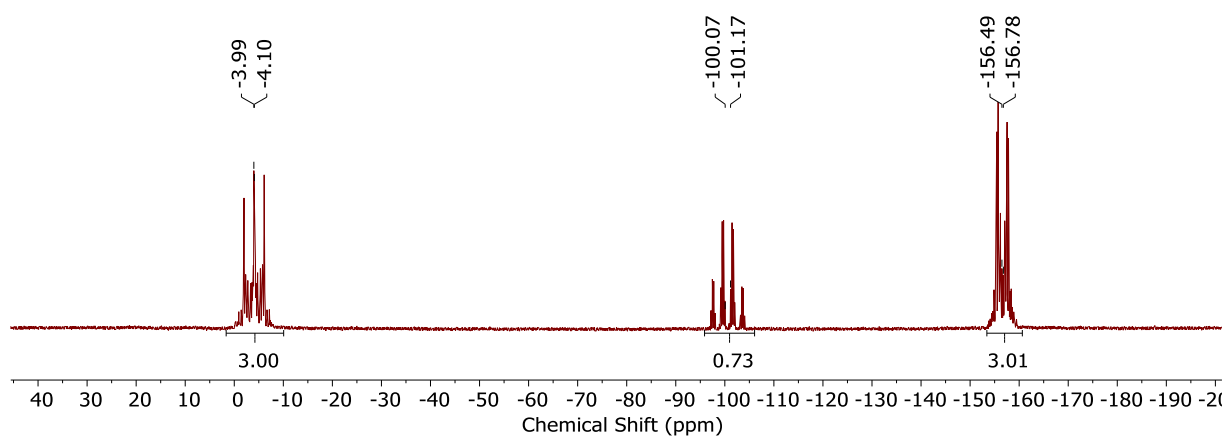


Figure S10. ^{31}P NMR spectrum (C_6D_6) of **2**.

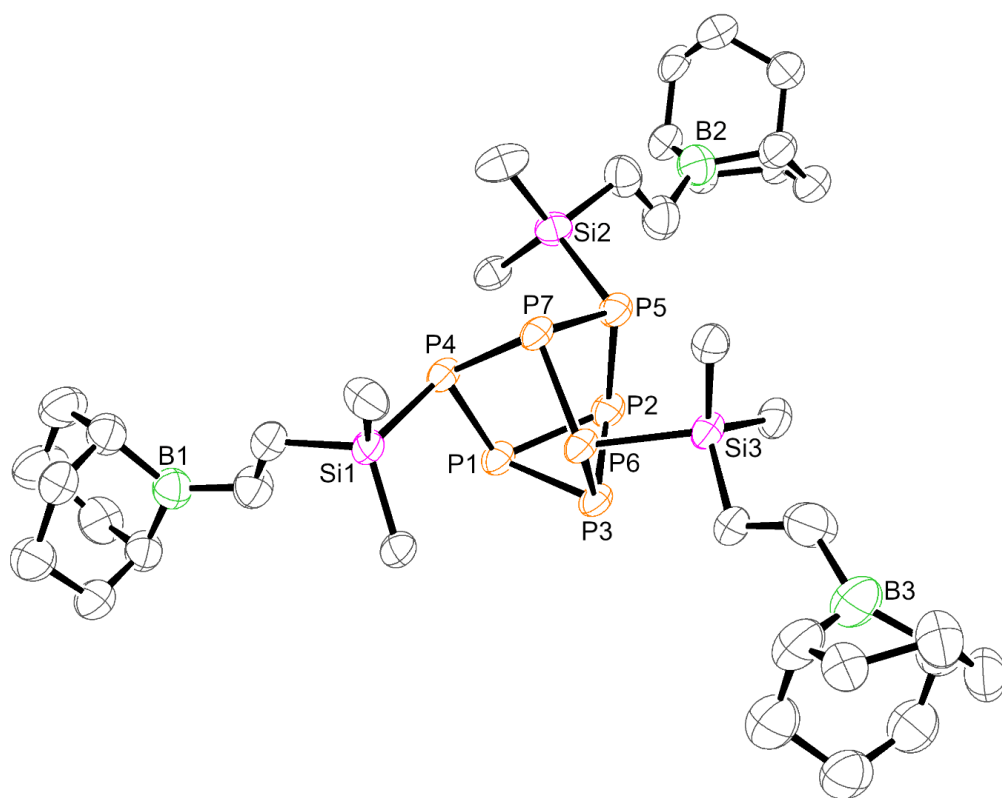


Figure S11. Molecular structure of **2**. Anisotropic displacement ellipsoids pictured at 50% probability. Hydrogen atoms and pentane omitted for clarity. Phosphorus: Orange; Silicon: Pink; Boron: Green; Carbon: Black.

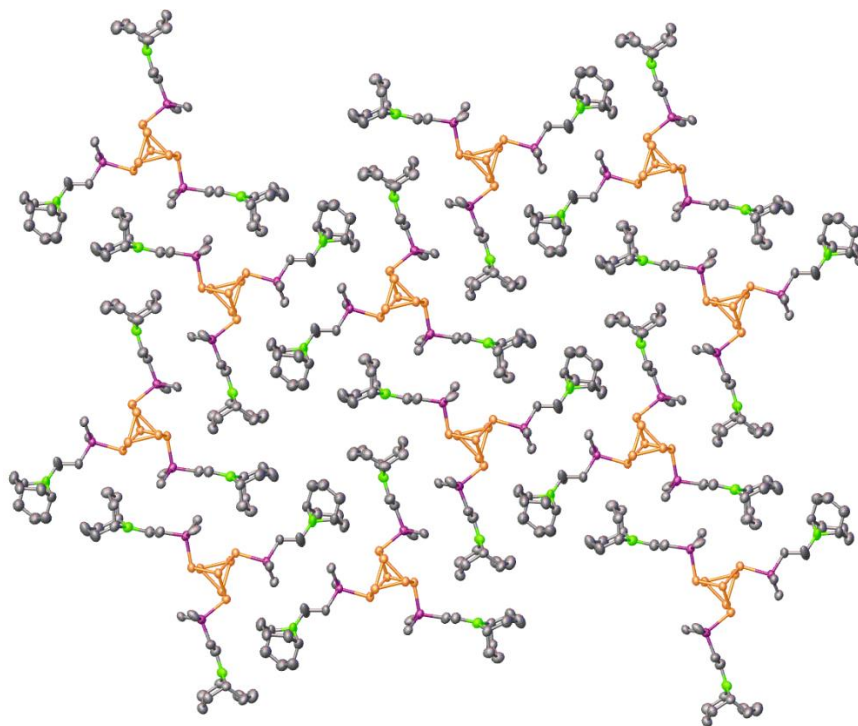
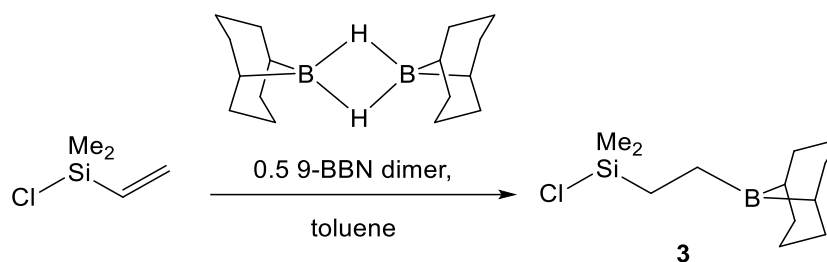


Figure S12. Crystal packing structure of **2**. Hydrogen atoms and pentane omitted for clarity. Phosphorus: Orange; Silicon: Pink; Boron: Green; Carbon: Grey.

2.3. Synthesis of ClSiMe₂CH₂CH₂(9-BBN) (**3**)



Scheme S5. Synthesis of ClSiMe₂CH₂CH₂(9-BBN) (**3**).

To a Schlenk flask charged with a stir bar, 9-BBN dimer (1.768 g, 7.24 mmol) was partially dissolved in toluene (15 mL). ClSiMe₂CH=CH₂ (2 mL, 1.748 g, 14.48 mmol) in toluene (5 mL) was added dropwise to the vigorously stirring solution at which point all remaining 9-BBN dimer dissolved. The reaction was stirred at room temperature for two days at which point volatiles were removed under reduced pressure and the resulting colourless oil dried for three hours yielding ClSiMe₂CH₂CH₂(9-BBN) (**3**).

Isolated Yield: 2.977 g, 12.27 mmol, 85 %.

¹H NMR (400 MHz, 298 K, C₆D₆): δ = 1.58 – 1.90 (m, 12H, CH₂), 1.37 (t, ¹J_{HH} = 8.2 Hz, 2H, CH₂), 1.12 – 1.24 (m, 2H, CH), 0.81 (t, ¹J_{HH} = 8.2 Hz, 2H, CH₂), 0.28 (s, 6H, SiCH₃) ppm.

¹¹B NMR (128 MHz, 298 K, C₆D₆): δ = 87.01 (s) ppm.

¹³C{¹H} NMR (101 MHz, 298 K, C₆D₆): δ = 33.62 (s, 9-BBN), 31.45 (s, 9-BBN), 23.64 (s, 9-BBN), 19.57 (s, CH₂), 12.12 (s, CH₂), 1.28 (s, SiCH₃) ppm.

²⁹Si{¹H} NMR (79 MHz, 298 K, C₆D₆): δ = 32.66 (s) ppm.

Mass spectrometry (APCI): C₁₂H₂₄BSiCl-H ([M-H]⁻); Calcd. = 241.1356, Found = 241.1351.

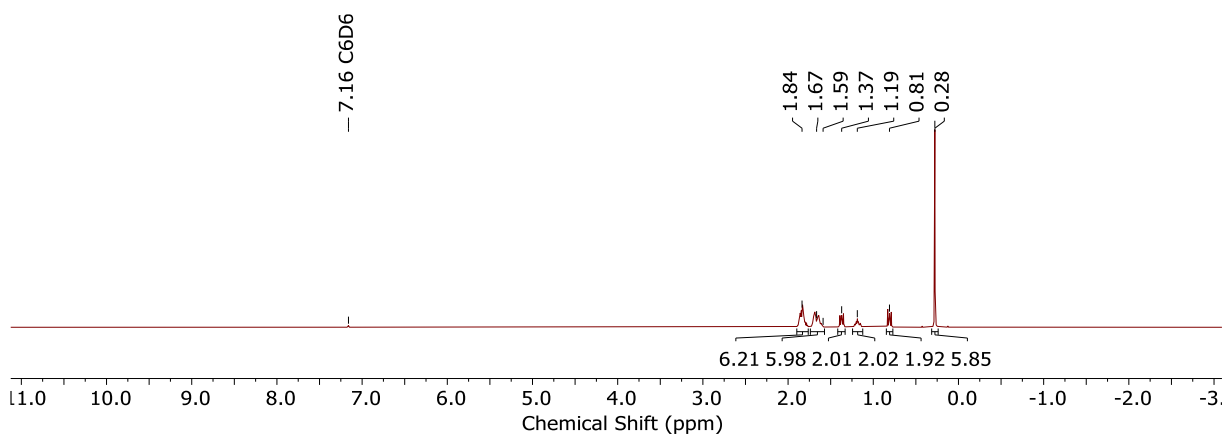


Figure S13. ¹H NMR spectrum (C₆D₆) of **3**.

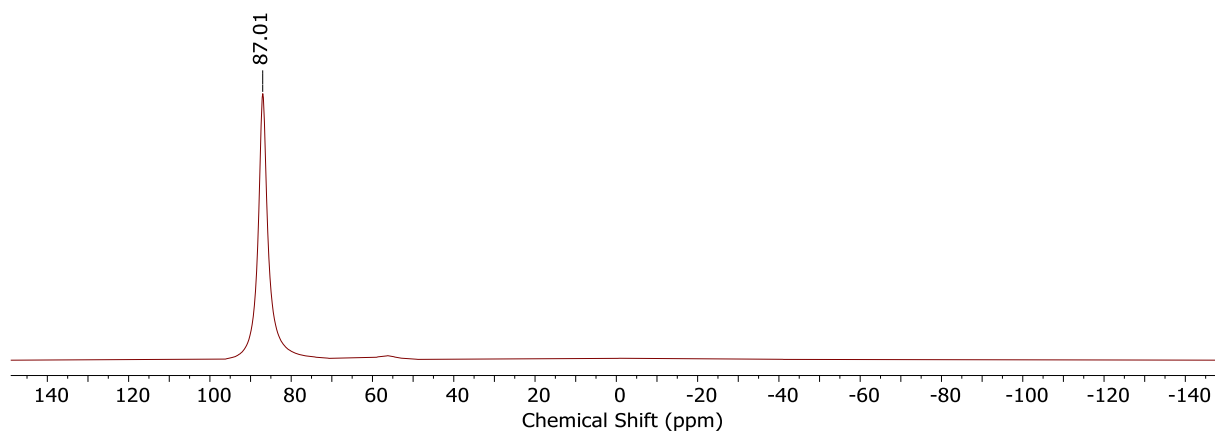


Figure S14. ^{11}B NMR spectrum (C_6D_6) of **3**.

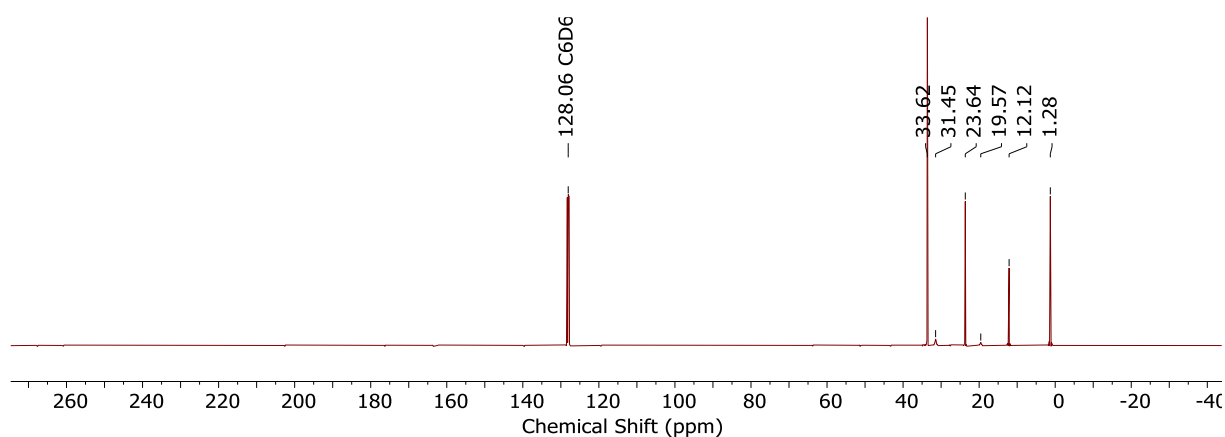


Figure S15. $^{13}\text{C}\{^1\text{H}\}$ NMR spectrum (C_6D_6) of **3**.

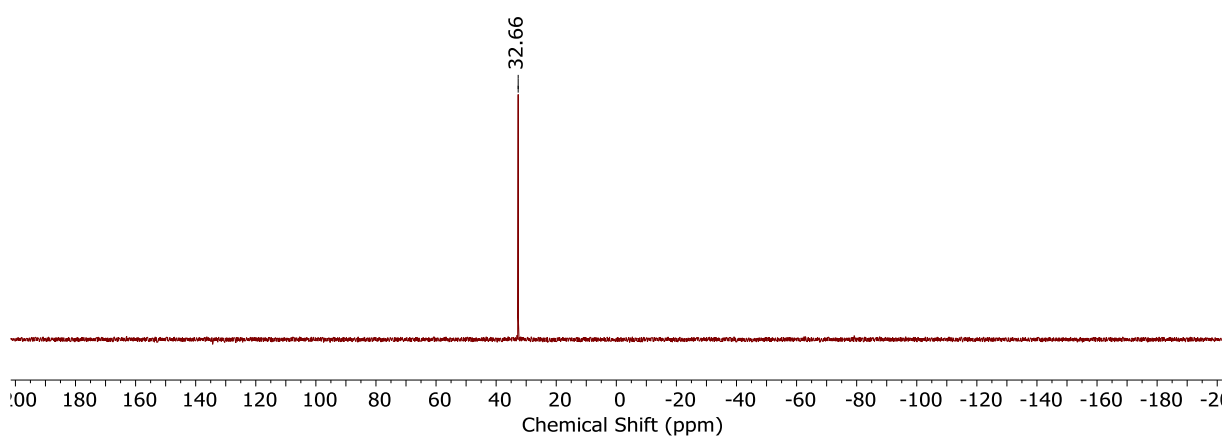


Figure S16. $^{29}\text{Si}\{^1\text{H}\}$ NMR spectrum (C_6D_6) of **3**.

2.4. Solution Stability of $(\{9\text{-BBN}\}\text{CH}_2\text{CH}_2\text{SiMe}_2)_3(\text{P}_7)$ (**2**)

33 mg of **2** was dissolved in 0.5 mL C_6D_6 and monitored by NMR spectroscopy at 25 °C, 50 °C and 110 °C. No evidence for decomposition was observed over 72 hours at 25 °C, 120 hours at 50 °C, and 168 hours at 110 °C. The small singlet in the ^{31}P NMR spectrum at -187.67 ppm observed after 168 hours at 110 °C accounts only for <4 % and no other decomposition in other NMR spectra was observed.

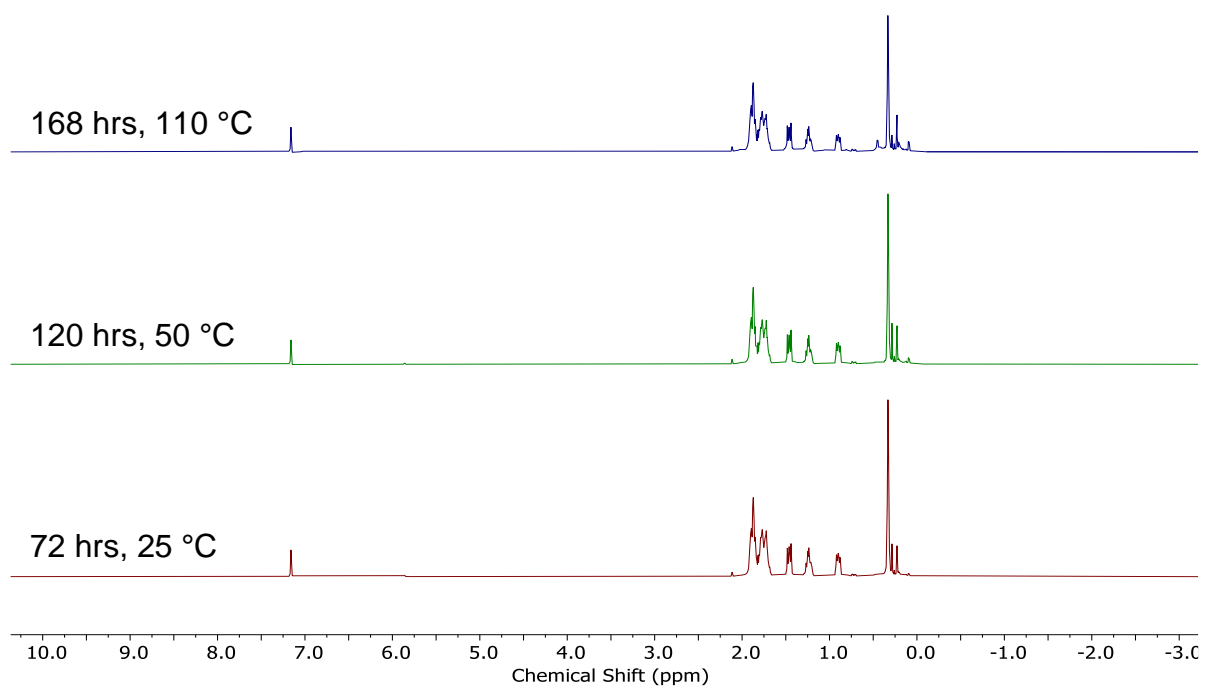


Figure S17. Stacked ^1H NMR spectrum (C_6D_6) of **2** after prolonged heating.

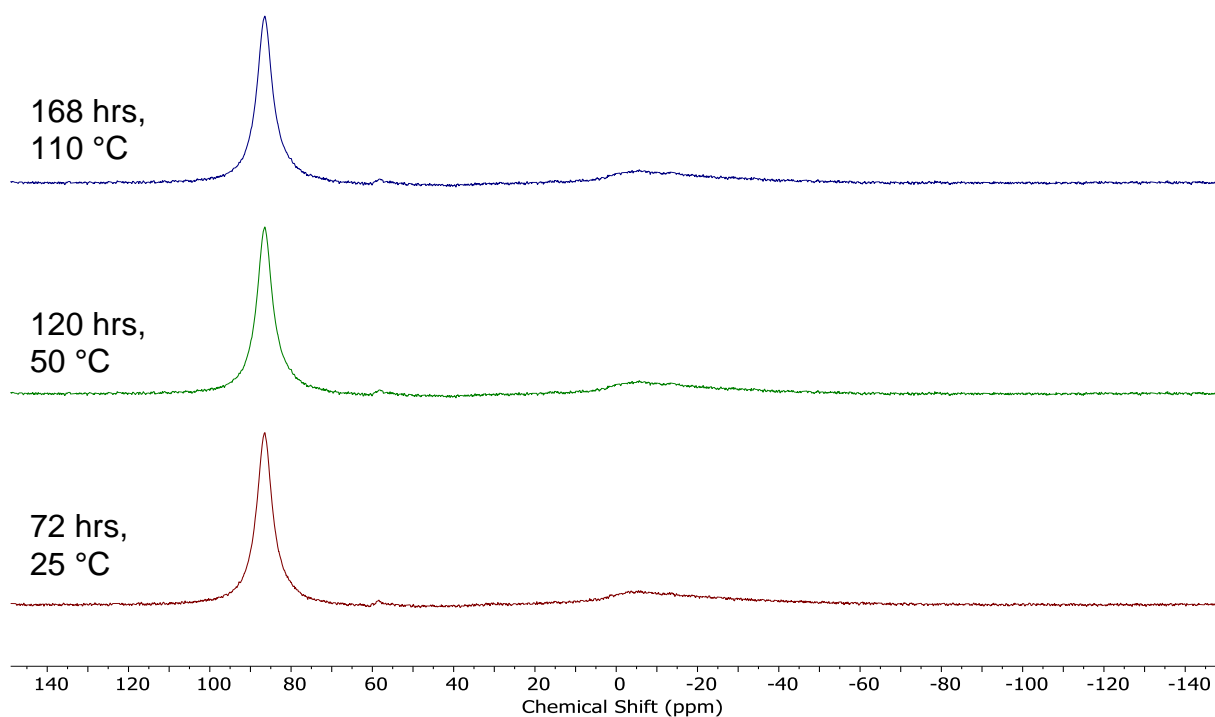


Figure S18. Stacked ^{11}B NMR spectrum (C_6D_6) of **2** after prolonged heating.

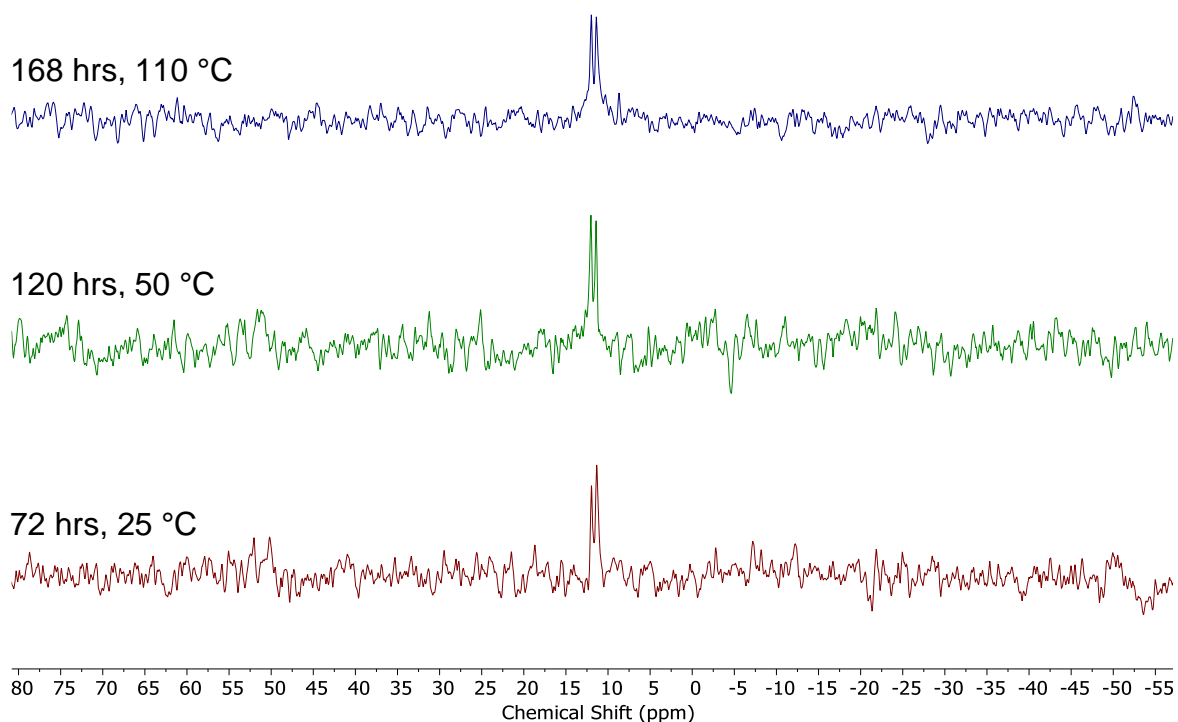


Figure S19. Stacked $^{29}\text{Si}\{^1\text{H}\}$ NMR spectrum (C_6D_6) of **2** after prolonged heating.

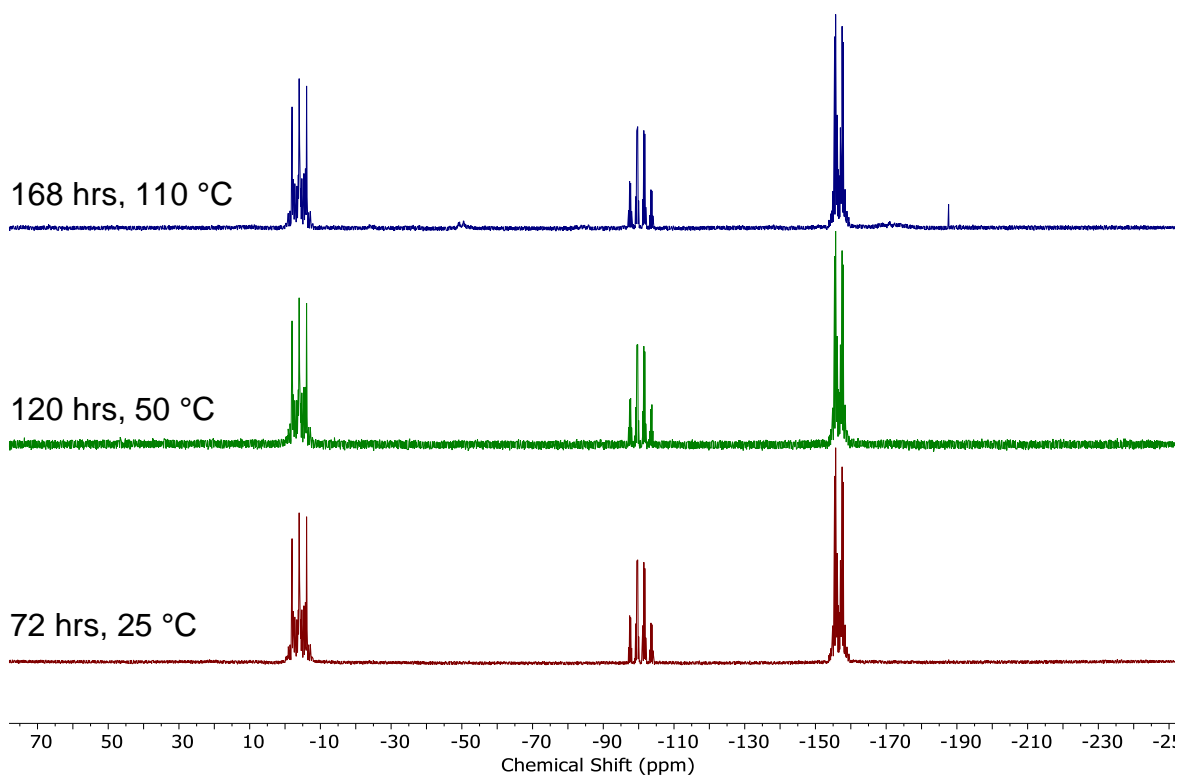


Figure S20. Stacked ^{31}P NMR spectrum (C_6D_6) of **2** after prolonged heating.

In order to study if **2** would undergo retro-hydroboration at elevated temperatures, 30 mg of **2** was dissolved in 0.5 mL toluene- d_8 , the sample was heated in the

spectrometer to 100 °C and ^1H , ^{11}B and ^{31}P analysis recorded, the temperature was maintained for two hours and analysis recorded again. No changes in the NMR spectrum were observed indicating that retrohydroboration does not occur in solution.

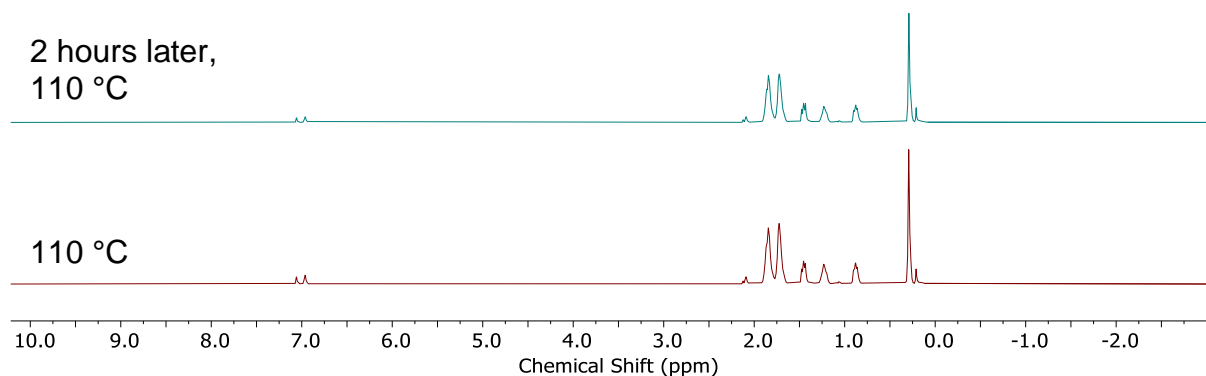


Figure S21. Stacked ^1H NMR spectrum ($\text{toluene-}d_8$) of **2** at $110\text{ }^\circ\text{C}$.

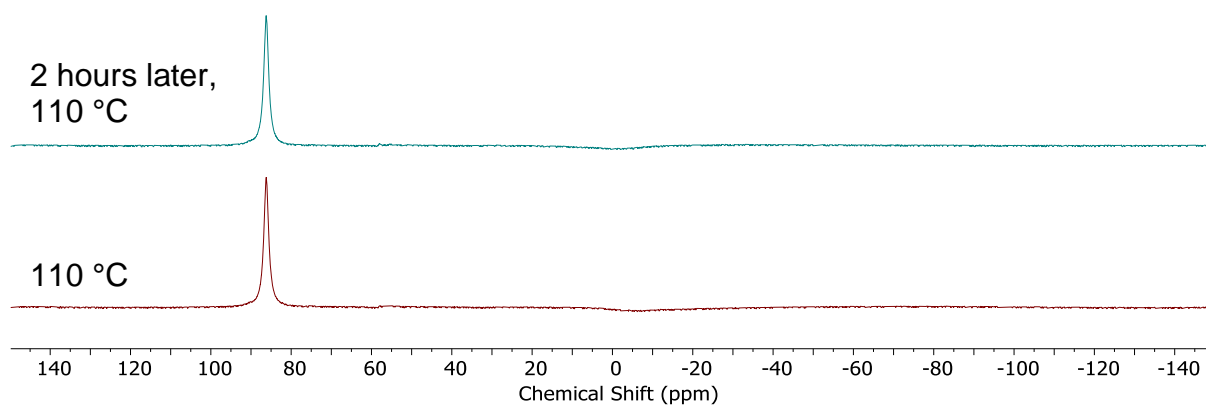


Figure S22. Stacked ^{11}B NMR spectrum ($\text{toluene-}d_8$) of **2** at $110\text{ }^\circ\text{C}$.

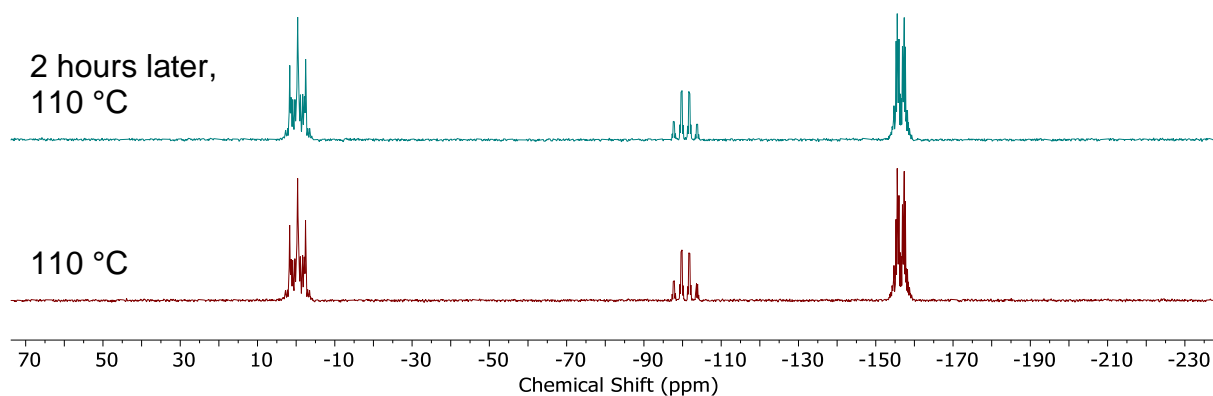
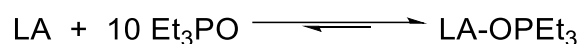


Figure S23. Stacked ^{31}P NMR spectrum ($\text{toluene-}d_8$) of **2** at $110\text{ }^\circ\text{C}$.

3. Lewis Acidity Examination

3.1. Gutmann-Beckett Test of **2** and **3**

The Gutmann-Beckett method assess Lewis acidity by complexation of Et₃PO to the Lewis acid and the difference in the ³¹P NMR chemical shift of Et₃PO and complexed Et₃PO. From this, a scale of Acceptor Number (AN) is generated, where the larger the AN the higher the Lewis acidity; the formula to calculate this is shown in Equation 1.⁹ To ensure complexation we used 10 equivalents of Et₃PO per Lewis acidic site and we compared the AN of **2** and **3**.



Scheme S6. Complexation of Et₃PO to the Lewis Acid.

$$\text{AN} = 2.21 \times (\delta_{\text{P(LA-OPEt}_3)} - 41) \text{ Eqn(1).}$$

Table 1. Determination of Acceptor Number (AN) for **2** and **3**.

Compound	Solvent	$\delta_{\text{P(LA-OPEt}_3)}$ / ppm	Acceptor Number (AN)
2	C ₆ D ₆	62.15	46.74
3	C ₆ D ₆	62.08	46.59

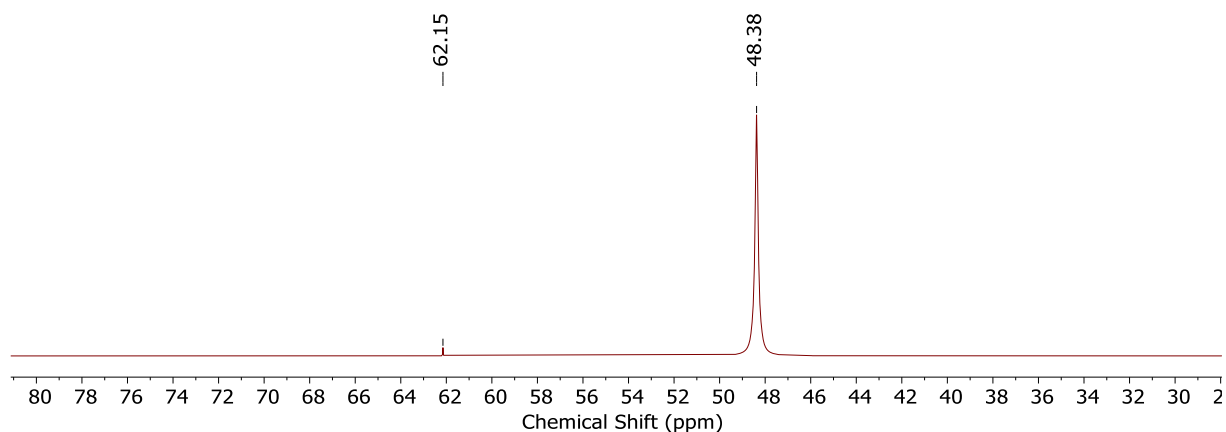


Figure S24. ³¹P NMR spectrum (C₆D₆) of **2** + 30 equivalents Et₃PO.

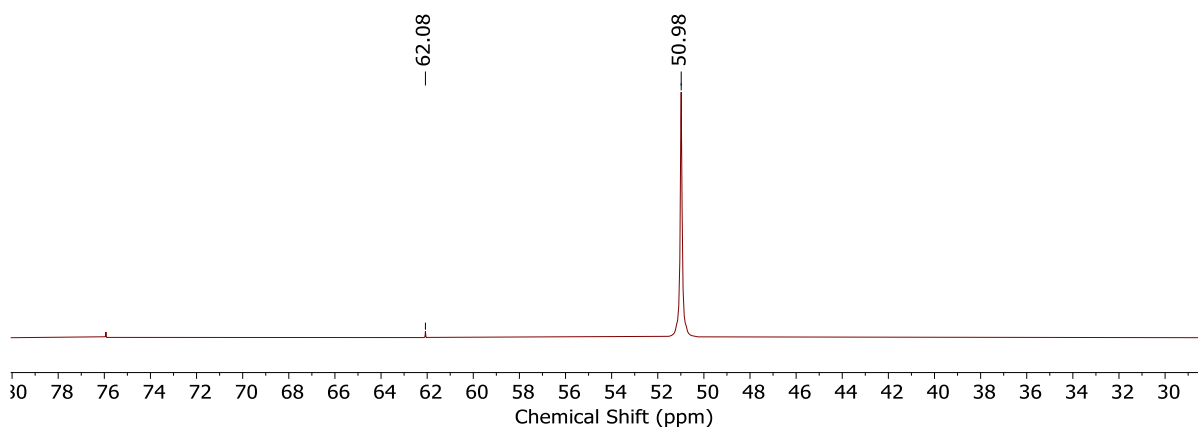
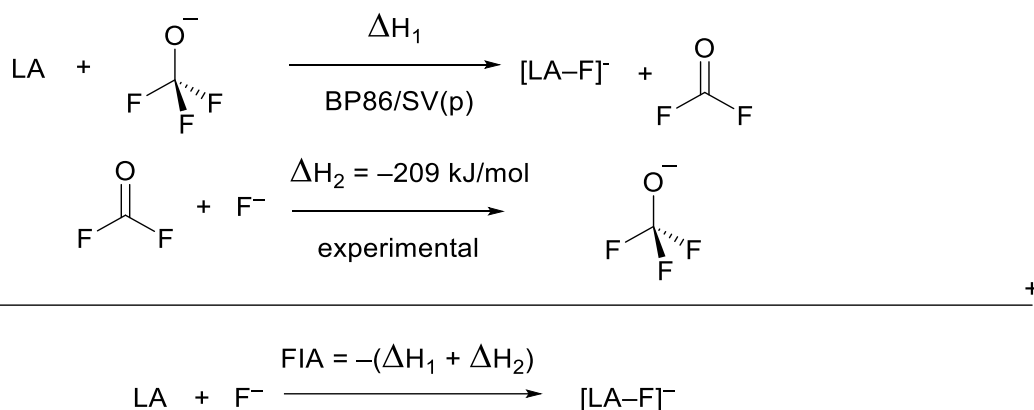


Figure S25. ^{31}P NMR spectrum (C_6D_6) of **3** + 10 equivalents Et_3PO .

3.2. Fluoride Ion Affinity (FIA)

The Lewis acidity of selected Lewis acids was probed by calculation of its Fluoride Ion Affinity (FIA) using the $\text{CF}_2\text{O}-\text{CF}_3\text{O}^-$ reference system (also known as Christie's method).¹⁰ This method has been extensively used in literature using the BP86/SV(p) level of theory. The calculated FIA of $\text{B}(\text{C}_6\text{F}_5)_3$, SbF_5 and Me_3Si^+ are consistent with literature values and used as benchmarks.¹¹



Scheme S7. FIA calculation.

Table S2. FIA values of selected Lewis Acids and **2** and **3**.

Compound	FIA (kJ/mol)
$\text{B}(\text{C}_6\text{F}_5)_3$	444
SbF_5	489
$[\text{Me}_3\text{Si}]^+$	948
$(\{9\text{-BBN}\}\text{CH}_2\text{CH}_2\text{SiMe}_2)_3(\text{P}_7)$ (2)	350
$[(\{9\text{-BBN}\}\text{CH}_2\text{CH}_2\text{SiMe}_2)_2(\{9\text{-BBN}\}\text{CH}_2\text{CH}_2\text{FSiMe}_2)(\text{P}_7)]^-$	220
$[(\{9\text{-BBN}\}\text{CH}_2\text{CH}_2\text{SiMe}_2)(\{9\text{-BBN}\}\text{CH}_2\text{CH}_2\text{FSiMe}_2)_2(\text{P}_7)]^{2-}$	113

ClSiMe ₂ CH ₂ CH ₂ (9-BBN) (3)	340
H-BBN	328
(H-BBN) ₂	327

Table S3. Computed FIA of selected Lewis Acids and **2** and **3**.

Compound	E [a.u.]	G [a.u.]
CF ₂ O	-312.7854163	-312.76742
[CF ₃ O] ⁻	-412.6141114	-412.594474
B(C ₆ F ₅) ₃	-2206.628214	-2206.448141
[FB(C ₆ F ₅) ₃] ⁻	-2306.547159	-2306.364788
SbF ₅	-6814.717684	-6814.698435
[SbF ₆] ⁻	-6914.652886	-6914.631992
[Me ₃ Si] ⁺	-408.8174622	-408.70319
Me ₃ SiF	-508.9311529	-508.81189
({9-BBN}CH ₂ CH ₂ SiMe ₂) ₃ (P ₇) (2)	-4746.14535	-4745.07617
[({9-BBN}CH ₂ CH ₂ SiMe ₂) ₂ ({9-BBN}FCH ₂ CH ₂ SiMe ₂)(P ₇)] ⁻	-4846.02792	-4844.95702
[({9-BBN}CH ₂ CH ₂ SiMe ₂)({9-BBN}FCH ₂ CH ₂ SiMe ₂) ₂ (P ₇)] ²⁻	-4945.85997	-4944.78814
[({9-BBN}CH ₂ CH ₂ FSiMe ₂) ₃ (P ₇)] ³⁻	-5045.65104	-5044.57845
ClSiMe ₂ CH ₂ CH ₂ (9-BBN) (3)	-1245.82099	-1245.47052
[ClSiMe ₂ CH ₂ CH ₂ F(9-BBN)] ⁻	-1345.69957	-1345.34757
H-BBN	-338.46179	-338.24158
[H-FBBN] ⁻	-438.33644	-438.11413
(H-BBN) ₂	-676.97627	-676.52912

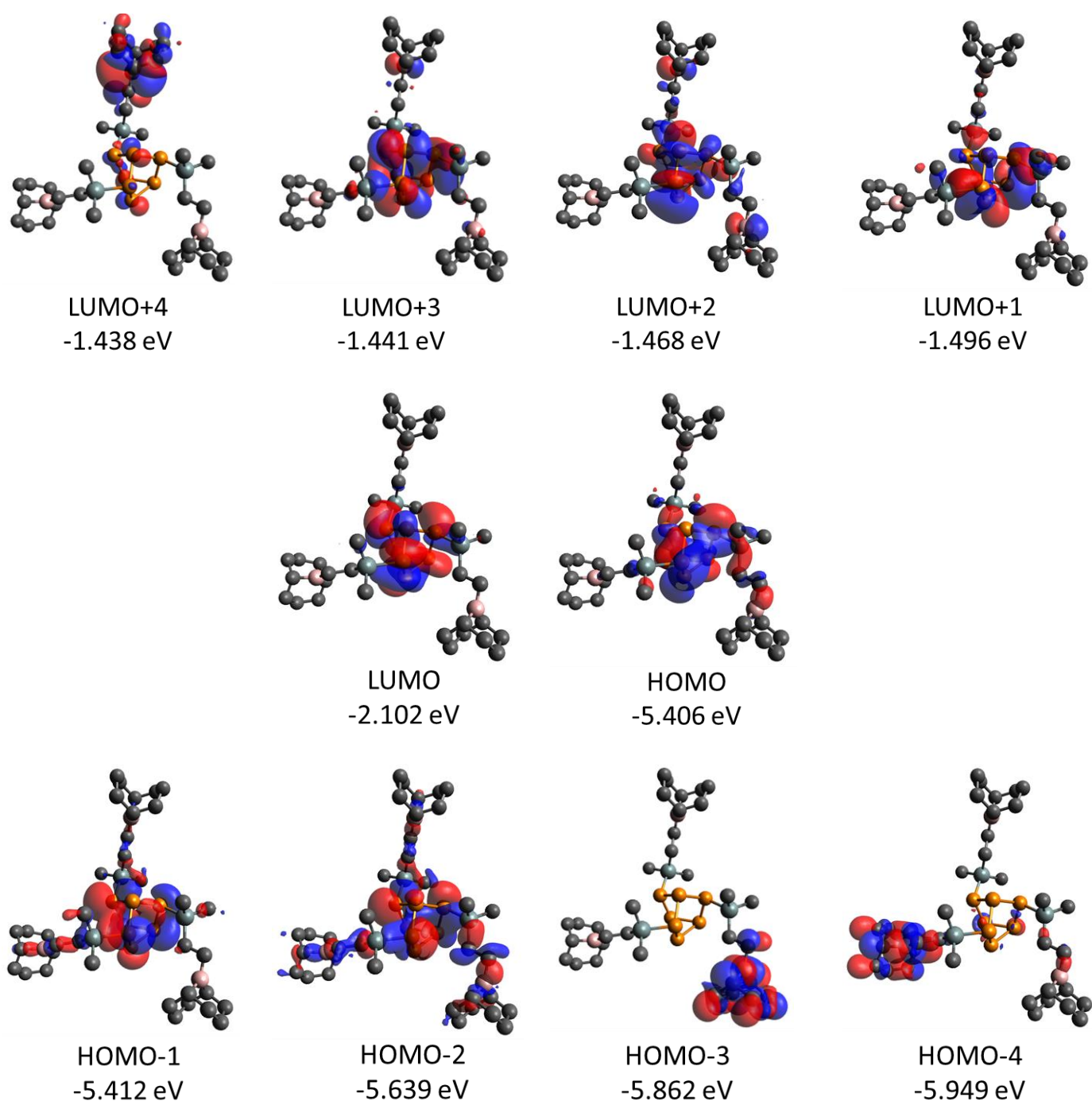


Figure S26. HOMO and LUMO Kohn-Sham images of **2**.

4. General Procedure for Hydroboration

Catalyst **2** (4.2 mg, 5 mol%) was dissolved in 0.5 mL C_6D_6 or THF and transferred to a J Young NMR tube. One (14.5 μ L, 0.1 mmol) or two (29 μ L, 0.2 mmol) equivalents of pinacol borane (HB(pin)) and substrate (0.1 mmol) were subsequently added via

microsyringe. The reaction progress was monitored by ^1H and ^{11}B NMR spectroscopy and conversion was determined by ^1H NMR spectroscopy based on the ratio of reagent and the target hydroborated product or using toluene (10.7 μL , 0.1 mmol, 1 equivalent) as an internal standard. The NMR resonance used to determine conversion is underlined under the substrate characterization data. Isolated yields were obtained by the removal of volatiles under reduced pressure, followed by extraction in cold ($-20\text{ }^\circ\text{C}$) pentane and filtration.

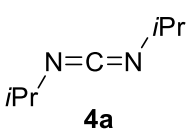
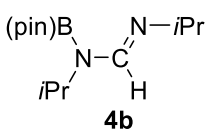
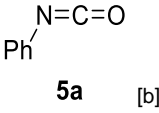
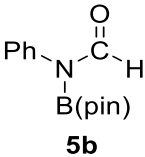
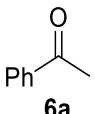
Integrations for aromatic signals in the ^1H NMR spectra were on occasion difficult to assign to crude compounds due to a mixture of hydroborated product, substrate and toluene internal standard. All key assignments have successfully been made.

5. Screening Catalytic Conditions

5.1. Temperature and Solvent Screening

We examined hydroboration of a wide variety of substrate functional groups in both C_6D_6 and THF at $25\text{ }^\circ\text{C}$, $50\text{ }^\circ\text{C}$ and $110\text{ }^\circ\text{C}$. Reactions were prepared and monitored according to the general procedure for hydroboration described in section 4. In general, higher reactivity was observed in C_6D_6 compared to THF.

Table S4. Solvent and Temperature Screening, Catalyst Loading = 5 mol%.

Entry	Substrate	Product	Solvent	<i>t</i> (h)	T ($^\circ\text{C}$)	Conv. (%) ^[a]
1	 4a	 4b	C_6D_6	12	25	92
2			C_6D_6	2	50	>99 (91)
3			THF	12	25	70
4			THF	2	50	95 (90)
5	 5a	 5b	C_6D_6	18	25	0
6			C_6D_6	72	50	43
7			C_6D_6	22	110	21
8			THF	18	25	0
9			THF	72	50	18
10			THF	22	110	12
11	 6a		C_6D_6	18	25	0
12			C_6D_6	40	50	0
13			C_6D_6	15	110	91

14			THF	18	25	0
15			THF	40	50	0
16			THF	15	110	20
17			C ₆ D ₆	24	25	0
18			C ₆ D ₆	48	50	0
19			C ₆ D ₆	72	110	80
20			THF	24	25	0
21			THF	48	50	0
22			THF	72	110	16
23			C ₆ D ₆	18	25	0
24			C ₆ D ₆	112	50	78
25			THF	18	25	0
26			THF	112	50	61
27			C ₆ D ₆	18	25	0
28			C ₆ D ₆	40	50	0
29			C ₆ D ₆	72	110	84
30			THF	18	25	0
31			THF	40	50	0
32			THF	72	110	26

[a] Conversion determined by ¹H NMR spectroscopy. Yields of the isolated product are given within parentheses.

[b] The hydroboration of isocyanates also led to the detectable formation product interactions with **2**, see section 7 for more information. The conversions stated are for the conversion to free **5b**. [c] Two equivalents HB(pin) added.

5.2. HB(pin) equivalents

We investigated the possibility of double hydroboration and hydrodeoxygenation/hydrodenitrogenation reactions. Our results showed that no double hydroboration of di-isopropylcarbodiimide (**4a**) or phenyl acetylene (**8a**) could be observed after 5 days at 110 °C. Under similar conditions, no deoxygenations of acetophenone (**6a**) was observed. However, with two or three equivalents of HB(pin) at either 50 °C or 110 °C we observed bis-hydroboration and hydrodeoxygenation of phenyl isocyanate PhNCO (**5a**).

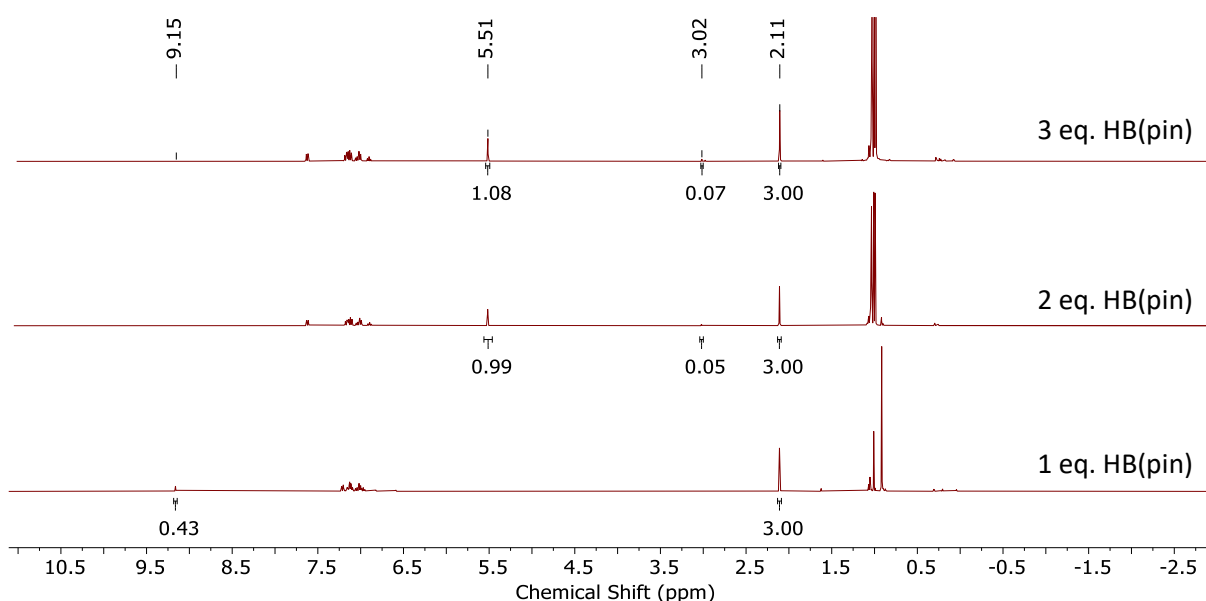


Figure S27. Stacked ^1H NMR spectra in C_6D_6 of phenylisocyanate (**16a**) hydroboration with one, two and three equivalents of HB(pin) respectively at 50 °C after 48 hours. δ 9.15 ppm = $\text{PhN}(\text{B}(\text{pin}))\text{CHO}$ (1H, **5b**); δ 5.51 ppm = $\text{PhN}(\text{B}(\text{pin}))\text{CH}_2\text{O}(\text{B}(\text{pin}))$ (2H, **5c**); δ 3.02 ppm = $\text{PhN}(\text{B}(\text{pin}))\text{CH}_3$ (3H, **5d**); δ 2.11 ppm = toluene internal standard resonance.

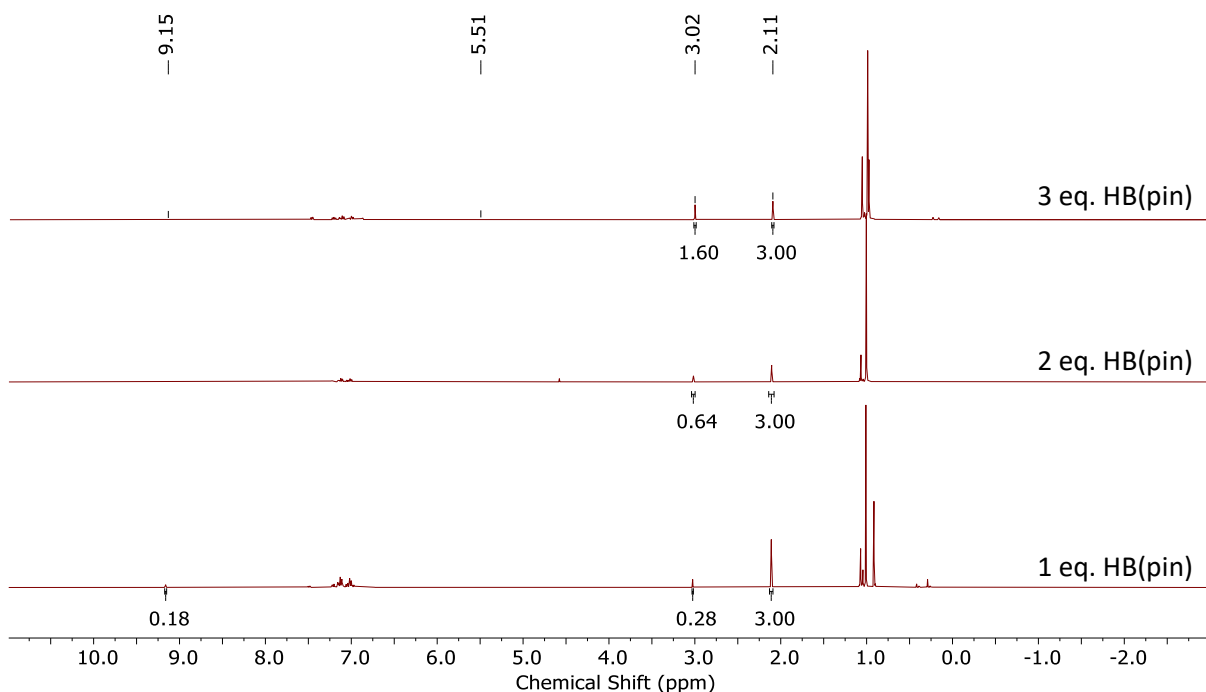


Figure S28. Stacked ^1H NMR spectra in C_6D_6 of phenylisocyanate (**16a**) hydroboration with one, two and three equivalents of HB(pin) respectively at 110 °C after 48 hours. δ 9.15 ppm = $\text{PhN}(\text{B}(\text{pin}))\text{CHO}$ (1H, **5b**); δ 5.51 ppm =

PhN(B(pin))CH₂O(B(pin)) (2H, **5c**); δ 3.02 ppm = PhN(B(pin))CH₃ (3H, **5d**); δ 2.11 ppm = toluene internal standard resonance.

5.3. Role of the Cluster in Catalysis

In order to investigate the role of the cluster in catalysis we investigated both the untethered chlorosilane **3** and (Me₃Si)₃(P)₇ as a hydroboration catalyst. (Me₃Si)₃(P)₇ remained inactive towards hydroboration catalysis.

For the untethered chlorosilane (3);

To a J Young NMR tube containing 0.4 mL C₆D₆, 0.1 mL of a stock solution of untethered chlorosilane **3** (21.8 mg in 0.6 mL C₆D₆, 15 mol%) was transferred. One equivalent (14.5 μ L, 0.1 mmol) for **4a–8a** or two equivalents (29 μ L, 0.2 mmol) for **9a** of pinacol borane (HB(pin)) and one equivalent of substrate (0.1 mmol) were subsequently added via microsyringe.

For (Me₃Si)₃(P)₇;

(Me₃Si)₃(P)₇ (2.2 mg, 5 mol%) was dissolved in 0.5 mL of C₆D₆ and transferred to a J Young NMR tube. One equivalent (14.5 μ L, 0.1 mmol) for **4a–8a** or two equivalents (29 μ L, 0.2 mmol) for **9a** of pinacol borane (HB(pin)) and one equivalent of substrate (0.1 mmol) were subsequently added via microsyringe.

Monitoring;

The catalysis was allowed to proceed under analogous conditions used for catalyst **2** and subsequently monitored by ¹H and ¹¹B NMR spectroscopy and conversion was determined by ¹H NMR spectroscopy based on the ratio of starting material and the hydroborated product or using toluene (10.7 μ L, 0.1 mmol, 1 equivalent) as an internal standard. ²⁹Si{¹H} and ³¹P{¹H} was used to confirm that **3** and (Me₃Si)₃(P)₇ do not decompose during the catalysis.

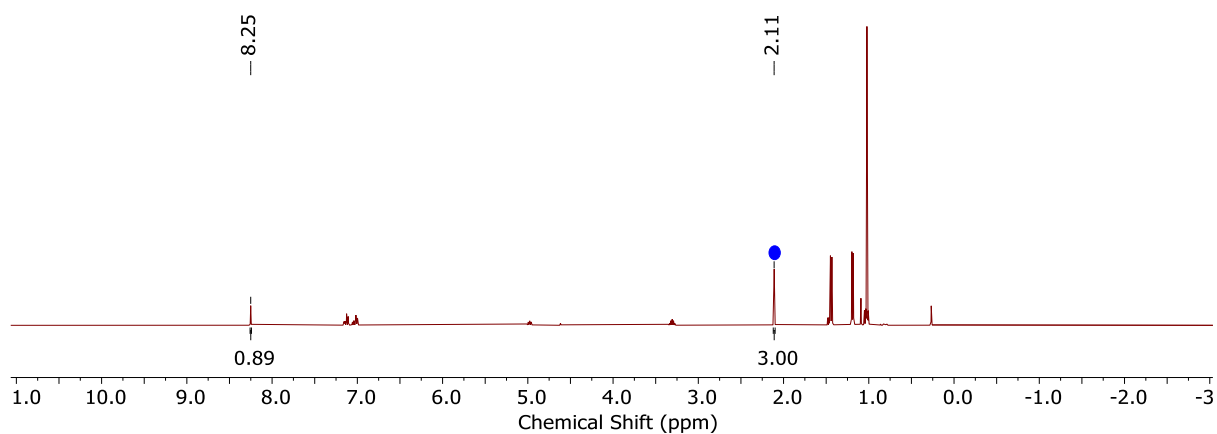


Figure S29. ^1H NMR spectrum (C_6D_6) of crude **4a**, catalyzed by $\text{ClSiMe}_2\text{CH}_2\text{CH}_2(9\text{-BBN})$ (**3**). • = toluene internal standard resonance.

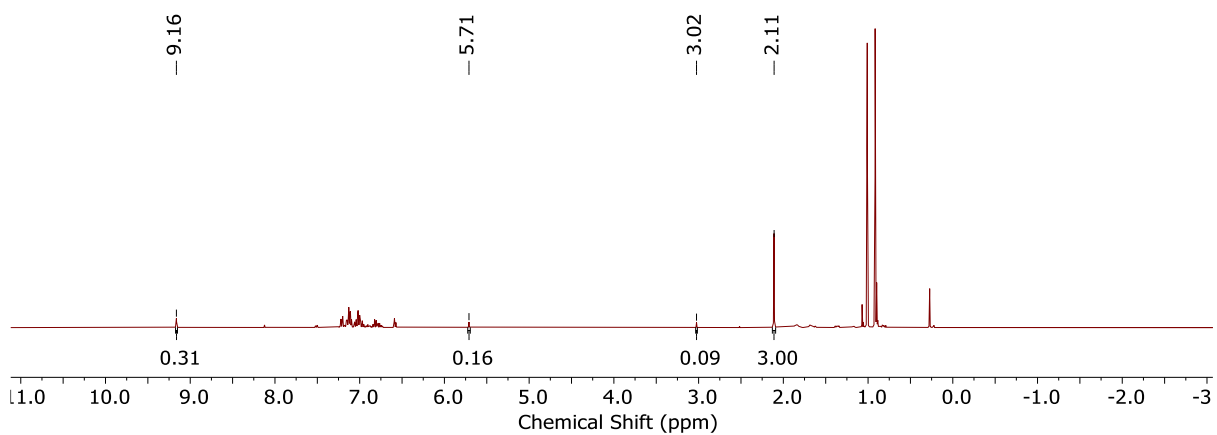


Figure S30. ^1H NMR spectrum (C_6D_6) of crude **5a**, catalyzed by $\text{ClSiMe}_2\text{CH}_2\text{CH}_2(9\text{-BBN})$ (**3**). δ 9.16 ppm = $\text{PhN}(\text{B}(\text{pin}))\text{CHO}$ (1H, **5b**); δ 5.71 ppm = $\text{PhN}(\text{B}(\text{pin}))\text{CH}_2\text{O}(\text{B}(\text{pin}))$ (2H, **5c**); δ 3.02 ppm = $\text{PhN}(\text{B}(\text{pin}))\text{CH}_3$ (3H, **5d**); • = toluene internal standard resonance.

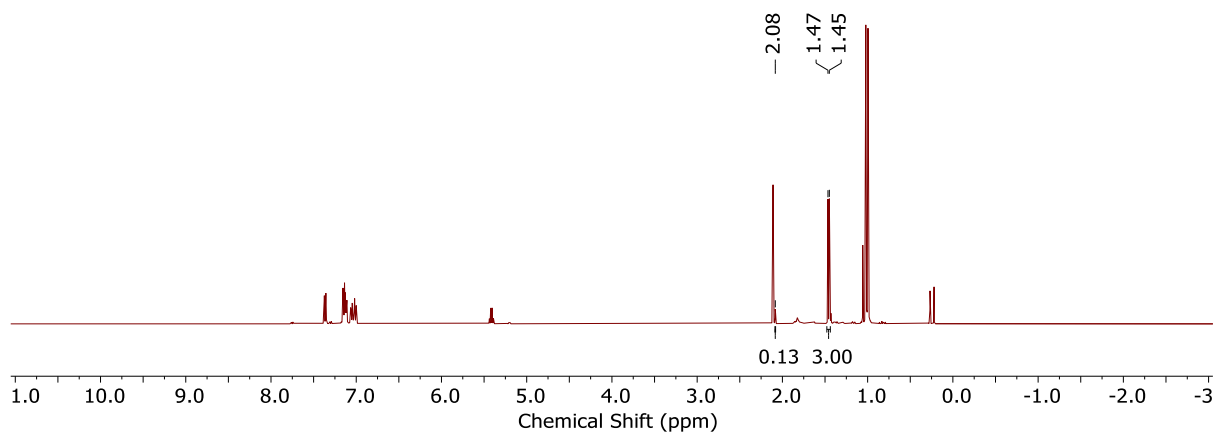


Figure S31. ^1H NMR spectrum (C_6D_6) of crude **6a**, catalyzed by $\text{ClSiMe}_2\text{CH}_2\text{CH}_2(9\text{-BBN})$ (**3**). ● = unreacted start material used to determine conversion.

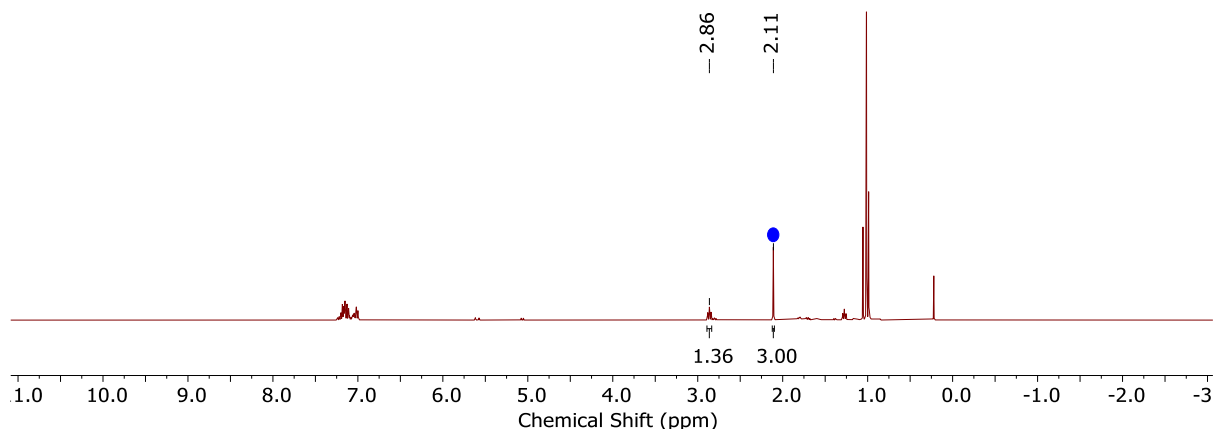


Figure S32. ^1H NMR spectrum (C_6D_6) of crude **7a**, catalyzed by $\text{ClSiMe}_2\text{CH}_2\text{CH}_2(9\text{-BBN})$ (**3**). ● = toluene internal standard resonance.

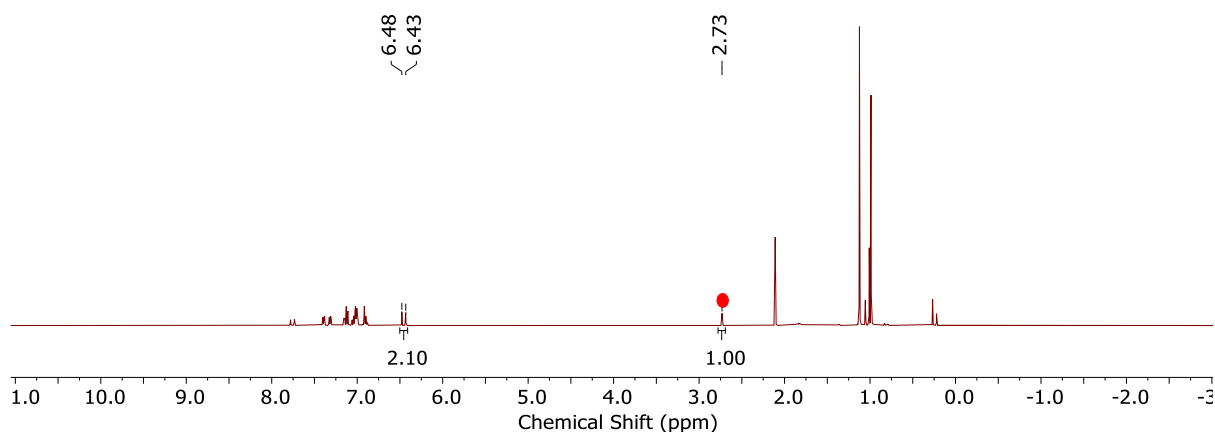


Figure S33. ^1H NMR spectrum (C_6D_6) of crude **8a**, catalyzed by $\text{ClSiMe}_2\text{CH}_2\text{CH}_2(9\text{-BBN})$ (**3**). ● = unreacted start material used to determine conversion.

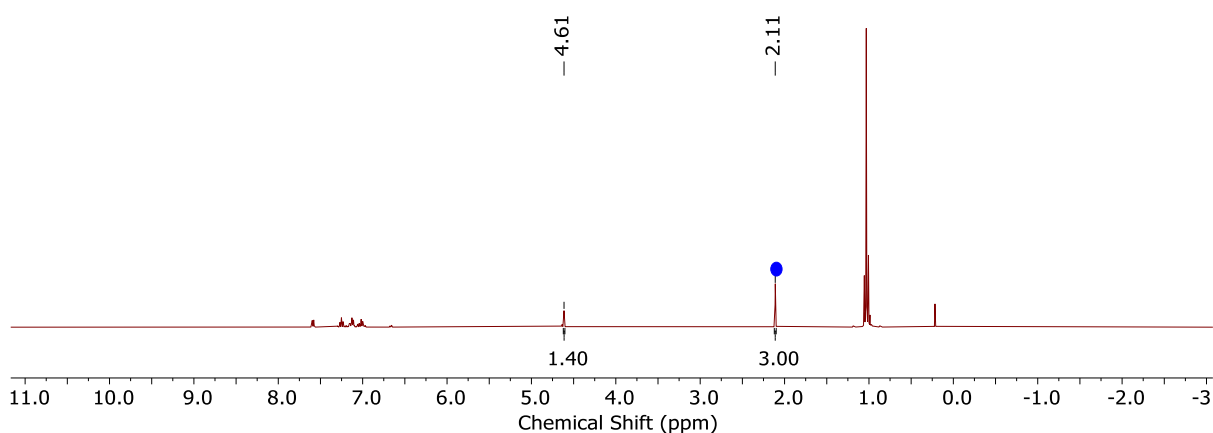


Figure S34. ^1H NMR spectrum (C_6D_6) of crude **9a**, catalyzed by $\text{ClSiMe}_2\text{CH}_2\text{CH}_2(9\text{-BBN})$ (**3**). ● = toluene internal standard resonance.

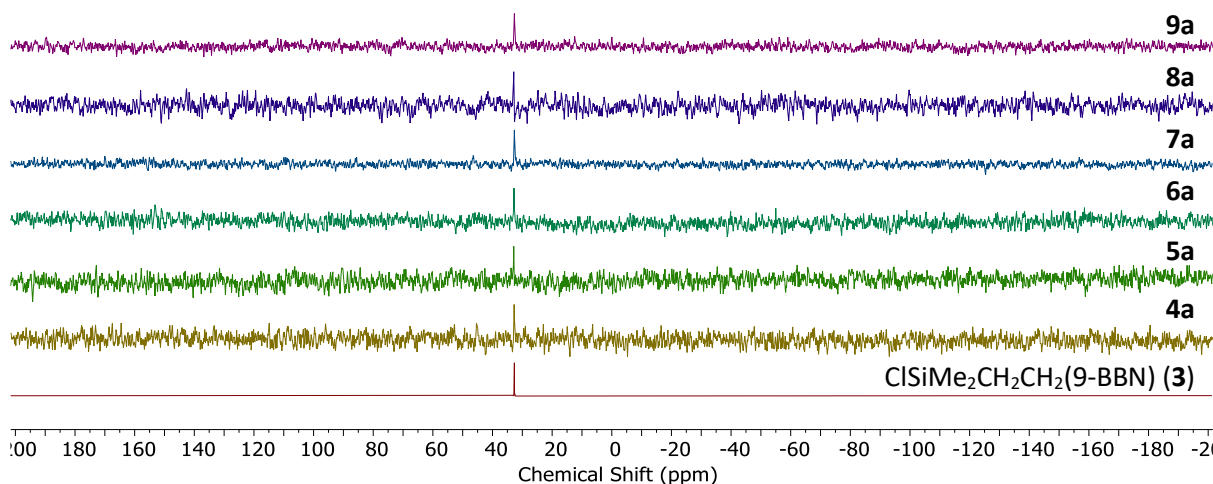


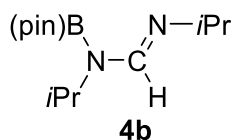
Figure S35. $^{29}\text{Si}\{^1\text{H}\}$ NMR spectrum (C_6D_6) of **3** and after the catalysis of substrates **4a – 9a** confirming that the Si–Cl bond remains intact. δ 32.66 ppm.

6. Characterization Data

6.1. Carbodiimides

We validated our analysis of hydroborated carbodiimides by comparison to various literature sources and found all data to be in agreement with those previously reported.^{12, 13}

6.1.1. **4b** – N,N'-diisopropyl-N-(4,4,5,5-tetramethyl-1,3,2-dioxaborolan-2-yl)formimidamide



^1H NMR (400 MHz, 298 K, C_6D_6): δ = 8.28 (s, 1H, $\text{HC}=\text{N}$), 5.00 (sept, $^3J_{\text{HH}}$ = 6.9 Hz, 1H, $\text{CH}(\text{CH}_3)_2$), 3.32 (sept, $^3J_{\text{HH}}$ = 6.3 Hz, 1H, $\text{CH}(\text{CH}_3)_2$), 1.46 (d, $^3J_{\text{HH}}$ = 6.9 Hz, 6H, $\text{CH}(\text{CH}_3)_2$), 1.20 (d, $^3J_{\text{HH}}$ = 6.3 Hz, 6H, $\text{CH}(\text{CH}_3)_2$), 1.02 (s, 12H, Bpin) ppm.

^{11}B NMR (128 MHz, 298 K, C_6D_6): δ = 25.3 (s) ppm.

$^{13}\text{C}\{^1\text{H}\}$ NMR (101 MHz, 298 K, C_6D_6): δ = 150.01 (HC=N), 82.75 ($\text{C}(\text{CH}_3)_2$), 57.30 ($\text{CH}(\text{CH}_3)_2$), 43.67 ($\text{CH}(\text{CH}_3)_2$), 25.71 ($\text{CH}(\text{CH}_3)_2$), 24.53 ($\text{C}(\text{CH}_3)_2$), 21.87 ($\text{CH}(\text{CH}_3)_2$) ppm.

Mass spectrometry (ESI): $\text{C}_{13}\text{H}_{27}\text{BN}_2\text{O}_2+\text{H}$ ($[\text{M}+\text{H}]^+$); Calcd. = 255.2238, Found = 255.2238.

Conversion: >99%

Isolated Yield: 91%

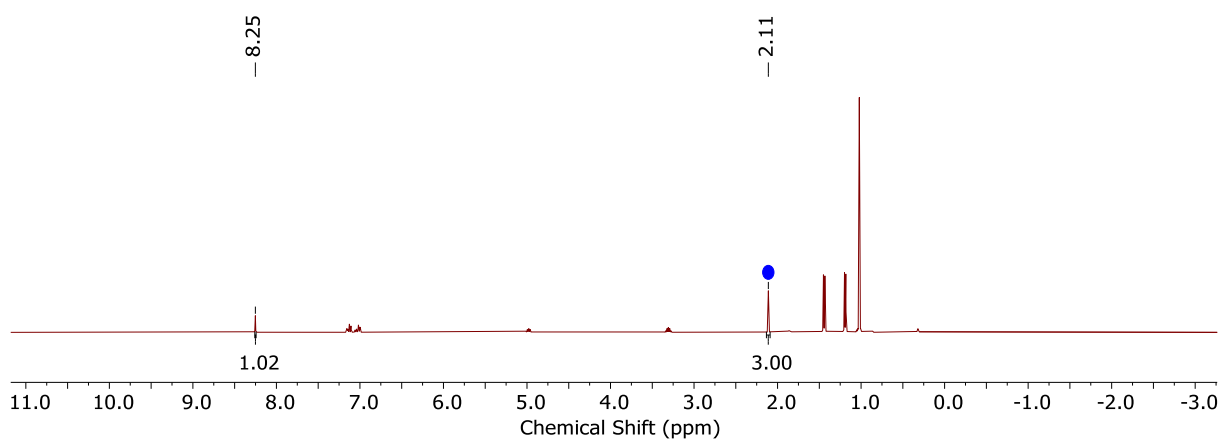


Figure S36. ^1H NMR spectrum (C_6D_6) of crude **4b**. • = toluene internal standard resonance.

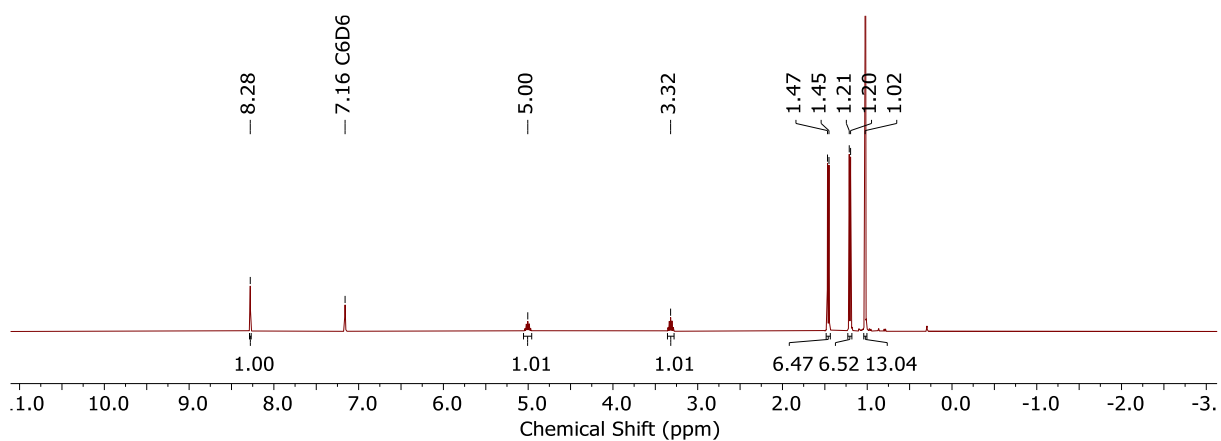


Figure S37. ^1H NMR spectrum (C_6D_6) of isolated **4b**.

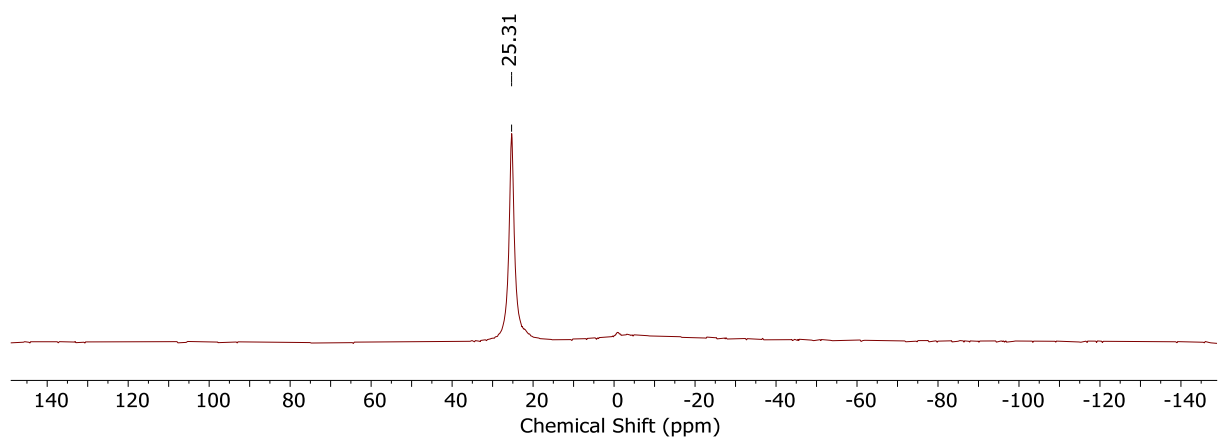


Figure S38. ^{11}B NMR spectrum (C_6D_6) of isolated **4b**.

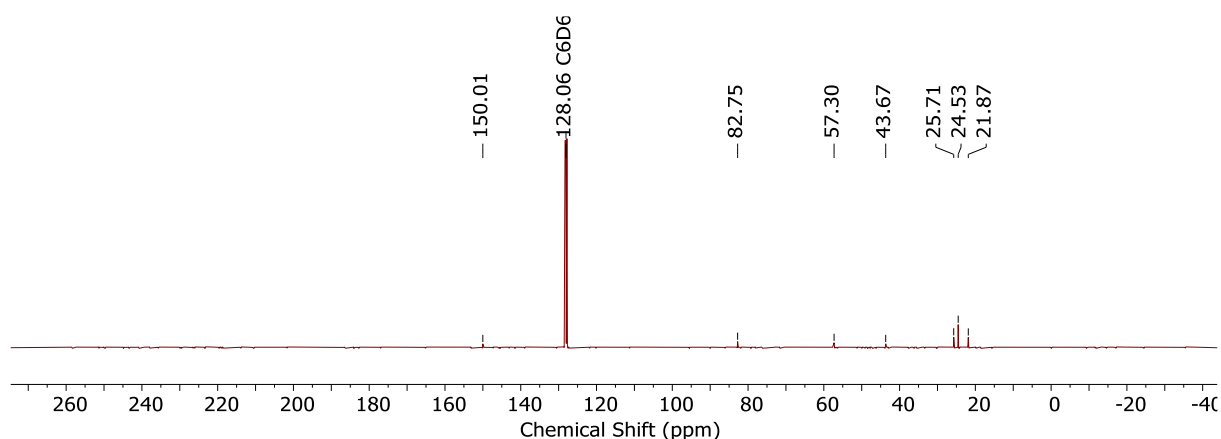
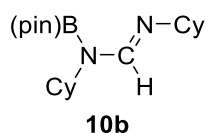


Figure S39. $^{13}\text{C}\{^1\text{H}\}$ NMR spectrum (C_6D_6) of isolated **4b**.

6.1.2. **10b** – N,N'-dicyclohexyl-N-(4,4,5,5-tetramethyl-1,3,2-dioxaborolan-2-yl)formimidamide



^1H NMR (400 MHz, 298 K, C_6D_6): $\delta = 8.34$ (s, 1H, $\text{HC}=\text{N}$), 4.62 (m, 1H, NCH), 2.99 (m, 1H, NCH), 1.12–1.96 (m, 20H, Cy), 1.05 (s, 12H, Bpin) ppm.

^{11}B NMR (128 MHz, 298 K, C_6D_6): $\delta = 25.4$ (s) ppm.

Mass spectrometry (ESI): $\text{C}_{19}\text{H}_{35}\text{BN}_2\text{O}_2+\text{H}$ ($[\text{M}+\text{H}]^+$); Calcd. = 335.2867, Found = 335.2867.

Conversion: 82%

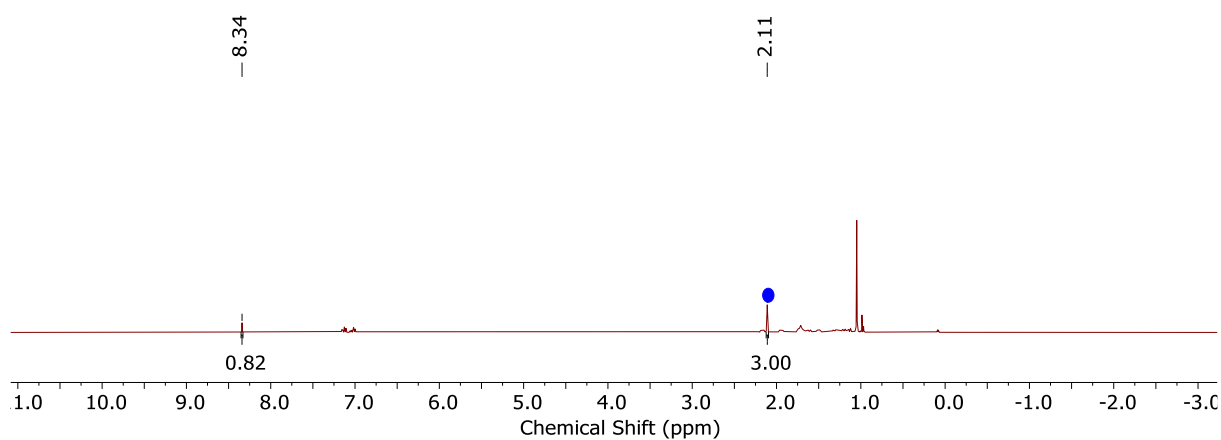


Figure S40. ^1H NMR spectrum (C_6D_6) of crude **10b**. ● = toluene internal standard resonance.

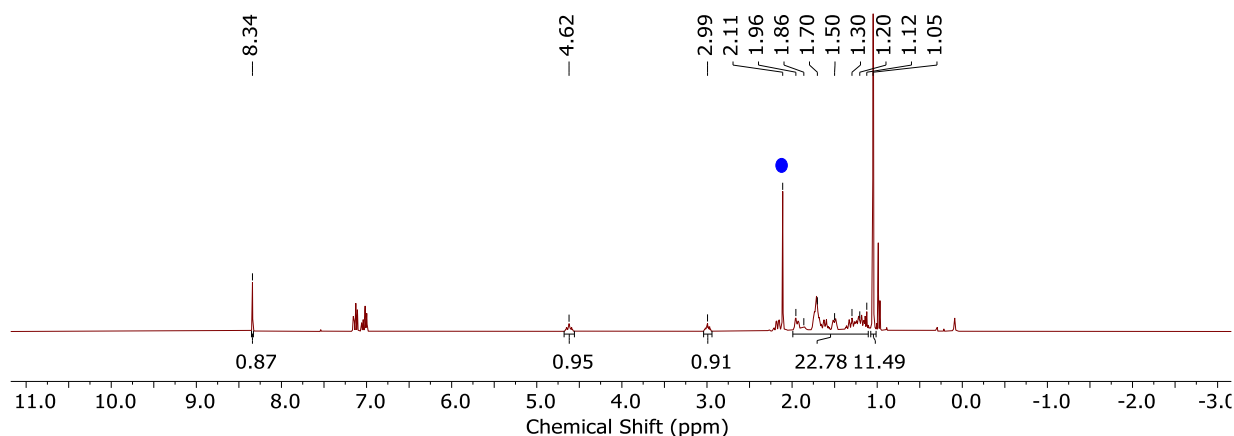


Figure S41. ^1H NMR spectrum (C_6D_6) of crude **10b**. • = toluene internal standard resonance.

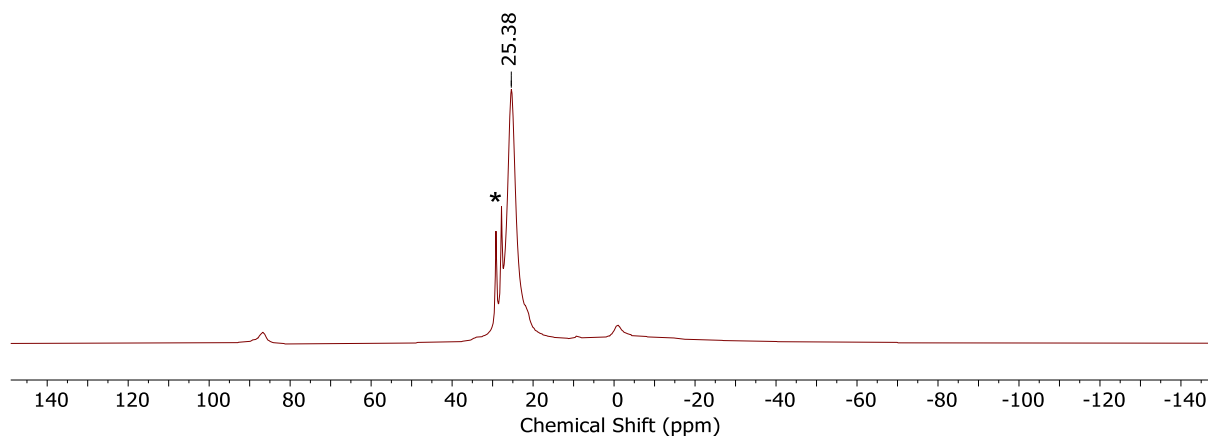
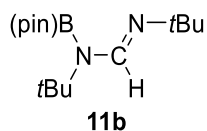


Figure S42. ^{11}B NMR spectrum (C_6D_6) of crude **10b**. * = HB(pin).

6.1.3. **11b** – N,N'-di-tert-butyl-N-(4,4,5,5-tetramethyl-1,3,2-dioxaborolan-2-yl)formimidamide



^1H NMR (400 MHz, 298 K, C_6D_6): δ = 8.34 (s, 1H, HC=N), 1.54 (s, 18H, $\text{C}(\text{CH}_3)_3$), 1.01 (s, 12H, Bpin) ppm.

^{11}B NMR (128 MHz, 298 K, C_6D_6): δ = 25.5 (s) ppm.

$^{13}\text{C}\{^1\text{H}\}$ NMR (101 MHz, 298 K, C_6D_6): δ = 149.23 (HC=N), 82.19 ($\text{C}(\text{CH}_3)_2$), 55.14 ($\text{C}(\text{CH}_3)_3$), 30.61 ($\text{C}(\text{CH}_3)_3$), 24.48 ($\text{C}(\text{CH}_3)_2$) ppm.

Mass spectrometry (APCI): $C_{15}H_{31}BN_2O_2+H$ ($[M+H]^+$); Calcd. = 283.2551, Found = 283.2552.

Conversion: >99%

Isolated Yield: 88%

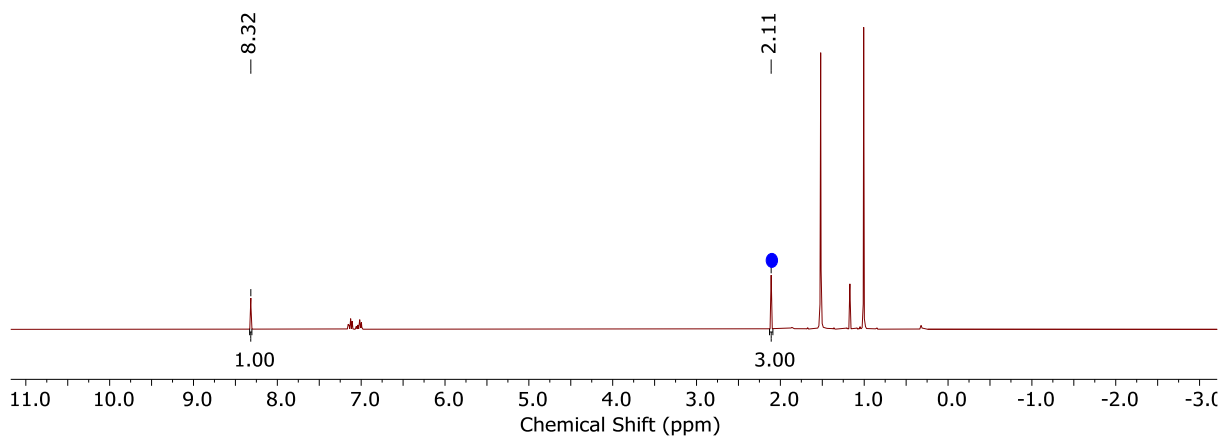


Figure S43. 1H NMR spectrum (C_6D_6) of crude **11b**. ● = toluene internal standard resonance.

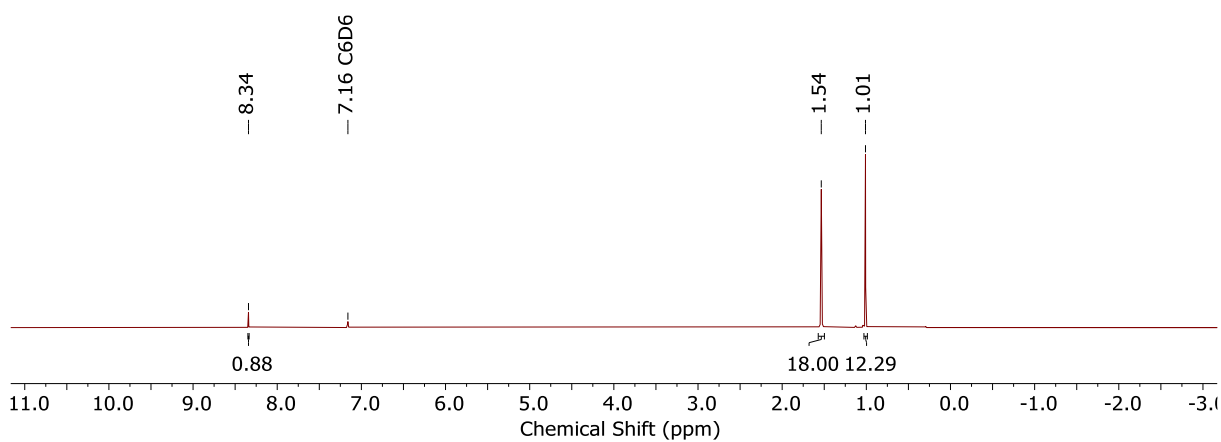


Figure S44. 1H NMR spectrum (C_6D_6) of isolated **11b**.

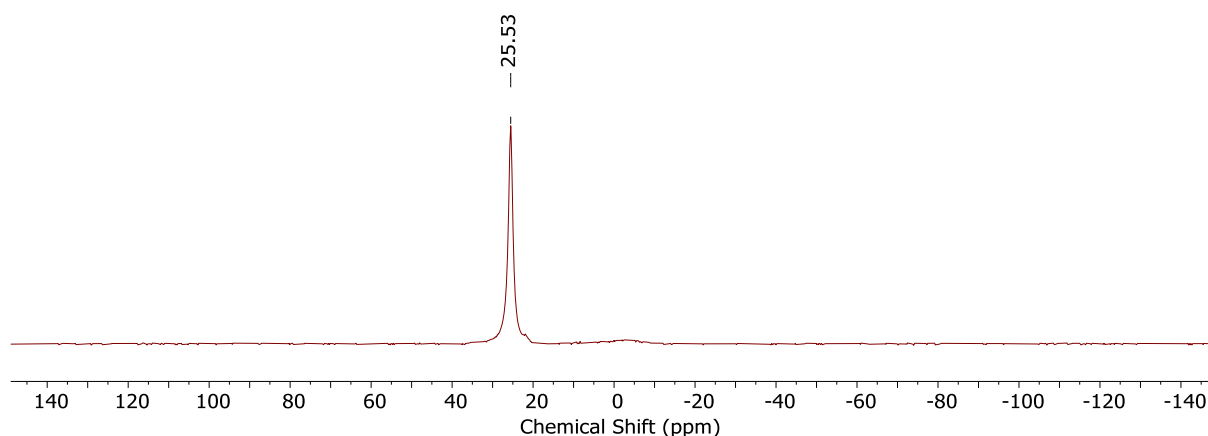


Figure S45. ^{11}B NMR spectrum (C_6D_6) of isolated **11b**.

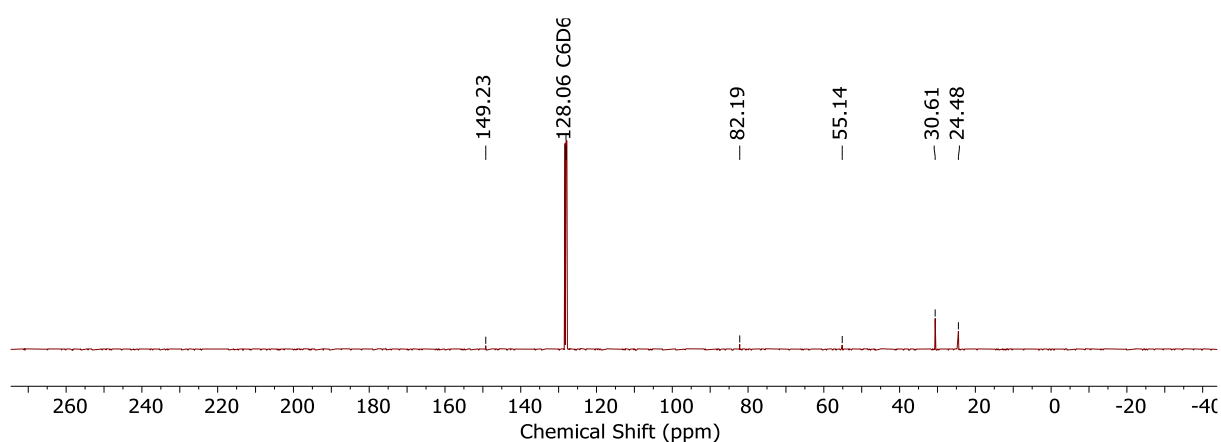
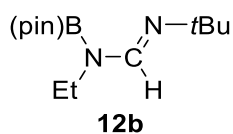


Figure S46. $^{13}\text{C}\{^1\text{H}\}$ NMR spectrum (C_6D_6) of isolated **11b**.

6.1.4. **12b** – N'-tert-butyl-N-ethyl-N-(4,4,5,5-tetramethyl-1,3,2-dioxaborolan-2-yl)formimidamide



^1H NMR (400 MHz, 298 K, C_6D_6): δ = 8.19 (s, 1H, $\text{HC}=\text{N}$), 3.80 (q, $^3J_{\text{HH}} = 6.9$ Hz, 2H, CH_2), 1.34 (t, $^3J_{\text{HH}} = 6.9$ Hz, 3H, CH_3), 1.22 (s, 9H, CH_3), 1.04 (s, 12H, Bpin) ppm.

^{11}B NMR (128 MHz, 298 K, C_6D_6): δ = 25.4 (s) ppm.

Mass spectrometry (APCI): $\text{C}_{13}\text{H}_{27}\text{BN}_2\text{O}_2+\text{H}$ ($[\text{M}+\text{H}]^+$); Calcd. = 255.2238, Found = 255.2249.

Conversion: 56%

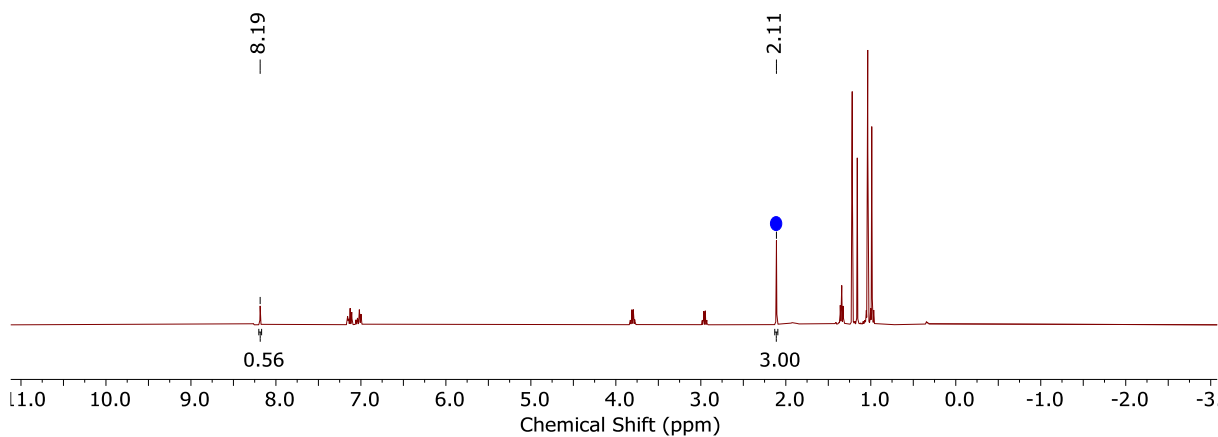


Figure S47. ^1H NMR spectrum (C_6D_6) of crude **12b**. ● = toluene internal standard resonance.

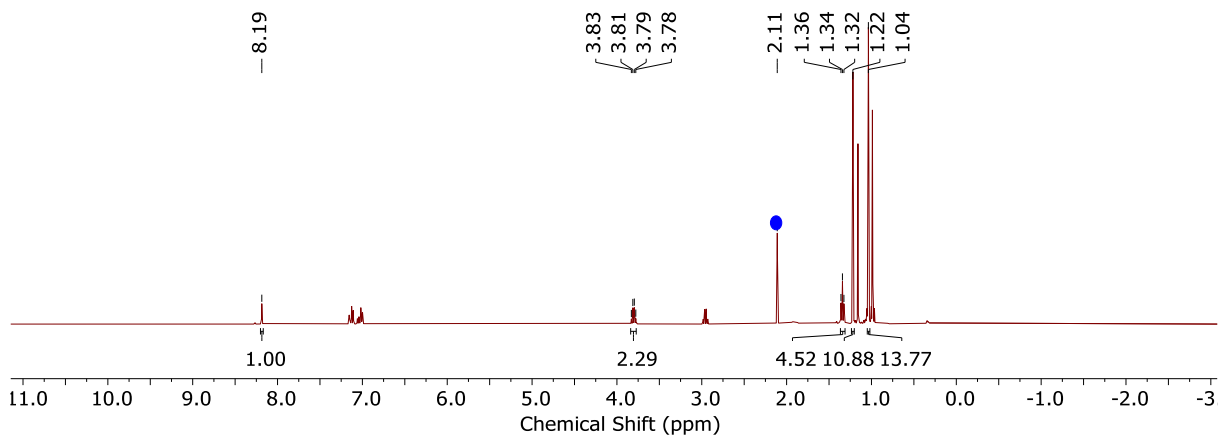


Figure S48. ^1H NMR spectrum (C_6D_6) of crude **12b**. ● = toluene internal standard resonance.

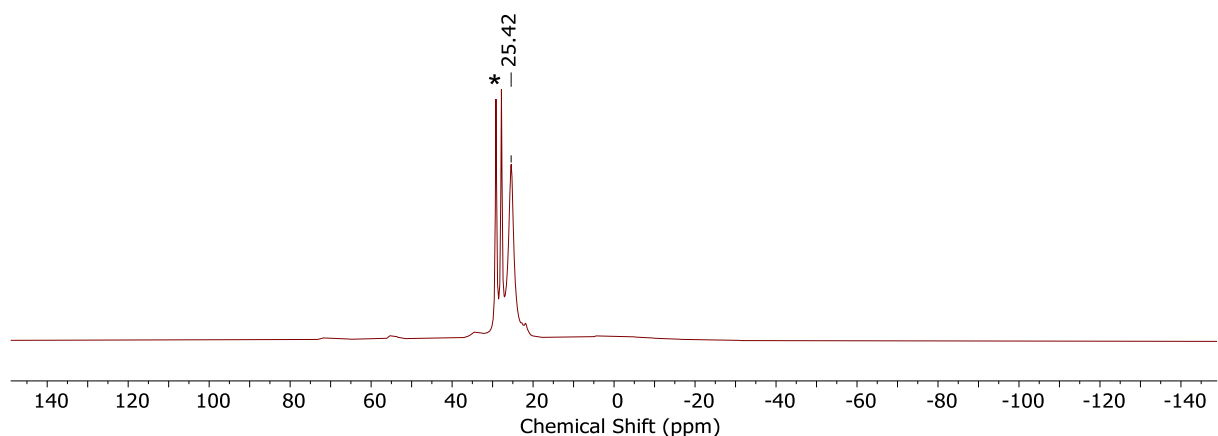
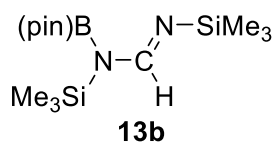


Figure S49. ^{11}B NMR spectrum (C_6D_6) of crude **12b**. * = HB(pin).

6.1.5. **13b** – N-(4,4,5,5-tetramethyl-1,3,2-dioxaborolan-2-yl)-N,N'-bis(trimethylsilyl)formimidamide



^1H NMR (400 MHz, 298 K, C_6D_6): $\delta = 8.71$ (s, 1H, $\text{HC}=\text{N}$), 1.00 (s, 12H, Bpin), 0.35 (s, br, 18H, CH_3) ppm.

^{11}B NMR (128 MHz, 298 K, C_6D_6): $\delta = 26.3$ (s) ppm.

$^{29}\text{Si}\{^1\text{H}\}$ NMR (79 MHz, 298 K, C_6D_6): not observed.

Mass spectrometry (APCI): $\text{C}_{13}\text{H}_{31}\text{BN}_2\text{O}_2\text{Si}_2+\text{H}$ ($[\text{M}+\text{H}]^+$); Calcd. = 315.2090, Found = 315.2107.

Conversion: 19%

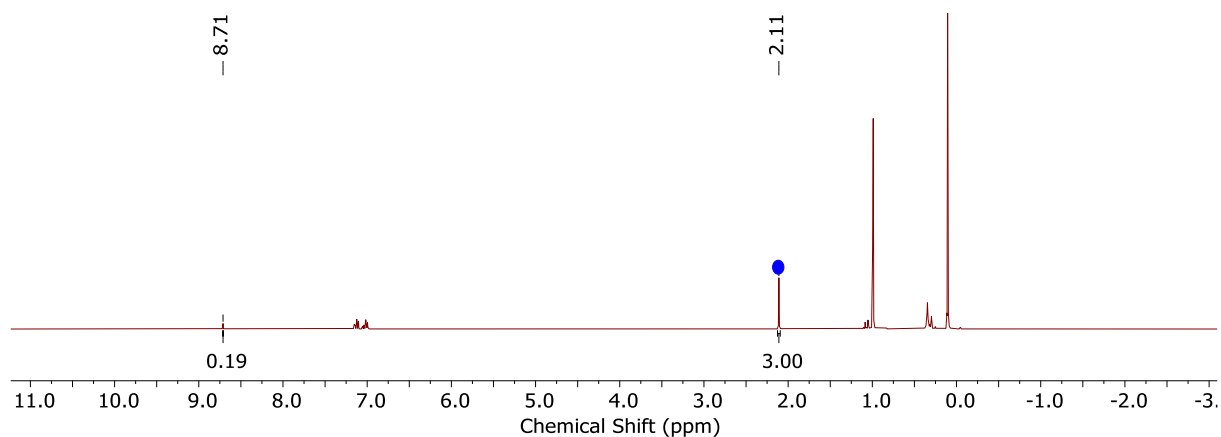


Figure S50. ^1H NMR spectrum (C_6D_6) of crude **13b**. ● = toluene internal standard resonance.

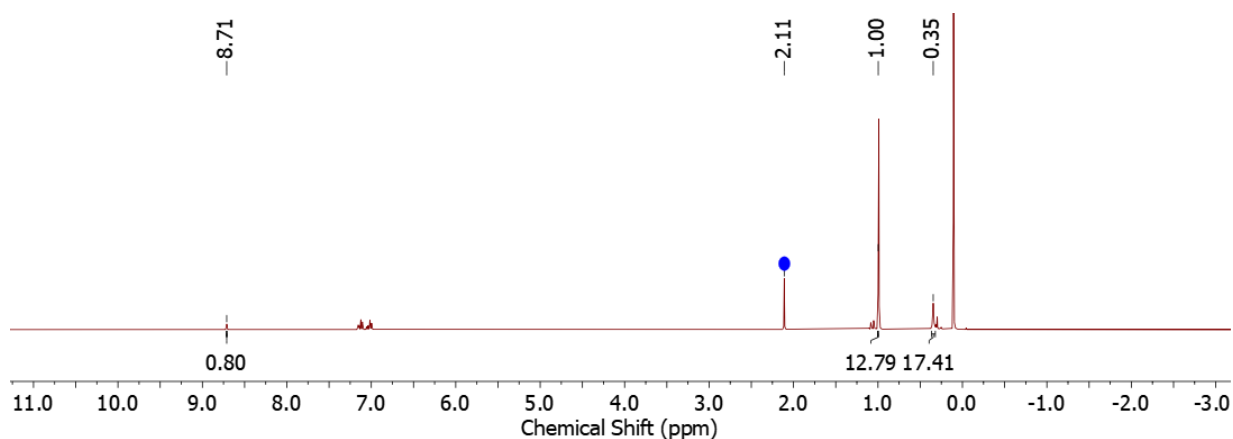


Figure S51. ^1H NMR spectrum (C_6D_6) of crude **13b**. • = toluene internal standard resonance.

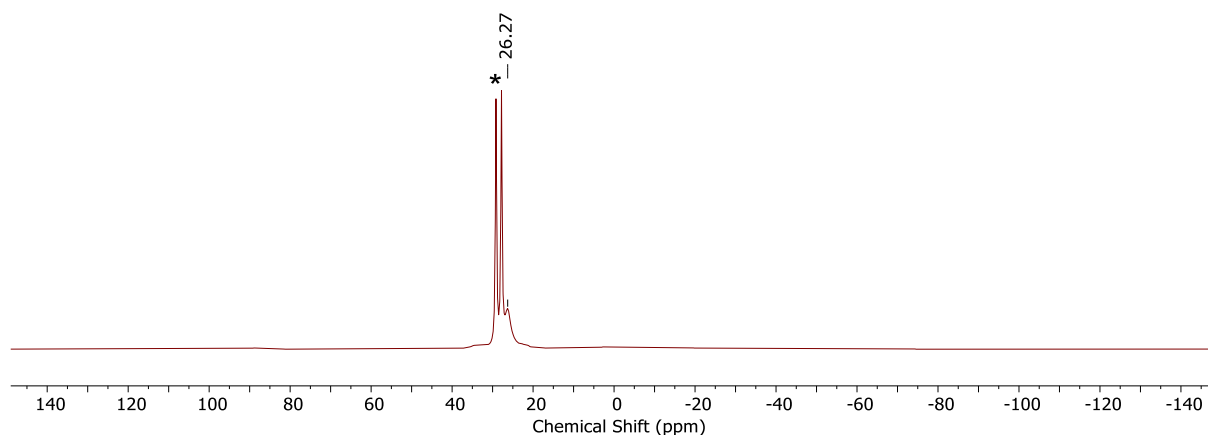
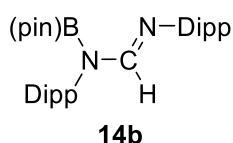


Figure S52. ^{11}B NMR spectrum (C_6D_6) of crude **13b**. * = HB(pin).

6.1.6. **14b** – N,N'-bis(2,6-diisopropylphenyl)-N-(4,4,5,5-tetramethyl-1,3,2-dioxaborolan-2-yl)formimidamide



^1H NMR (400 MHz, 298 K, C_6D_6): δ = 8.32 (s, 1H, $\text{HC}=\text{N}$), 7.00 – 7.24 (m, 6H, *Ar*), 3.36 (sept, $^3J_{\text{HH}}$ = 6.9 Hz, 2H, *CH*), 3.28 (~sept, $^3J_{\text{HH}}$ = 6.9 Hz, 2H, *CH*), 1.38 (t, $^3J_{\text{HH}}$ = 6.9 Hz, 12H, CH_3), 1.20 (d, $^3J_{\text{HH}}$ = 6.9 Hz, 12H, CH_3), 0.96 (s, 12H, *Bpin*) ppm.

^{11}B NMR (128 MHz, 298 K, C_6D_6): δ = 25.4 (s) ppm.

Mass spectrometry (APCI): $\text{C}_{31}\text{H}_{47}\text{BN}_2\text{O}_2+\text{H}$ ($[\text{M}+\text{H}]^+$); Calcd. = 491.3803, Found = 491.3803.

Conversion: 88%

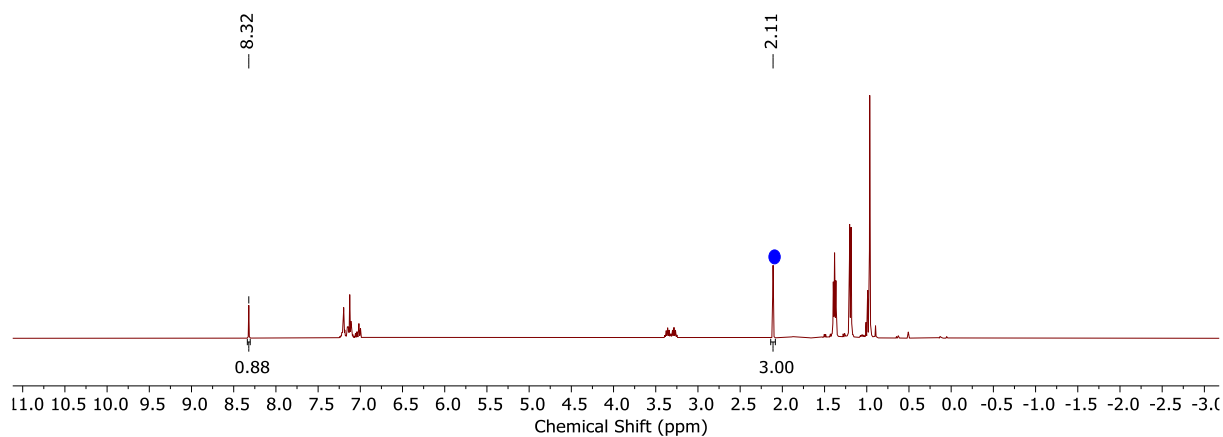


Figure S53. ^1H NMR spectrum (C_6D_6) of crude **14b**. ● = toluene internal standard resonance.

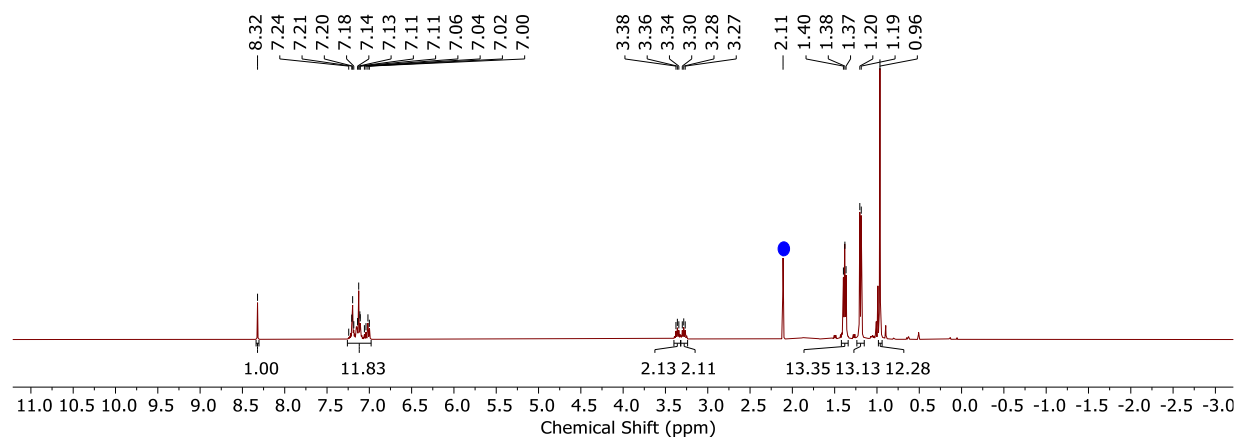


Figure S54. ^1H NMR spectrum (C_6D_6) of crude **14b**. ● = toluene internal standard resonance.

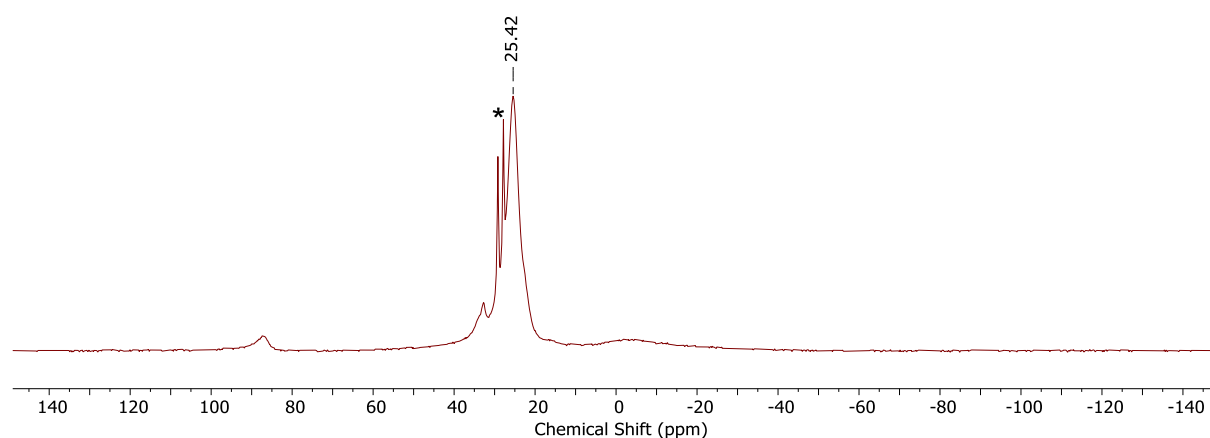
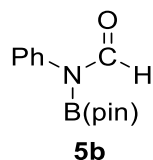


Figure S55. ^{11}B NMR spectrum (C_6D_6) of crude **14b**. * = HB(pin).

6.2. Isocyanates

We validated our analysis of hydroborated isocyanates by comparison to various literature sources and found all data to be in agreement with those previously reported.¹⁴

6.2.1. **5b** - N-phenyl-N-(4,4,5,5-tetramethyl-1,3,2-dioxaborolan-2-yl)formamide



¹H NMR (400 MHz, 298 K, C₆D₆): δ = 9.16 (s, 1H, CH), 6.95 – 7.22 (m, 5H, Ar), 0.92 (s, 12H, Bpin) ppm.

¹¹B NMR (128 MHz, 298 K, C₆D₆): δ = 25.7 (s) ppm.

Mass spectrometry (ESI): C₁₃H₁₈BNO₃+H ([M+H]⁺); Calcd. = 248.15, Found = 248.17.

Conversion: 43%

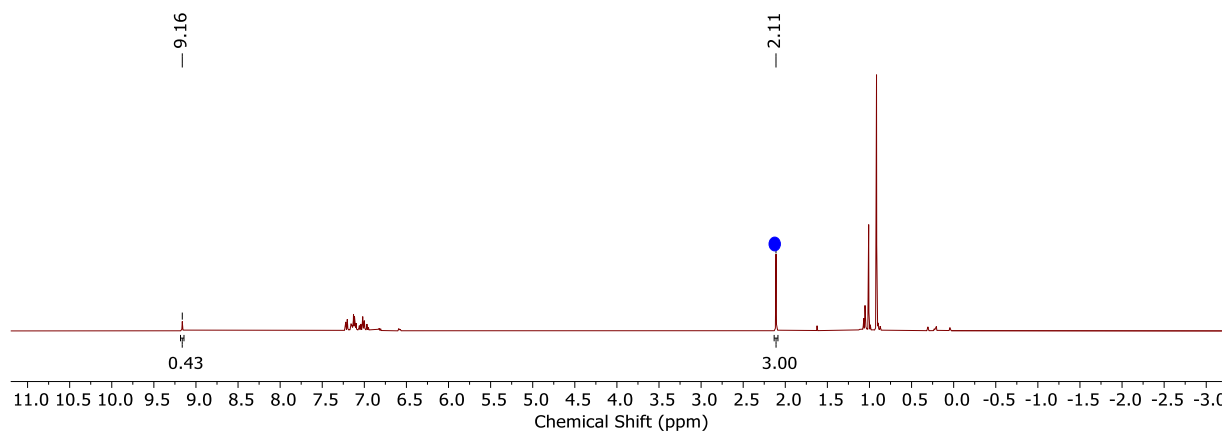


Figure S56. ¹H NMR spectrum (C₆D₆) of crude **5b**. ● = toluene internal standard resonance.

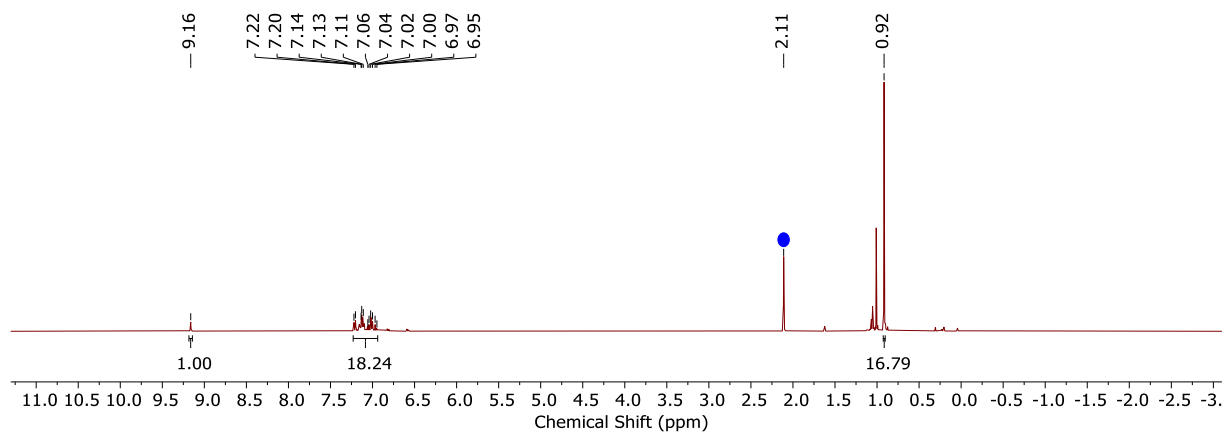


Figure S57. ^1H NMR spectrum (C_6D_6) of crude **5b**. • = toluene internal standard resonance.

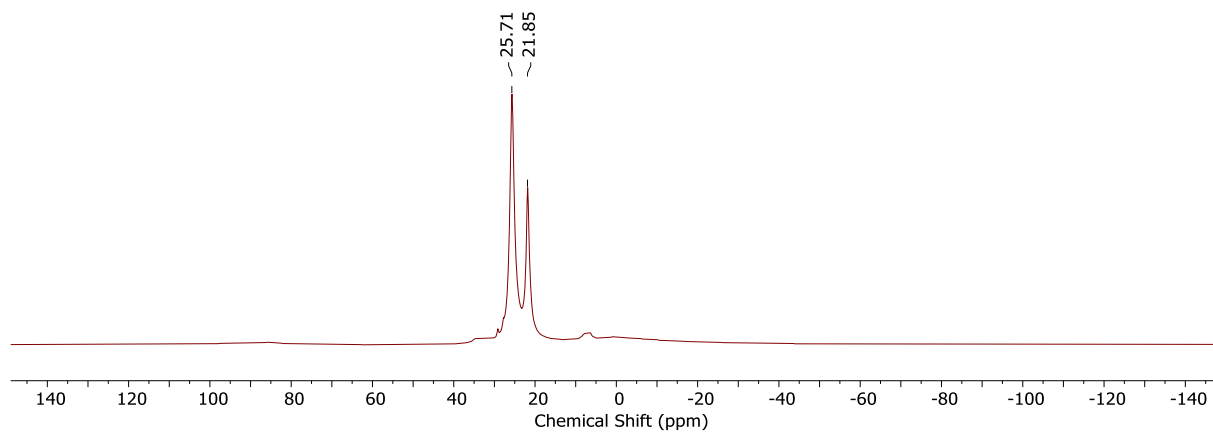
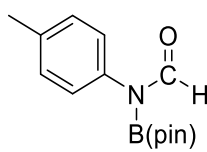


Figure S58. ^{11}B NMR spectrum (C_6D_6) of crude **5b**.

6.2.2. **15b** – N-(4,4,5,5-tetramethyl-1,3,2-dioxaborolan-2-yl)-N-(p-tolyl)formamide



15b

^1H NMR (400 MHz, 298 K, C_6D_6): $\delta = 9.18$ (s, 1H, CH), 6.92 – 7.14 (m, 4H, Ar), 2.02 (s, 3H, CH_3), 0.93 (s, 12H, Bpin) ppm.

^{11}B NMR (128 MHz, 298 K, C_6D_6): $\delta = 25.7$ (s) ppm.

Mass spectrometry (APCI): $\text{C}_{14}\text{H}_{20}\text{BNO}_3 + \text{H}$ ($[\text{M} + \text{H}]^+$); Calcd. = 262.1609, Found = 262.1608.

Conversion: 42%

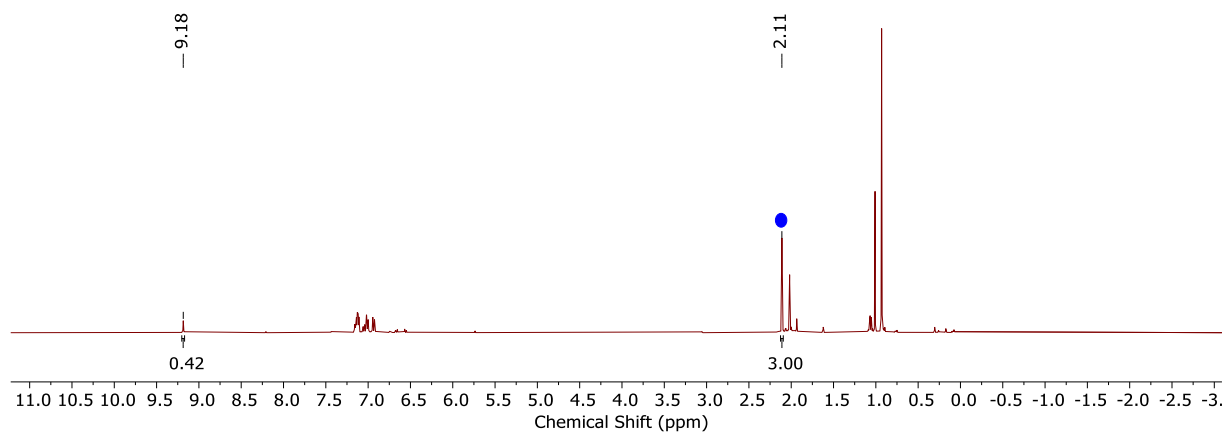


Figure S59. ^1H NMR spectrum (C_6D_6) of crude **15b**. ● = toluene internal standard resonance.

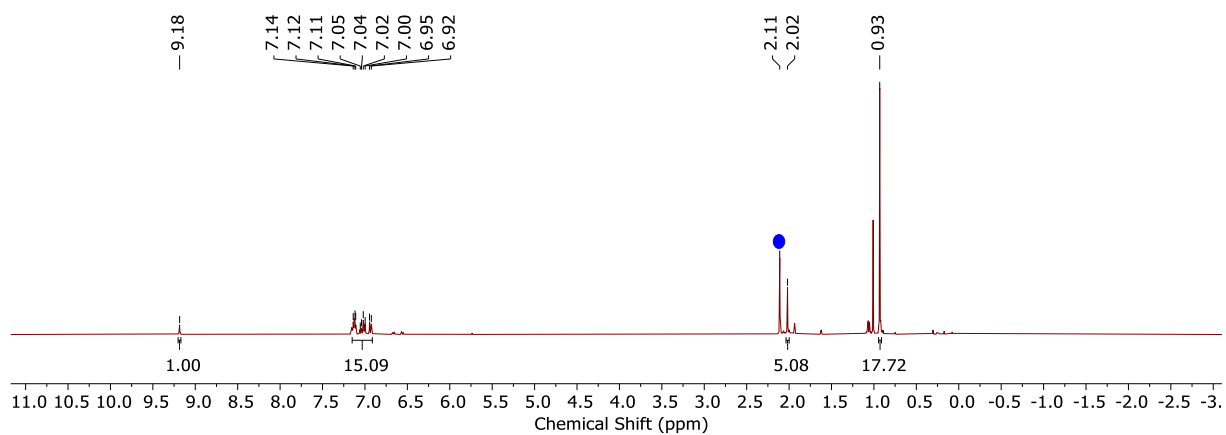


Figure S60. ^1H NMR spectrum (C_6D_6) of crude **15b**. ● = toluene internal standard resonance.

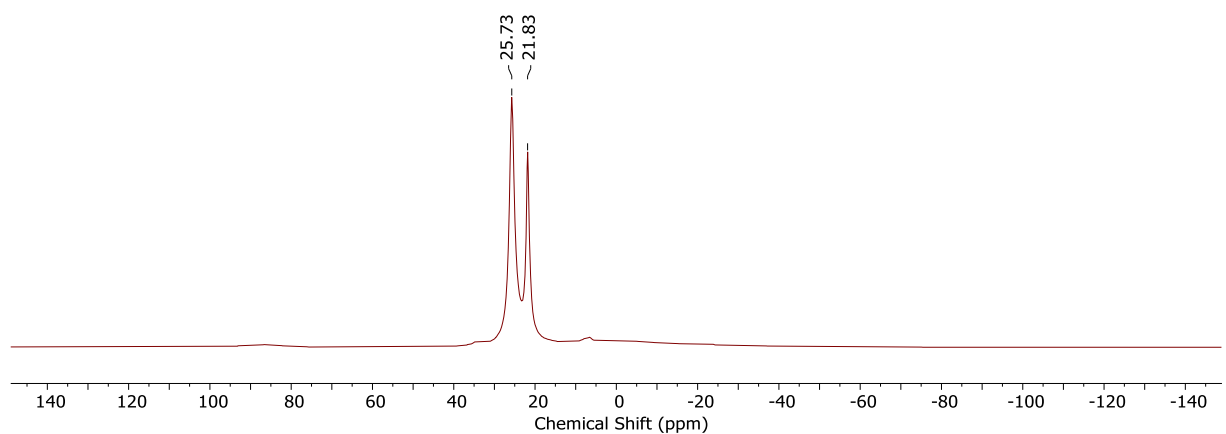
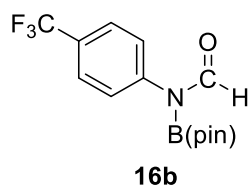


Figure S61. ^{11}B NMR spectrum (C_6D_6) of crude **15b**.

6.2.3. **16b** - N-(4,4,5,5-tetramethyl-1,3,2-dioxaborolan-2-yl)-N-(4-(trifluoromethyl)phenyl)formamide



^1H NMR (400 MHz, 298 K, C_6D_6): $\delta = 9.03$ (s, 1H, CH), 7.00 – 7.30 (m, 4H, Ar), 0.92 (s, 12H, Bpin) ppm.

^{11}B NMR (128 MHz, 298 K, C_6D_6): $\delta = 25.5$ (s) ppm.

$^{19}\text{F}\{^1\text{H}\}$ NMR (376 MHz, 298 K, C_6D_6): $\delta = -69.2$ (s) ppm.

Mass spectrometry (ESI): $\text{C}_{14}\text{H}_{17}\text{BF}_3\text{NO}_3 + \text{NH}_4$ ($[\text{M} + \text{NH}_4]^+$); Calcd. = 333.16, Found = 333.08.

Conversion: 34%

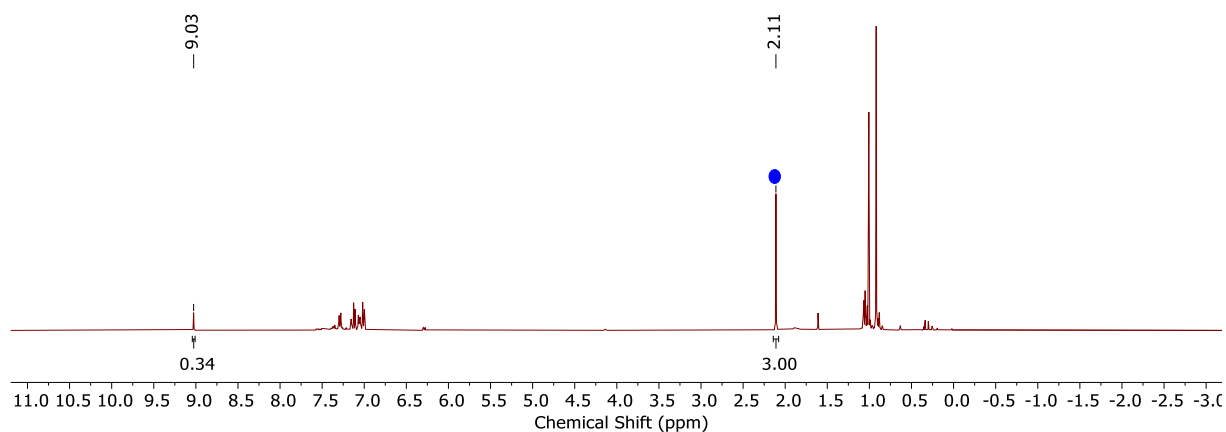


Figure S62. ^1H NMR spectrum (C_6D_6) of crude **16b**. ● = toluene internal standard resonance.

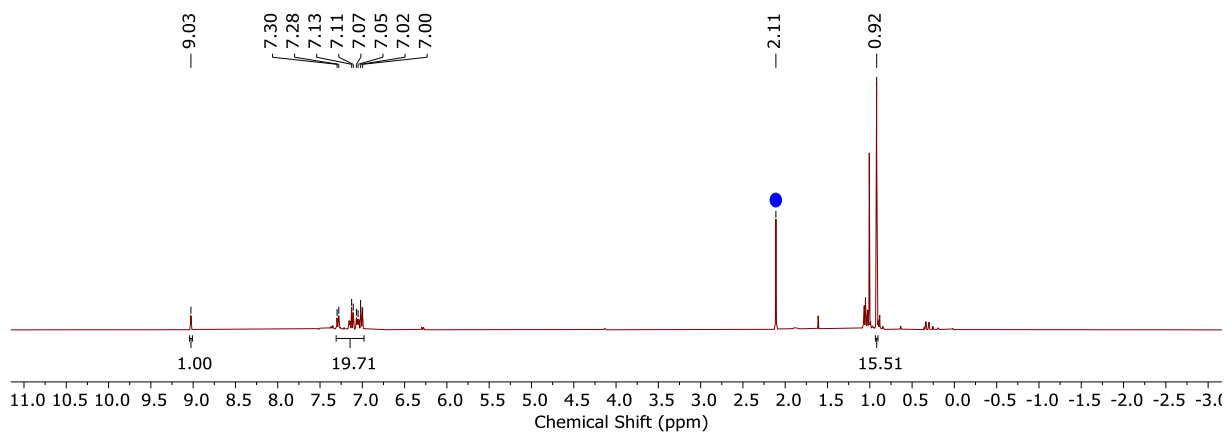


Figure S63. ^1H NMR spectrum (C_6D_6) of crude **16b**. ● = toluene internal standard resonance.

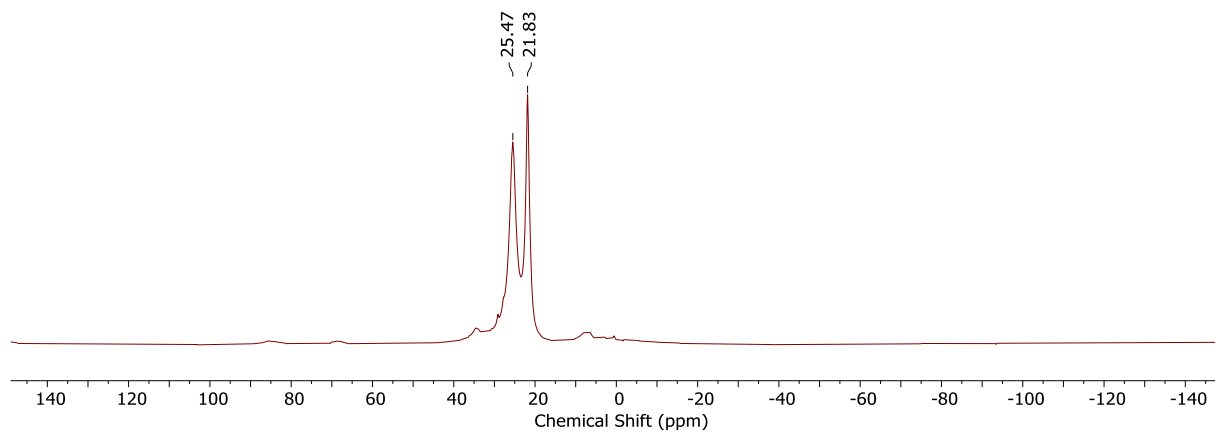


Figure S64. ^{11}B NMR spectrum (C_6D_6) of crude **16b**.

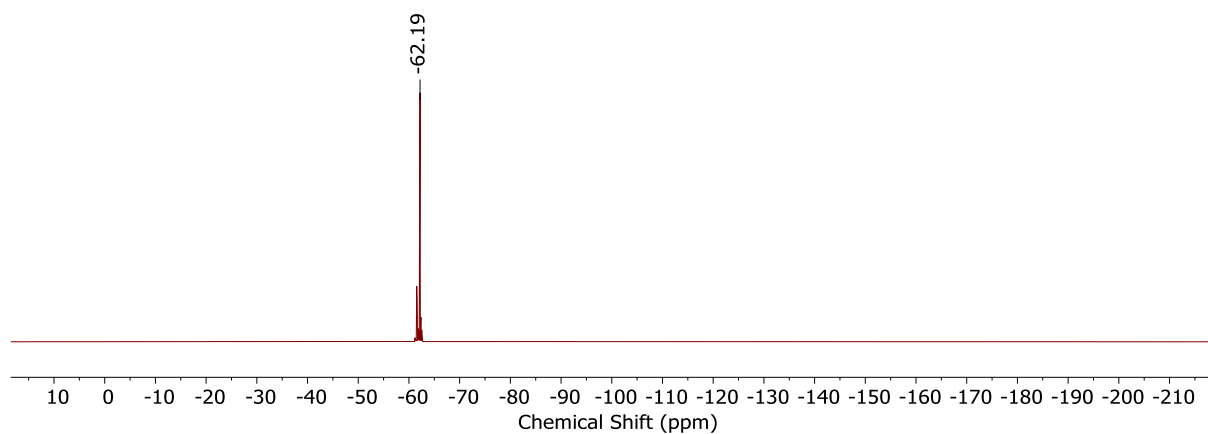
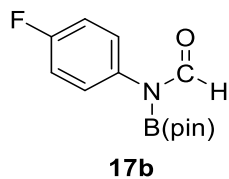


Figure S65. $^{19}\text{F}\{^1\text{H}\}$ NMR spectrum (C_6D_6) of crude **16b**.

6.2.4. **17b** – N-(4-fluorophenyl)-N-(4,4,5,5-tetramethyl-1,3,2-dioxaborolan-2-yl)formamide



^1H NMR (400 MHz, 298 K, C_6D_6): $\delta = 9.08$ (s, 1H, CH), 6.72 – 7.16 (m, 4H, Ar), 0.92 (s, 12H, Bpin) ppm.

^{11}B NMR (128 MHz, 298 K, C_6D_6): $\delta = 25.6$ (s) ppm.

$^{19}\text{F}\{^1\text{H}\}$ NMR (376 MHz, 298 K, C_6D_6): $\delta = -118.2$ (s) ppm.

Mass spectrometry (APCI): $\text{C}_{13}\text{H}_{17}\text{BFNO}_3 + \text{H}$ ($[\text{M} + \text{H}]^+$); Calcd. = 266.1358, Found = 266.1356.

Conversion: 32%

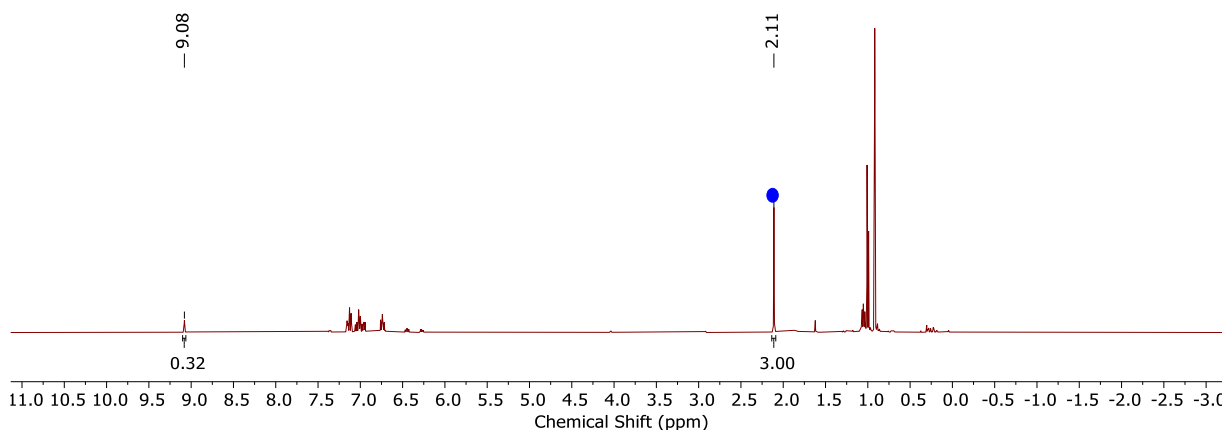


Figure S66. ^1H NMR spectrum (C_6D_6) of crude **17b**. ● = toluene internal standard resonance.

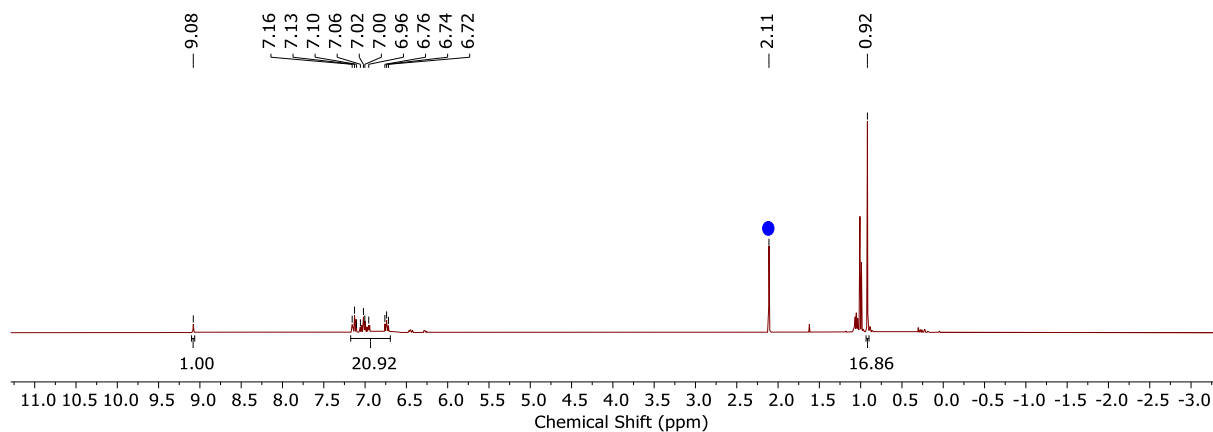


Figure S67. ^1H NMR spectrum (C_6D_6) of crude **17b**. ● = toluene internal standard resonance.

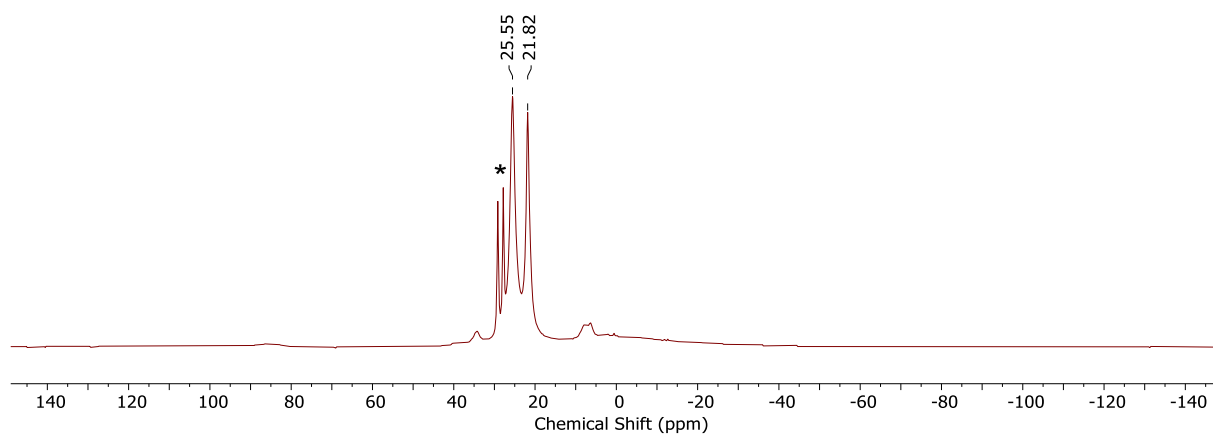


Figure S68. ^{11}B NMR spectrum (C_6D_6) of crude **17b**. * = HB(pin).

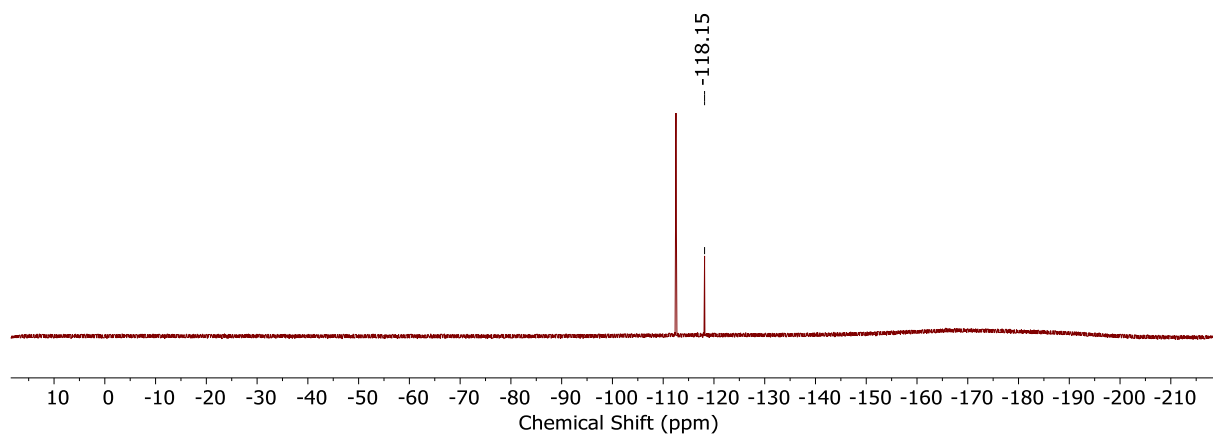
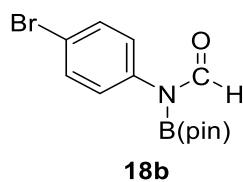


Figure S69. $^{19}\text{F}\{^1\text{H}\}$ NMR spectrum (C_6D_6) of crude **17b**.

6.2.5. **18b** – N-(4-bromophenyl)-N-(4,4,5,5-tetramethyl-1,3,2-dioxaborolan-2-yl)formamide



^1H NMR (400 MHz, 298 K, C_6D_6): $\delta = 9.04$ (s, 1H, CH), 6.84 – 7.25 (m, 4H, Ar), 0.91 (s, 12H, Bpin) ppm.

^{11}B NMR (128 MHz, 298 K, C_6D_6): $\delta = 25.4$ (s) ppm.

Mass spectrometry (ESI): $\text{C}_{13}\text{H}_{17}\text{BBrNO}_3 + \text{H}$ ($[\text{M} + \text{H}]^+$); Calcd. = 327.06, Found = 327.08.

Conversion: 36%

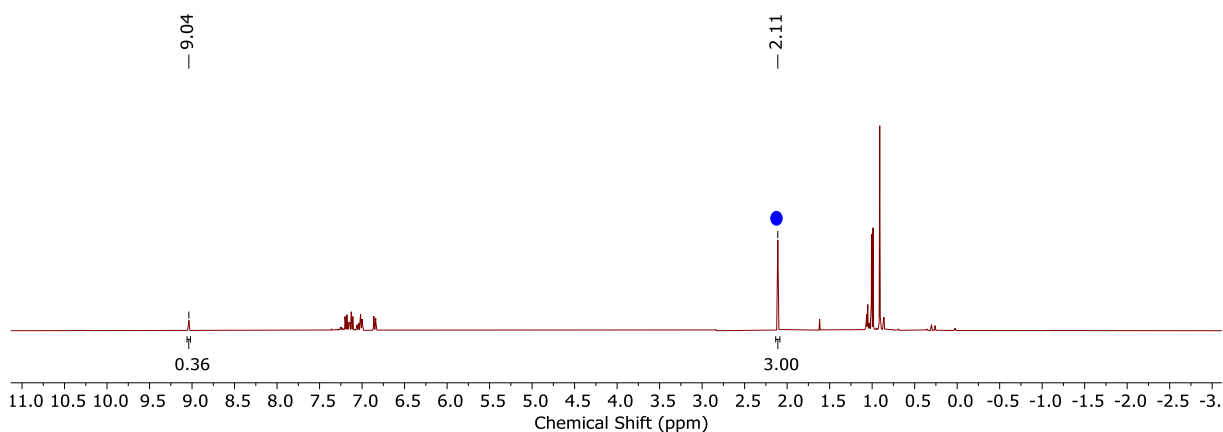


Figure S70. ^1H NMR spectrum (C_6D_6) of crude **18b**. ● = toluene internal standard resonance.

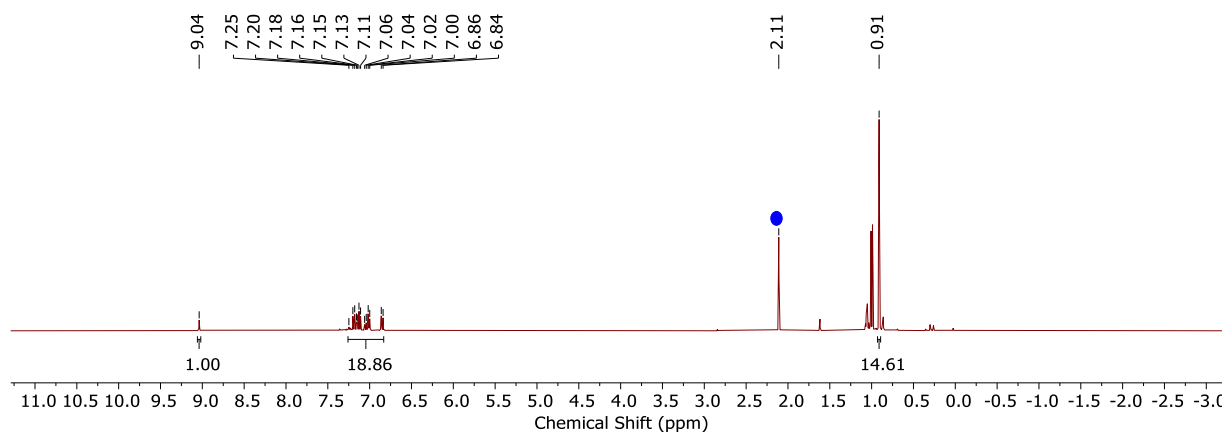


Figure S71. ^1H NMR spectrum (C_6D_6) of crude **18b**. • = toluene internal standard resonance.

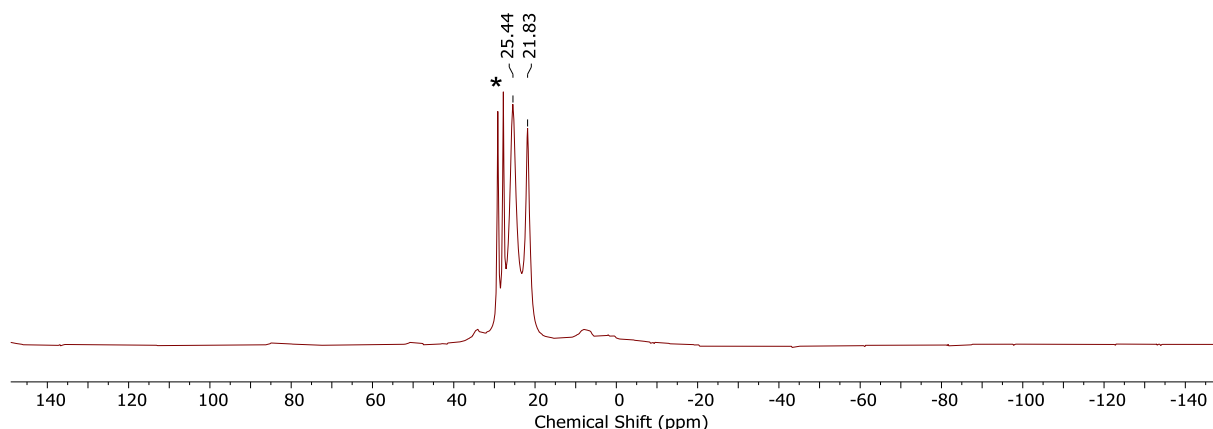
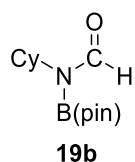


Figure S72. ^{11}B NMR spectrum (C_6D_6) of crude **18b**. * = HB(pin).

6.2.6. **19b** – N-cyclohexyl-N-(4,4,5,5-tetramethyl-1,3,2-dioxaborolan-2-yl)formamide



^1H NMR (400 MHz, 298 K, C_6D_6): $\delta = 9.10$ (s, 1H, CH), 4.34 (m, 1H, Cy), 1.62 – 2.01 (m, 10H, Cy), 0.95 (s, 12H, Bpin) ppm.

^{11}B NMR (128 MHz, 298 K, C_6D_6): $\delta = 25.9$ (s) ppm.

Mass spectrometry (ESI): $\text{C}_{13}\text{H}_{24}\text{BNO}_3 + \text{H}$ ($[\text{M} + \text{H}]^+$); Calcd. = 254.19, Found = 254.17.

Conversion: 60%

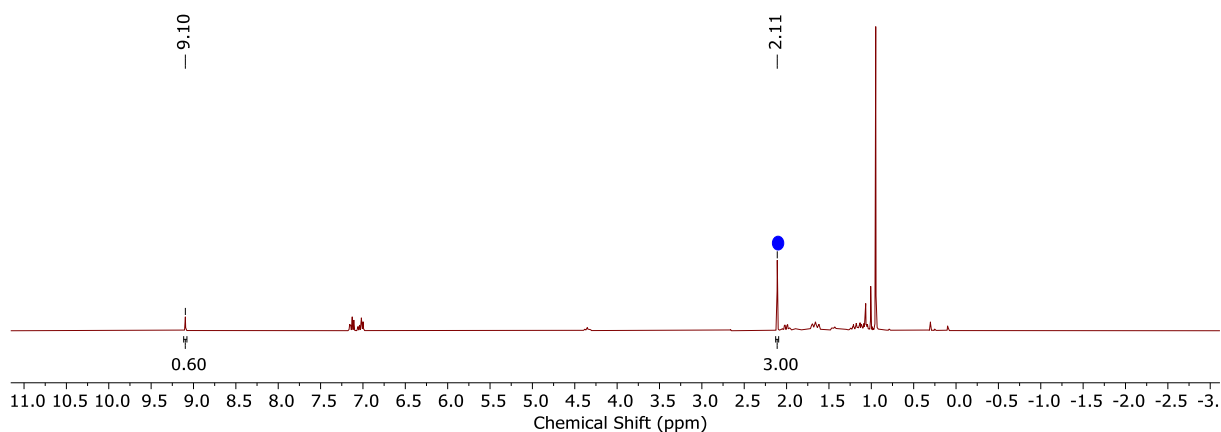


Figure S73. ^1H NMR spectrum (C_6D_6) of crude **19b**. ● = toluene internal standard resonance.

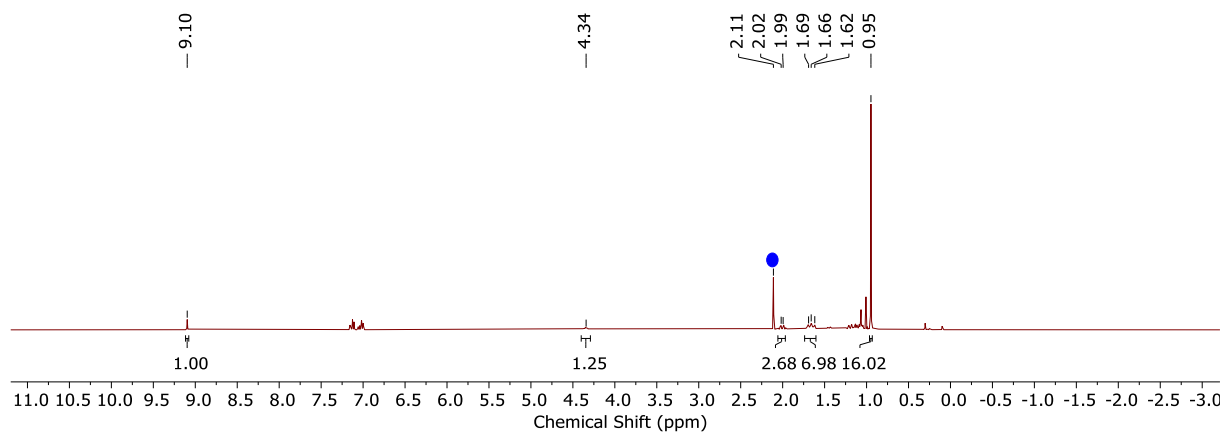


Figure S74. ^1H NMR spectrum (C_6D_6) of crude **19b**. ● = toluene internal standard resonance.

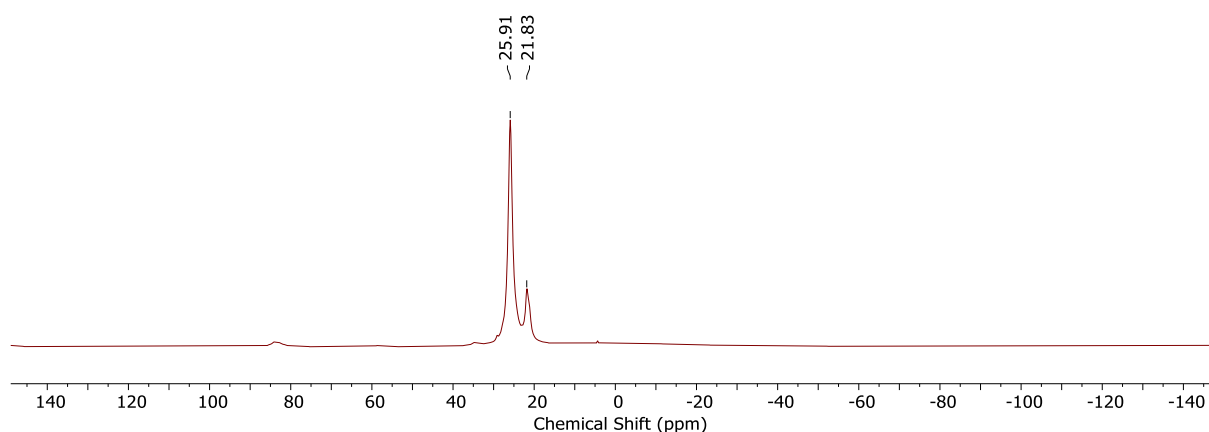
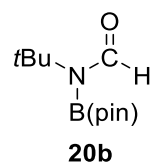


Figure S75. ^{11}B NMR spectrum (C_6D_6) of crude **19b**.

6.2.7. **20b** – N-tert-butyl-N-(4,4,5,5-tetramethyl-1,3,2-dioxaborolan-2-yl)formamide



^1H NMR (400 MHz, 298 K, C_6D_6): δ = 9.14 (s, 1H, CH), 1.55 (s, 9H, CH_3), 0.91 (s, 12H, Bpin) ppm.

^{11}B NMR (128 MHz, 298 K, C_6D_6): δ = 26.1 (s) ppm.

Mass spectrometry (ESI): $C_{11}H_{22}BNO_3+Na$ ($[M+Na]^+$); Calcd. = 250.16, Found = 249.92.

Conversion: 49%

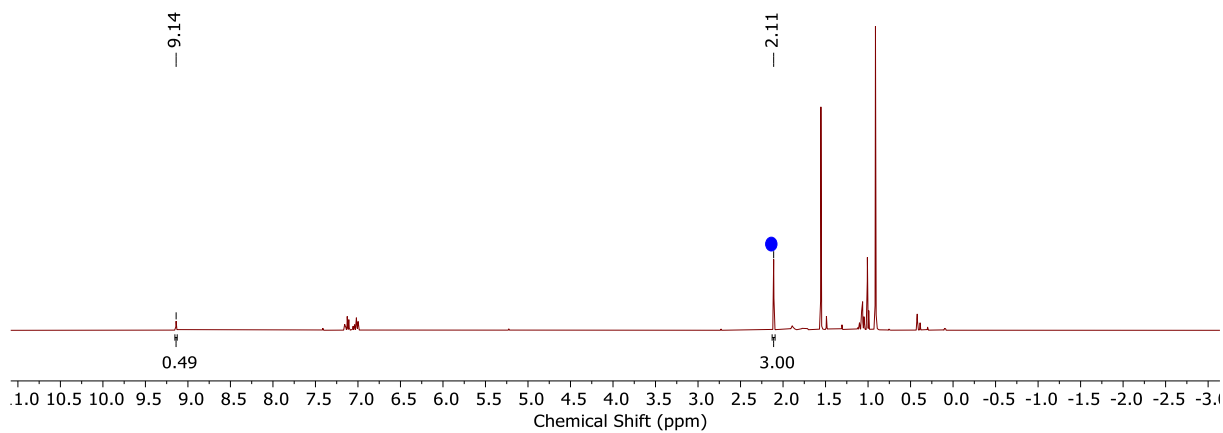


Figure S76. 1H NMR spectrum (C_6D_6) of crude **20b**. ● = toluene internal standard resonance.

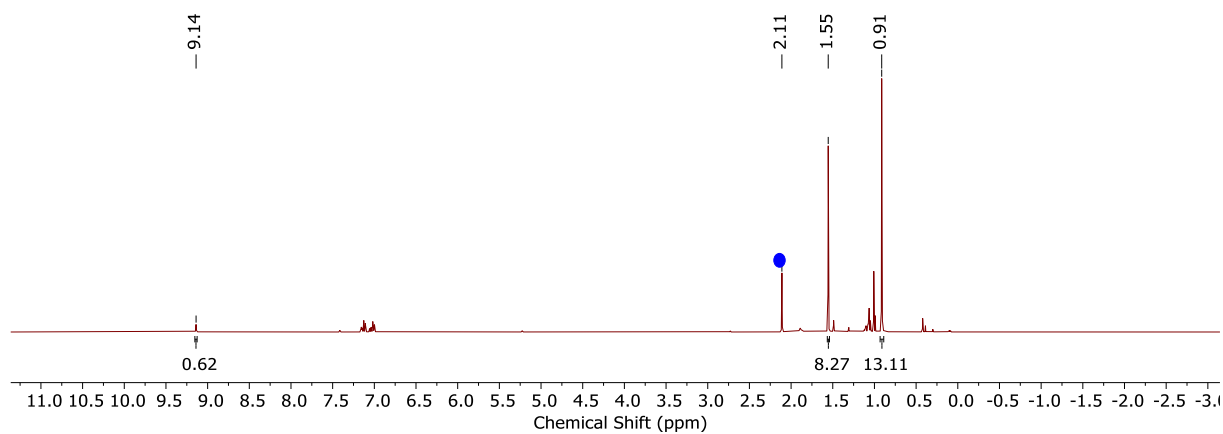


Figure S77. 1H NMR spectrum (C_6D_6) of crude **20b**. ● = toluene internal standard resonance.

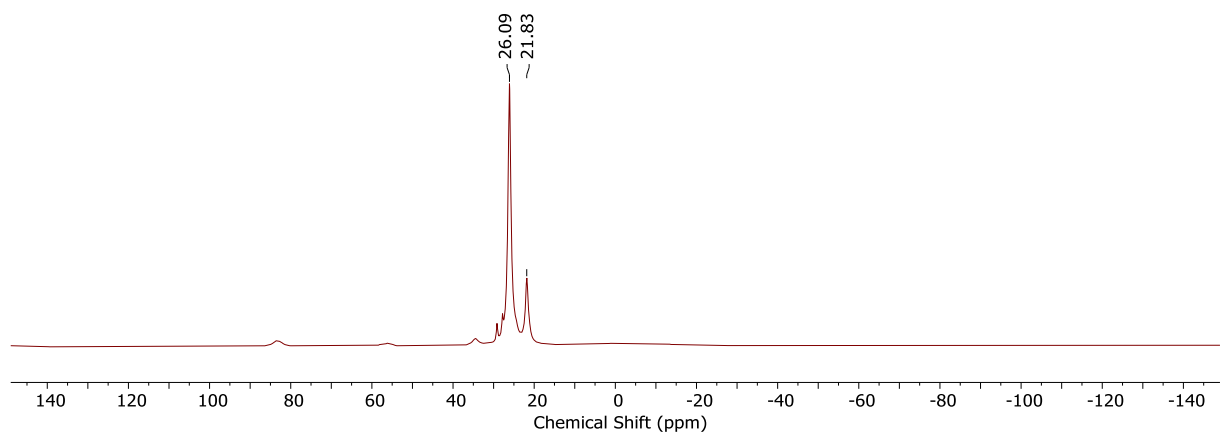
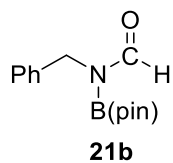


Figure S78. ^{11}B NMR spectrum (C_6D_6) of crude **20b**.

6.2.8. **21b** – N-benzyl-N-(4,4,5,5-tetramethyl-1,3,2-dioxaborolan-2-yl)formamide



^1H NMR (400 MHz, 298 K, C_6D_6): $\delta = 8.98$ (s, 1H, CH), 7.00 – 7.47 (m, 5H, Ar), 4.57 (s, 2H, CH_2), 0.90 (s, 12H, Bpin) ppm.

^{11}B NMR (128 MHz, 298 K, C_6D_6): $\delta = 25.8$ (s) ppm.

Mass spectrometry (ESI): $\text{C}_{14}\text{H}_{20}\text{BNO}_3 + \text{H}$ ($[\text{M} + \text{H}]^+$); Calcd. = 262.16, Found = 262.00.

Conversion: 41%

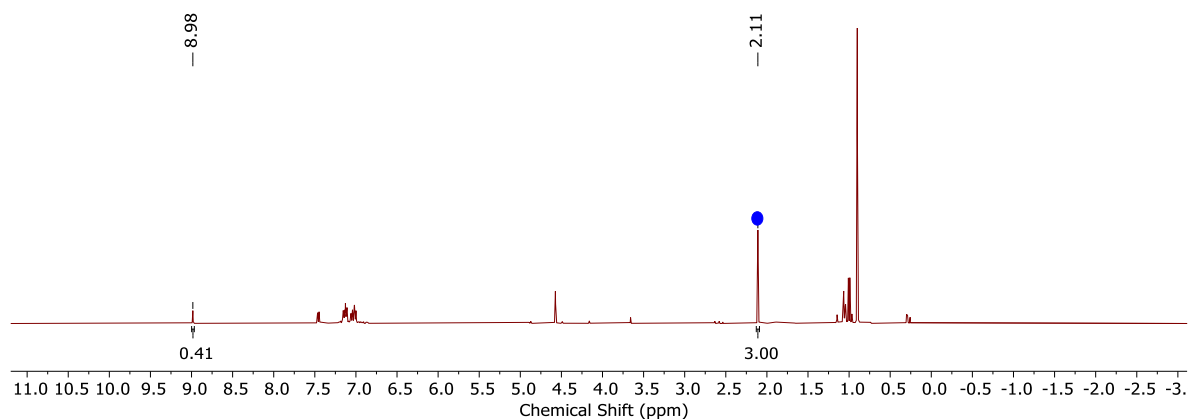


Figure S79. ^1H NMR spectrum (C_6D_6) of crude **21b**. ● = toluene internal standard resonance.

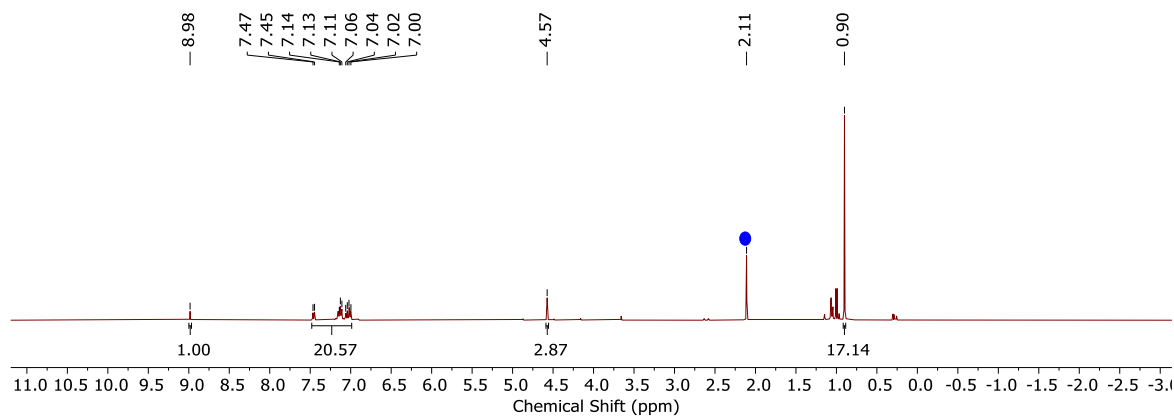


Figure S80. ^1H NMR spectrum (C_6D_6) of crude **21b**. • = toluene internal standard resonance.

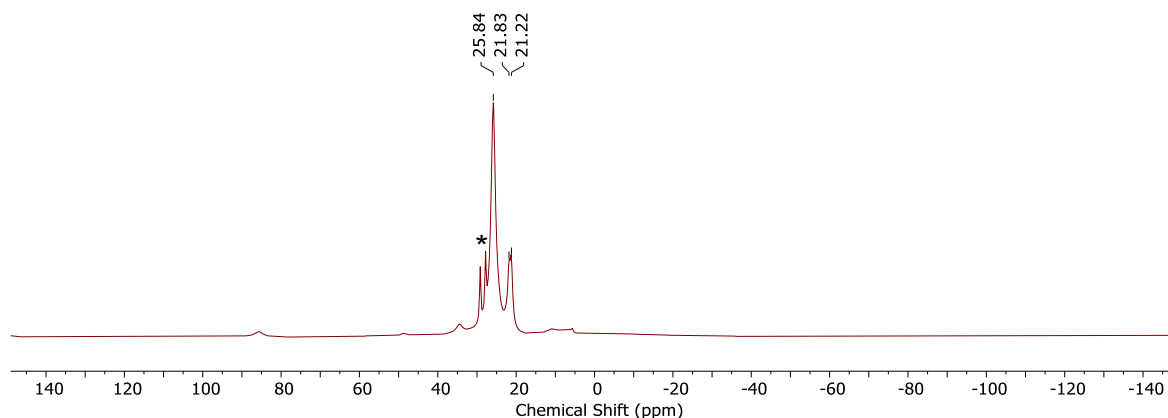
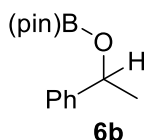


Figure S81. ^{11}B NMR spectrum (C_6D_6) of crude **21b**. * = HB(pin).

6.3. Ketones

We validated our analysis of hydroborated ketones by comparison to various literature sources and found all data to be in agreement with those previously reported.^{13, 15}

6.3.1. **6b** – 4,4,5,5-tetramethyl-2-(1-phenylethoxy)-1,3,2-dioxaborolane



^1H NMR (400 MHz, 298 K, C_6D_6): δ = 7.38 (d, $^3J_{\text{HH}}$ = 7.7 Hz, 2H, Ar), 7.14 (t, $^3J_{\text{HH}}$ = 7.7 Hz, 2H, Ar), 7.05 (t, $^3J_{\text{HH}}$ = 7.7 Hz, 1H, Ar), 5.42 (q, $^3J_{\text{HH}}$ = 6.5 Hz, 1H, CH), 1.47 (d, $^3J_{\text{HH}}$ = 6.5 Hz, 3H, CH_3), 1.03 (s, 6H, Bpin), 1.00 (s, 6H, Bpin) ppm.

^{11}B NMR (128 MHz, 298 K, C_6D_6): δ = 22.6 (s) ppm.

Mass spectrometry (ESI): $\text{C}_{14}\text{H}_{21}\text{BO}_3 + \text{H}$ ($[\text{M} + \text{H}]^+$); Calcd. = 249.17, Found = 249.67.

Conversion: 90%

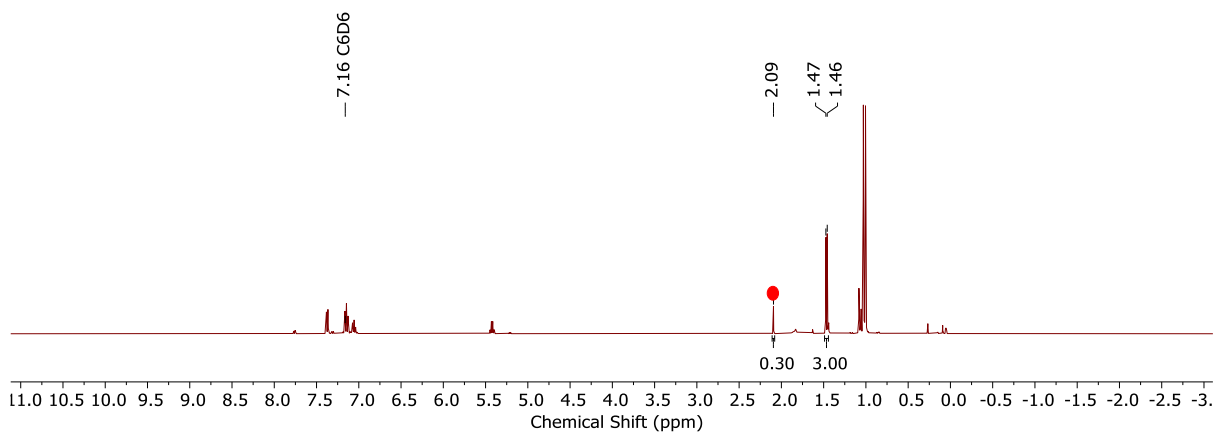


Figure S82. ^1H NMR spectrum (C_6D_6) of crude **6b**. ● = unreacted start material used to determine conversion.

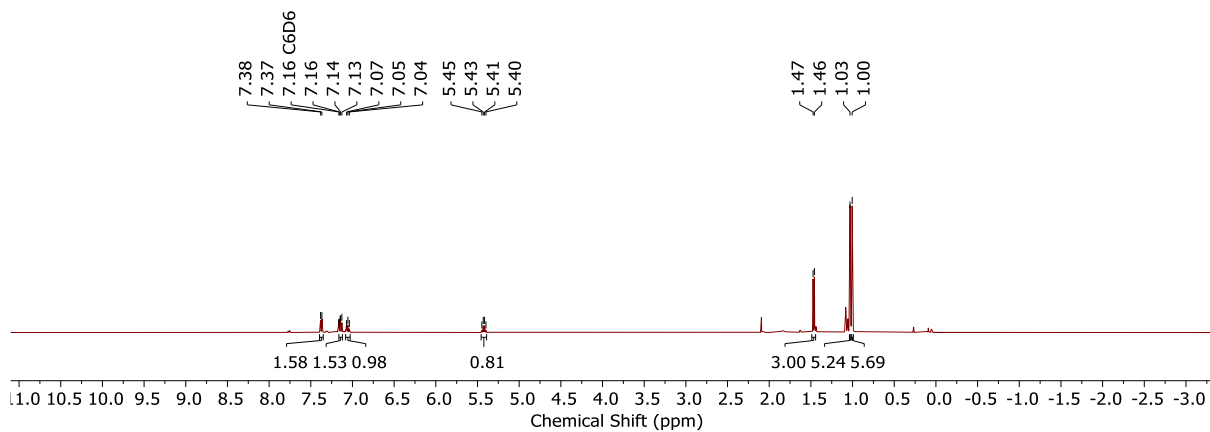


Figure S83. ^1H NMR spectrum (C_6D_6) of crude **6b**.

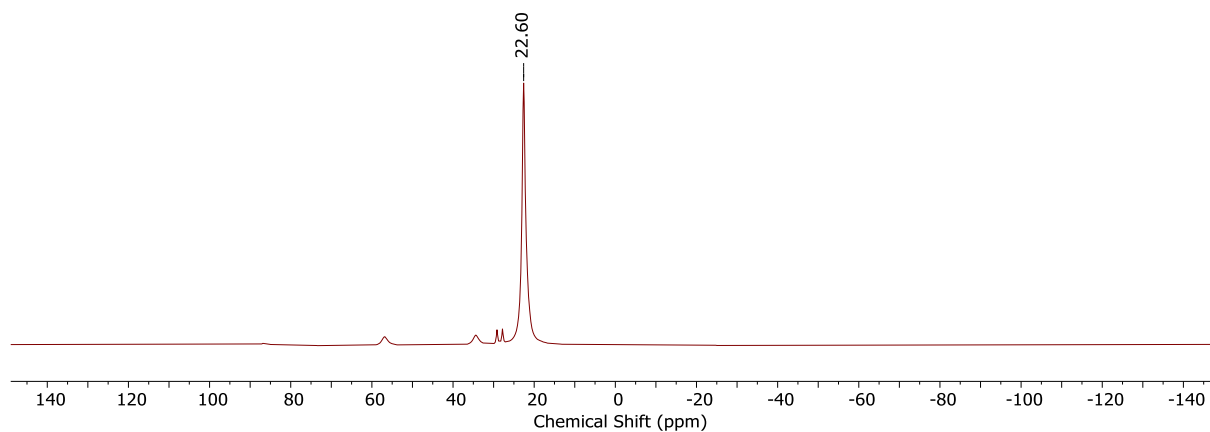
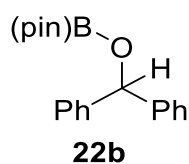


Figure S84. ^{11}B NMR spectrum (C_6D_6) of crude **6b**.

6.3.2. **22b** – 2-(benzhydryloxy)-4,4,5,5-tetramethyl-1,3,2-dioxaborolane



^1H NMR (400 MHz, 298 K, C_6D_6): $\delta = 7.00 - 7.71$ (m, 10H, Ar), 6.44 (s, 1H, CH), 0.99 (s, 12H, Bpin) ppm.

^{11}B NMR (128 MHz, 298 K, C_6D_6): $\delta = 22.9$ (s) ppm.

Mass spectrometry (APCI): $\text{C}_{19}\text{H}_{23}\text{O}_3\text{B}+\text{Na}$ ($[\text{M}+\text{Na}]^+$); Calcd = 333.1632, Found = 333.1640.

Conversion: 42%

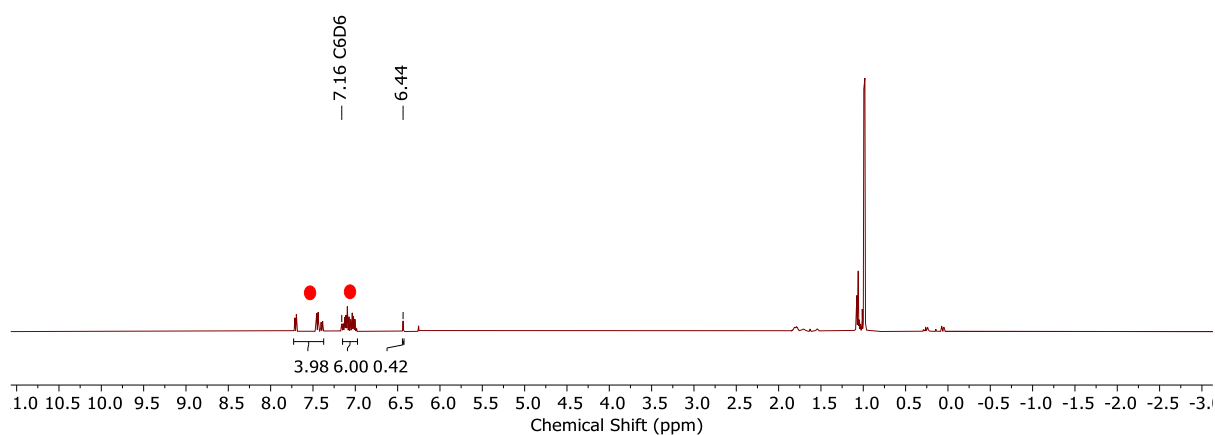


Figure S85. ^1H NMR spectrum (C_6D_6) of crude **22b**. ● = unreacted start material used to determine conversion.

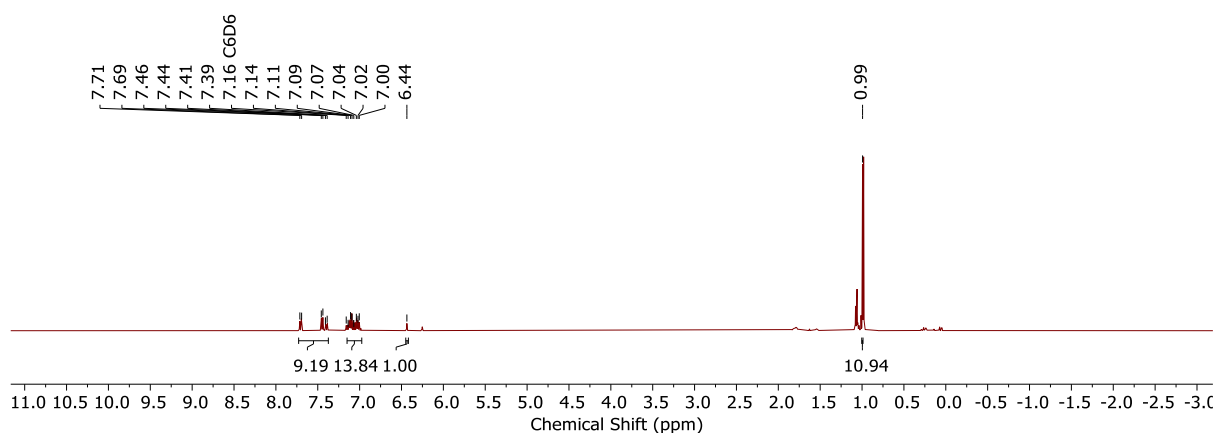


Figure S86. ^1H NMR spectrum (C_6D_6) of crude **22b**.

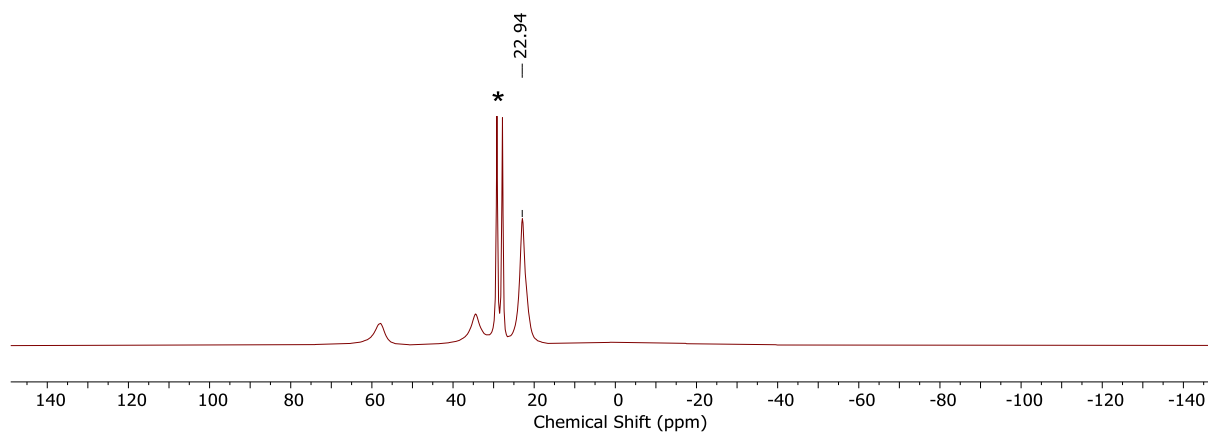
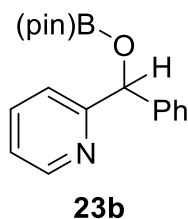


Figure S87. ^{11}B NMR spectrum (C_6D_6) of crude **22b**. * = HB(pin).

6.3.3. **23b** – 2-(phenyl((4,4,5,5-tetramethyl-1,3,2-dioxaborolan-2-yl)oxy)methyl)pyridine



^1H NMR (400 MHz, 298 K, C_6D_6): δ = 6.39 – 8.31 (m, 9H, Ar), 6.32 (s, 1H, CH), 1.27 (s, 12H, Bpin) ppm.

^{11}B NMR (128 MHz, 298 K, C_6D_6): δ = 17.7 (s) ppm.

Mass spectrometry (ESI): $\text{C}_{18}\text{H}_{22}\text{BNO}_3 + \text{H}$ ($[\text{M} + \text{H}]^+$); Calcd. = 312.18, Found = 312.08.

Conversion: 86%

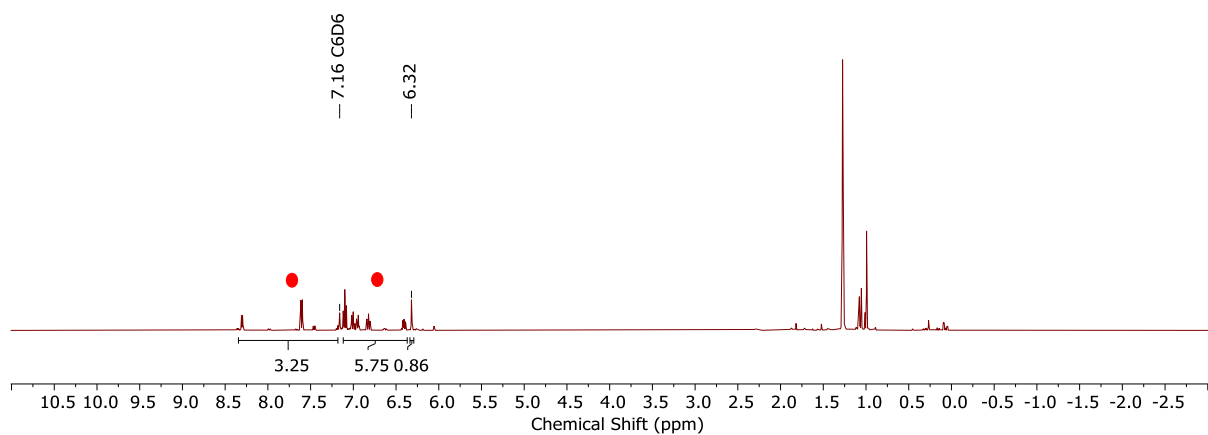


Figure S88. ^1H NMR spectrum (C_6D_6) of crude **23b**. ● = unreacted start material used to determine conversion.

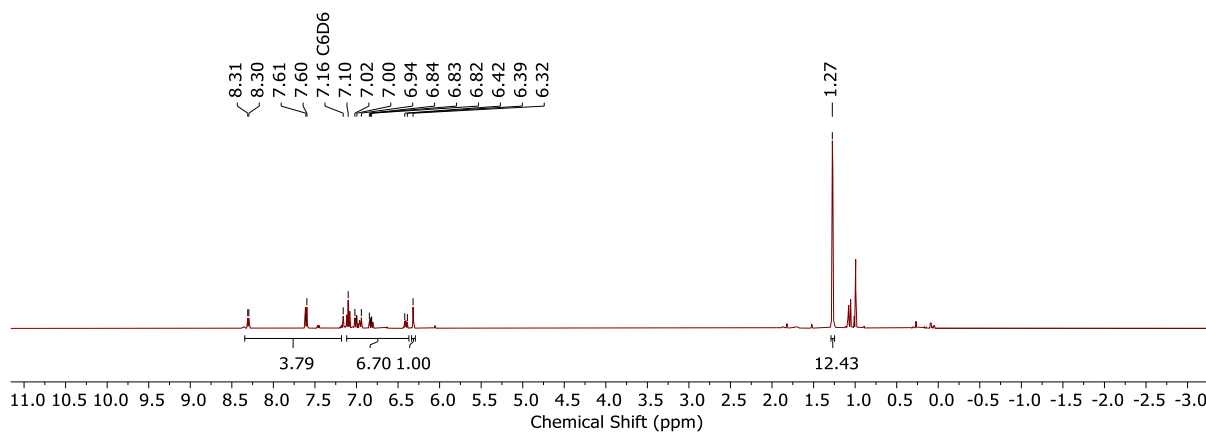


Figure S89. ^1H NMR spectrum (C_6D_6) of crude **23b**.

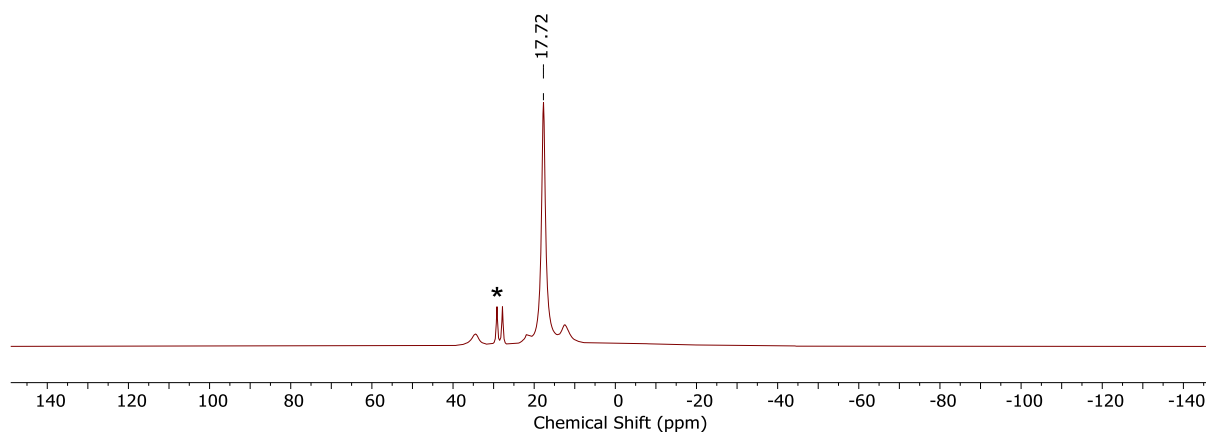
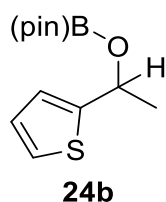


Figure S90. ^{11}B NMR spectrum (C_6D_6) of crude **23b**. * = HB(pin).

6.3.4. **24b** – 4,4,5,5-tetramethyl-2-(1-(thiophen-2-yl)ethoxy)-1,3,2-dioxaborolane



^1H NMR (400 MHz, 298 K, C_6D_6): δ = 6.82 – 6.88 (m, 2H, Ar), 6.68 – 6.70 (m, 1H, Ar), 5.63 & 5.41 (q, $^3J_{\text{HH}}$ = 6.4 Hz, 1H, CH), 1.52 & 1.50 (d, $^3J_{\text{HH}}$ = 6.4 Hz, 3H, CH_3), 1.03 & 1.01 (12H, s, Bpin) ppm.

^{11}B NMR (128 MHz, 298 K, C_6D_6): δ = 22.6 (s) ppm.

Mass spectrometry (ESI): $C_{12}H_{19}BO_3S+H$ ($[M+H]^+$); Calcd. = 255.12, Found = 255.00.

Conversion: 82%

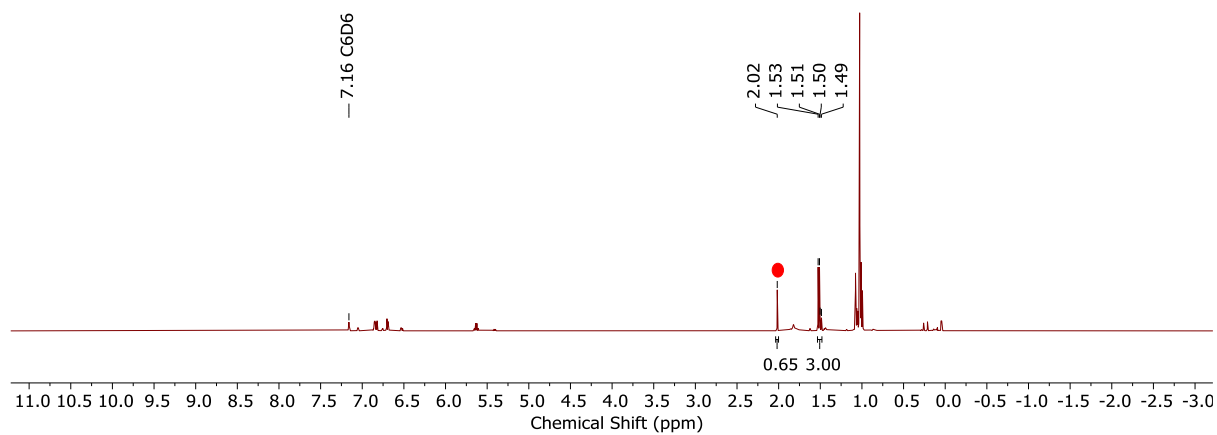


Figure S91. 1H NMR spectrum (C_6D_6) of crude **24b**. ● = unreacted start material used to determine conversion.

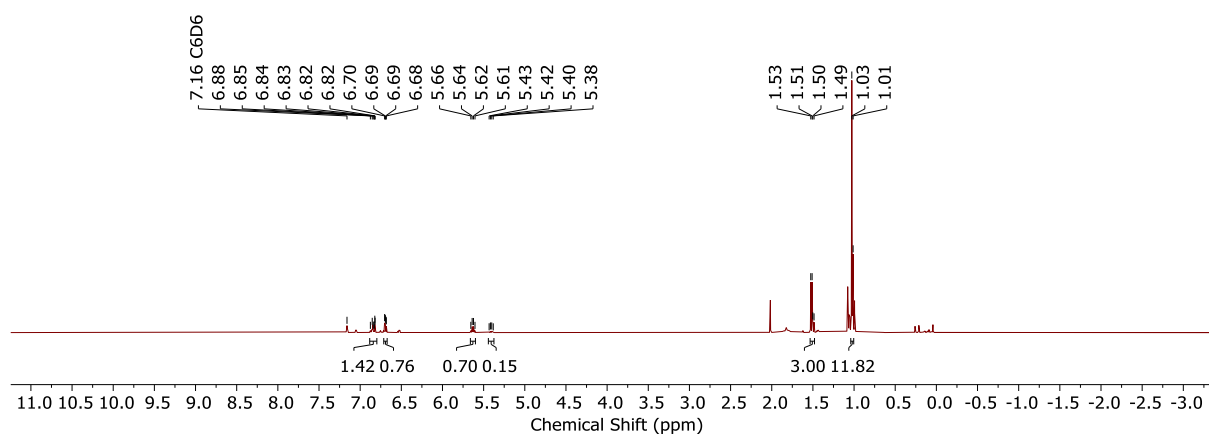


Figure S92. 1H NMR spectrum (C_6D_6) of crude **24b**.

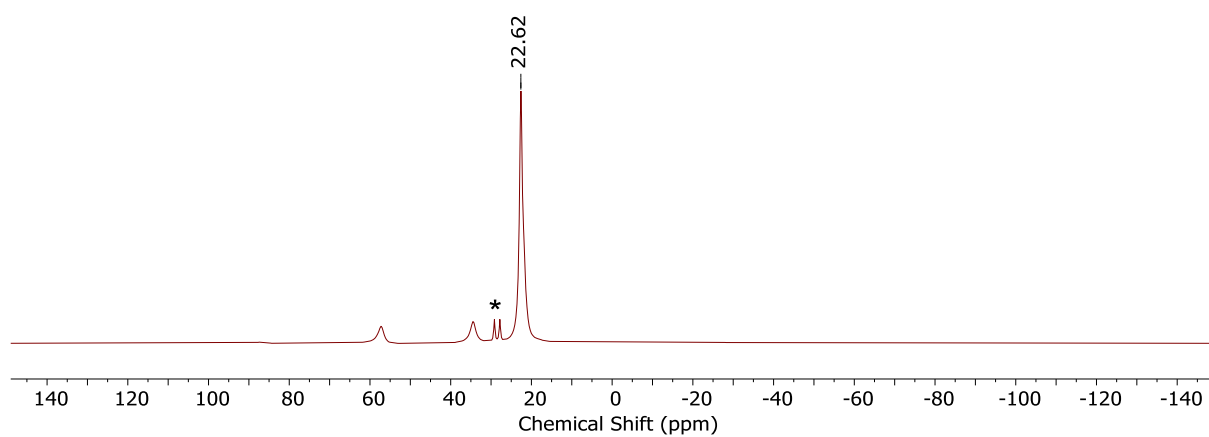
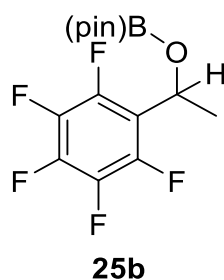


Figure S93. ^{11}B NMR spectrum (C_6D_6) of crude **24b**. * = HB(pin).

6.3.5. **25b** – 4,4,5,5-tetramethyl-2-(1-(perfluorophenyl)ethoxy)-1,3,2-dioxaborolane



^1H NMR (400 MHz, 298 K, C_6D_6): δ = 5.65 & 5.52 (q, $^3J_{\text{HH}}$ = 6.7 Hz, 1H, CH), 1.44 & 1.42 (d, $^3J_{\text{HH}}$ = 6.7 Hz, 3H, CH_3), 1.00 & 1.09 (s, 12H, Bpin) ppm.

^{11}B NMR (128 MHz, 298 K, C_6D_6): δ = 22.5 (s) ppm.

$^{19}\text{F}\{^1\text{H}\}$ NMR (376 MHz, 298 K, C_6D_6): δ = -162.9 (m, 2F, *ortho-F*), -156.3 (t, $^3J_{\text{FF}}$ = 21.6 Hz, 1F, *para-F*), -143.4 (m, 2F, *meta-F*) ppm.

Mass spectrometry (ESI): $\text{C}_{14}\text{H}_{16}\text{BF}_5\text{O}_3+\text{Na}$ ($[\text{M}+\text{Na}]^+$); Calcd. = 361.10, Found = 361.00.

Conversion: 69%

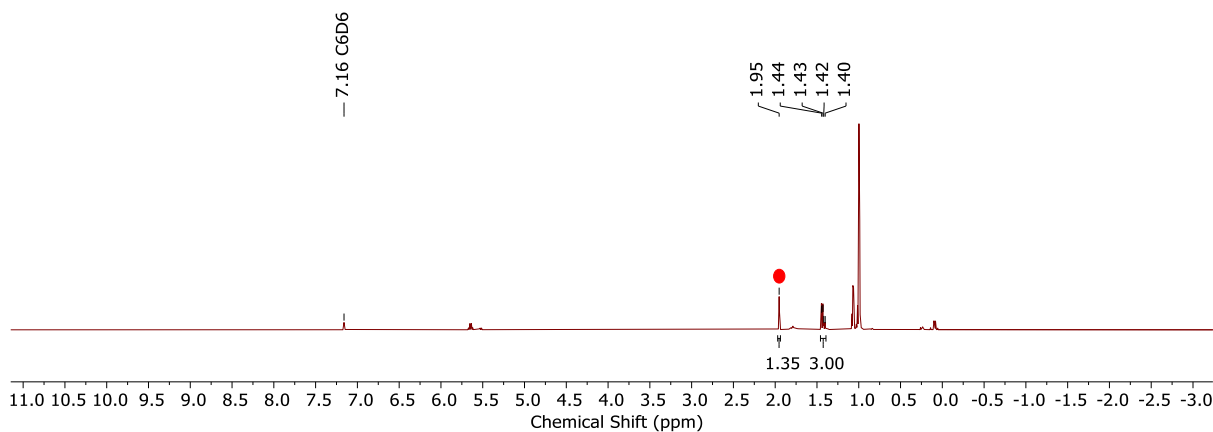


Figure S94. ^1H NMR spectrum (C_6D_6) of crude **25b**. ● = unreacted start material used to determine conversion.

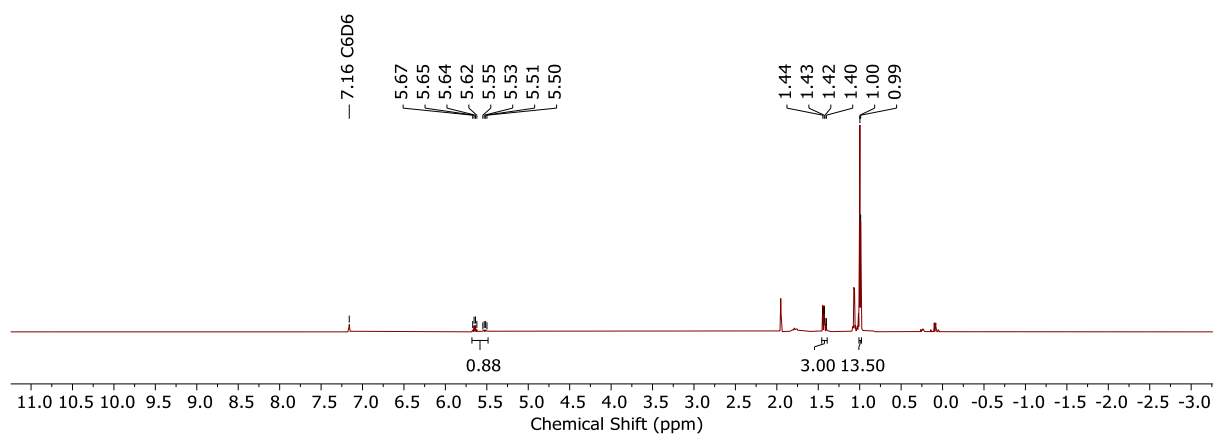


Figure S95. ^1H NMR spectrum (C_6D_6) of crude **25b**.

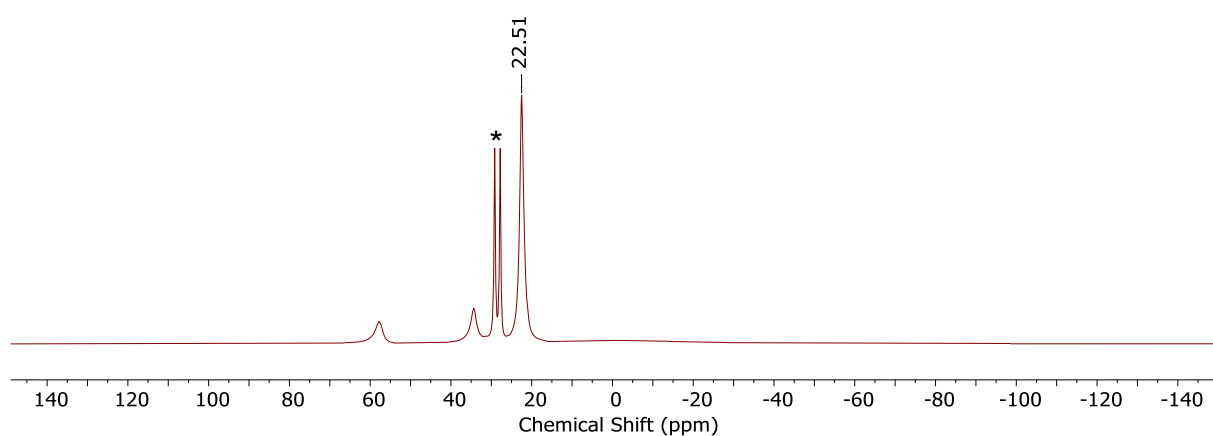


Figure S96. ^{11}B NMR spectrum (C_6D_6) of crude **25b**. * = HB(pin).

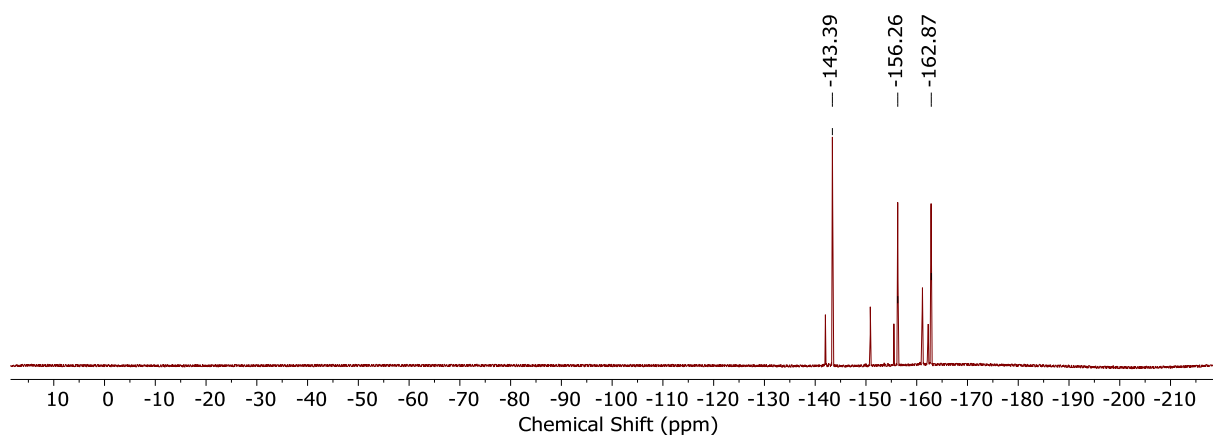
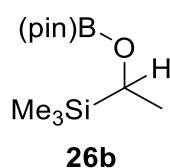


Figure S97. $^{19}\text{F}\{^1\text{H}\}$ NMR spectrum (C_6D_6) of crude **25b**.

6.3.6. **26b** - trimethyl(1-((4,4,5,5-tetramethyl-1,3,2-dioxaborolan-2-yl)oxy)ethyl)silane



^1H NMR (400 MHz, 298 K, C_6D_6): $\delta = 4.15$ (q, $^3J_{\text{HH}} = 7.4$ Hz, 1H, CH), 1.31 (d, $^3J_{\text{HH}} = 7.4$ Hz, 3H, CH_3), 1.08 (s, 12H, Bpin), 0.03 (s, 9H, Si- CH_3) ppm.

^{11}B NMR (128 MHz, 298 K, C_6D_6): $\delta = 22.7$ (s) ppm.

$^{29}\text{Si}\{^1\text{H}\}$ NMR (79 MHz, 298 K, C_6D_6): $\delta = 1.82$ (s) ppm.

Mass spectrometry (APCI): $\text{C}_{11}\text{H}_{25}\text{BO}_3\text{Si}+\text{H}$ ($[\text{M}+\text{H}]^+$); Calcd. = 245.1739, Found = 245.1747.

Conversion: >99%

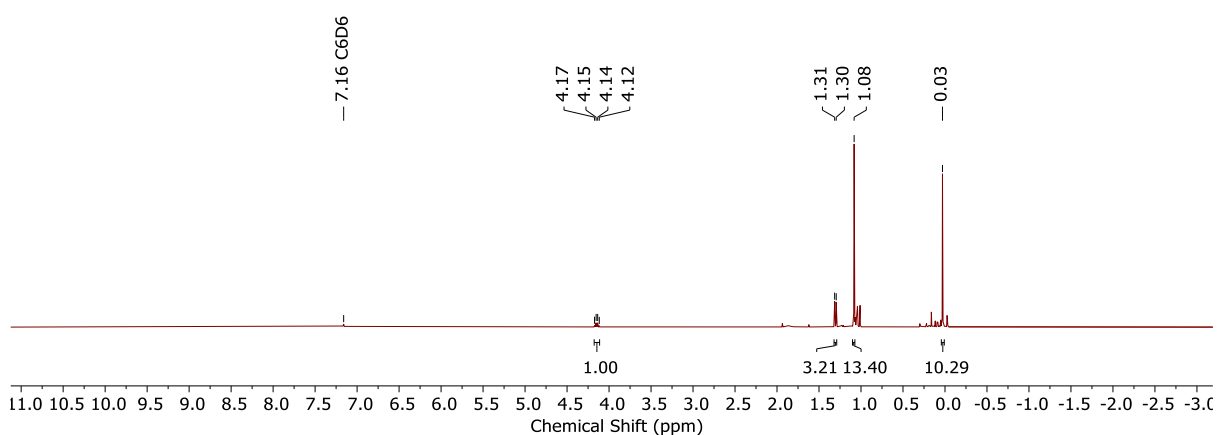


Figure S98. ^1H NMR spectrum (C_6D_6) of crude **26b**.

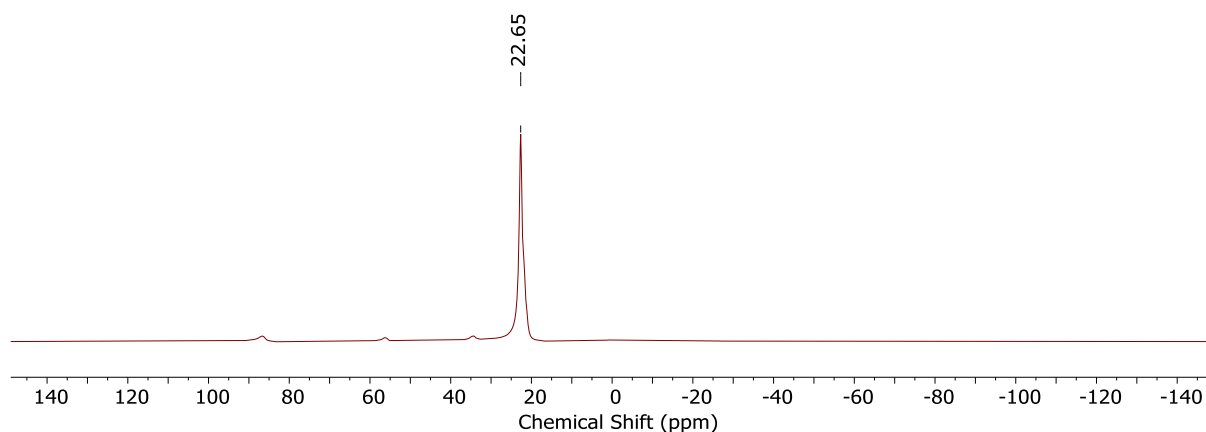


Figure S99. ^{11}B NMR spectrum (C_6D_6) of crude **26b**.

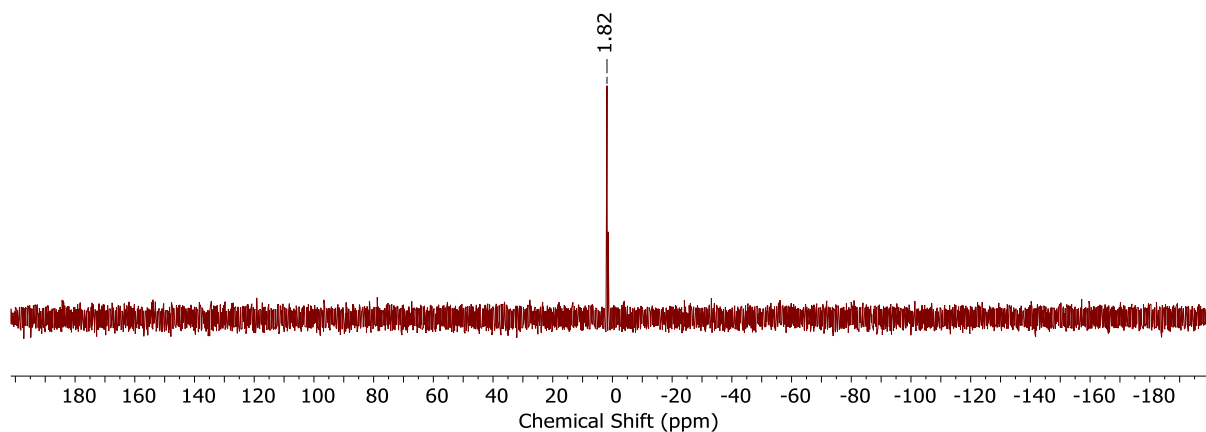
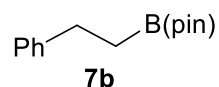


Figure S100. $^{29}\text{Si}\{^1\text{H}\}$ NMR spectrum (C_6D_6) of crude **26b**.

6.4. Alkenes

We validated our analysis of hydroborated alkenes by comparison to various literature sources and found all data to be in agreement with those previously reported.¹⁶

6.4.1. **7b** – 4,4,5,5-tetramethyl-2-phenethyl-1,3,2-dioxaborolane



^1H NMR (400 MHz, 298 K, C_6D_6): $\delta = 7.00 - 7.24$ (m, 5H, Ar), 2.86 (t, $^3J_{\text{HH}} = 8.0$ Hz, 2H, CH_2), 1.27 (t, $^3J_{\text{HH}} = 8.0$ Hz, 2H, CH_2), 1.01 (s, 12H, Bpin) ppm.

^{11}B NMR (128 MHz, 298 K, C_6D_6): $\delta = 34.1$ (s) ppm.

Mass spectrometry (ESI): $\text{C}_{14}\text{H}_{21}\text{BO}_2 + \text{H}$ ($[\text{M} + \text{H}]^+$); Calcd. = 233.17, Found = 233.08.

Conversion: 80%

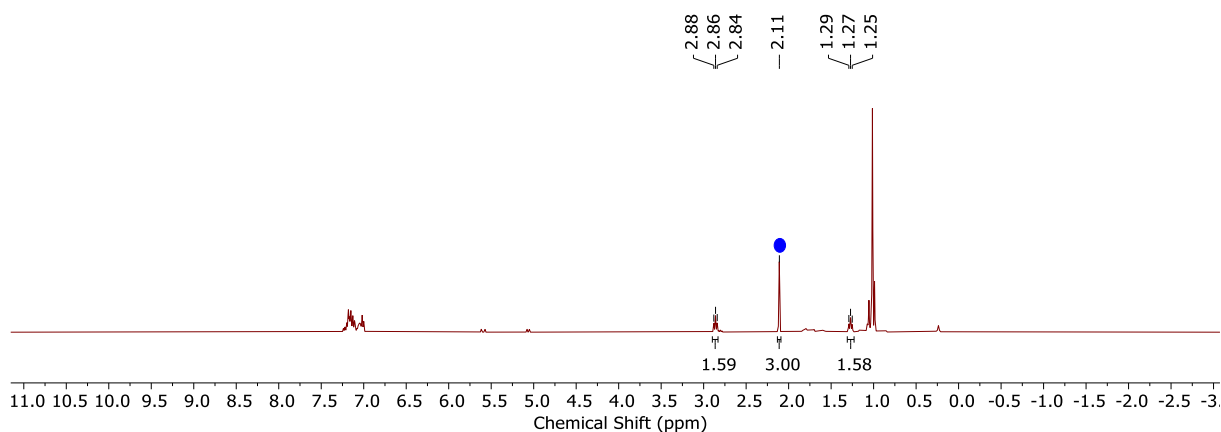


Figure S101. ^1H NMR spectrum (C_6D_6) of crude **7b**. ● = toluene internal standard resonance.

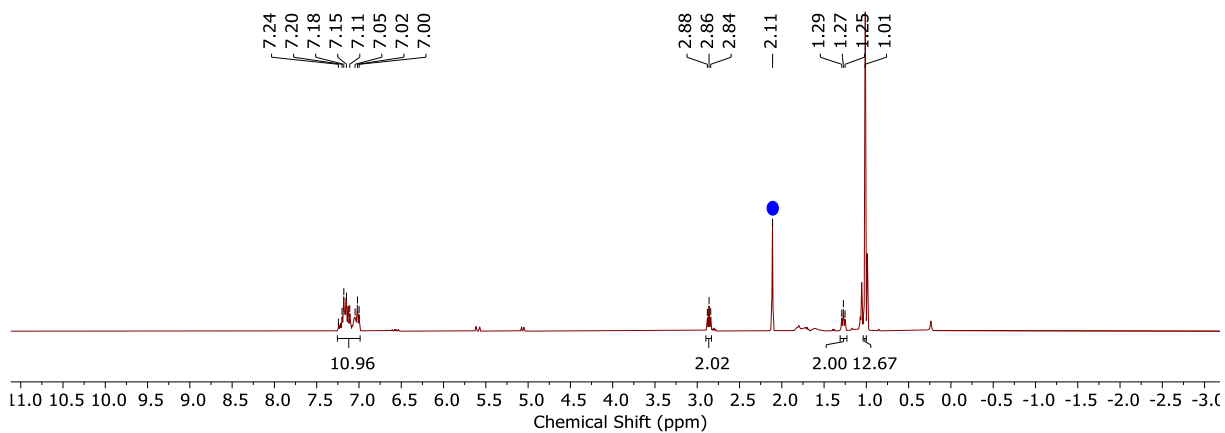


Figure S102. ^1H NMR spectrum (C_6D_6) of crude **7b**. ● = toluene internal standard resonance.

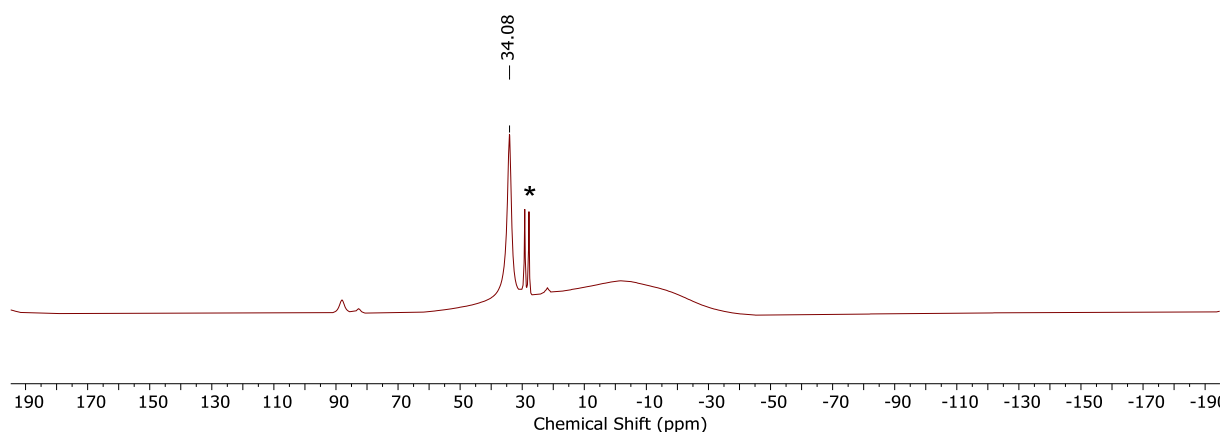
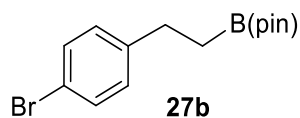


Figure S103. ^{11}B NMR spectrum (C_6D_6) of crude **7b**. * = HB(pin).

6.4.2. **27b** - 2-(4-bromophenethyl)-4,4,5,5-tetramethyl-1,3,2-dioxaborolane



^1H NMR (400 MHz, 298 K, C_6D_6): $\delta = 6.78 - 7.24$ (m, 4H, Ar), 2.64 (t, $^3J_{\text{HH}} = 7.9$ Hz, 2H, CH_2), 1.12 (t, $^3J_{\text{HH}} = 7.9$ Hz, 2H, CH_2), 1.00 (s, br, 14H, Bpin & CH_2) ppm.

^{11}B NMR (128 MHz, 298 K, C_6D_6): $\delta = 33.9$ (s) ppm.

Mass spectrometry (ESI): $\text{C}_{14}\text{H}_{20}\text{BBrO}_2 + \text{H}$ ($[\text{M} + \text{H}]^+$); Calcd. = 312.08, Found = 312.00.

Conversion: 78%

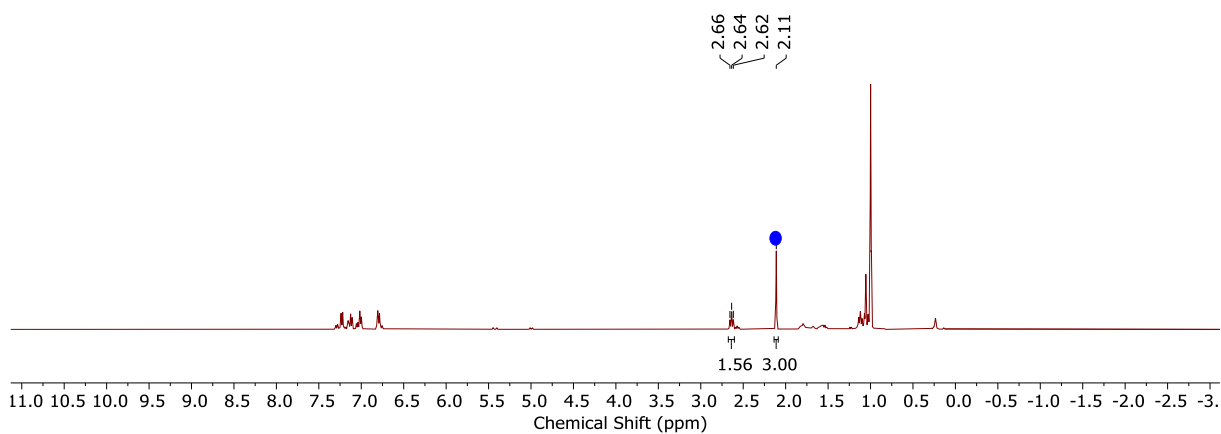


Figure S104. ^1H NMR spectrum (C_6D_6) of crude **27b**. ● = toluene internal standard resonance.

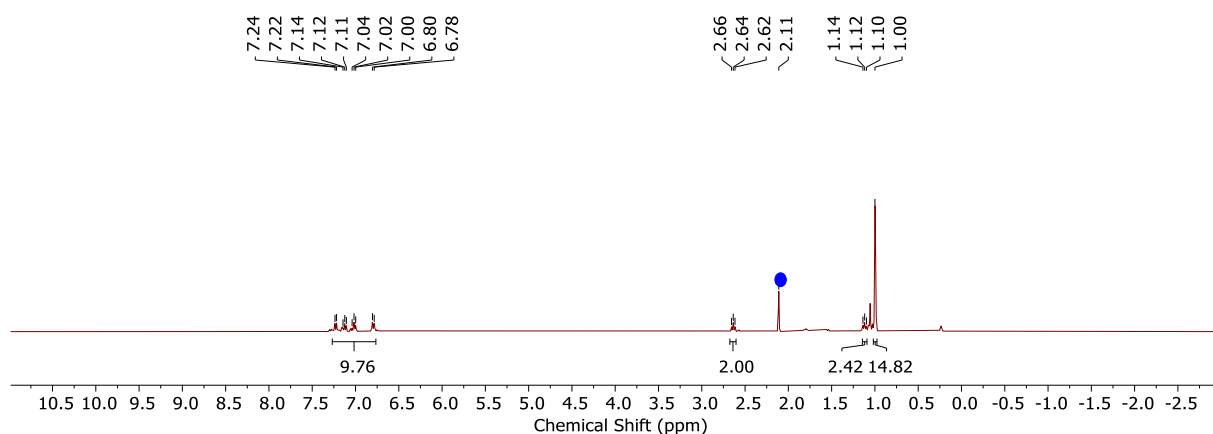


Figure S105. ^1H NMR spectrum (C_6D_6) of crude **27b**. ● = toluene internal standard resonance.

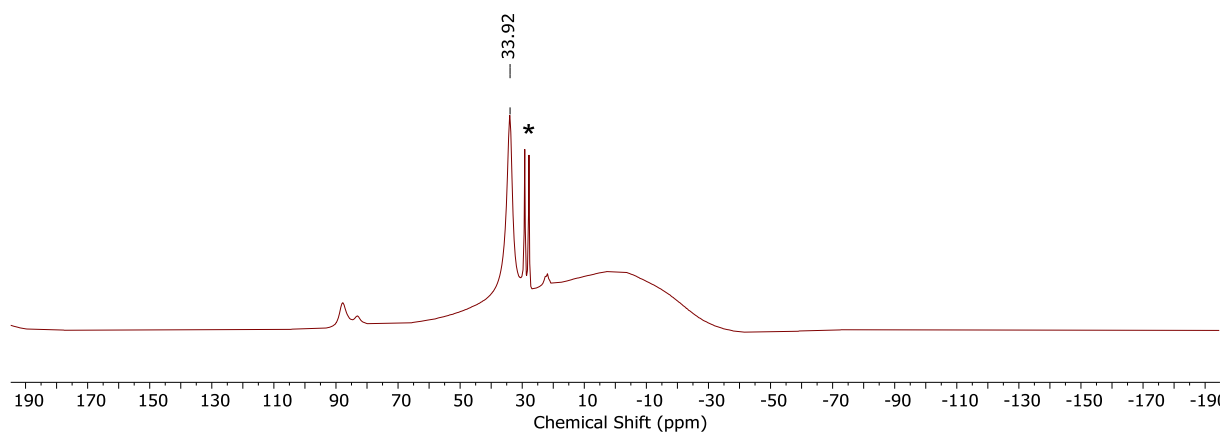
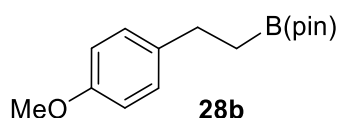


Figure S106. ^{11}B NMR spectrum (C_6D_6) of crude **27b**. * = HB(pin).

6.4.3. **28b** – 2-(4-methoxyphenethyl)-4,4,5,5-tetramethyl-1,3,2-dioxaborolane



^1H NMR (400 MHz, 298 K, C_6D_6): δ = 6.71 – 7.21 (m, 4H, Ar), 3.33 (s, 3H, CH_3), 2.86 (t, $^3J_{\text{HH}}$ = 7.9 Hz, 2H, CH_2), 1.29 (t, $^3J_{\text{HH}}$ = 7.9 Hz, 2H, CH_2), 1.03 (s, 12H, Bpin) ppm.

^{11}B NMR (128 MHz, 298 K, C_6D_6): δ = 34.2 (s) ppm.

Mass spectrometry (ESI): $\text{C}_{15}\text{H}_{23}\text{BO}_3+\text{Na}$ ($[\text{M}+\text{Na}]^+$); Calcd. = 285.16, Found = 285.08.

Conversion: 79%

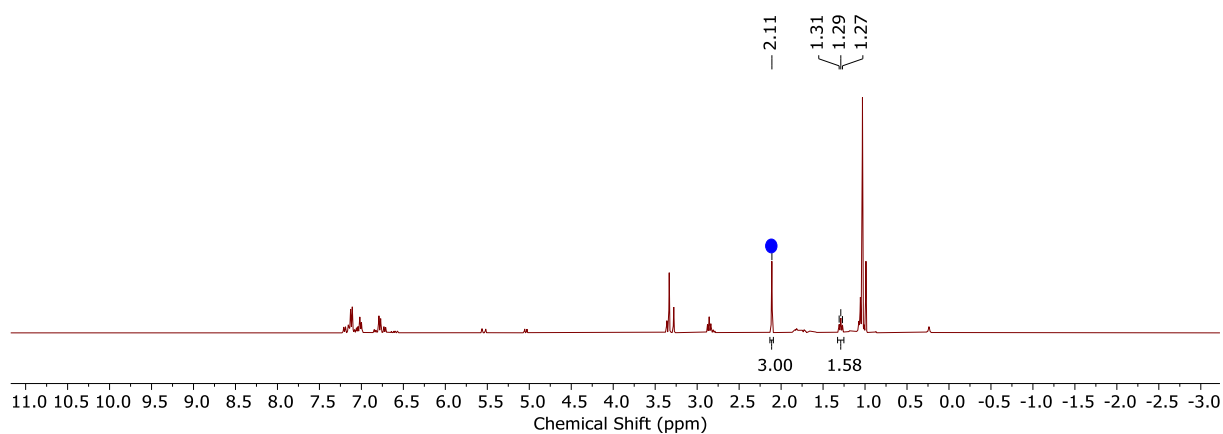


Figure S107. ^1H NMR spectrum (C_6D_6) of crude **28b**. ● = toluene internal standard resonance.

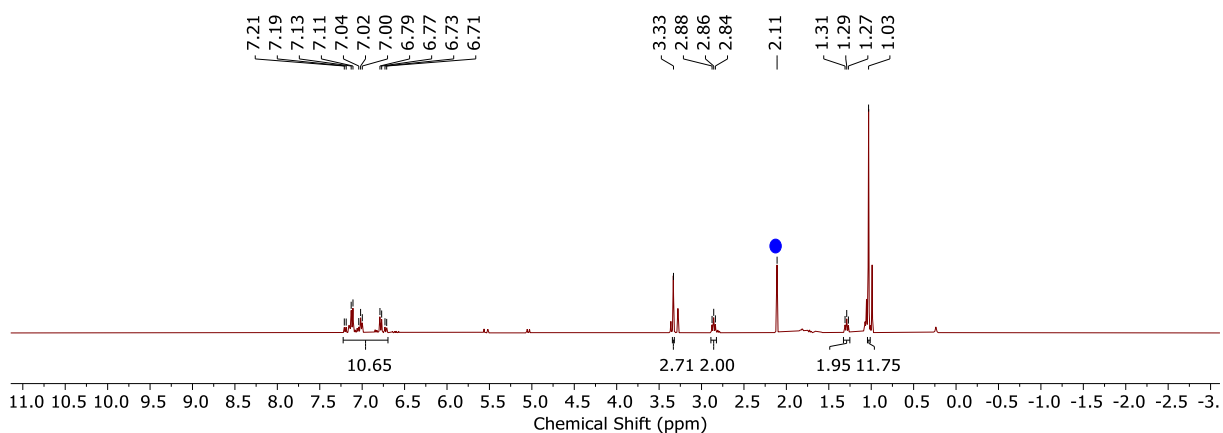


Figure S108. ^1H NMR spectrum (C_6D_6) of crude **28b**. ● = toluene internal standard resonance.

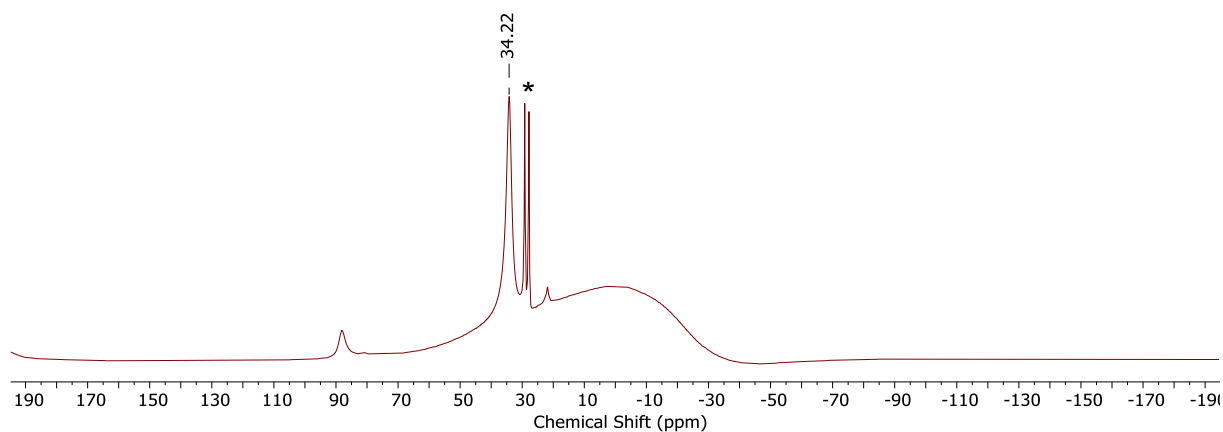
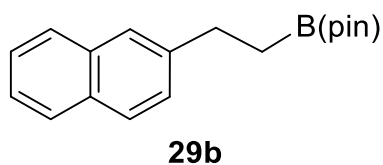


Figure S109. ^{11}B NMR spectrum (C_6D_6) of crude **28b**. * = HB(pin).

6.4.4. **29b** – 4,4,5,5-tetramethyl-2-(2-(naphthalen-2-yl)ethyl)-1,3,2-dioxaborolane



^1H NMR (400 MHz, 298 K, C_6D_6): $\delta = 7.00 - 7.67$ (m, 7H, Ar), 3.00 (t, $^3J_{\text{HH}} = 7.9$ Hz, 2H, CH_2), 1.35 (t, $^3J_{\text{HH}} = 7.9$ Hz, 2H, CH_2), 1.01 (s, 12H, Bpin) ppm.

^{11}B NMR (128 MHz, 298 K, C_6D_6): $\delta = 34.2$ (s) ppm.

Mass spectrometry (ESI): $\text{C}_{18}\text{H}_{23}\text{BO}_2 + \text{H}$ ($[\text{M} + \text{H}]^+$); Calcd. = 283.19, Found = 283.17.

Conversion: 76%

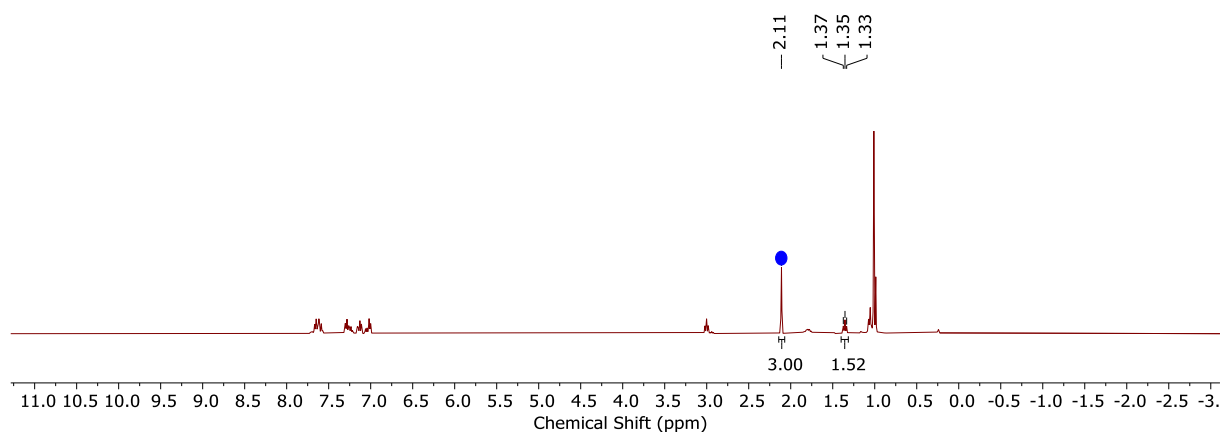


Figure S110. ^1H NMR spectrum (C_6D_6) of crude **29b**. ● = toluene internal standard resonance.

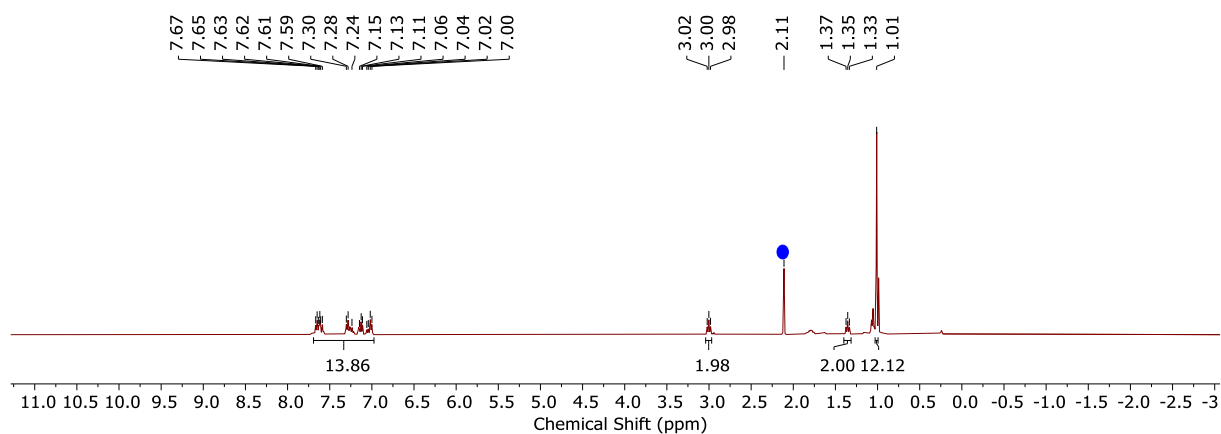


Figure S111. ^1H NMR spectrum (C_6D_6) of crude **29b**. ● = toluene internal standard resonance.

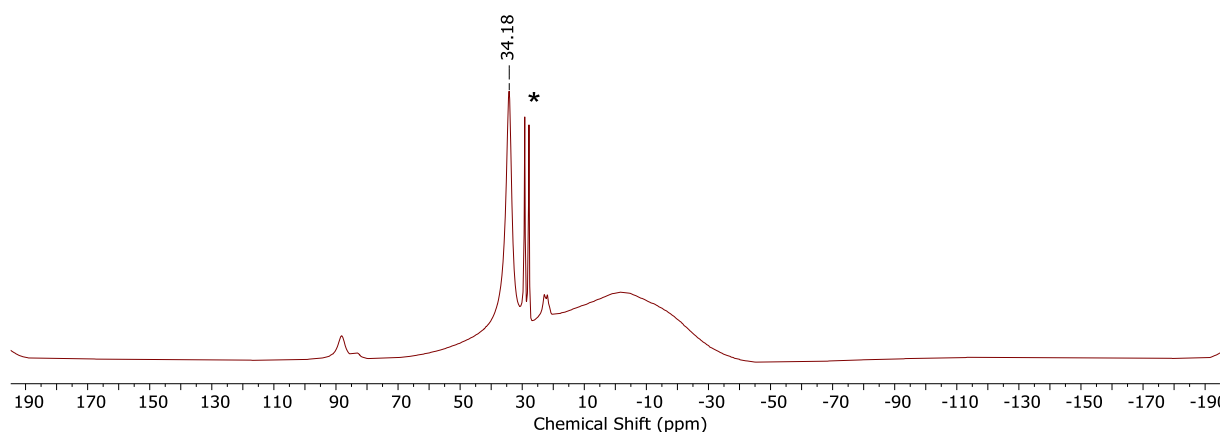
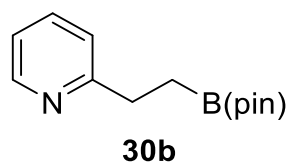


Figure S112. ^{11}B NMR spectrum (C_6D_6) of crude **29b**.

6.4.5. **30b** – 2-(2-(4,4,5,5-tetramethyl-1,3,2-dioxaborolan-2-yl)ethyl)pyridine



^1H NMR (400 MHz, 298 K, C_6D_6): δ = 6.35 – 7.13 (m, 4H, Ar), 2.80 (t, $^3J_{\text{HH}}$ = 7.4 Hz, 2H, CH_2), 1.25 (t, $^3J_{\text{HH}}$ = 7.4 Hz, 2H, CH_2), unable to identify Bpin signals because of multiple overlapping resonances from unreacted HBpin.

^{11}B NMR (128 MHz, 298 K, C_6D_6): δ = 33.7 (s, uncoordinated Bpin), 4.5 (s, tetracoordinated NBpin)] ppm.

Mass spectrometry (ESI): $\text{C}_{13}\text{H}_{20}\text{BNO}_2+\text{H}$ ($[\text{M}+\text{H}]^+$); Calcd. = 234.17, Found = 234.17.

Conversion: 49%

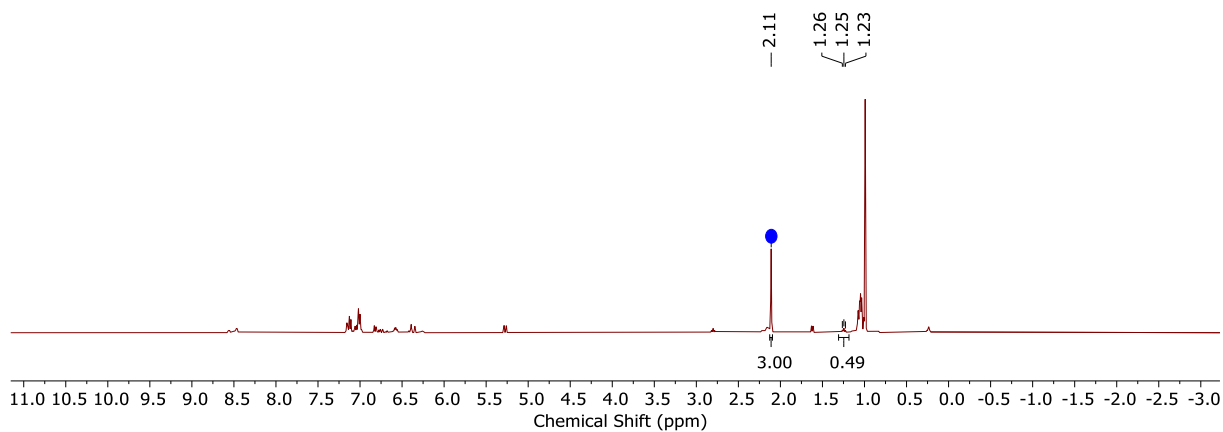


Figure S113. ^1H NMR spectrum (C_6D_6) of crude **30b**. ● = toluene internal standard resonance.

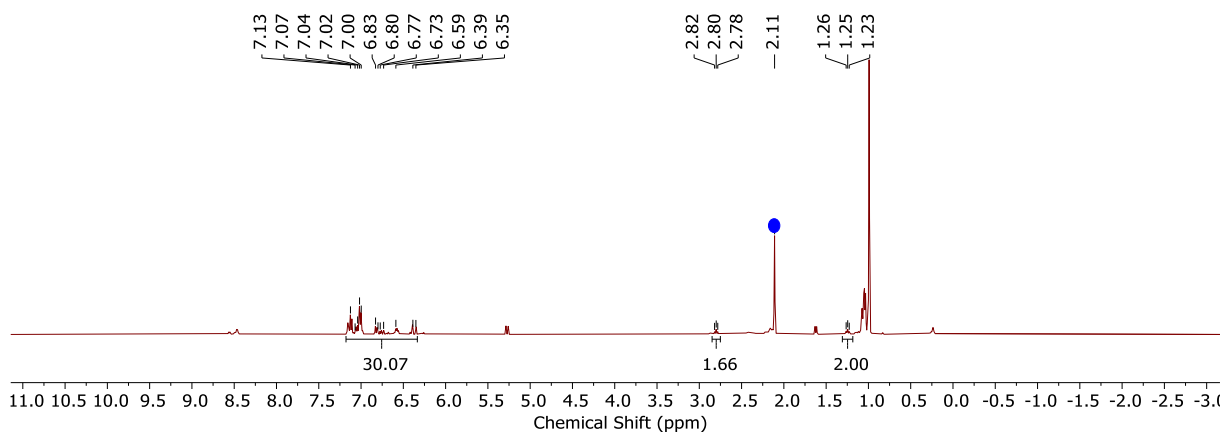


Figure S114. ^1H NMR spectrum (C_6D_6) of crude **30b**. ● = toluene internal standard resonance.

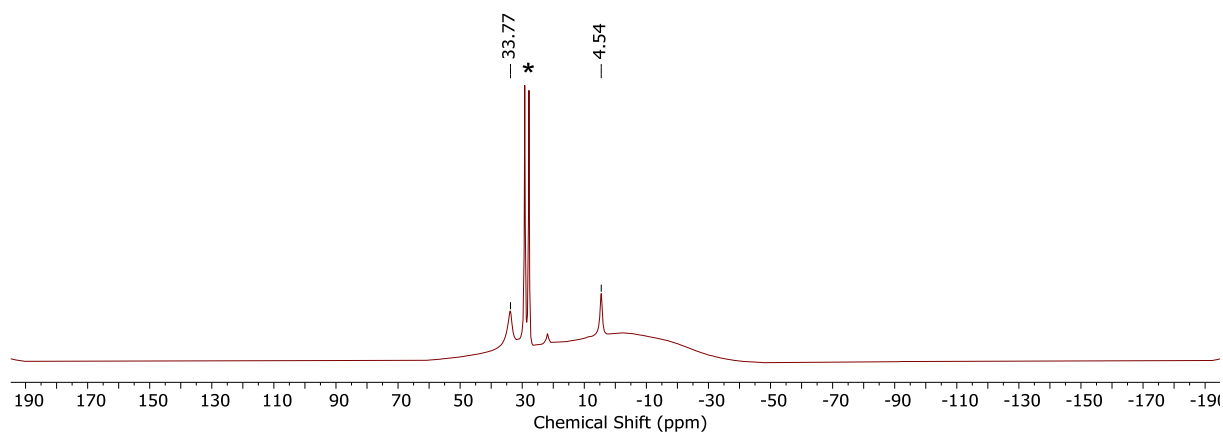
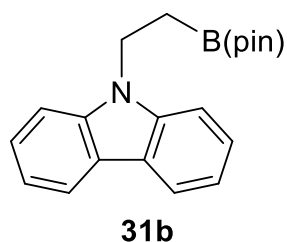


Figure S115. ^{11}B NMR spectrum (C_6D_6) of crude **30b**. * = HB(pin).

6.4.6. **31b** – 9-(2-(4,4,5,5-tetramethyl-1,3,2-dioxaborolan-2-yl)ethyl)-9H-carbazole



^1H NMR (400 MHz, 298 K, C_6D_6): δ = 7.00 – 8.11 (m, 8H, Ar), 4.22 (t, $^3J_{\text{HH}} = 8.0$ Hz, 2H, CH_2), 1.35 (t, $^3J_{\text{HH}} = 8.0$ Hz, 2H, CH_2), 0.92 (s, 12H, Bpin) ppm.

^{11}B NMR (128 MHz, 298 K, C_6D_6): δ = 33.5 (s) ppm.

Mass spectrometry (APCI): $\text{C}_{20}\text{H}_{42}\text{BNO}_2 + \text{H}$ ($[\text{M} + \text{H}]^+$); Calcd. = 322.20, Found = 322.25.

Conversion: 54%

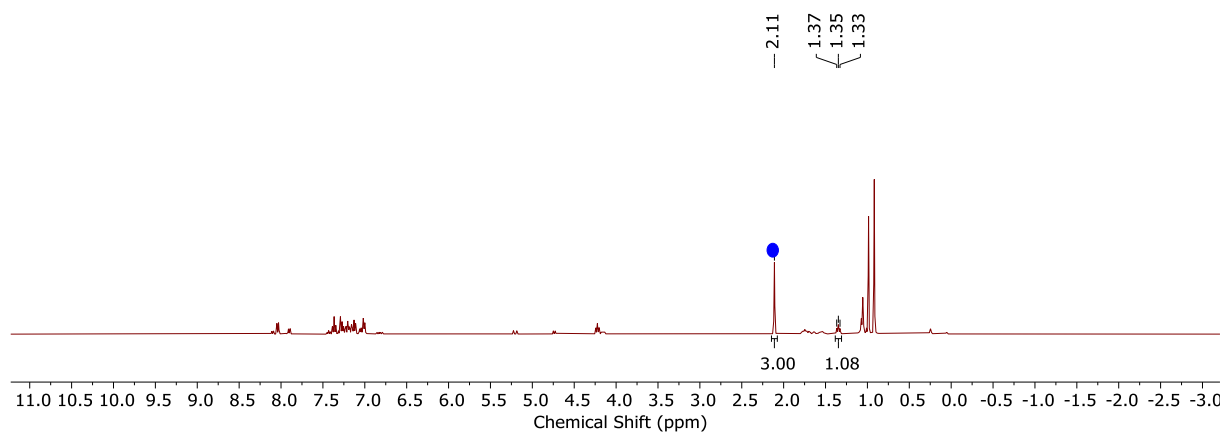


Figure S116. ^1H NMR spectrum (C_6D_6) of crude **31b**. ● = toluene internal standard resonance.

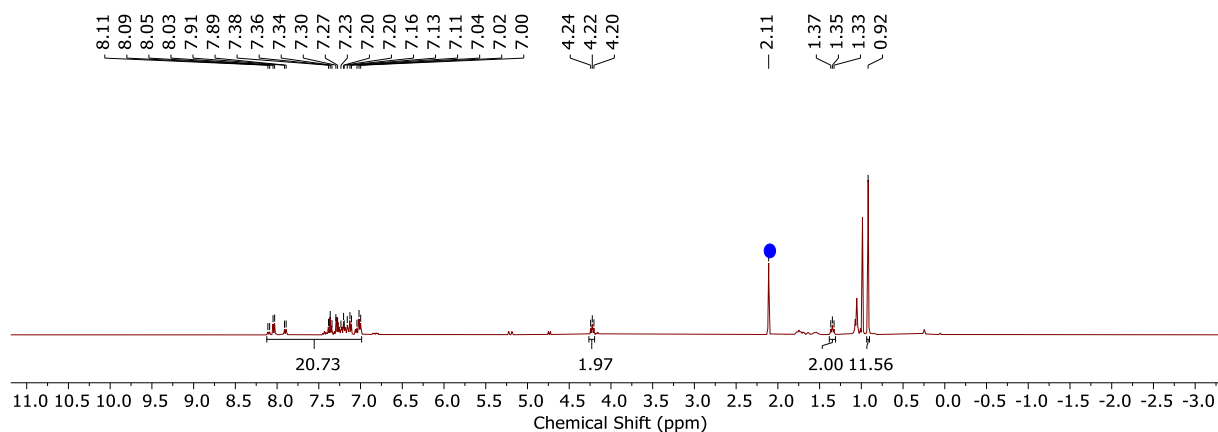


Figure S117. ^1H NMR spectrum (C_6D_6) of crude **31b**. • = toluene internal standard resonance.

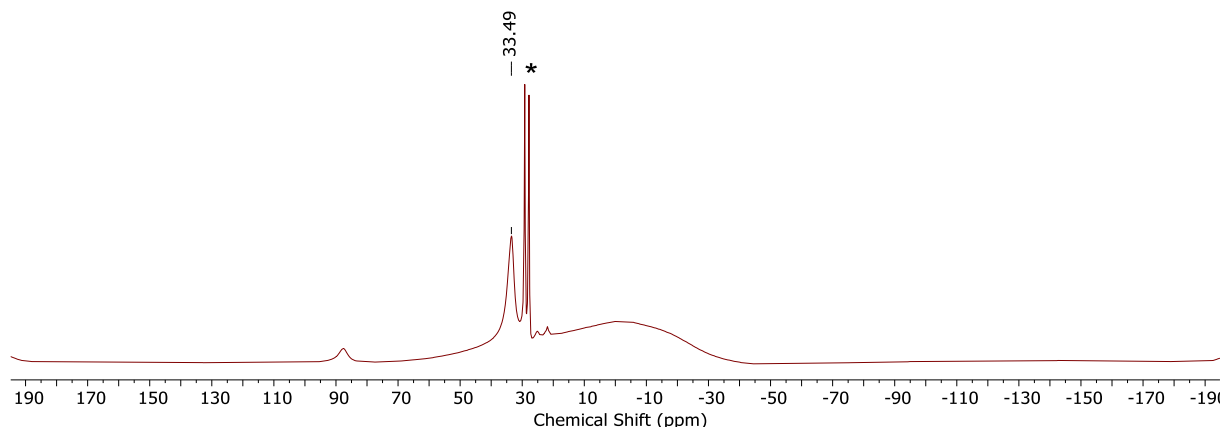
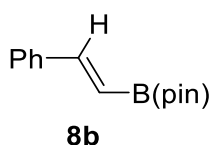


Figure S118. ^{11}B NMR spectrum (C_6D_6) of crude **31b**. * = HB(pin).

6.5. Alkynes

We validated our analysis of hydroborated alkynes by comparison to various literature sources and found all data to be in agreement with those previously reported.¹⁷

6.5.1. **8b** – (E)-4,4,5,5-tetramethyl-2-styryl-1,3,2-dioxaborolane



^1H NMR (400 MHz, 298 K, C_6D_6): δ = 7.76 (d, $^3J_{\text{HH}}$ = 18.5 Hz, 1H, CH), 6.88 – 7.31 (m, 5H, Ar), 6.46 (d, $^3J_{\text{HH}}$ = 18.5 Hz, 1H, CH), 1.13 (s, 12H, Bpin) ppm.

^{11}B NMR (128 MHz, 298 K, C_6D_6): δ = 30.6 (s) ppm.

Mass spectrometry (APCI): $\text{C}_{14}\text{H}_{19}\text{BO}_2 + \text{H}$ ($[\text{M} + \text{H}]^+$); Calcd. = 231.1551, Found = 231.1554.

Conversion: 79%

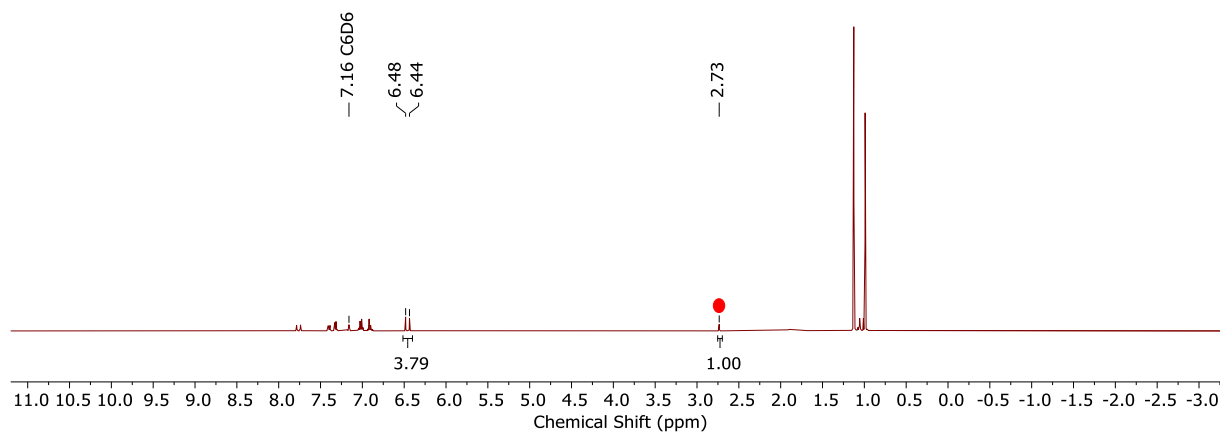


Figure S119. ^1H NMR spectrum (C_6D_6) of crude **8b**. • = unreacted start material used to determine conversion.

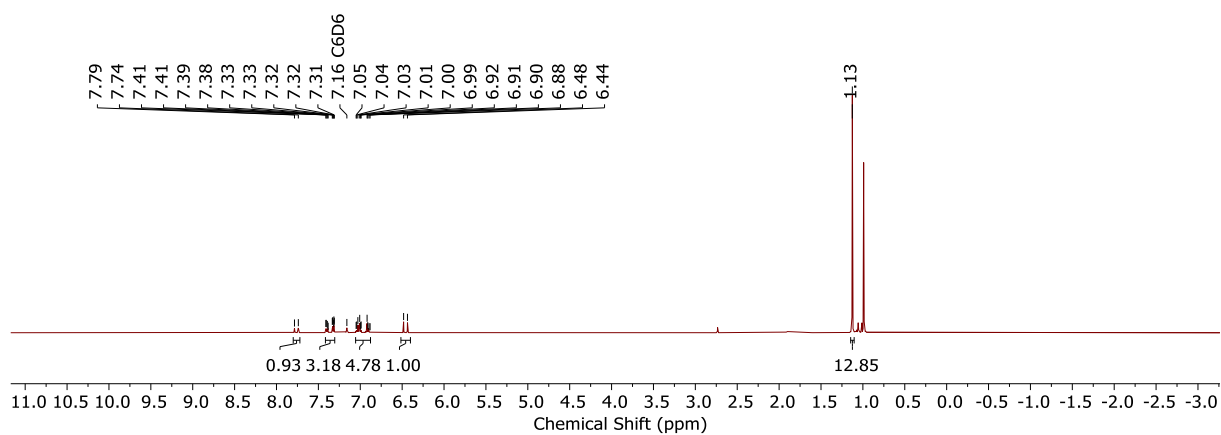


Figure S120. ^1H NMR spectrum (C_6D_6) of crude **8b**.

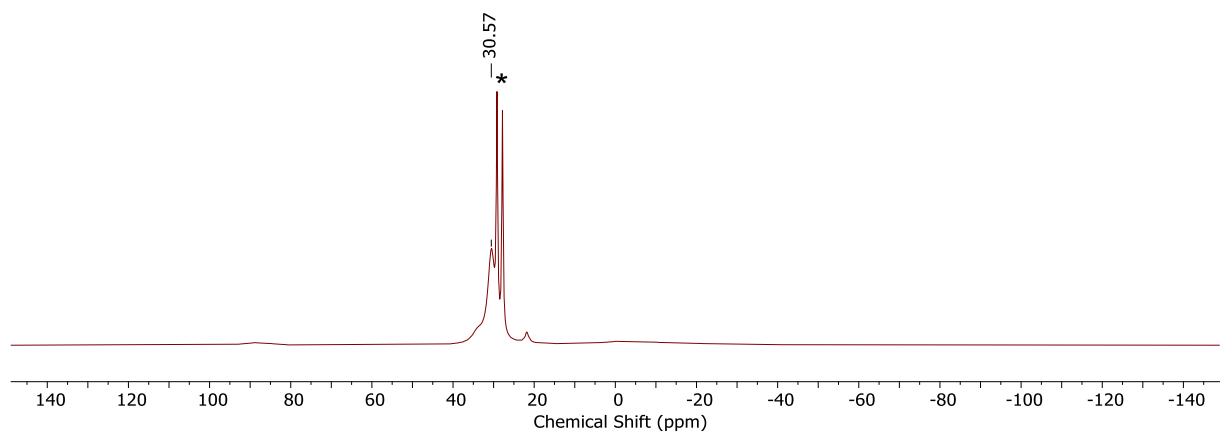
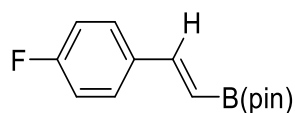


Figure S121. ^{11}B NMR spectrum (C_6D_6) of crude **8b**. * = HB(pin).

6.5.2. **32b** – (E)-2-(4-fluorostyryl)-4,4,5,5-tetramethyl-1,3,2-dioxaborolane



32b

^1H NMR (400 MHz, 298 K, C_6D_6): δ = 7.60 (d, $^3J_{\text{HH}}$ = 18.4 Hz, 1H, CH), 6.49 – 7.13 (m, 4H, Ar), 6.26 (d, $^3J_{\text{HH}}$ = 18.4 Hz, 1H, CH), 1.13 (s, 12H, Bpin) ppm.

^{11}B NMR (128 MHz, 298 K, C_6D_6): δ = 30.5 (s) ppm.

$^{19}\text{F}\{^1\text{H}\}$ NMR (376 MHz, 298 K, C_6D_6): δ = -112.6 (s) ppm.

Mass spectrometry (APCI): $\text{C}_{14}\text{H}_{18}\text{O}_2\text{BF}+\text{H}$ ($[\text{M}+\text{H}]^+$); Calcd. = 249.1457, Found = 249.1462.

Conversion: 80%

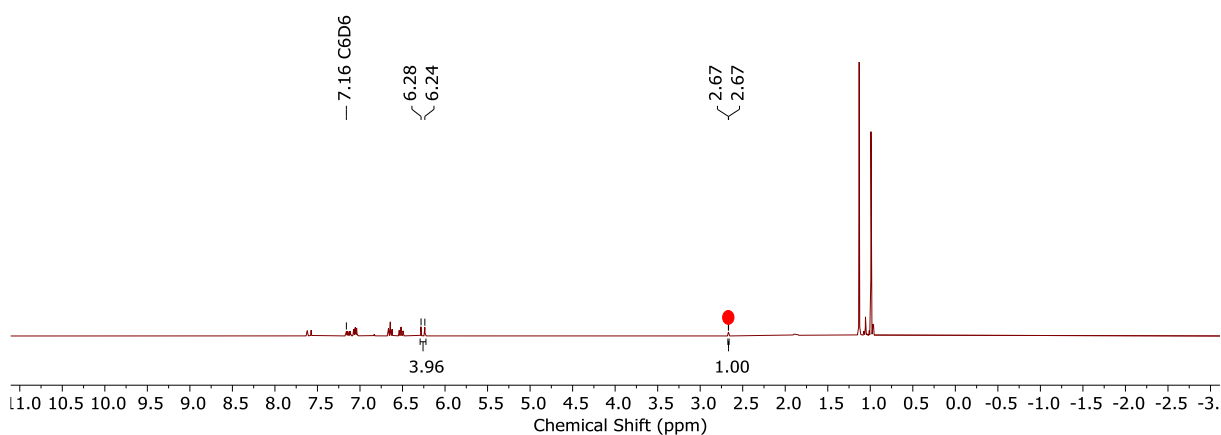


Figure S122. ^1H NMR spectrum (C_6D_6) of crude **32b**. ● = unreacted start material used to determine conversion.

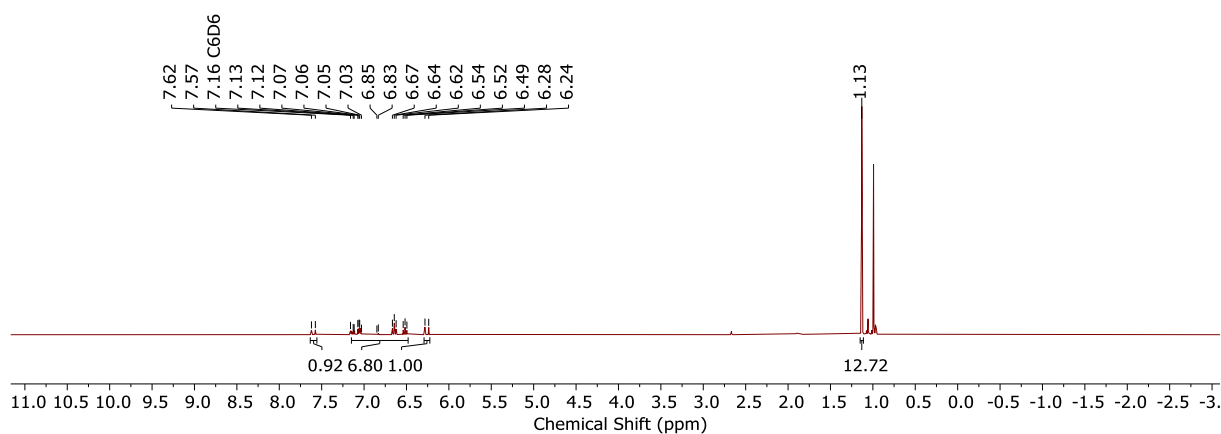


Figure S123. ^1H NMR spectrum (C_6D_6) of crude **32b**.

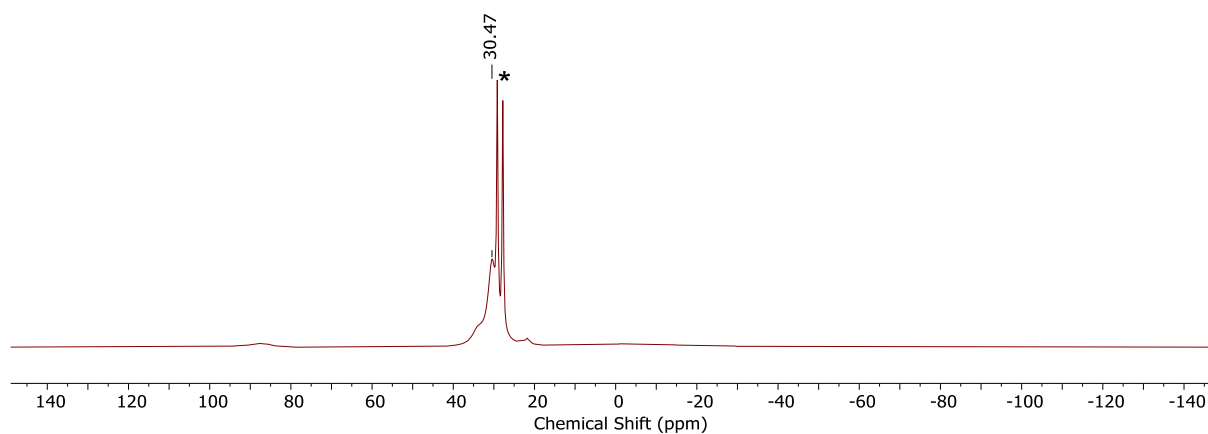


Figure S124. ^{11}B NMR spectrum (C_6D_6) of crude **32b**. * = HB(pin).

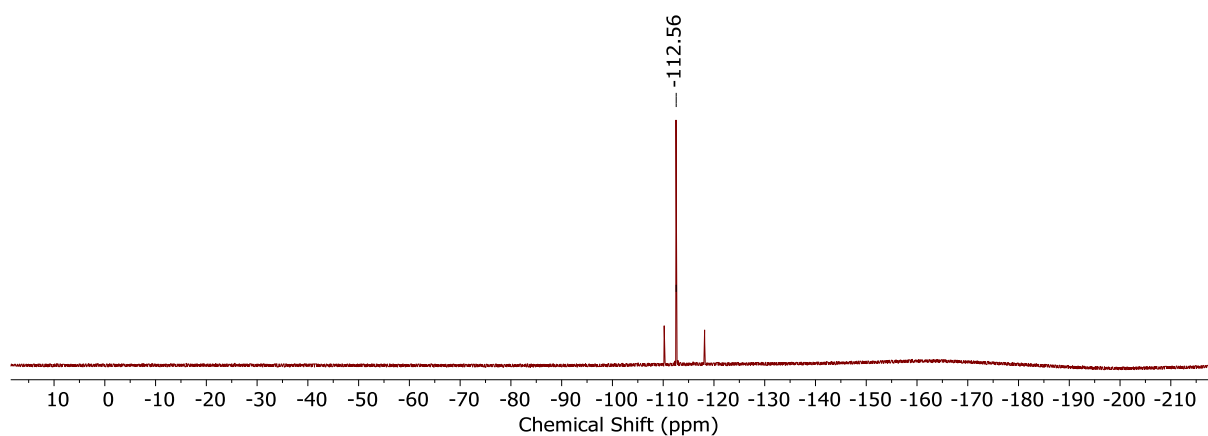
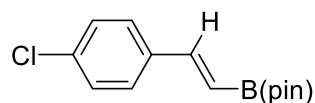


Figure S125. $^{19}\text{F}\{^1\text{H}\}$ NMR spectrum (C_6D_6) of crude **32b**.

6.5.3. **32b** – (E)-2-(4-chlorostyryl)-4,4,5,5-tetramethyl-1,3,2-dioxaborolane



32b

^1H NMR (400 MHz, 298 K, C_6D_6): δ = 7.55 (d, $^3J_{\text{HH}}$ = 18.4 Hz, 1H, CH), 6.81 – 7.05 (m, 4H, Ar), 6.28 (d, $^3J_{\text{HH}}$ = 18.4 Hz, 1H, CH), 1.12 (s, 12H, Bpin) ppm.

^{11}B NMR (128 MHz, 298 K, C_6D_6): δ = 30.4 (s).

Mass spectrometry (APCI): $\text{C}_{14}\text{H}_{18}\text{O}_2\text{BCl}+\text{H}$ ($[\text{M}+\text{H}]^+$); Calcd. = 265.1161, Found = 265.1167.

Conversion: 81%

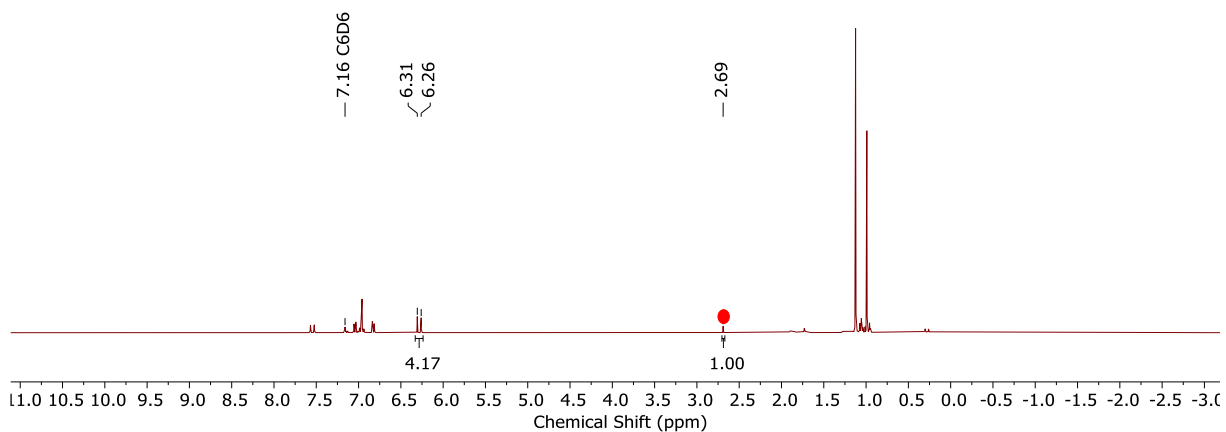


Figure S126. ^1H NMR spectrum (C_6D_6) of crude **33b**. ● = unreacted start material used to determine conversion.

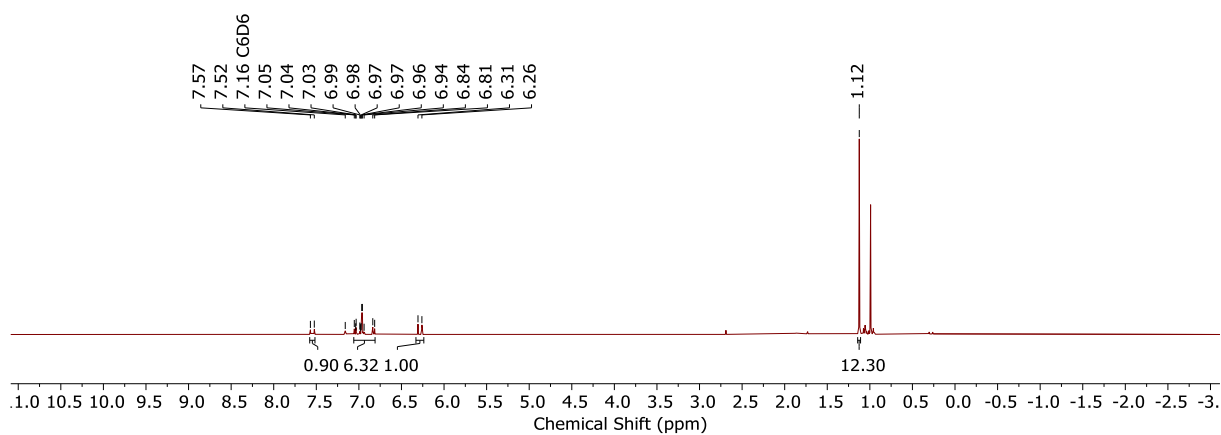


Figure S127. ^1H NMR spectrum (C_6D_6) of crude **33b**.

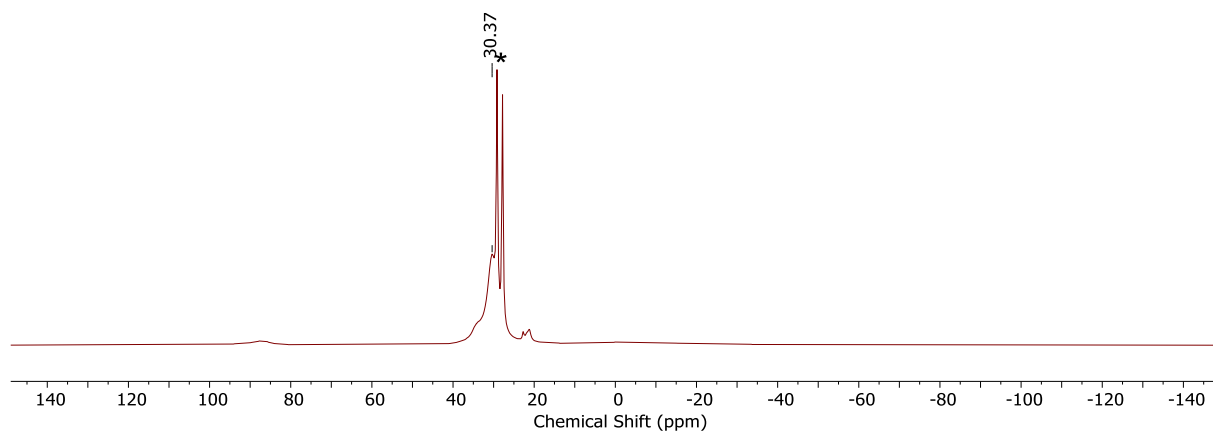
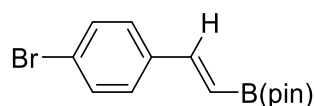


Figure S128. ^{11}B NMR spectrum (C_6D_6) of crude **33b**. * = HB(pin).

6.5.4. **34b** – (E)-2-(4-bromostyryl)-4,4,5,5-tetramethyl-1,3,2-dioxaborolane



34b

¹H NMR (400 MHz, 298 K, C₆D₆): δ = 7.52 (d, $^3J_{\text{HH}}$ = 18.5 Hz, 1H, CH), 6.89 – 7.12 (m, 4H, Ar), 6.29 (d, $^3J_{\text{HH}}$ = 18.5 Hz, 1H, CH), 1.12 (s, 12H, Bpin) ppm.

¹¹B NMR (128 MHz, 298 K, C₆D₆): δ = 30.2 (s) ppm.

Mass spectrometry (APCI): C₁₄H₁₈O₂BBR+H ([M+H]⁺); Calcd. = 309.0656, Found = 309.0660.

Conversion: 80%

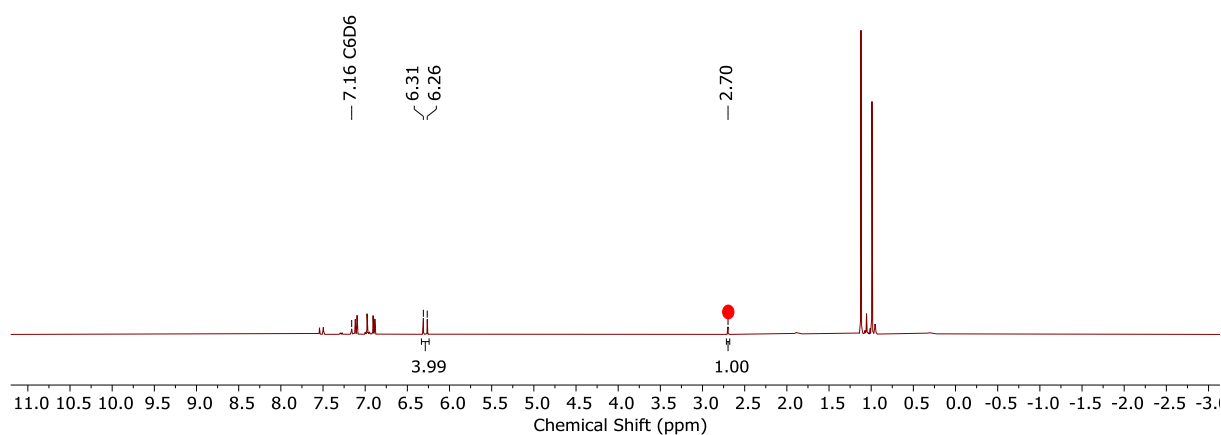


Figure S129. ¹H NMR spectrum (C₆D₆) of crude **34b**. ● = unreacted start material used to determine conversion.

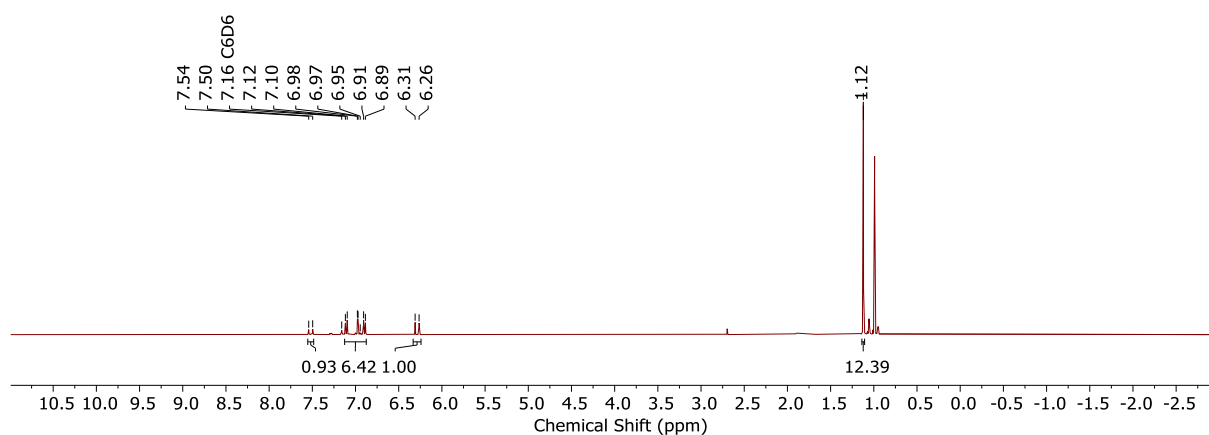


Figure S130. ¹H NMR spectrum (C₆D₆) of crude **34b**.

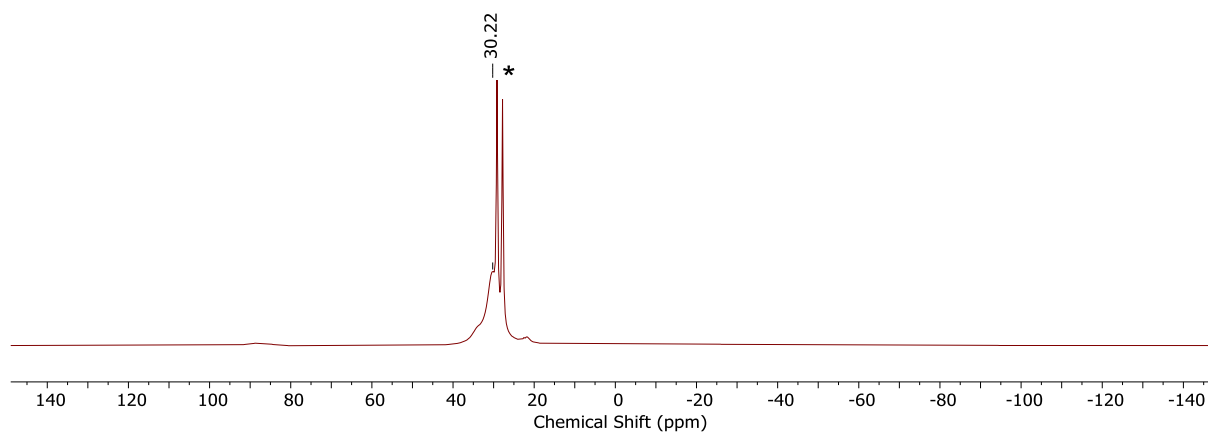
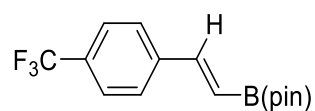


Figure S131. ^{11}B NMR spectrum (C_6D_6) of crude **34b**. * = HB(pin).

6.5.5. **35b** – (E)-4,4,5,5-tetramethyl-2-(4-(trifluoromethyl)styryl)-1,3,2-dioxaborolane



35b

^1H NMR (400 MHz, 298 K, C_6D_6): δ = 7.55 (d, $^3J_{\text{HH}}$ = 18.3 Hz, 1H, CH), 7.04 – 7.20 (m, 4H, Ar), 6.35 (d, $^3J_{\text{HH}}$ = 18.3 Hz, 1H, CH), 1.13 (s, 12H, Bpin) ppm.

^{11}B NMR (128 MHz, 298 K, C_6D_6): δ = 30.2 (s) ppm.

$^{19}\text{F}\{^1\text{H}\}$ NMR (376 MHz, 298 K, C_6D_6): δ = -62.4 (s) ppm.

Mass spectrometry (APCI): $\text{C}_{15}\text{H}_{18}\text{O}_2\text{BF}_3 + \text{H}$ ($[\text{M} + \text{H}]^+$); Calcd. 299.1425, Found = 299.1428.

Conversion: 76%

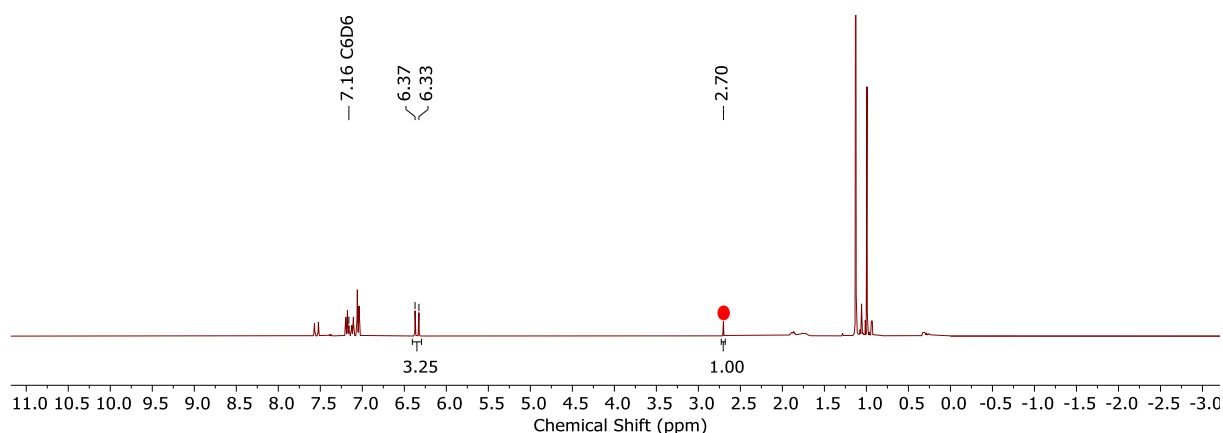


Figure S132. ^1H NMR spectrum (C_6D_6) of crude **35b**. ● = unreacted start material used to determine conversion.

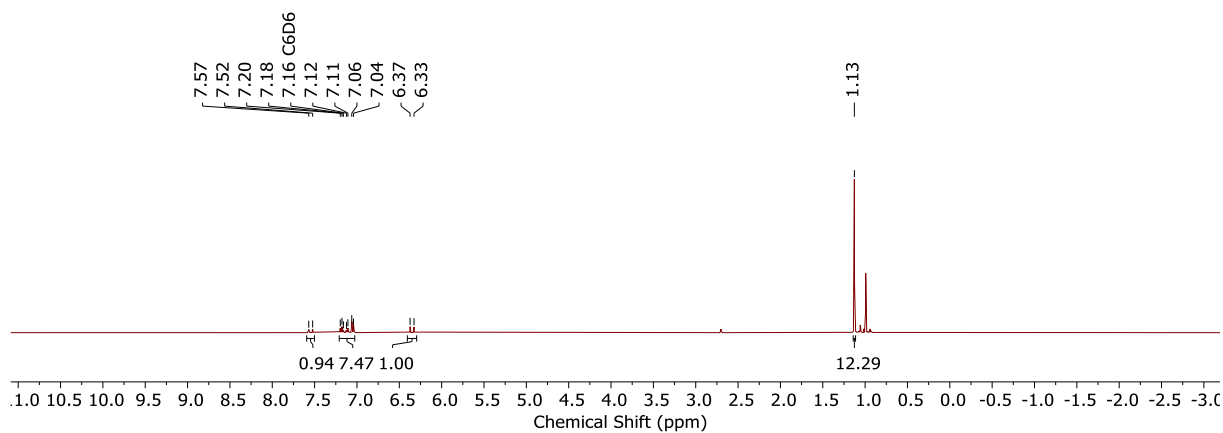


Figure S133. ^1H NMR spectrum (C_6D_6) of crude **35b**.

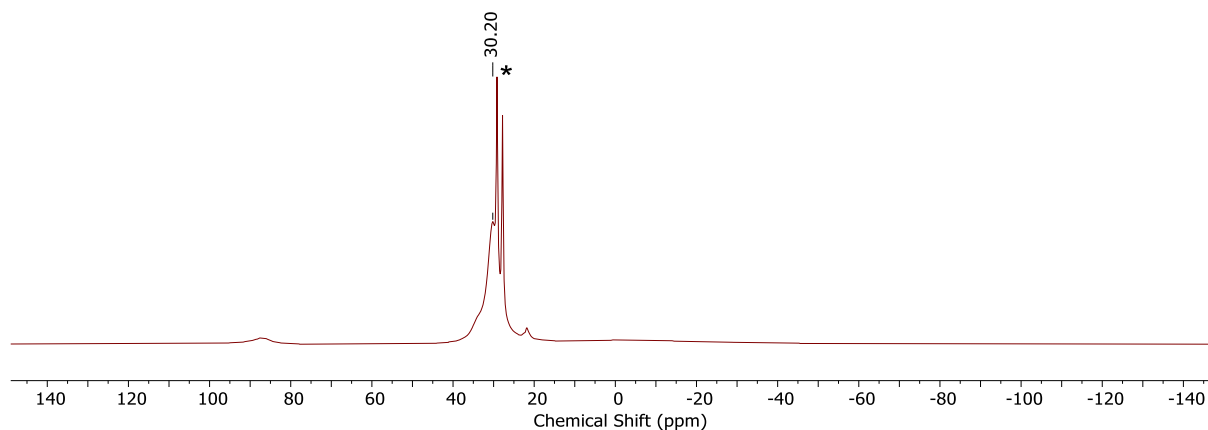


Figure S134. ^{11}B NMR spectrum (C_6D_6) of crude **35b**. * = HB(pin).

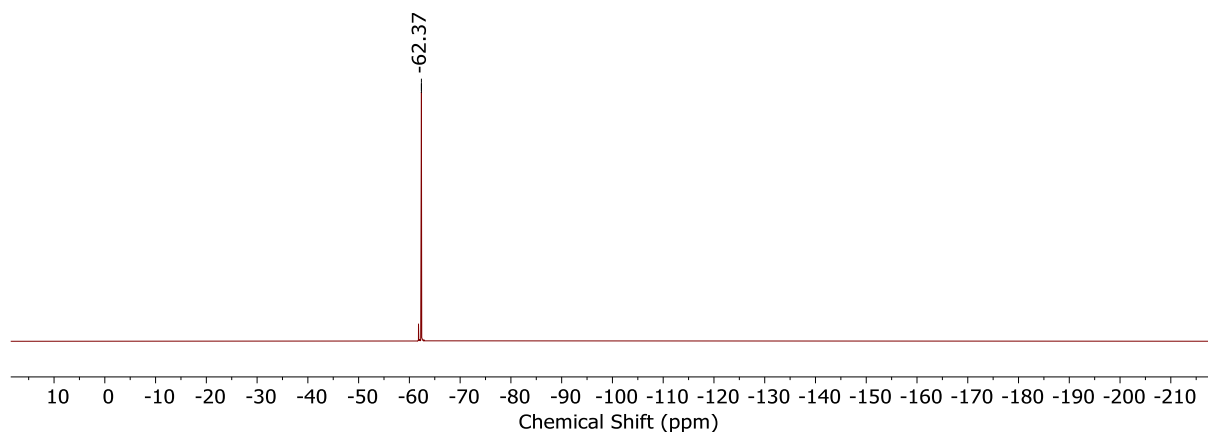
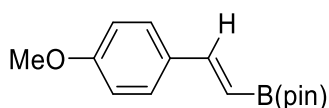


Figure S135. $^{19}\text{F}\{^1\text{H}\}$ NMR spectrum (C_6D_6) of crude **35b**.

6.5.6. **36b** – (E)-2-(4-methoxystyryl)-4,4,5,5-tetramethyl-1,3,2-dioxaborolane



36b

^1H NMR (400 MHz, 298 K, C_6D_6): $\delta = 7.77$ (d, $^3J_{\text{HH}} = 18.3$ Hz, 1H, CH), 7.29 (d, $^3J_{\text{HH}} = 9.0$ Hz, 2H, Ar), 6.62 (d, $^3J_{\text{HH}} = 9.0$ Hz, 2H, Ar), 6.36 (d, $^3J_{\text{HH}} = 18.3$ Hz, 1H, CH), 3.22 (s, 3H, CH_3), 1.15 (s, 12H, Bpin) ppm.

^{11}B NMR (128 MHz, 298 K, C_6D_6): $\delta = 30.6$ (s) ppm.

Mass spectrometry (APCI): $\text{C}_{15}\text{H}_{21}\text{O}_3\text{B}+\text{H}$ ($[\text{M}+\text{H}]^+$); Calcd. = 261.1657, Found = 261.1663.

Conversion: 87%

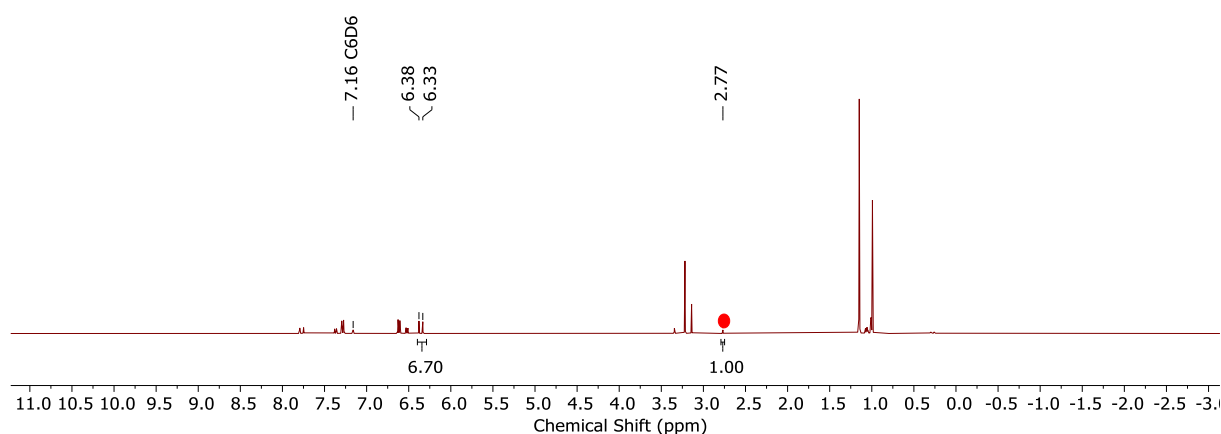


Figure S136. ^1H NMR spectrum (C_6D_6) of crude **36b**. ● = unreacted start material used to determine conversion.

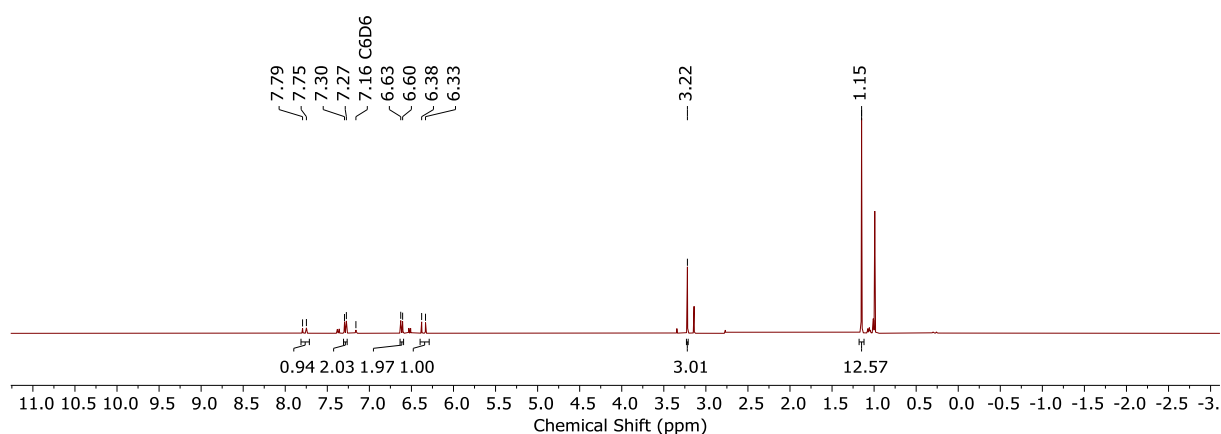


Figure S137. ^1H NMR spectrum (C_6D_6) of crude **36b**.

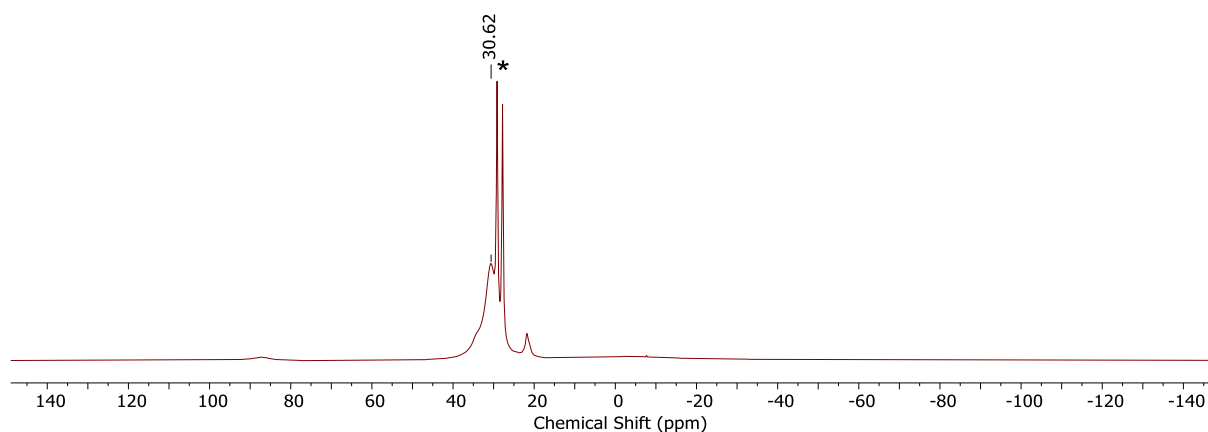
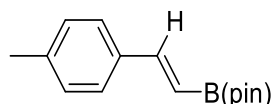


Figure S138. ^{11}B NMR spectrum (C_6D_6) of crude **36b**. * = HB(pin).

6.5.7. **37b** – (E)-4,4,5,5-tetramethyl-2-(4-methylstyryl)-1,3,2-dioxaborolane



37b

^1H NMR (400 MHz, 298 K, C_6D_6): δ = 7.79 (d, $^3J_{\text{HH}}$ = 18.3 Hz, 1H, CH), 7.29 (d, $^3J_{\text{HH}}$ = 7.9 Hz, 2H, Ar), 6.86 (d, $^3J_{\text{HH}}$ = 7.9 Hz, Ar), 6.46 (d, $^3J_{\text{HH}}$ = 18.3 Hz, 1H, CH), 2.02 (s, 3H, CH_3), 1.14 (s, 12H, Bpin) ppm.

^{11}B NMR (128 MHz, 298 K, C_6D_6): δ = 30.6 (s) ppm.

Mass spectrometry (ESI): $\text{C}_{15}\text{H}_{21}\text{BO}_2 + \text{H}$ ($[\text{M} + \text{H}]^+$); Calcd. = 245.17, Found = 244.83.

Conversion: 90%

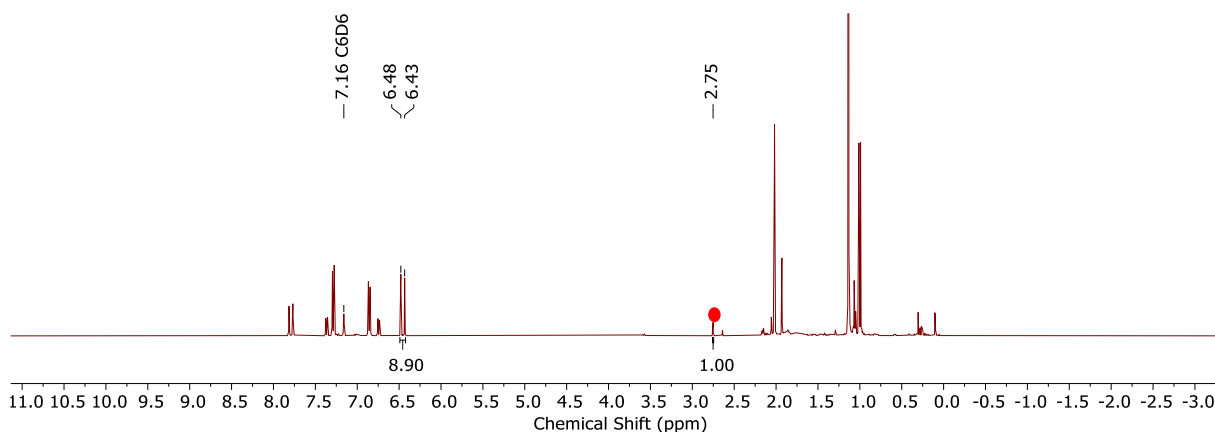


Figure S139. ^1H NMR spectrum (C_6D_6) of crude **37b**. ● = unreacted start material used to determine conversion.

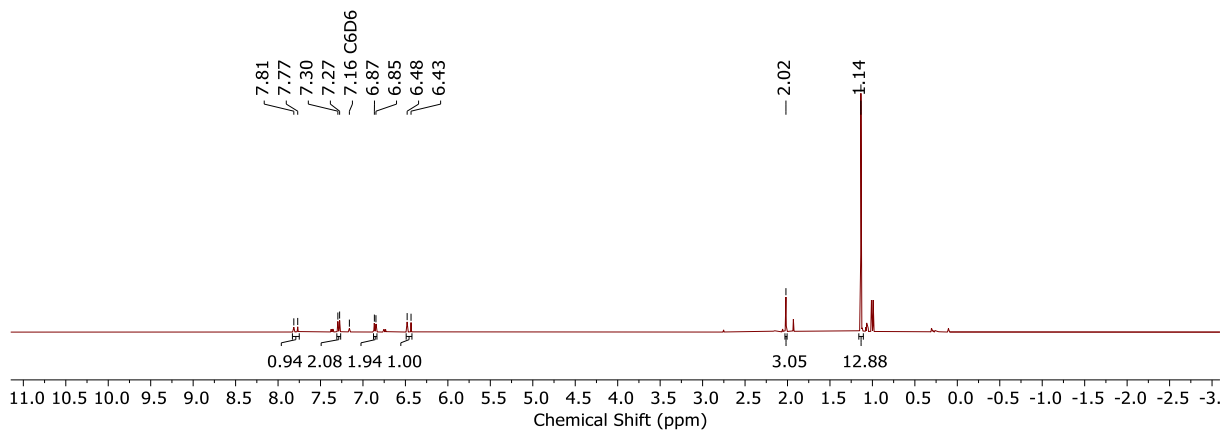


Figure S140. ^1H NMR spectrum (C_6D_6) of crude **37b**.

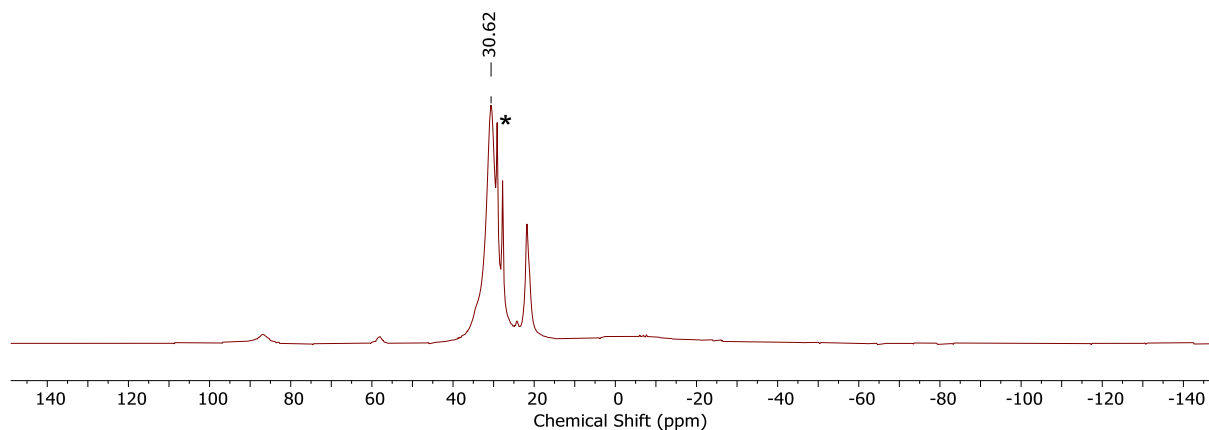
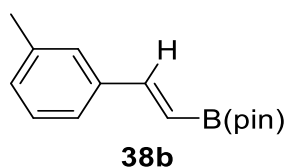


Figure S141. ^{11}B NMR spectrum (C_6D_6) of crude **37b**. * = HB(pin).

6.5.8. **38b** – (E)-4,4,5,5-tetramethyl-2-(3-methylstyryl)-1,3,2-dioxaborolane



^1H NMR (400 MHz, 298 K, C_6D_6): δ = 7.69 (d, $^3J_{\text{HH}}$ = 18.3 Hz, 1H, CH), 6.69 – 7.22 (m, 4H, Ar), 6.40 (d, $^3J_{\text{HH}}$ = 18.3 Hz, 1H, CH), 1.93 (s, 3H, CH_3), 1.05 (s, 12H, Bpin) ppm.

^{11}B NMR (128 MHz, 298 K, C_6D_6): δ = 30.6 (s) ppm.

Mass spectrometry (APCI): $\text{C}_{15}\text{H}_{21}\text{BO}_2 + \text{H}$ ($[\text{M} + \text{H}]^+$); Calcd. = 245.1707, Found = 245.1712.

Conversion: 86%

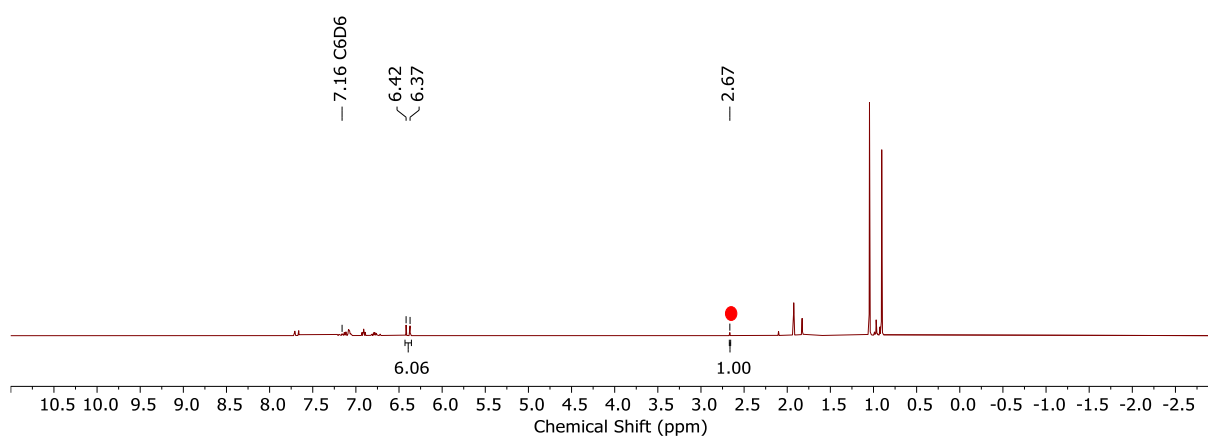


Figure S142. ^1H NMR spectrum (C_6D_6) of crude **38b**. ● = unreacted start material used to determine conversion.

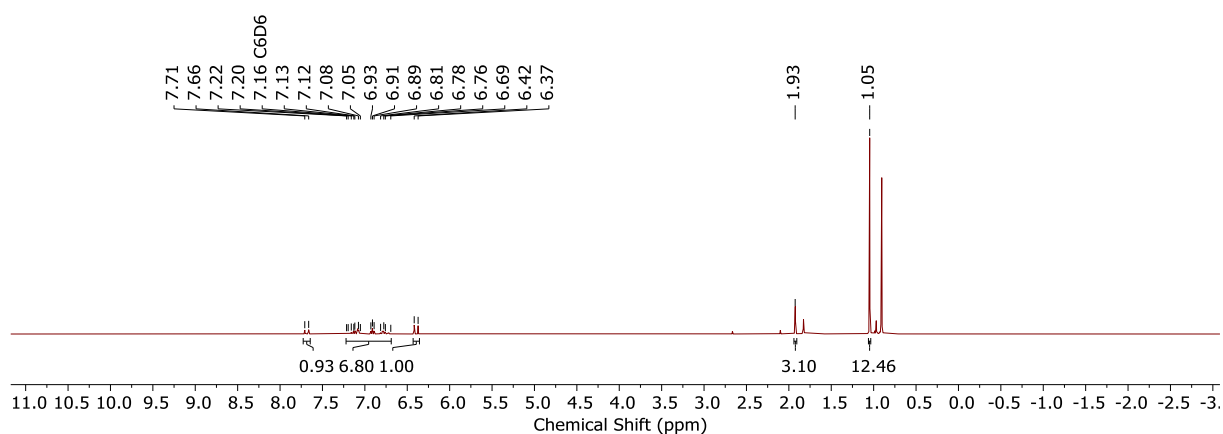


Figure S143. ^1H NMR spectrum (C_6D_6) of crude **38b**.

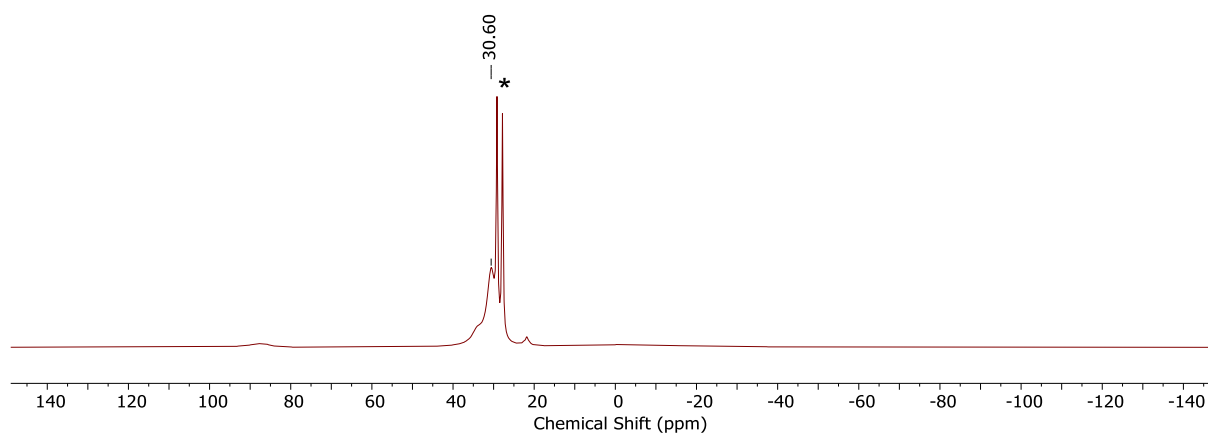
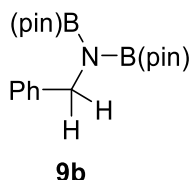


Figure S144. ^{11}B NMR spectrum (C_6D_6) of crude **38b**. * = HB(pin).

6.6. Nitriles

We validated our analysis of hydroborated nitriles by comparison to various literature sources and found all data to be in agreement with those previously reported.¹⁷⁻¹⁹

6.6.1. **9b** – N-benzyl-4,4,5,5-tetramethyl-N-(4,4,5,5-tetramethyl-1,3,2-dioxaborolan-2-yl)-1,3,2-dioxaborolan-2-amine



¹H NMR (400 MHz, 298 K, C₆D₆): δ = 7.00 – 7.60 (m, 5H, Ar), 4.61 (s, 2H, CH₂), 1.03 (s, 24H, Bpin) ppm.

¹¹B NMR (128 MHz, 298 K, C₆D₆): δ = 26.5 (s) ppm.

Mass spectrometry (APCI): C₁₉H₃₁B₂NO₄+H ([M+H]⁺); Calcd. = 360.2512, Found = 360.2511

Conversion: 84%

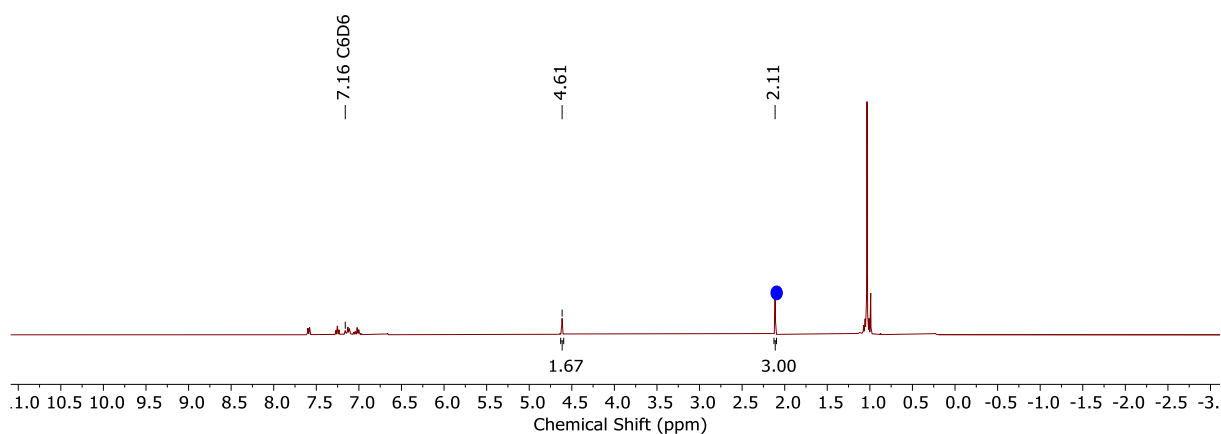


Figure S145. ¹H NMR spectrum (C₆D₆) of crude **9b**. ● = toluene internal standard resonance.

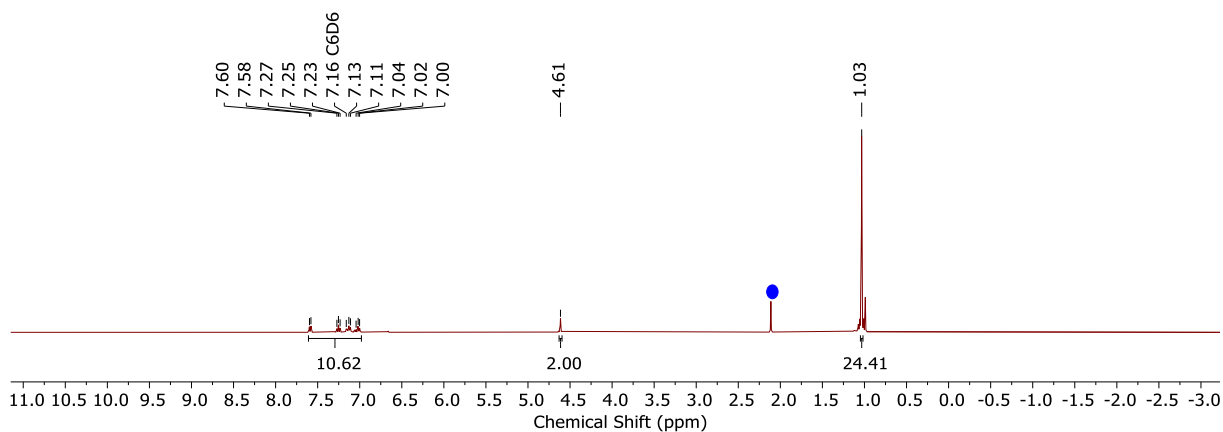


Figure S146. ^1H NMR spectrum (C_6D_6) of crude **9b**. ● = toluene internal standard resonance.

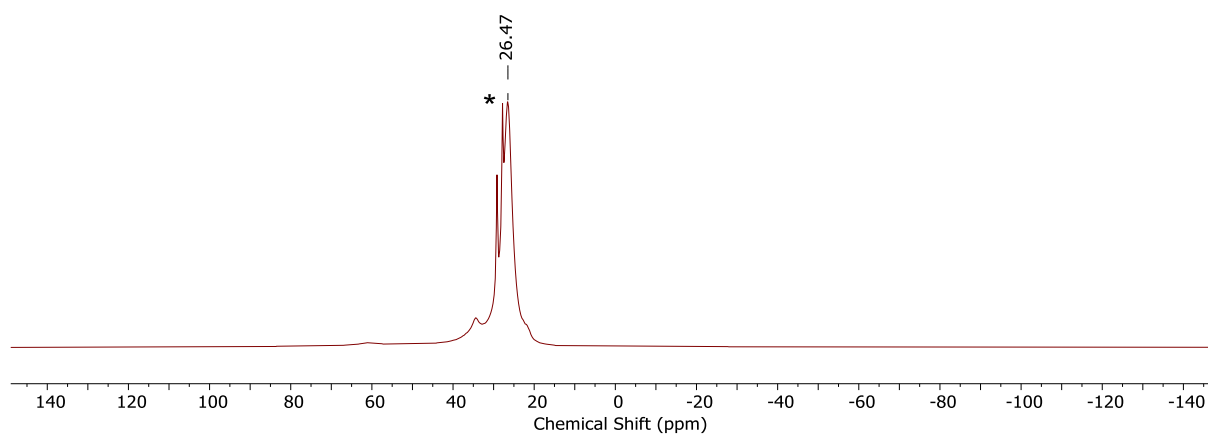
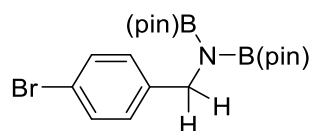


Figure S147. ^{11}B NMR spectrum (C_6D_6) of crude **9b**. * = $\text{HB}(\text{pin})$.

6.6.2. **39b** – N-(4-bromobenzyl)-4,4,5,5-tetramethyl-N-(4,4,5,5-tetramethyl-1,3,2-dioxaborolan-2-yl)-1,3,2-dioxaborolan-2-amine



39b

^1H NMR (400 MHz, 298 K, C_6D_6): δ = 6.96 – 7.35 (m, 4H, Ar), 4.42 (s, 2H, NCH_2), 1.01 (s, 24H, Bpin) ppm.

^{11}B NMR (128 MHz, 298 K, C_6D_6): δ = 26.4 (s) ppm.

Mass spectrometry (APCI): $\text{C}_{19}\text{H}_{30}\text{B}_2\text{BrNO}_4 + \text{H}$ ($[\text{M} + \text{H}]^+$); Calcd. = 438.1617, Found = 438.1617.

Conversion: 68%

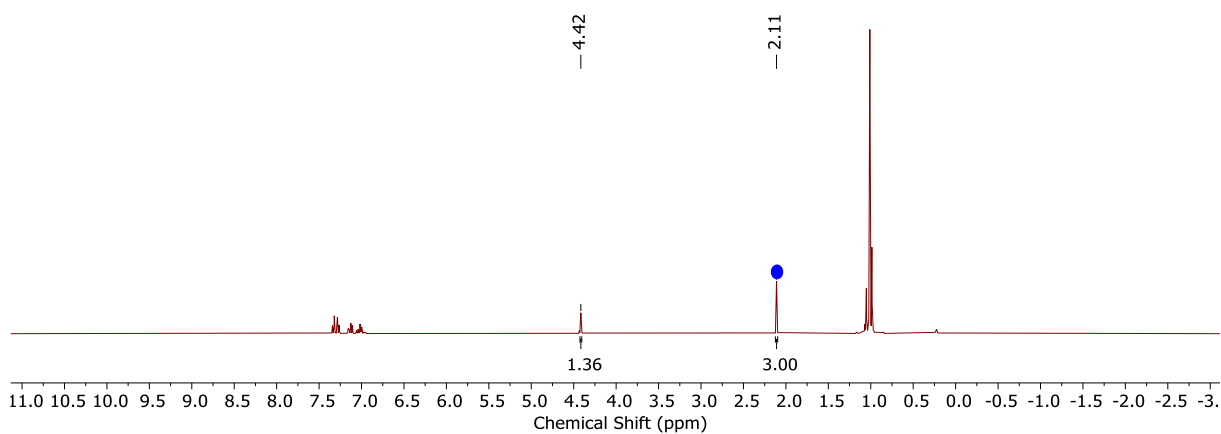


Figure S148. ^1H NMR spectrum (C_6D_6) of crude **39b**. ● = toluene internal standard resonance.

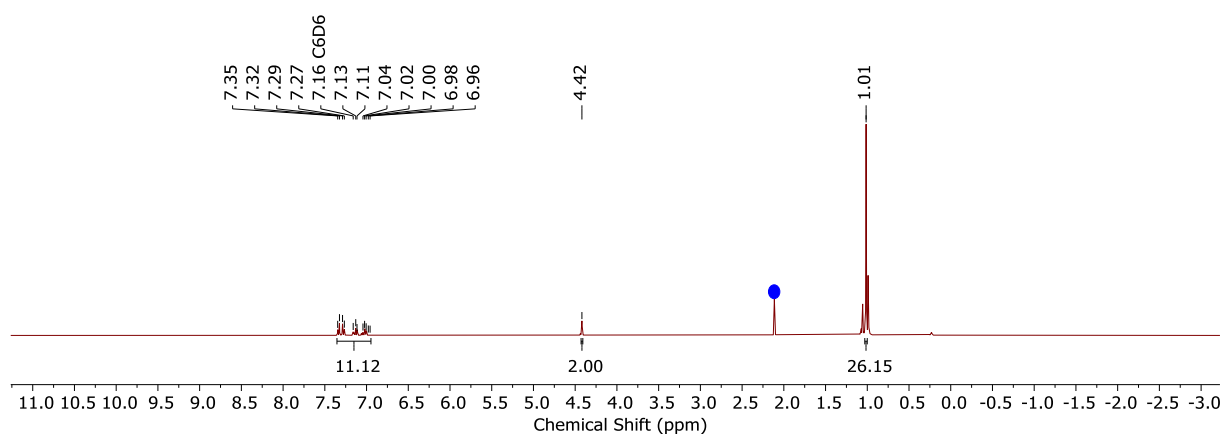


Figure S149. ^1H NMR spectrum (C_6D_6) of crude **39b**. ● = toluene internal standard resonance.

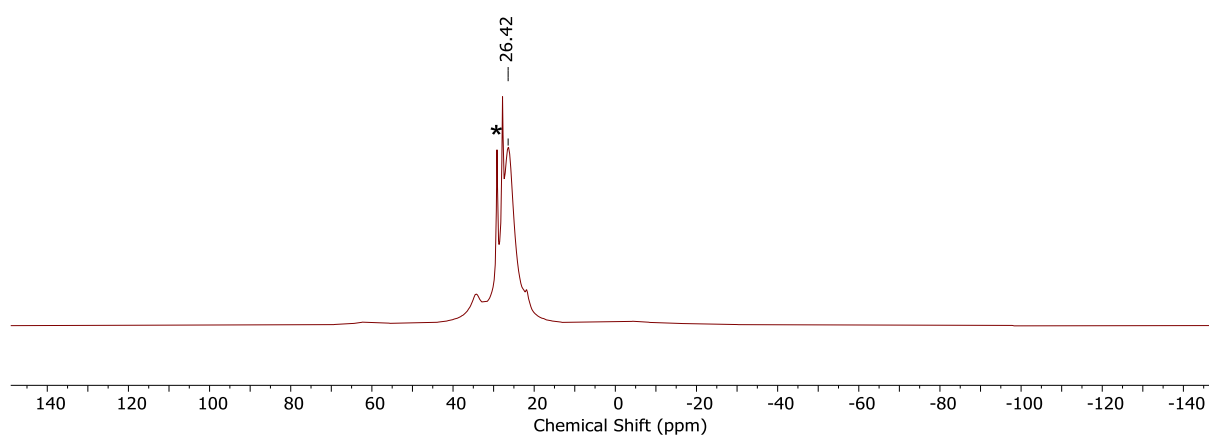
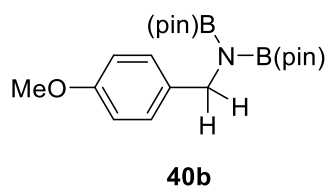


Figure S150. ^{11}B NMR spectrum (C_6D_6) of crude **39b**. * = HB(pin).

6.6.3. **40b** – N-(4-methoxybenzyl)-4,4,5,5-tetramethyl-N-(4,4,5,5-tetramethyl-1,3,2-dioxaborolan-2-yl)-1,3,2-dioxaborolan-2-amine



^1H NMR (400 MHz, 298 K, C_6D_6): δ = 6.86 – 7.58 (m, 4H, Ar), 4.58 (s, 2H, NCH_2), 3.35 (s, 3H, CH_3), 1.05 (s, 24H, Bpin) ppm.

^{11}B NMR (128 MHz, 298 K, C_6D_6): δ = 26.6 (s) ppm.

Mass spectrometry (APCI): $\text{C}_{20}\text{H}_{33}\text{B}_2\text{NO}_5 + \text{H}$ ($[\text{M} + \text{H}]^+$); Calcd. = 390.2618, Found = 390.2616.

Conversion: 66%

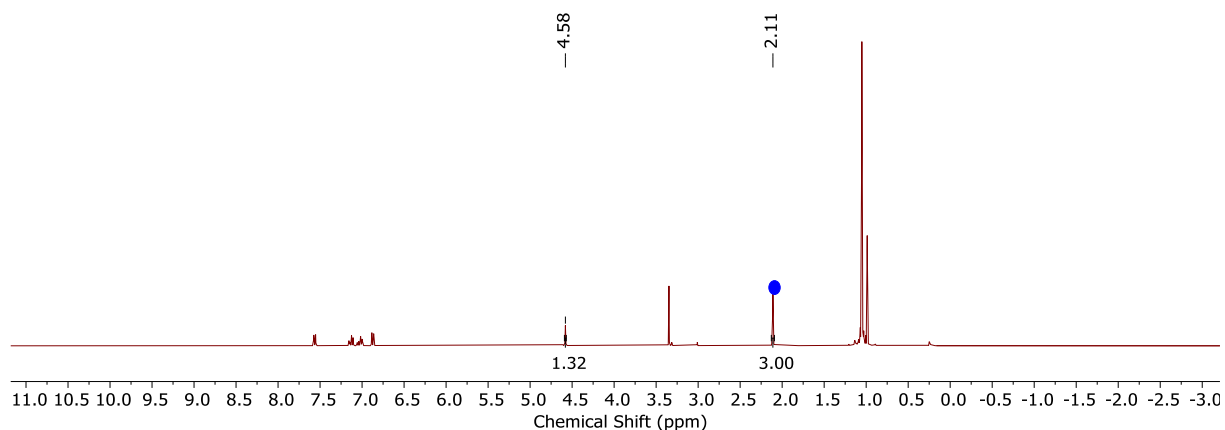


Figure S151. ^1H NMR spectrum (C_6D_6) of crude **40b**. ● = toluene internal standard resonance.

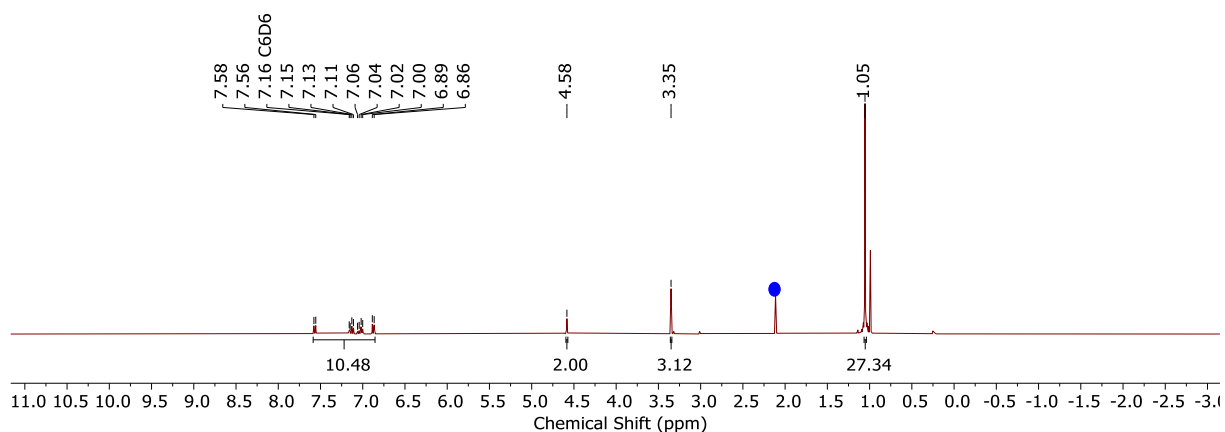


Figure S152. ^1H NMR spectrum (C_6D_6) of crude **40b**. • = toluene internal standard resonance.

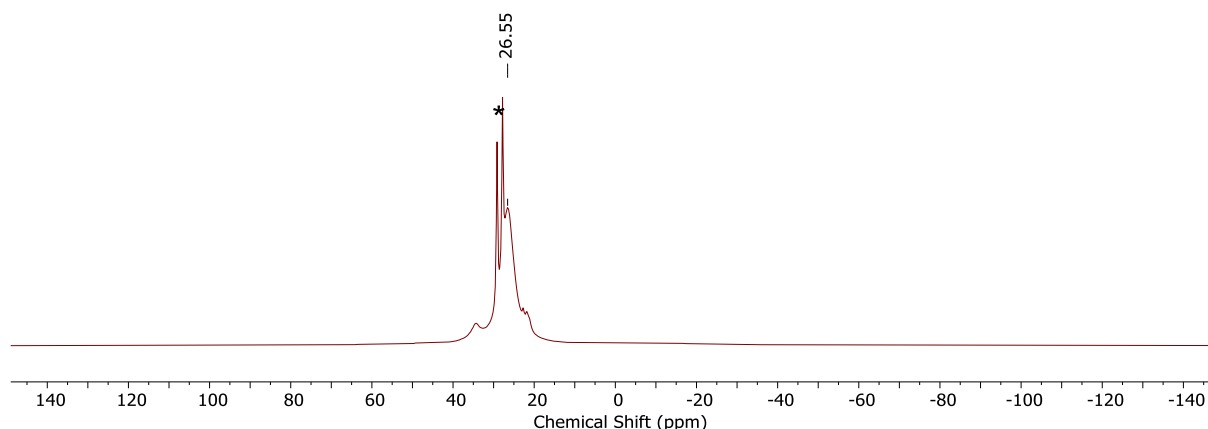
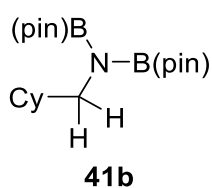


Figure S153. ^{11}B NMR spectrum (C_6D_6) of crude **40b**. * = HB(pin).

6.6.4. **41b** – N-(cyclohexylmethyl)-4,4,5,5-tetramethyl-N-(4,4,5,5-tetramethyl-1,3,2-dioxaborolan-2-yl)-1,3,2-dioxaborolan-2-amine



^1H NMR (400 MHz, 298 K, C_6D_6): $\delta = 3.34$ (d, $^3J_{\text{HH}} = 7.16$ Hz, 2H, NCH_2), 1.89 – 1.95 (m, 2H, Cy), 1.70 – 1.80 (m, 5H, Cy), 1.14 – 1.33 (m, 4H, Cy), 1.08 (s, 24H, Bpin) ppm.

^{11}B NMR (128 MHz, 298 K, C_6D_6): $\delta = 26.3$ (s) ppm.

Mass spectrometry (APCI): $\text{C}_{19}\text{H}_{37}\text{B}_2\text{NO}_4 + \text{H}$ ($[\text{M} + \text{H}]^+$); Calcd. = 366.2981, Found = 366.2987.

Conversion: 74%

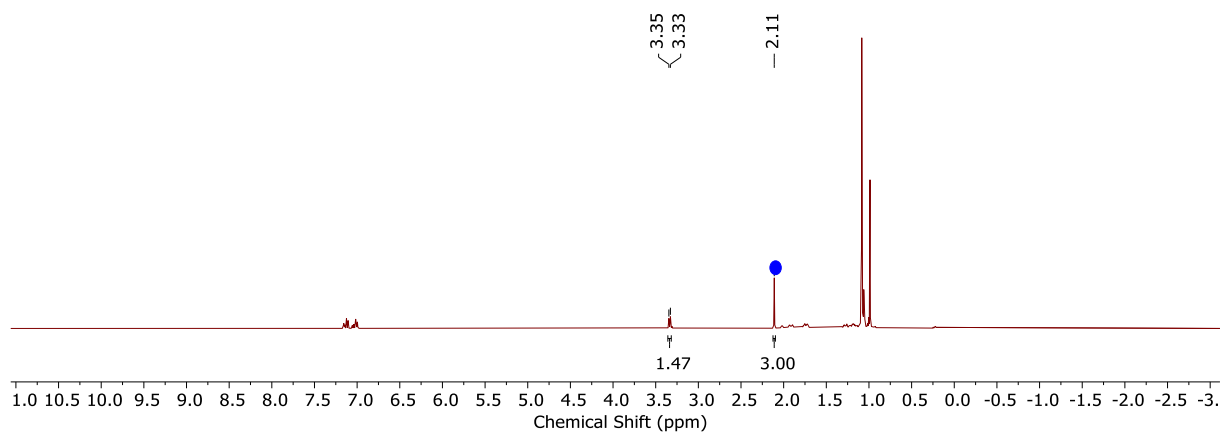


Figure S154. ^1H NMR spectrum (C_6D_6) of crude **41b**. • = toluene internal standard resonance.

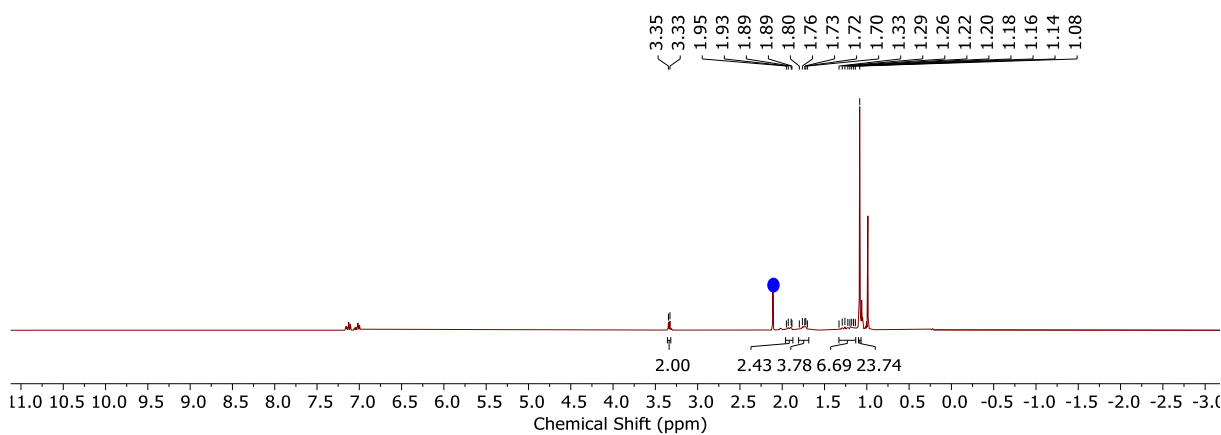


Figure S155. ^1H NMR spectrum (C_6D_6) of crude **41b**. • = toluene internal standard resonance.

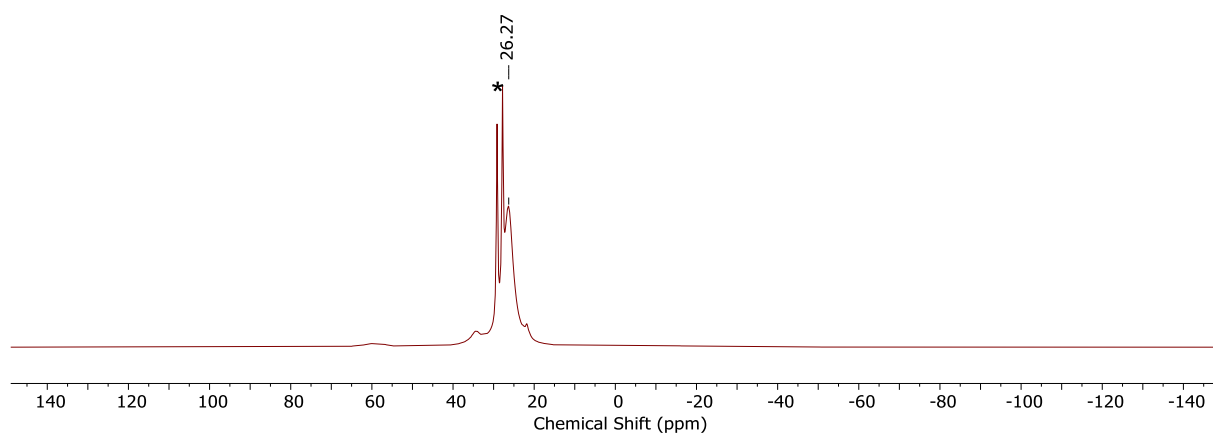
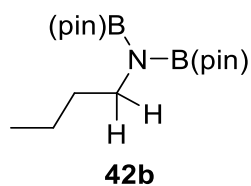


Figure S156. ^{11}B NMR spectrum (C_6D_6) of crude **41b**. * = HB(pin).

6.6.5. **42b** – N-butyl-4,4,5,5-tetramethyl-N-(4,4,5,5-tetramethyl-1,3,2-dioxaborolan-2-yl)-1,3,2-dioxaborolan-2-amine



^1H NMR (400 MHz, 298 K, C_6D_6): $\delta = 3.47$ (t, $^3J_{\text{HH}} = 7.0$ Hz, 2H, NCH_2), 1.75 (m, 2H, CH_2), 1.43 (m, 2H, CH_2), 1.08 (s, 24H, Bpin), 0.96 (t, $^3J_{\text{HH}} = 7.4$ Hz, 3H, CH_3) ppm.

^{11}B NMR (128 MHz, 298 K, C_6D_6): $\delta = 26.33$ (s) ppm.

Mass spectrometry (APCI): $\text{C}_{16}\text{H}_{33}\text{B}_2\text{NO}_4 + \text{H}$ ($[\text{M} + \text{H}]^+$); Calcd. 326.2668, Found = 326.2658.

Conversion: 95%

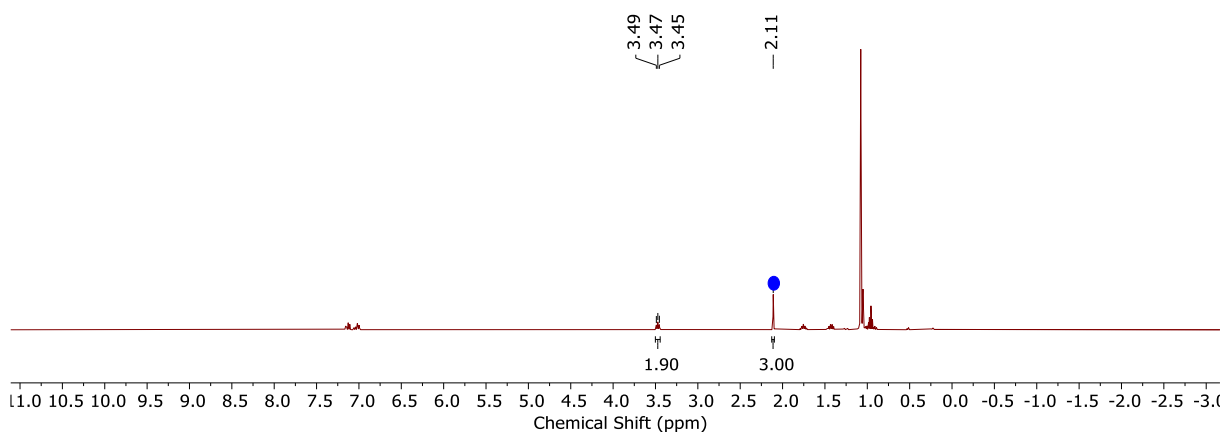


Figure S157. ^1H NMR spectrum (C_6D_6) of crude **42b**. ● = toluene internal standard resonance.

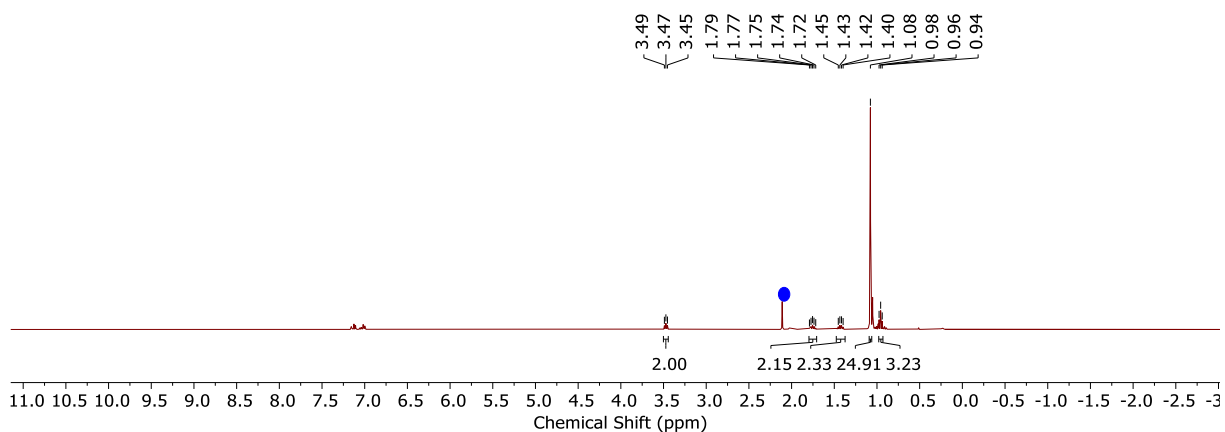


Figure S158. ^1H NMR spectrum (C_6D_6) of crude **42b**. • = toluene internal standard resonance.

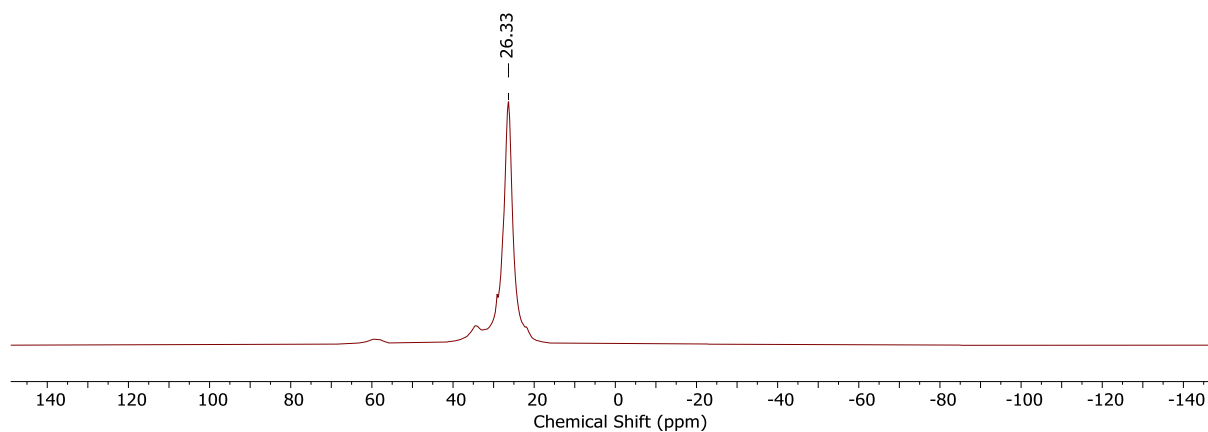
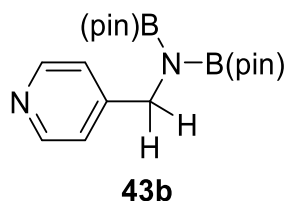


Figure S159. ^{11}B NMR spectrum (C_6D_6) of crude **42b**.

6.6.6. **43b** - 4,4,5,5-tetramethyl-N-(pyridin-4-ylmethyl)-N-(4,4,5,5-tetramethyl-1,3,2-dioxaborolan-2-yl)-1,3,2-dioxaborolan-2-amine



^1H NMR (400 MHz, 298 K, C_6D_6): δ = 8.61 (d, $^3J_{\text{HH}}$ = 5.7 Hz, 1H, *Py*), 8.13 (d, $^3J_{\text{HH}}$ = 6.0 Hz, 1H, *Py*), 7.15 (m, 1H, *Py*), 6.42 (d, $^3J_{\text{HH}}$ = 6.0 Hz, 1H, *Py*), 4.40 (s, 2H, NCH_2), 1.00 (s, 24H, *Bpin*) ppm.

^{11}B NMR (128 MHz, 298 K, C_6D_6): δ = 24.0 (s) ppm.

Mass spectrometry (ESI): $\text{C}_{18}\text{H}_{30}\text{B}_2\text{N}_2\text{O}_4+\text{Na}$ ($[\text{M}+\text{Na}]^+$); Calcd. = 383.23, Found = 383.33

Conversion: 16%

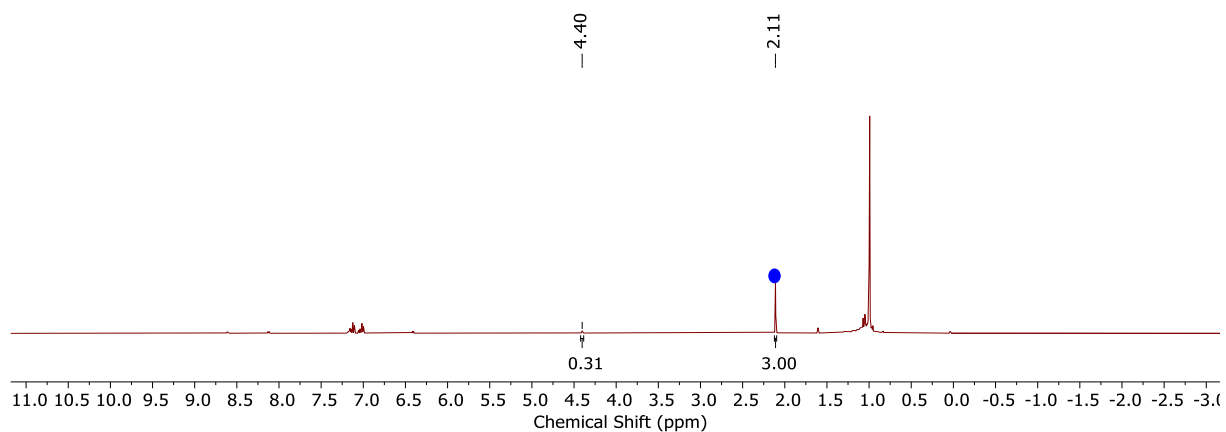


Figure S160. ^1H NMR spectrum (C_6D_6) of crude **43b**. ● = toluene internal standard resonance.

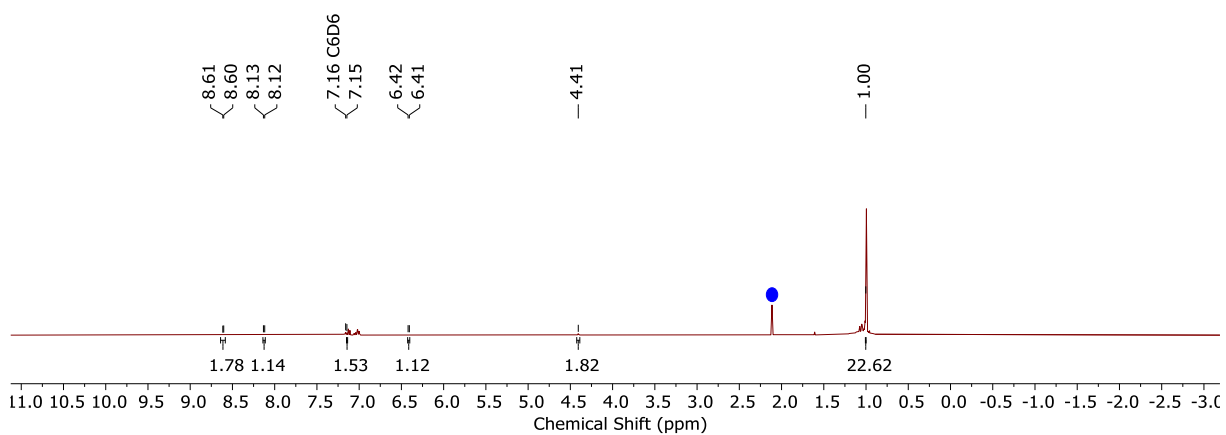


Figure S161. ^1H NMR spectrum (C_6D_6) of crude **43b**. ● = toluene internal standard resonance.

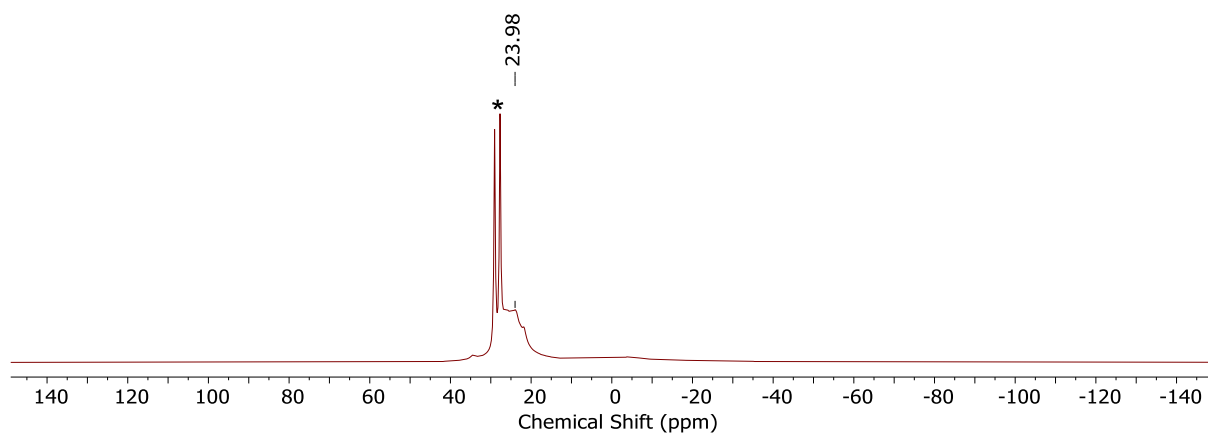
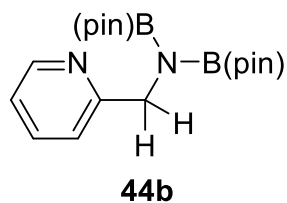


Figure S162. ^{11}B NMR spectrum (C_6D_6) of crude **43b**. * = HB(pin).

6.6.7. **44b** – 4,4,5,5-tetramethyl-N-(pyridin-2-ylmethyl)-N-(4,4,5,5-tetramethyl-1,3,2-dioxaborolan-2-yl)-1,3,2-dioxaborolan-2-amine



^1H NMR (400 MHz, 298 K, C_6D_6): $\delta = 4.90$ (s, 2H, NCH_2), 1.03 (s, 24H, *Bpin*) ppm; pyridine *CH* could not be identified due to low conversion.

^{11}B NMR (128 MHz, 298 K, C_6D_6): $\delta = 25.7$ ppm.

Mass spectrometry (ESI): $\text{C}_{18}\text{H}_{30}\text{B}_2\text{N}_2\text{O}_4 + \text{H}$ ($[\text{M} + \text{H}]^+$); Calcd. = 361.25, Found = 361.17

Conversion: 10%

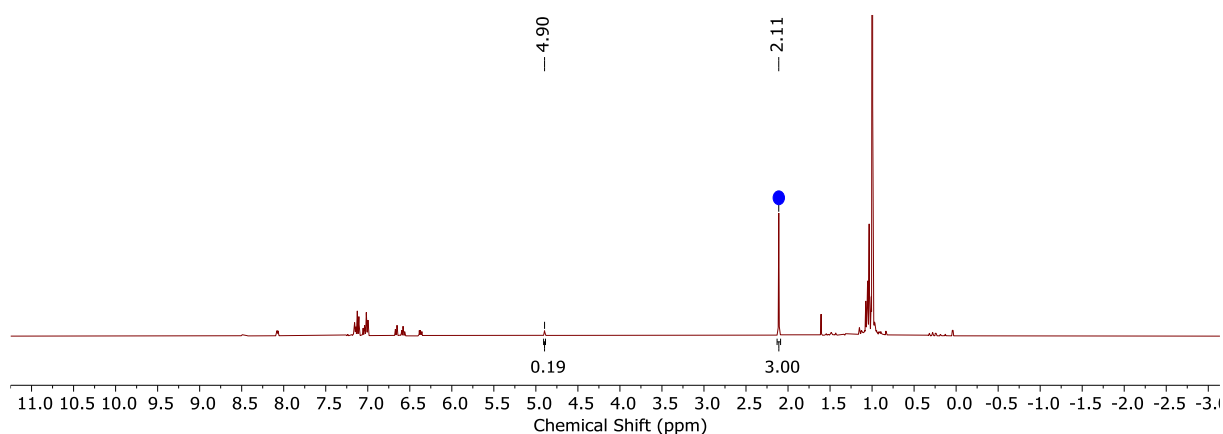


Figure S163. ^1H NMR spectrum (C_6D_6) of crude **44b**. ● = toluene internal standard resonance.

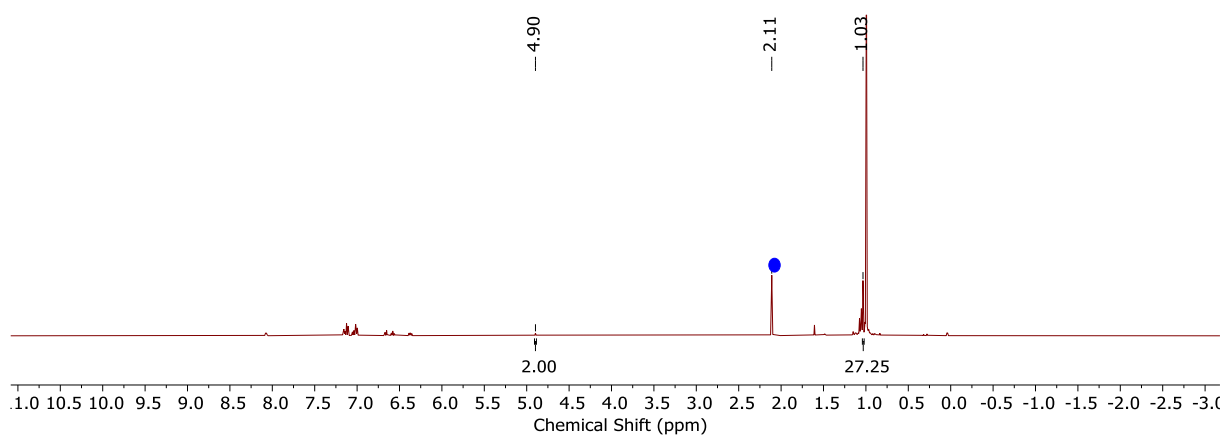


Figure S164. ^1H NMR spectrum (C_6D_6) of crude **44b**. • = toluene internal standard resonance.

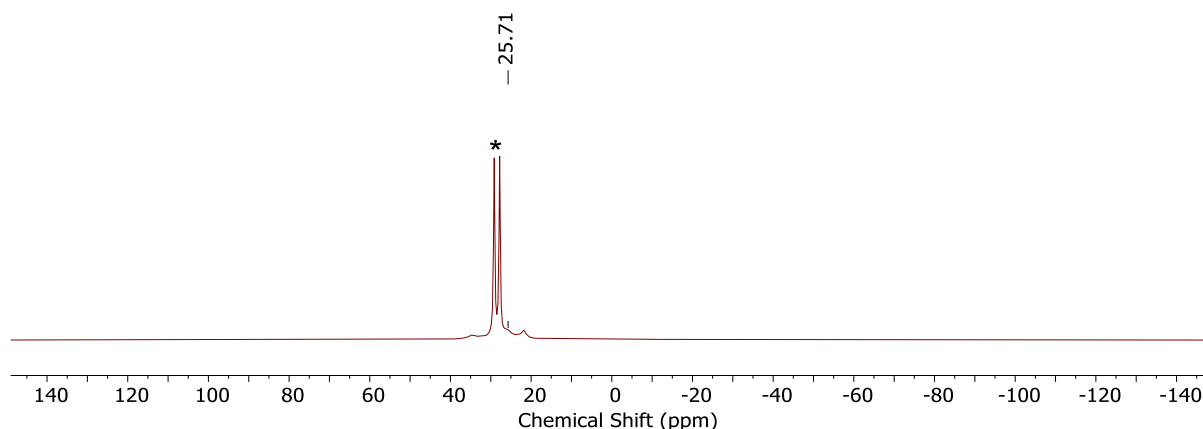


Figure S165. ^{11}B NMR spectrum (C_6D_6) of crude **44b**. * = HB(pin).

7. Studies into Catalyst-Product Interactions

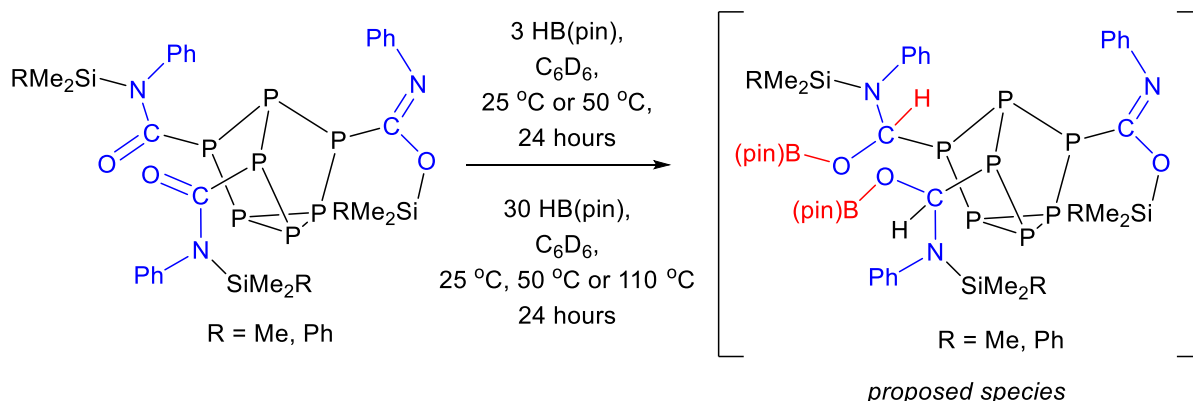
We observed consistent low conversions in the hydroboration of isocyanates (average = 42 %), with a second ^{11}B NMR signal with a δ of ~ 21 ppm can also be observed. A signal in this region has also been reported by other groups who have investigated isocyanate hydroboration, and was left unidentified.¹⁴

Here we probe the identity of this signal.

Test 1: (pin)B–O–B(pin)

(pin)B–O–B(pin) is a possible by-product from isocyanate deoxygenation. However, we do not believe that the signal at ~ 21 ppm in the ^{11}B NMR spectrum is (pin)B–O–B(pin), because no (pin)B–O–B(pin) could be detected by MS of these reaction mixtures. Further, no evidence for deoxygenation could be observed by ^1H NMR spectroscopy of these reactions.

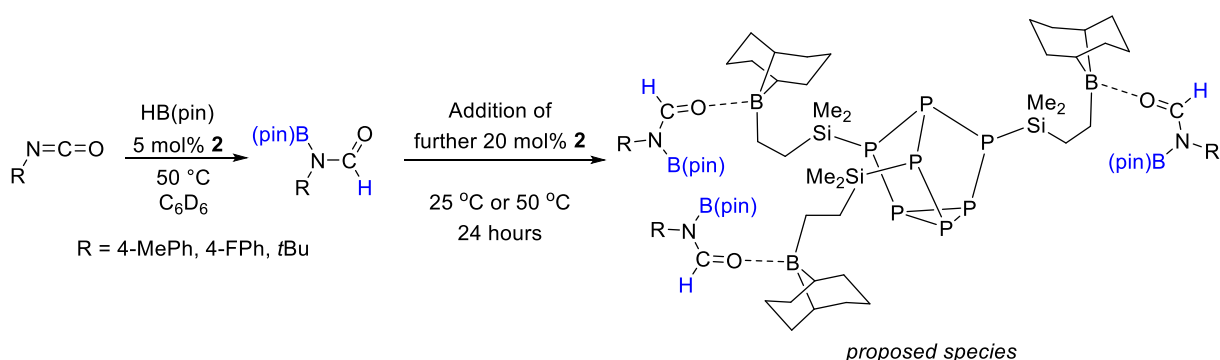
Test 2: Insertion of Isocyanate into the P–Si Bonds of the Catalyst and Reaction with HB(pin)



Scheme S8. Postulated reaction of HB(pin) with inserted isocyanates.

We have previously demonstrated insertion into the P–Si bonds of silyl functionalized P_7 clusters is possible.²⁰ Previously prepared, N,N,O-bound $(\text{PhNCO-SiMe}_3)_3(\text{P}_7)$ (15 mg, 0.02 mmol) and $(\text{PhNCO-SiMe}_2\text{Ph})_3(\text{P}_7)$ (15 mg, 0.015 mmol) were dissolved in C_6D_6 (0.5 mL), transferred to a J Young NMR tube and three equivalents of HB(pin) was added. The reaction was sequentially monitored after 24 hours at 25 °C and 50 °C by ^1H , ^{11}B , and ^{31}P NMR spectroscopy where no changes were observed. To mimic the catalytic nature of our hydroboration reactions we added an additional 27 equivalents of HB(pin) to the reaction mixture and monitored the reaction in the same manner, and again no reaction was observed by NMR spectroscopy. Further, stoichiometric studies between phenyl isocyanate and catalyst **2**, showed no change in the ^{31}P or ^{29}Si NMR spectra, consistent with no isocyanate insertion.

Test 3: Interaction of catalyst **2** with hydroborated isocyanate product.



Scheme S9. Proposed interaction of hydroborated isocyanate with catalyst **2**.

Because the integration of the signal at 21 ppm in the ^{11}B NMR spectrum was approximately 15% or under, and our loading of catalyst Lewis acidic sites is 15% we postulated is this signal is the result of catalyst-product coordination. Under the reaction conditions discussed in section 4, once hydroboration of 4-MePhN(B(pin))CHO (**15b**), 4-FPhN(B(pin))CHO (**17b**) and *t*BuN(B(pin))CHO (**20b**) substrates was completed, an additional 16.8 mg (20 mol%) of catalyst **2** was added to each of the reaction mixtures. The reaction was then monitored at 25 °C by ^1H , ^{11}B , and ^{31}P NMR spectroscopy. In the ^1H NMR spectra of all case, we see a decrease in the CH_3 signal of the B(pin) moiety (12H) of **15b**, **17b**, and **20b** (products) to the proposed interaction. Further, we see the relative intensities of the product signal in ^{11}B NMR spectrum decrease, while the resonance at 21 ppm increase. From these results, we speculate the resonance at 21 ppm is the adduct between catalyst **2** and the isocyanate hydroborated product, as shown in Scheme S9.

Similarly, there are small unidentified ^{11}B NMR resonances from the hydroboration of alkynes. Similar testing to isocyanates indicated no interaction with the catalyst and alkyne hydroborate products. Further, these unidentified ^{11}B NMR resonance are not consistent with previously reported branched alkene or *cis*-alkene products.^{21, 22}

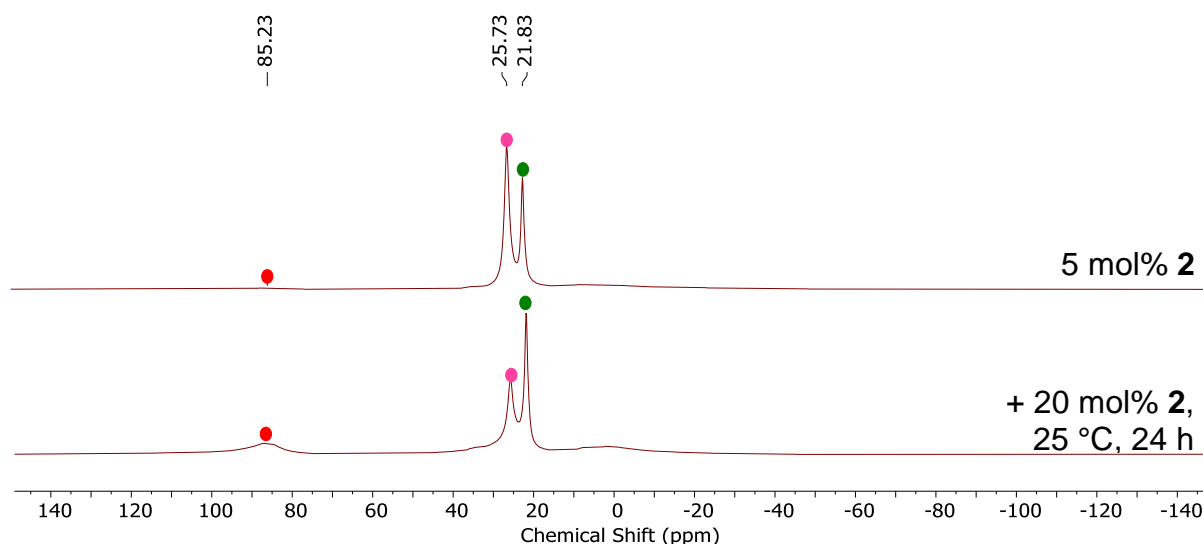
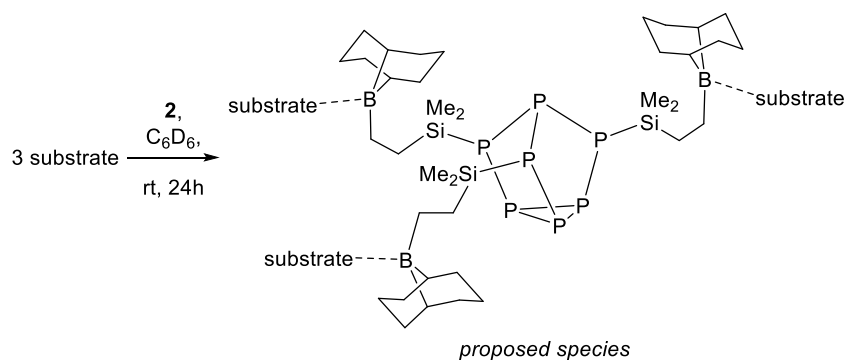


Figure S166. Stacked ^{11}B NMR spectra in C_6D_6 of crude **15b** and the changes with an increase in catalyst loading. ● = “free” hydroborated product (**15b**), ● = proposed adduct of **15b** with catalyst **2**, ● = catalyst **2**.

8. Studies into Catalyst-Substrate Interactions

Coordination of substrate to the Lewis acidic site was probed by ^{11}B NMR spectroscopy. Compound **2** (30 mg, 0.036 mmol) in C_6D_6 (0.5 mL) was reacted with three equivalents of substrate (0.108 mmol). The reaction was monitored by ^1H , ^{11}B , $^{29}\text{Si}\{^1\text{H}\}$, and ^{31}P NMR spectroscopy at room temperature.



Scheme S10. Proposed interaction of 3 equivalents of substrate with catalyst **2**.

We observed no interactions by NMR spectroscopy between catalyst **2** and substrates **5a** – **8a** or HB(pin). In the case of HB(pin), the NMR spectrum was also collected in d_8 -toluene at $-70\text{ }^\circ\text{C}$ after cooling the sample in the instrument for 1 hour and again no adduct formation or change could be detected by ^1H , ^{31}P or ^{11}B NMR spectroscopy. Substrates **4a** (diisopropylcarbodiimide) and **9a** (benzonitrile) do show a detectable interaction by ^{11}B NMR spectroscopy with a small shift from 86.5 ppm (**2**) to 74.9 ppm (**2** + 3 eq **4a**) or 80.3 ppm (**2** + 3 eq **9a**).

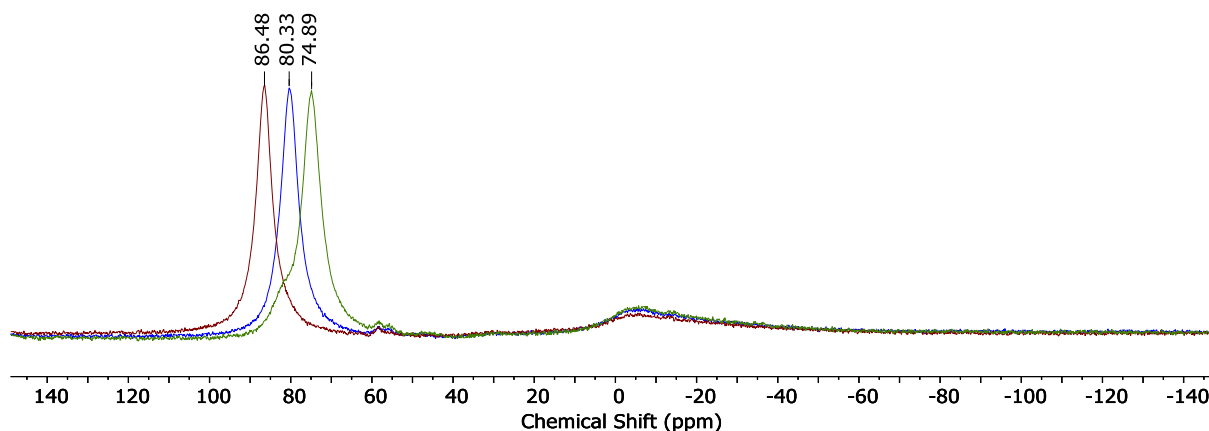


Figure S167. Overlaid ^{11}B NMR spectra in C_6D_6 of **2** (red), **2** + 3 PhCN (**9a**, blue) and **2** + 3 $i\text{PrNCNiPr}$ (**4a**, green).

9. Testing for Hidden Catalysis

Thomas and co-workers have previously reported the ‘hidden role’ that BH_3 can play in hydroboration catalysis when $\text{HB}(\text{pin})$ is used as the hydroborating agent in the presence of a Lewis acid catalyst.²³ First, the commercial pinacol borane was investigated by NMR spectroscopy for contaminants, none were found. Next, benzonitrile (**9a**) converted to **9b** using catalysts **2** 120h at 110 °C. These are the harshest conditions employed when investigating **2** as a hydroboration catalyst with $\text{HB}(\text{pin})$. The reaction mixture was investigated by NMR spectroscopy. Next, an excess of tetramethylethylenediamine (TMEDA) was added to the reaction mixture and investigated by NMR spectroscopy. To allow for direct comparisons of the NMR spectra, the $\text{TMEDA}\cdot\text{BH}_3$ adduct was independently prepared by reaction of excess TMEDA with $\text{BH}_3\cdot\text{SMe}_2$. No evidence of $\text{TMEDA}\cdot\text{BH}_3$ or any other borohydride was detected during the catalysis.

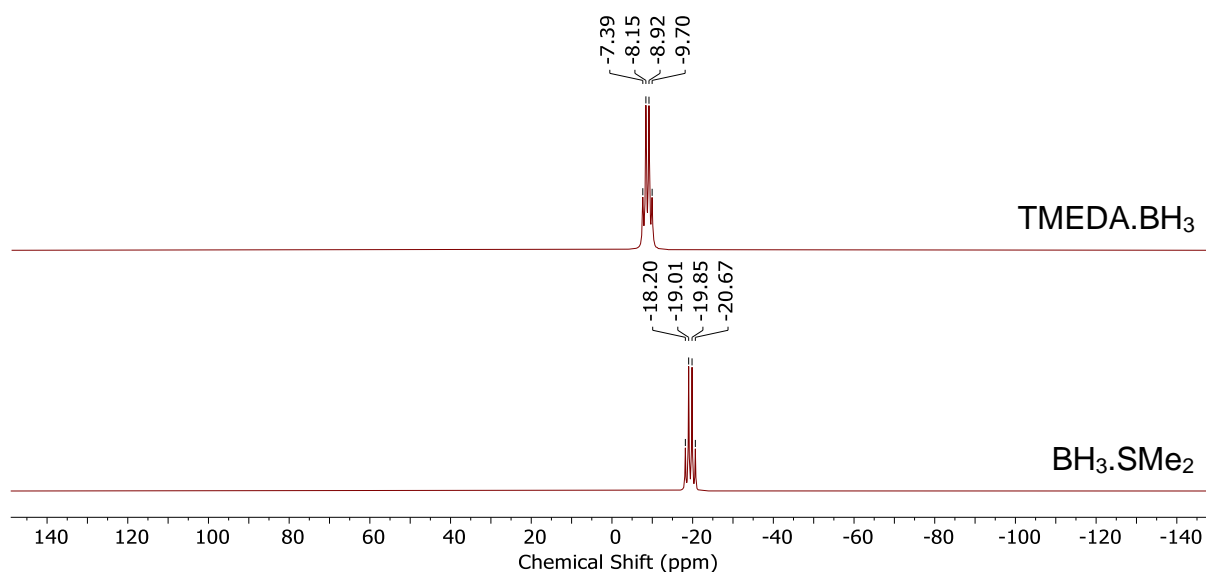


Figure S168. ^{11}B NMR spectra in C_6D_6 of $\text{TMEDA}\cdot\text{BH}_3$ (top) and $\text{BH}_3\cdot\text{SMe}_2$ (bottom). $\text{TMEDA}\cdot\text{BH}_3$: δ -8.53 (q, $^1J_{\text{BH}} = 95.8$ Hz); $\text{BH}_3\cdot\text{SMe}_2$: δ -19.43 (q, $^1J_{\text{BH}} = 105.9$ Hz).

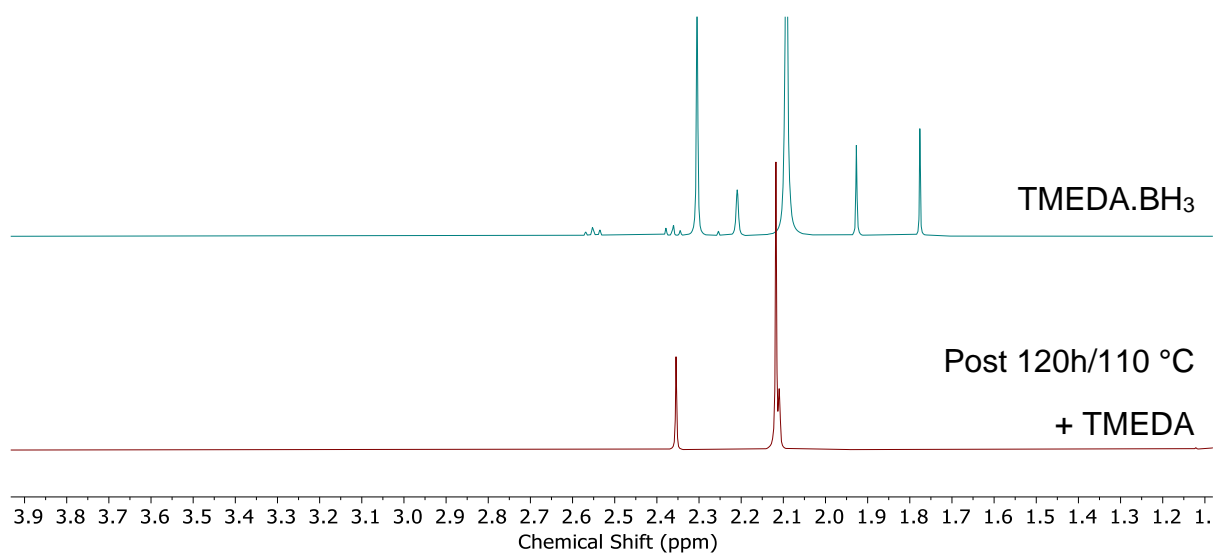


Figure S169. ^1H NMR spectra in C_6D_6 of **9a** catalyzed to **9b** by catalyst **2** (5 mol%) followed by TMEDA addition (red); ^1H NMR spectra in C_6D_6 of $\text{TMEDA}\cdot\text{BH}_3$ (blue).

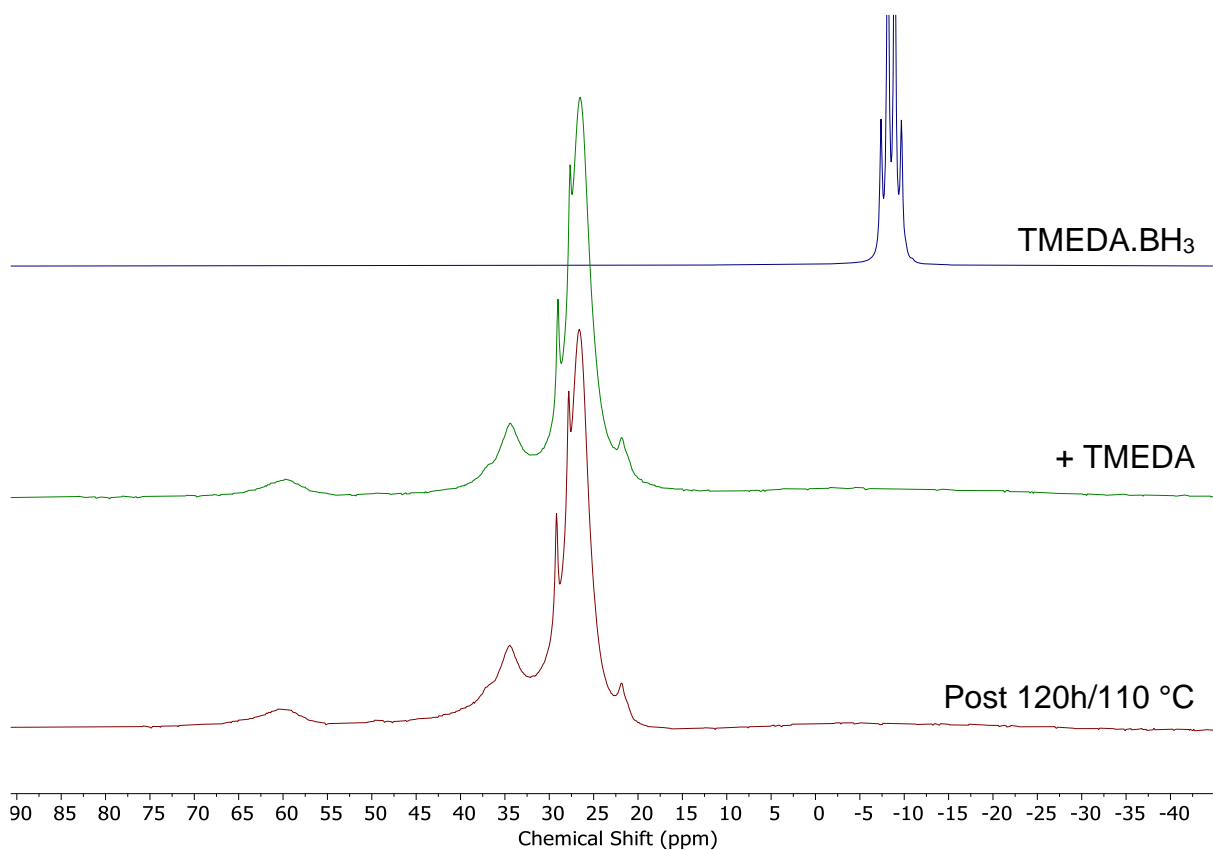


Figure S170. ^{11}B NMR spectra in C_6D_6 of **9a** catalyzed to **9b** by catalyst **2** (5 mol%) (red); ^{11}B NMR spectra in C_6D_6 of **9a** catalyzed to **9b** by catalyst **2** (5 mol%) and subsequent addition of TMEDA (green); ^{11}B NMR spectra of $\text{TMEDA}\cdot\text{BH}_3$ (blue).

10. Catalyst Recycling

We investigated the ability to recycle catalyst **2** with the hydroboration of diisopropylcarbodiimide (**4a**). Following the general procedure outlined in section 4, once hydroboration of **4a** was complete we reloaded the reaction mixture with more substrates and reused the catalyst. We repeated this for a total of 9 cycles, after which catalyst **2** could no longer be reliably detected by $^{31}\text{P}\{^1\text{H}\}$ NMR spectroscopy. One equivalent of toluene was added in the first cycle and was used as the internal reference standard throughout.

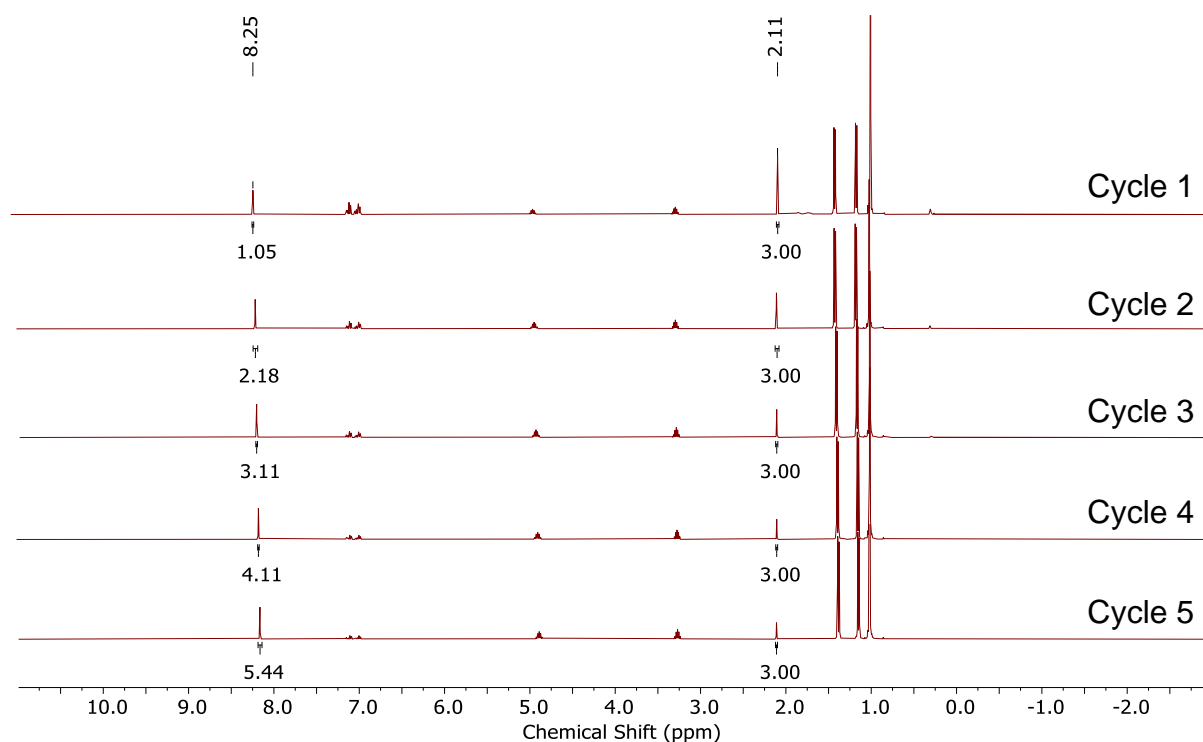


Figure S171. Stacked ^1H NMR spectra in C_6D_6 of cycle 1 – 5 of diisopropylcarbodiimide (**4a**) hydroboration. δ 8.25 ppm = $i\text{PrN}(\text{B}(\text{pin})\text{CHN}i\text{Pr})$ (1H, **4b**); δ 2.11 ppm = toluene internal standard resonance.

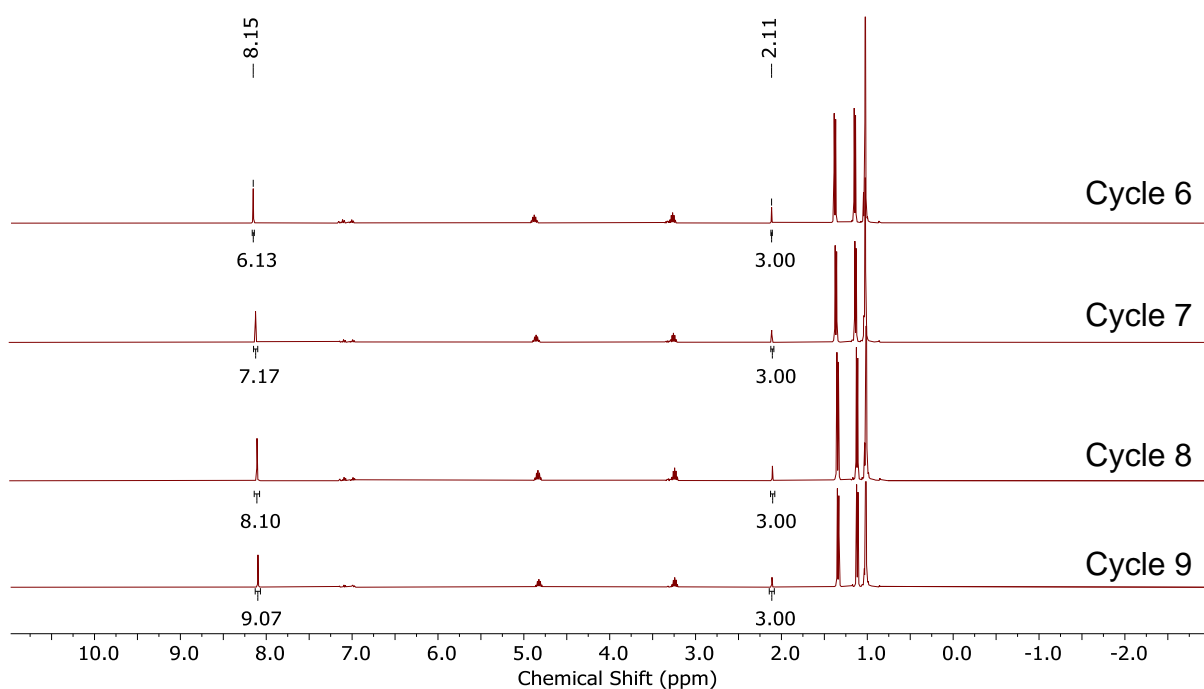


Figure S172. Stacked ^1H NMR spectra in C_6D_6 of cycle 6 – 9 of diisopropylcarbodiimide (**4a**) hydroboration. δ 8.15 ppm = $i\text{PrN}(\text{B}(\text{pin})\text{CHN})\text{Pr}$ (1H, **4b**); δ 2.11 ppm = toluene internal standard resonance.

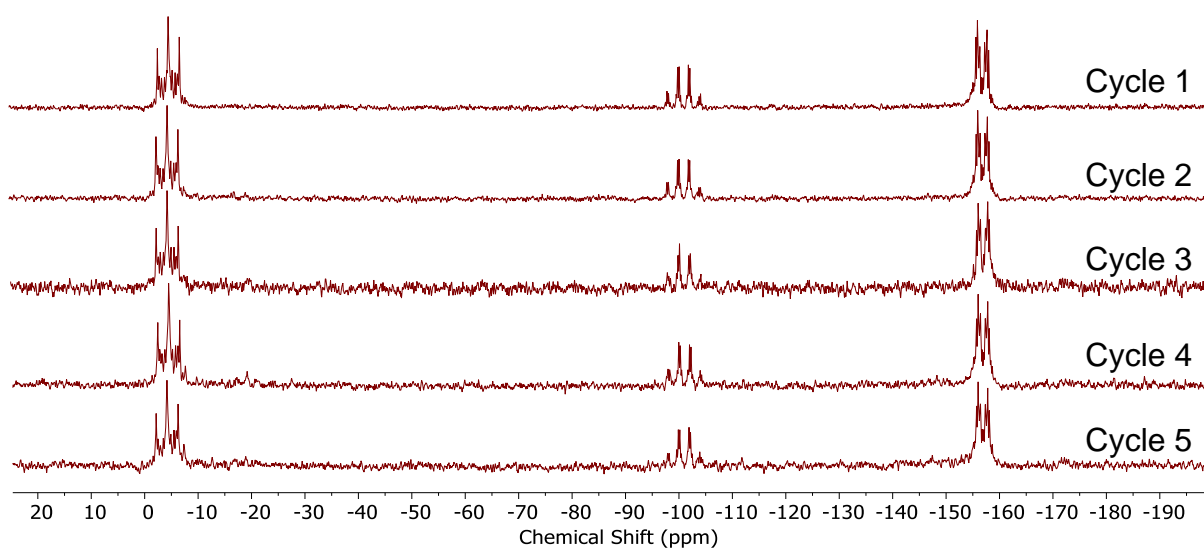


Figure S173. Stacked $^{31}\text{P}\{^1\text{H}\}$ NMR spectra in C_6D_6 of cycle 1 – 5 of diisopropylcarbodiimide (**4a**) hydroboration.

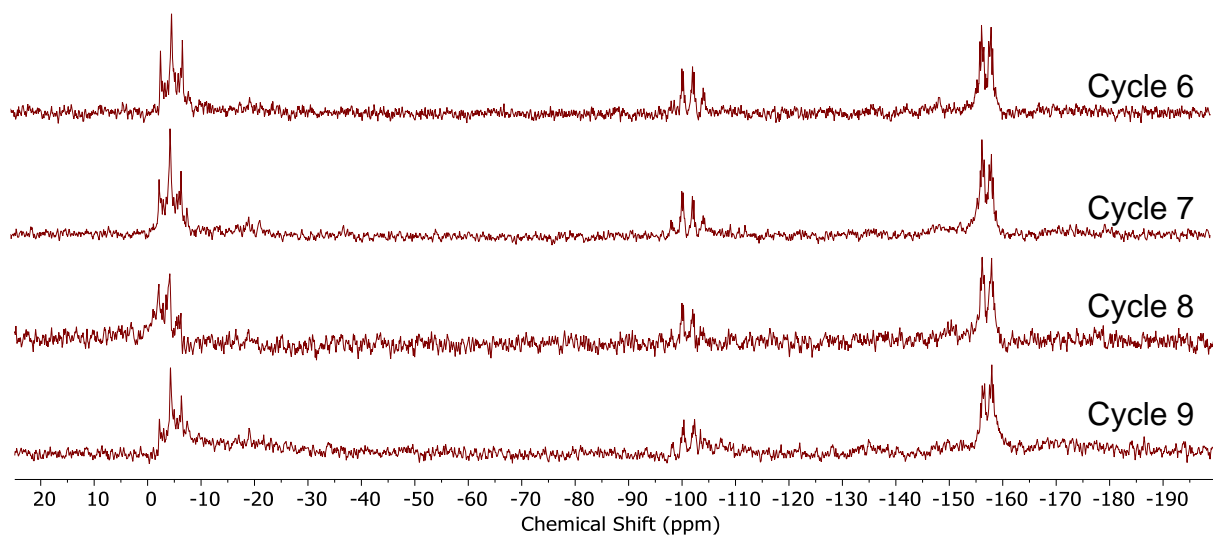


Figure S174. Stacked $^{31}\text{P}\{^1\text{H}\}$ NMR spectra in C_6D_6 of cycle 6 – 9 of diisopropylcarbodiimide (**4a**) hydroboration.

11. Crystallographic Data

Table S5. Crystallographic data for **1** and **2**.

	P ₇ (SiMe ₂ CHCH ₂) ₃ (1)	P ₇ (SiMe ₂ CH ₂ CH ₂ BBN) ₃ (2)
Formula	C ₁₂ H ₂₇ P ₇ Si ₃	C _{37.67} H ₇₆ B ₃ P ₇ Si ₃
Fw	472.39	862.45
cryst size, mm	0.521 x 0.193 x 0.161	0.205 x 0.085 x 0.029
cryst syst	monoclinic	triclinic
space group	P121/c1	P-1
collection temperature, K	100.00(10)	100.00(14)
a, Å	6.8678(3)	6.7553(2)
b, Å	18.0666(9)	19.7337(10)
c, Å	19.2147(10)	20.2549(11)
α, °	90	118.487(6)
β, °	96.980(5)	90.481(3)
γ, °	90	90.417(3)
V, Å ³	2366.4(2)	2372.9(2)
Z	4	2
ρ _{calcd} , g cm ⁻³	1.326	1.207
μ, mm ⁻¹	0.668	3.340
no. of reflections made	11320	31328
no. of unique reflns, R _{int}	5447, 0.0428	9147, 0.0990
no. of reflns with F ² > 2σ(F ²)	3974	6867
transmn coeff range	0.51249-1.00000	0.75897-1.00000
R, R _w ^a (F ² > 2σ(F ²))	0.0430, 0.0842	0.1272, 0.3401
R, R _w ^a (all data)	0.0697, 0.0982	0.1502, 0.3568
S ^a	1.022	1.050
Parameters	253, 160	657, 1423
max., min. diff map, e Å ⁻³	0.513, -0.362	1.344, -0.891
CCDC	2192816	2192817

^a Conventional R = $\sum||F_o| - |F_c||/\sum|F_o|$; R_w = $[\sum w(F_o^2 - F_c^2)^2/\sum w(F_o^2)^2]^{1/2}$; S = $[\sum w(F_o^2 - F_c^2)^2/\text{no. data} - \text{no. params}]^{1/2}$ for all data.

12. Geometry Optimized Structures

12.1. CF₂O

Charge = 0 Multiplicity = 1

O	-0.0466230000	-0.7269130000	0.7078620000
C	-0.0198320000	0.4570640000	0.6604760000
F	-1.0755860000	1.2641720000	0.6177690000
F	1.0710410000	1.2166780000	0.6398920000

12.2. [CF₃O]⁻

Charge = -1 Multiplicity = 1

O	-0.0024660000	-0.0727380000	0.7919310000
C	-0.0077480000	-1.2197580000	1.2200720000
F	-0.0372870000	-1.3904350000	2.6566080000
F	1.1166540000	-2.0616680000	0.8724600000
F	-1.1111530000	-2.0694010000	0.8259280000

12.3. B(C₆F₅)₃

Charge = 0 Multiplicity = 1

B	-0.1527200000	0.4557970000	-0.1605200000
C	-0.5860590000	1.3581700000	-1.3766080000
C	-0.1083040000	-1.1107320000	-0.3176840000
C	0.2355380000	1.1209860000	1.2133700000
C	-0.0238350000	-3.9535890000	-0.6022600000
C	0.3991710000	-3.1282370000	-1.6617220000
C	0.3396250000	-1.7339100000	-1.5065250000
C	-0.5130710000	-1.9823330000	0.7209530000
C	-0.4887670000	-3.3807870000	0.5971040000
F	0.0160700000	-5.2789060000	-0.7349120000
F	0.8493990000	-3.6771200000	-2.7944170000
F	0.7672890000	-0.9904480000	-2.5413400000
F	-0.9782470000	-1.4844150000	1.8795460000
F	-0.8990550000	-4.1686170000	1.5960760000
C	0.9379580000	2.3272340000	3.7079460000
C	1.6577230000	1.2114750000	3.2392850000
C	1.2910990000	0.6273090000	2.0161560000
C	-0.4498370000	2.2498640000	1.7217490000
C	-0.1271350000	2.8499490000	2.9495890000
F	1.2651870000	2.8894560000	4.8708630000
F	2.6748620000	0.7255680000	3.9577470000
F	2.0184480000	-0.4257380000	1.6056550000
F	-1.4829100000	2.7773710000	1.0427140000
F	-0.8136720000	3.9032240000	3.4036760000
C	-1.3737740000	2.9974720000	-3.5815760000
C	-2.0361030000	1.7786450000	-3.3397880000
C	-1.6274720000	0.9825950000	-2.2575660000
C	0.0416280000	2.5951620000	-1.6551120000
C	-0.3235410000	3.4096670000	-2.7390890000
F	-1.7413530000	3.7617730000	-4.6093870000
F	-3.0391770000	1.3964250000	-4.1365090000
F	-2.3001260000	-0.1641980000	-2.0603520000
F	1.0588850000	3.0253600000	-0.8892410000
F	0.3092550000	4.5625400000	-2.9788190000

12.4. [FB(C₆F₅)₃]⁻

Charge = -1 Multiplicity = 1

B	-1.0312930000	0.2232650000	0.0282600000
C	-0.9890050000	1.2531340000	-1.2823180000
C	-0.3707440000	-1.2773630000	-0.2797500000
C	-0.2759520000	1.0317420000	1.2858070000
C	0.5070170000	-3.9914620000	-0.6547500000
C	0.4773630000	-3.0981990000	-1.7352940000
C	0.0361790000	-1.7742170000	-1.5287690000
C	-0.3270790000	-2.2166340000	0.7693280000
C	0.1011300000	-3.5465250000	0.6148250000
F	0.9186910000	-5.2624450000	-0.8310130000
F	0.8572570000	-3.5187830000	-2.9597680000
F	0.0221920000	-0.9984240000	-2.6379190000
F	-0.6982780000	-1.8584350000	2.0180080000
F	0.1283960000	-4.3989990000	1.6599830000
C	0.8329230000	2.5318650000	3.4745310000
C	1.5555730000	1.4758250000	2.8979060000
C	0.9954700000	0.7624780000	1.8202290000
C	-0.9522780000	2.1116220000	1.8861300000
C	-0.4358920000	2.8532150000	2.9663140000
F	1.3509140000	3.2296770000	4.5048280000
F	2.7781100000	1.1653470000	3.3773000000
F	1.7704130000	-0.2248360000	1.3162040000
F	-2.1605890000	2.5039580000	1.4302660000
F	-1.1318830000	3.8755200000	3.5062330000
C	-0.8508750000	3.1531150000	-3.4367820000
C	-2.0824890000	2.6064350000	-3.0465420000
C	-2.1310160000	1.6724020000	-1.9899130000
C	0.2195170000	1.8229440000	-1.7215220000
C	0.3193290000	2.7532990000	-2.7702760000
F	-0.7891280000	4.0449120000	-4.4458020000
F	-3.2081690000	2.9781200000	-3.6917710000
F	-3.3572600000	1.1913170000	-1.7056160000
F	1.3867140000	1.4601540000	-1.1373620000
F	1.5113150000	3.2615440000	-3.1462110000
F	-2.3785710000	-0.0295660000	0.4192040000

12.5. SbF₅

Charge = 0 Multiplicity = 1

F	-1.9354430000	0.7880830000	0.0118850000
F	0.1865520000	1.0762600000	-1.6358360000
F	-1.0232240000	-1.7224270000	-0.3860040000
F	0.2213570000	0.5881340000	1.6245680000
F	1.5235260000	-0.8318660000	-0.2673920000
Sb	-0.2057670000	-0.0211940000	-0.1292210000

12.6. [SbF₆]⁻

Charge = -1 Multiplicity = 1

F	0.6934610000	1.8491390000	0.2844740000
F	0.2883260000	-0.4182980000	1.7840280000
F	-1.8501630000	0.8765200000	0.6436940000
F	-0.6454980000	0.6963010000	-1.8202990000
F	1.4930270000	-0.5985220000	-0.6799630000
F	-1.0505750000	-1.5711420000	-0.3207950000

Sb -0.1785690000 0.1390010000 -0.0181390000

12.7. MeSi⁺

Charge = +1 Multiplicity = 1

Si	-0.0002000000	-0.0001130000	-0.0000860000
C	-1.8306730000	-0.2180430000	-0.0001470000
C	1.1043370000	-1.4757570000	0.0000570000
C	0.7265010000	1.6938980000	0.0000840000
H	1.7763700000	-1.4347240000	-0.8884030000
H	0.5543200000	-2.4369350000	0.0008830000
H	1.7777070000	-1.4337300000	0.8874080000
H	-2.1314140000	-0.8264600000	-0.8843510000
H	-2.3870780000	0.7394000000	-0.0054770000
H	-2.1314250000	-0.8157220000	0.8914840000
H	0.3534440000	2.2567190000	0.8870480000
H	0.3559000000	2.2553790000	-0.8888160000
H	1.8339950000	1.6970620000	0.0014590000

12.8. MeSiF

Charge = 0 Multiplicity = 1

F	-2.4514360000	-0.5755960000	-1.3668210000
Si	-3.2706670000	0.5824720000	-2.2238730000
C	-2.7366820000	2.2546910000	-1.5424270000
C	-5.1083400000	0.2732700000	-1.9531520000
C	-2.7852850000	0.3766130000	-4.0314760000
H	-5.7247850000	1.0162240000	-2.5030130000
H	-5.3718330000	0.3455110000	-0.8770980000
H	-5.4010510000	-0.7374200000	-2.3071960000
H	-3.2481490000	3.0850840000	-2.0745550000
H	-1.6423760000	2.4030790000	-1.6563780000
H	-2.9807280000	2.3435440000	-0.4630480000
H	-1.6909750000	0.5038270000	-4.1688000000
H	-3.2961870000	1.1270910000	-4.6718380000
H	-3.0595060000	-0.6313930000	-4.4073280000

12.9. ({9-BBN}CH₂CH₂SiMe₂)₃P₇ (2)

Charge = 0 Multiplicity = 1

P	-0.6739050000	0.7135590000	0.5579860000
P	-1.2933050000	-1.0028710000	-0.7200560000
P	-0.3013540000	2.1986540000	-1.0606950000
P	1.4369510000	0.0951840000	0.9047810000
P	1.1122900000	1.1036760000	-2.4121640000
P	2.1197740000	-0.4892570000	-1.1485310000
P	0.2543570000	-0.9951630000	-2.3385080000
Si	-3.2252910000	-0.3225750000	-1.8219680000
Si	1.0572970000	3.8463500000	-0.1309610000
Si	1.3425460000	-1.9430580000	2.0310830000
C	-0.0793020000	-1.8128280000	3.2812880000
C	3.0034050000	-2.0147930000	2.9513840000
C	1.1586390000	-3.4546620000	0.8887680000
C	0.4286990000	4.1624320000	1.6299640000
C	0.7354860000	5.3650920000	-1.2247130000
C	2.9167420000	3.4185870000	-0.1451410000
C	-4.2850820000	0.5660710000	-0.5088940000

C	-4.0319550000	-1.9575730000	-2.3578810000
C	-2.9362710000	0.7658100000	-3.3451620000
H	-4.3171470000	-0.0770770000	0.3991270000
C	-5.7190310000	0.9331640000	-0.9556160000
H	-3.7318830000	1.4805200000	-0.1972370000
H	-2.4309420000	1.7132260000	-3.0676930000
H	-3.9085840000	1.0092570000	-3.8267260000
H	-2.3066810000	0.2449250000	-4.0961300000
H	-4.2311030000	-2.6171190000	-1.4879030000
H	-3.3785080000	-2.5124770000	-3.0632740000
H	-4.9966250000	-1.7649450000	-2.8752460000
H	1.2946920000	6.2459940000	-0.8426180000
H	-0.3434410000	5.6239860000	-1.2394020000
H	1.0570750000	5.1855570000	-2.2720310000
H	3.1871700000	3.1193160000	-1.1833860000
H	3.0525980000	2.5074920000	0.4798480000
C	3.8373910000	4.5855820000	0.3466300000
H	0.9602200000	5.0315840000	2.0738770000
H	0.6019830000	3.2812420000	2.2811310000
H	-0.6576810000	4.3882670000	1.6355460000
H	3.0652900000	-2.9329730000	3.5746560000
H	3.1272900000	-1.1388130000	3.6211220000
H	3.8584400000	-2.0257580000	2.2433490000
H	-0.0747510000	-2.6951840000	3.9572210000
H	-1.0631050000	-1.7740360000	2.7702870000
H	0.0198320000	-0.9037790000	3.9098690000
H	0.2274070000	-3.3180920000	0.2960360000
C	1.1433450000	-4.8231100000	1.6095370000
H	1.9873420000	-3.4159500000	0.1461700000
H	-6.2904180000	0.0211030000	-1.2620490000
H	-5.7056570000	1.5331620000	-1.8999610000
H	3.5513690000	4.8806950000	1.3802960000
H	3.7046140000	5.4703420000	-0.3143170000
H	0.3316390000	-4.8709370000	2.3750980000
H	2.0689420000	-4.9615800000	2.2276870000
B	1.0737620000	-6.1430180000	0.7381240000
C	0.8067370000	-7.5698660000	1.3796640000
H	0.7404110000	-7.5343410000	2.4907980000
C	-0.5943150000	-8.0141450000	0.8475170000
H	-0.8341590000	-9.0354790000	1.2244670000
H	-1.3603400000	-7.3440970000	1.3029570000
C	-0.7557580000	-7.9762350000	-0.6889050000
H	-1.8345430000	-8.0747440000	-0.9427190000
H	-0.2720640000	-8.8673880000	-1.1379250000
C	-0.1991460000	-6.6931920000	-1.3464050000
H	-0.1724260000	-6.8205000000	-2.4534290000
H	-0.9148460000	-5.8586870000	-1.1629980000
C	1.2079580000	-6.2368510000	-0.8363060000
H	1.4241400000	-5.2564110000	-1.3135680000
C	2.3749240000	-7.2060810000	-1.1918310000
H	2.4289130000	-7.3466940000	-2.2962930000
H	3.3288810000	-6.7016310000	-0.9127800000
C	2.3241480000	-8.5857470000	-0.4993350000
H	3.3074360000	-9.0910770000	-0.6249490000
H	1.5977840000	-9.2406330000	-1.0225740000
C	1.9789290000	-8.5242510000	1.0051690000
H	2.8819420000	-8.1846970000	1.5638620000
H	1.7697230000	-9.5528770000	1.3808020000
B	-6.6603680000	1.7164020000	0.0473210000
C	-6.2944850000	2.1921960000	1.5129560000

H	-5.2808830000	1.8678210000	1.8350820000
C	-6.2866230000	3.7551640000	1.4714180000
H	-6.0783730000	4.1564150000	2.4903510000
H	-5.4205230000	4.0747060000	0.8465060000
C	-7.5692690000	4.4078390000	0.9095190000
H	-7.3681970000	5.4823080000	0.7023760000
H	-8.3602740000	4.4088970000	1.6867050000
C	-8.1026400000	3.7386660000	-0.3772220000
H	-9.1217940000	4.1279610000	-0.6061480000
H	-7.4657340000	4.0577430000	-1.2348590000
C	-8.1244530000	2.1764860000	-0.3560350000
H	-8.4149890000	1.8365440000	-1.3758930000
C	-9.1347870000	1.5532750000	0.6539870000
H	-10.1655600000	1.9171910000	0.4354270000
H	-9.1646360000	0.4545150000	0.4677950000
C	-8.8091030000	1.7925060000	2.1450370000
H	-9.4373090000	1.1163300000	2.7662810000
H	-9.1183200000	2.8171980000	2.4355370000
C	-7.3237550000	1.5734480000	2.5073530000
H	-7.1277470000	0.4773580000	2.5578270000
H	-7.1318420000	1.9546140000	3.5371860000
B	5.2863560000	3.9663390000	0.2589380000
C	6.0329520000	3.2593260000	1.4640810000
H	5.3877600000	3.1454710000	2.3638470000
C	6.5365190000	1.8469780000	1.0504440000
H	7.1533420000	1.4041830000	1.8670450000
H	5.6429390000	1.1875620000	0.9625090000
C	7.3264500000	1.7859530000	-0.2765250000
H	7.4114700000	0.7241690000	-0.5974980000
H	8.3716660000	2.1170620000	-0.1061830000
C	6.7003020000	2.6078740000	-1.4255280000
H	7.4269060000	2.6755230000	-2.2686240000
H	5.8287050000	2.0445890000	-1.8304370000
C	6.1994700000	4.0273810000	-1.0343610000
H	5.6738470000	4.4618110000	-1.9142190000
C	7.3330270000	5.0330170000	-0.6356040000
H	8.0587280000	5.1311970000	-1.4759730000
H	6.8728900000	6.0421870000	-0.5220010000
C	8.0888050000	4.6844820000	0.6666620000
H	8.7007780000	5.5606200000	0.9763620000
H	8.8209320000	3.8762810000	0.4685330000
C	7.1665240000	4.2749800000	1.8365910000
H	6.6846960000	5.1918680000	2.2493310000
H	7.7798230000	3.8619590000	2.6708200000

12.10. $[(\{9\text{-BBN}\}\text{CH}_2\text{CH}_2\text{SiMe}_2)_2(\{9\text{-BBN}\}\text{FCH}_2\text{CH}_2\text{SiMe}_2)\text{P}_7]^-$

Charge = -1 Multiplicity = 1

P	-0.1768540000	0.8965930000	0.4641230000
P	-1.1692340000	-0.6307540000	-0.8053860000
P	0.4634900000	2.2877050000	-1.1572530000
P	1.7855690000	-0.1275790000	0.7583610000
P	1.6004650000	0.9443570000	-2.5435670000
P	2.2887600000	-0.8370330000	-1.3093380000
P	0.3212280000	-0.9277470000	-2.4423710000
Si	-3.0674370000	0.3698450000	-1.7649930000
Si	2.1175660000	3.6332680000	-0.2565690000
Si	1.2730150000	-2.0974450000	1.8757980000
C	0.0142080000	-1.6464550000	3.2239320000

C	2.9171900000	-2.6065080000	2.6932840000
C	0.6352660000	-3.5109260000	0.7689370000
C	1.5150030000	4.1944260000	1.4526860000
C	2.1853340000	5.1246050000	-1.4352070000
C	3.8529640000	2.8361420000	-0.1437590000
C	-4.0474380000	1.1511220000	-0.3572230000
C	-3.9405680000	-1.1534280000	-2.4992210000
C	-2.6422780000	1.5704000000	-3.1711900000
H	-4.1956800000	0.3922020000	0.4441740000
C	-5.4325590000	1.6815490000	-0.8071790000
H	-3.4417400000	1.9639400000	0.1041380000
H	-2.0226490000	2.4150350000	-2.8068380000
H	-3.5903090000	1.9818120000	-3.5808090000
H	-2.0948630000	1.0650670000	-3.9938600000
H	-4.1767240000	-1.8953340000	-1.7086990000
H	-3.3252800000	-1.6506150000	-3.2782910000
H	-4.8989860000	-0.8360460000	-2.9632570000
H	2.8987470000	5.8916410000	-1.0643020000
H	1.1850330000	5.5976200000	-1.5204930000
H	2.5053670000	4.8202540000	-2.4539060000
H	4.0804300000	2.3791190000	-1.1332750000
H	3.7710250000	1.9845120000	0.5686540000
C	4.9842070000	3.8362330000	0.2741890000
H	2.2020430000	4.9591080000	1.8752450000
H	1.4650110000	3.3409510000	2.1597370000
H	0.5019290000	4.6426010000	1.3874200000
H	2.7759090000	-3.5067490000	3.3301930000
H	3.3107060000	-1.7917900000	3.3361410000
H	3.6904960000	-2.8445940000	1.9328500000
H	-0.1749030000	-2.5198890000	3.8851410000
H	-0.9526560000	-1.3313950000	2.7799940000
H	0.3859930000	-0.8148740000	3.8578210000
H	-0.2949400000	-3.1424480000	0.2829640000
C	0.3828890000	-4.8539380000	1.4900420000
H	1.3636310000	-3.6469550000	-0.0624800000
H	-5.9710000000	0.8897220000	-1.3844150000
H	-5.3018500000	2.5353460000	-1.5117350000
H	4.7276300000	4.3179000000	1.2434760000
H	5.0722940000	4.6351550000	-0.4949240000
H	-0.3377630000	-4.7207720000	2.3385150000
H	1.2995320000	-5.2219580000	2.0145460000
B	-0.2073190000	-6.0682640000	0.6681720000
C	-0.3797870000	-7.5141880000	1.3051010000
H	-0.0539800000	-7.5522530000	2.3696260000
C	-1.8939490000	-7.8835880000	1.2640430000
H	-2.0442280000	-8.9220730000	1.6424350000
H	-2.4218720000	-7.2246660000	1.9917110000
C	-2.5717370000	-7.7341780000	-0.1163400000
H	-3.6756430000	-7.7770690000	0.0165400000
H	-2.3253820000	-8.6105930000	-0.7505770000
C	-2.2059680000	-6.4303600000	-0.8603380000
H	-2.5663930000	-6.4896100000	-1.9135150000
H	-2.7731290000	-5.5874820000	-0.4036280000
C	-0.6937320000	-6.0476860000	-0.8390030000
H	-0.5965500000	-5.0458920000	-1.3096760000
C	0.2380800000	-7.0240910000	-1.6245930000
H	-0.0921770000	-7.0876230000	-2.6875520000
H	1.2554720000	-6.5700060000	-1.6596560000
C	0.3523260000	-8.4472780000	-1.0333660000
H	1.2041930000	-8.9752880000	-1.5176480000

H	-0.5456900000	-9.0380080000	-1.3065300000
C	0.5473190000	-8.4766780000	0.4995830000
H	1.6036190000	-8.2021030000	0.7284040000
H	0.4264520000	-9.5215360000	0.8710020000
B	6.2552740000	2.9121110000	0.3525720000
C	6.8404910000	2.2866880000	1.6876680000
H	6.1860290000	2.4688200000	2.5692370000
C	7.0450690000	0.7527830000	1.5474190000
H	7.5646360000	0.3483660000	2.4479500000
H	6.0362830000	0.2814370000	1.5496930000
C	7.7983500000	0.2971790000	0.2769290000
H	7.6607350000	-0.7996150000	0.1499680000
H	8.8906560000	0.4336750000	0.4195670000
C	7.3484010000	1.0113840000	-1.0176980000
H	8.0662250000	0.7725930000	-1.8373780000
H	6.3739420000	0.5794790000	-1.3407560000
C	7.1608140000	2.5498340000	-0.8984600000
H	6.7342690000	2.9201170000	-1.8575540000
C	8.4803820000	3.3528490000	-0.6446840000
H	9.2132340000	3.1430730000	-1.4587350000
H	8.2422080000	4.4385090000	-0.7319310000
C	9.1463250000	3.1032840000	0.7286100000
H	9.9231810000	3.8814530000	0.9022520000
H	9.7000060000	2.1427720000	0.7056960000
C	8.1570920000	3.1042590000	1.9169210000
H	7.8722680000	4.1583890000	2.1430130000
H	8.6738330000	2.7340270000	2.8332150000
C	-7.9339070000	2.4750470000	0.0685610000
H	-8.3800290000	1.6697000000	-0.5673540000
C	-7.2176250000	4.9808230000	-0.1274250000
H	-7.8906910000	5.4453660000	0.6246550000
H	-7.0598050000	5.7733140000	-0.8976460000
C	-8.7881620000	2.5524820000	1.3580690000
H	-9.8503910000	2.8311800000	1.1340250000
H	-8.8210380000	1.5260730000	1.7866800000
C	-8.2480640000	3.5133640000	2.4465110000
H	-8.7783300000	3.3119450000	3.4080420000
H	-8.5228150000	4.5591470000	2.1867800000
C	-7.9374330000	3.7721170000	-0.7756570000
H	-7.4394850000	3.5493060000	-1.7479820000
H	-8.9792330000	4.0862430000	-1.0438030000
B	-6.3912990000	2.0667300000	0.5004550000
F	-6.4211030000	0.8562440000	1.3397110000
C	-5.8565170000	3.3488190000	1.3969020000
H	-4.8024760000	3.1883190000	1.7348640000
C	-6.7192740000	3.4262350000	2.6824720000
H	-6.4124810000	4.2834130000	3.3358080000
H	-6.5111820000	2.5019670000	3.2661020000
C	-5.8638810000	4.6417560000	0.5449270000
H	-5.0954460000	4.5292920000	-0.2556840000
H	-5.5369720000	5.5312360000	1.1427010000

12.11. $[(\{9\text{-BBN}\}\text{CH}_2\text{CH}_2\text{SiMe}_2)(\{9\text{-BBN}\}\text{FCH}_2\text{CH}_2\text{SiMe}_2)_2\text{P}_7]^{2-}$

Charge = -2 Multiplicity = 1

P	0.0511980000	0.9239340000	0.5636920000
P	-1.3840850000	-0.2168920000	-0.6920310000
P	1.1158770000	2.0812190000	-1.0144450000
P	1.5971600000	-0.6759530000	0.8047300000

P	1.7143830000	0.4837170000	-2.4553280000
P	1.8251090000	-1.4569580000	-1.2877710000
P	-0.0877800000	-0.8945290000	-2.3848350000
Si	-2.9438140000	1.2431950000	-1.6489100000
Si	3.1669130000	2.7826660000	-0.0851570000
Si	0.5082140000	-2.4224540000	1.8650150000
C	-0.6110090000	-1.6678480000	3.2042570000
C	1.9037370000	-3.4069150000	2.7145620000
C	-0.4778150000	-3.5977030000	0.7281410000
C	2.8034520000	3.1135980000	1.7537410000
C	3.3872990000	4.4559870000	-0.9747460000
C	4.6802910000	1.6802120000	-0.3535970000
C	-4.1338880000	1.8162820000	-0.2924460000
C	-3.8311180000	0.0876250000	-2.8799680000
C	-2.1658430000	2.6774440000	-2.6166480000
H	-4.6096040000	0.9134520000	0.1544230000
C	-5.2354300000	2.7674490000	-0.8319370000
H	-3.5637220000	2.2978840000	0.5337750000
H	-1.5540050000	3.3283520000	-1.9599760000
H	-2.9788970000	3.2888460000	-3.0652850000
H	-1.5069990000	2.3070630000	-3.4287970000
H	-4.2542190000	-0.7989260000	-2.3633430000
H	-3.1463340000	-0.2642530000	-3.6796670000
H	-4.6733760000	0.6379570000	-3.3519330000
H	4.3016440000	4.9649830000	-0.6020700000
H	2.5155630000	5.1232870000	-0.8103420000
H	3.5075400000	4.3072820000	-2.0686900000
H	4.8152690000	1.5208670000	-1.4479240000
H	4.4837480000	0.6735280000	0.0781780000
C	5.9717590000	2.3062230000	0.2377620000
H	3.6741370000	3.6358820000	2.2054930000
H	2.6518820000	2.1608760000	2.3018960000
H	1.9020190000	3.7456370000	1.8936320000
H	1.4915980000	-4.2437490000	3.3202930000
H	2.4919010000	-2.7517990000	3.3905370000
H	2.6058310000	-3.8346660000	1.9681590000
H	-1.0410730000	-2.4614820000	3.8536660000
H	-1.4463540000	-1.0997870000	2.7458130000
H	-0.0390200000	-0.9705340000	3.8512060000
H	-1.2150970000	-2.9715830000	0.1786690000
C	-1.1855660000	-4.7688750000	1.4451370000
H	0.2225800000	-3.9799130000	-0.0484050000
H	-5.6627630000	2.3498610000	-1.7782730000
H	-4.7681500000	3.7368510000	-1.1234090000
H	5.8895140000	2.3414900000	1.3495530000
H	6.0516890000	3.3740500000	-0.0860600000
H	-1.8703660000	-4.3988030000	2.2483760000
H	-0.4539940000	-5.3875180000	2.0299740000
B	-1.9913510000	-5.8260940000	0.5958950000
C	-2.8952540000	-6.9463340000	1.2739250000
H	-2.8256270000	-6.9327630000	2.3857150000
C	-4.3684740000	-6.5863990000	0.8976230000
H	-5.0646680000	-7.3588120000	1.3026280000
H	-4.6321680000	-5.6424240000	1.4277950000
C	-4.6319990000	-6.3909600000	-0.6131040000
H	-5.6252270000	-5.9078730000	-0.7477440000
H	-4.7202900000	-7.3806110000	-1.1075680000
C	-3.5578560000	-5.5426410000	-1.3312330000
H	-3.7098410000	-5.6027800000	-2.4341260000
H	-3.7141610000	-4.4709130000	-1.0719060000

C	-2.0770730000	-5.9078240000	-0.9839660000
H	-1.4299940000	-5.1569420000	-1.4859640000
C	-1.6269010000	-7.3202130000	-1.4580550000
H	-1.7705780000	-7.4179150000	-2.5598040000
H	-0.5265180000	-7.3951450000	-1.2974370000
C	-2.3105120000	-8.5090960000	-0.7454110000
H	-1.7479740000	-9.4430140000	-0.9721320000
H	-3.3211900000	-8.6704130000	-1.1738770000
C	-2.4216540000	-8.3466030000	0.7872590000
H	-1.4204180000	-8.5401080000	1.2387030000
H	-3.0889640000	-9.1425410000	1.1958020000
C	-7.6929940000	3.9562890000	-0.4262170000
H	-7.9996000000	3.5883280000	-1.4377850000
C	-6.5207420000	6.0324240000	0.6494360000
H	-7.3298980000	6.4177610000	1.3071500000
H	-5.9408790000	6.9392980000	0.3527350000
C	-8.9421160000	3.8600160000	0.4832830000
H	-9.7812310000	4.5043570000	0.1102070000
H	-9.3045860000	2.8095110000	0.4220590000
C	-8.6934950000	4.1945020000	1.9753560000
H	-9.5744800000	3.8626100000	2.5767820000
H	-8.6622350000	5.2986270000	2.1072530000
C	-7.1522570000	5.3943500000	-0.6133280000
H	-6.3780230000	5.3666180000	-1.4149800000
H	-7.9462520000	6.0880390000	-0.9962540000
B	-6.5196880000	2.9694020000	0.2037720000
F	-7.0890620000	1.6269880000	0.4257490000
C	-6.1518300000	3.6521130000	1.6657020000
H	-5.3500040000	3.0685880000	2.1816780000
C	-7.4076050000	3.5656280000	2.5685630000
H	-7.2254430000	4.0198120000	3.5774900000
H	-7.6026300000	2.4844570000	2.7463050000
C	-5.6067220000	5.0859410000	1.4668520000
H	-4.6269480000	5.0078790000	0.9409930000
H	-5.3766370000	5.5813870000	2.4456220000
C	7.5969870000	0.0179450000	0.2808090000
H	6.7232640000	-0.6260730000	0.0140230000
C	8.7871060000	0.9487950000	2.4169710000
H	9.7843720000	0.4654460000	2.3284650000
H	8.6202150000	1.0540280000	3.5162330000
C	8.8238400000	-0.5782360000	-0.4535890000
H	9.0365670000	-1.6285730000	-0.1235800000
H	8.5542730000	-0.6411750000	-1.5313420000
C	10.1314060000	0.2450220000	-0.3325960000
H	10.8675810000	-0.1244070000	-1.0873300000
H	10.6095500000	0.0394630000	0.6506000000
C	7.7098440000	0.0058200000	1.8240270000
H	6.7188340000	0.3025840000	2.2392440000
H	7.8960080000	-1.0274720000	2.2171010000
B	7.3716190000	1.5637100000	-0.2666760000
F	7.3307630000	1.5586920000	-1.7392910000
C	8.7285840000	2.3767010000	0.2292220000
H	8.6620370000	3.4503350000	-0.0798540000
C	9.9488430000	1.7733320000	-0.5079970000
H	10.9059430000	2.2804470000	-0.2153970000
H	9.8057670000	1.9813510000	-1.5918730000
C	8.8438200000	2.3563290000	1.7718870000
H	8.0050770000	2.9633120000	2.1855120000
H	9.7786140000	2.8663330000	2.1247830000

12.12. $[(9\text{-BBN})\text{CH}_2\text{CH}_2\text{FSiMe}_2)_3\text{P}_7]^{3-}$

Charge = -3 Multiplicity = 1

P	0.0673940000	0.4554300000	0.5499620000
P	-0.5288750000	1.8084400000	-1.1179970000
P	1.8680330000	-0.4832480000	-0.3957520000
P	-1.3984890000	-1.1919900000	0.1711750000
P	1.0365770000	-1.2370920000	-2.3264060000
P	-1.2041000000	-1.4856840000	-2.0374700000
P	-0.3752120000	0.4504870000	-2.8912330000
Si	1.0675760000	3.4738840000	-1.5138230000
Si	2.3976310000	-2.4552710000	0.7567880000
Si	-3.5787900000	-0.3733770000	0.4363450000
C	-4.1207690000	0.8088870000	-0.9484240000
C	-3.5185280000	0.5618690000	2.0941430000
C	-4.7444890000	-1.8740440000	0.5328600000
C	1.2203180000	-3.8951430000	0.3746120000
C	2.2539980000	-1.9824740000	2.5961740000
C	4.1904310000	-2.8953000000	0.2986830000
C	0.6984370000	4.9440690000	-0.3692380000
C	0.6880280000	3.9601030000	-3.3206730000
C	2.8742380000	2.9035530000	-1.4003110000
H	-0.3631150000	5.2392270000	-0.5334580000
C	1.6156800000	6.1730600000	-0.6196520000
H	0.7558020000	4.6162090000	0.6938160000
H	3.1313130000	2.5761390000	-0.3726480000
H	3.5365540000	3.7542470000	-1.6729320000
H	3.0797700000	2.0517350000	-2.0797470000
H	-0.3842530000	4.2187220000	-3.4457440000
H	0.9331860000	3.1409340000	-4.0284070000
H	1.2872620000	4.8567270000	-3.5902610000
H	2.6198760000	-2.8237540000	3.2236910000
H	1.2025110000	-1.7638920000	2.8752170000
H	2.8705140000	-1.0893580000	2.8292220000
H	4.8469230000	-2.0386010000	0.5732760000
H	4.2650710000	-2.9779160000	-0.8106200000
C	4.7099200000	-4.1917240000	0.9772970000
H	1.5039170000	-4.7741150000	0.9932680000
H	1.2917630000	-4.1912980000	-0.6929890000
H	0.1675470000	-3.6193820000	0.5897640000
H	-4.5454600000	0.8825730000	2.3729530000
H	-2.8715030000	1.4610540000	2.0297930000
H	-3.1323290000	-0.0888180000	2.9063630000
H	-5.1512370000	1.1701010000	-0.7401630000
H	-4.1320410000	0.2869070000	-1.9284030000
H	-3.4364180000	1.6780480000	-1.0283530000
H	-4.6538190000	-2.4482910000	-0.4184760000
C	-6.2248660000	-1.4865820000	0.7965850000
H	-4.3865600000	-2.5658380000	1.3283260000
H	1.7105800000	6.3486060000	-1.7211320000
H	2.6497600000	5.9351740000	-0.2756650000
H	4.0860400000	-5.0537320000	0.6408930000
H	4.5360790000	-4.1229670000	2.0809270000
H	-6.5674760000	-0.7927300000	-0.0074790000
H	-6.2821250000	-0.8862030000	1.7389740000
C	1.9707210000	8.9053050000	-0.3714550000
H	2.1041330000	8.9523670000	-1.4818220000
C	3.4098150000	8.5503010000	1.7807510000
H	3.2465360000	9.5188600000	2.3022060000
H	4.4355080000	8.2310110000	2.0862500000

C	1.2005170000	10.1835390000	0.0404800000
H	1.7748590000	11.1164710000	-0.2052400000
H	0.2758340000	10.2142490000	-0.5780400000
C	0.7830070000	10.2455090000	1.5313010000
H	0.0355000000	11.0649800000	1.6691120000
H	1.6567730000	10.5543360000	2.1467260000
C	3.3822570000	8.7862340000	0.2495650000
H	3.9007520000	7.9314910000	-0.2433880000
H	4.0138210000	9.6861000000	0.0222780000
B	1.0398320000	7.5894220000	0.0280130000
F	-0.3135710000	7.7847100000	-0.5258050000
C	0.9604300000	7.6389910000	1.6823090000
H	0.3628530000	6.7781720000	2.0702870000
C	0.1983480000	8.9239470000	2.0911680000
H	0.1110480000	9.0215950000	3.2053080000
H	-0.8403250000	8.8175320000	1.7065400000
C	2.3768400000	7.5155720000	2.2930980000
H	2.7600460000	6.4957690000	2.0591660000
H	2.3517890000	7.5723010000	3.4127480000
C	6.8066820000	-4.7741530000	-0.7953510000
H	6.4963700000	-3.9310370000	-1.4602870000
C	6.3219700000	-7.3265340000	-0.4833180000
H	7.3251470000	-7.7583810000	-0.6928860000
H	5.5999990000	-8.1104960000	-0.8175100000
C	8.3544300000	-4.8110390000	-0.8265080000
H	8.7474070000	-5.0022030000	-1.8601040000
H	8.7051840000	-3.7934560000	-0.5439890000
C	9.0108180000	-5.8295900000	0.1395850000
H	10.1028230000	-5.6054800000	0.2218670000
H	8.9656710000	-6.8473750000	-0.3081640000
C	6.1262650000	-6.0514970000	-1.3420910000
H	5.0333090000	-5.8478660000	-1.4181290000
H	6.4565620000	-6.2824830000	-2.3889340000
B	6.3290190000	-4.4868450000	0.7667290000
F	7.0529270000	-3.3097180000	1.2792590000
C	6.8436290000	-5.8309900000	1.5971900000
H	6.5482510000	-5.7467440000	2.6734000000
C	8.3903340000	-5.8621810000	1.5590790000
H	8.8058590000	-6.7501430000	2.1063270000
H	8.7446550000	-4.9628390000	2.1108060000
C	6.1697790000	-7.1086620000	1.0430260000
H	5.0822780000	-7.0498180000	1.2797620000
H	6.5361270000	-8.0318730000	1.5661480000
C	-7.4342570000	-3.7394900000	-0.3531940000
H	-6.4370920000	-4.1333040000	-0.6692590000
C	-9.3308140000	-2.1908630000	-1.2750140000
H	-10.1745010000	-2.9112590000	-1.3520590000
H	-9.5146010000	-1.4522280000	-2.0925060000
C	-8.2850260000	-4.9696150000	0.0480520000
H	-8.4318230000	-5.6743720000	-0.8125140000
H	-7.6994320000	-5.5290620000	0.8112900000
C	-9.6735540000	-4.6450020000	0.6539860000
H	-10.0909600000	-5.5663300000	1.1297610000
H	-10.3881650000	-4.4013010000	-0.1635610000
C	-7.9993380000	-2.9352320000	-1.5482070000
H	-7.2328710000	-2.1828910000	-1.8447410000
H	-8.1421110000	-3.5819920000	-2.4534640000
B	-7.2747060000	-2.7601030000	0.9746830000
F	-6.7996960000	-3.5655550000	2.1135140000
C	-8.8271390000	-2.2579100000	1.2908040000

H	-8.8292080000	-1.5669400000	2.1711510000
C	-9.6654050000	-3.4952940000	1.6919290000
H	-10.7289190000	-3.2226470000	1.9269040000
H	-9.2280520000	-3.8885350000	2.6369080000
C	-9.4030520000	-1.4657090000	0.0931440000
H	-8.8357590000	-0.5099190000	0.0119830000
H	-10.4687820000	-1.1609560000	0.2709820000

12.13. H-BBN

Charge = 0 Multiplicity = 1

H	0.4435980000	0.0554540000	-0.0586360000
B	1.6652350000	0.0374300000	-0.0378100000
C	2.5237510000	-1.2842380000	0.0370640000
H	1.9048540000	-2.2072270000	0.0596060000
C	3.4049920000	-1.3380350000	-1.2519330000
H	4.0818610000	-2.2225040000	-1.2063610000
H	2.7292670000	-1.5284760000	-2.1176560000
C	4.2323230000	-0.0654070000	-1.5404980000
H	4.6214910000	-0.1153710000	-2.5814890000
H	5.1350880000	-0.0520660000	-0.8965380000
C	3.4447540000	1.2517780000	-1.3613400000
H	4.1484730000	2.1157780000	-1.3896140000
H	2.7740860000	1.3891660000	-2.2409280000
C	2.5639310000	1.3338300000	-0.0735730000
H	1.9735000000	2.2738750000	-0.1297670000
C	3.3707650000	1.3638510000	1.2647570000
H	4.0734480000	2.2291320000	1.2585380000
H	2.6521440000	1.5738020000	2.0905210000
C	4.1441330000	0.0686240000	1.5991230000
H	4.4742160000	0.1084120000	2.6607620000
H	5.0815870000	0.0292790000	1.0079720000
C	3.3310790000	-1.2259240000	1.3741830000
H	2.6074610000	-1.3434310000	2.2137950000
H	4.0069630000	-2.1097330000	1.4418240000

12.14. [H-FBBN]⁻

Charge = -1 Multiplicity = 1

H	-2.4984360000	0.0000000000	-2.5854480000
C	-4.4713860000	-1.3083610000	-2.1089430000
H	-3.9023120000	-2.2549780000	-1.9323260000
C	-5.5676860000	0.0000000000	-4.0856510000
H	-6.6326480000	0.0000000000	-3.7640560000
H	-5.6082140000	0.0000000000	-5.2022240000
C	-5.6484870000	-1.3012680000	-1.1039000000
H	-6.3443390000	-2.1686170000	-1.2570450000
H	-5.2031760000	-1.4396650000	-0.0917430000
C	-6.4879300000	0.0000000000	-1.0812760000
H	-7.1422200000	0.0000000000	-0.1753310000
H	-7.1954530000	0.0000000000	-1.9397770000
C	-4.8851640000	-1.3025830000	-3.5983760000
H	-3.9554670000	-1.4487610000	-4.1975980000
H	-5.5538200000	-2.1666530000	-3.8558620000
B	-3.5058940000	0.0000000000	-1.8124220000
F	-3.0512190000	0.0000000000	-0.4232250000
C	-4.4713860000	1.3083610000	-2.1089430000
H	-3.9023120000	2.2549780000	-1.9323260000

C	-5.6484870000	1.3012680000	-1.1039000000
H	-6.3443390000	2.1686170000	-1.2570450000
H	-5.2031760000	1.4396650000	-0.0917430000
C	-4.8851640000	1.3025830000	-3.5983760000
H	-3.9554670000	1.4487610000	-4.1975980000
H	-5.5538200000	2.1666530000	-3.8558620000

12.15. (H-BBN)₂

Charge = 0 Multiplicity = 1

C	-0.8112350000	-1.3176790000	-0.6067410000
H	-1.3844660000	-2.2531000000	-0.7864320000
C	0.2779860000	0.0000000000	1.3824300000
H	1.3428800000	0.0000000000	1.0719770000
H	0.3037770000	0.0000000000	2.4946490000
C	0.3823380000	-1.3014130000	-1.6060590000
H	1.0565550000	-2.1670970000	-1.4117290000
H	-0.0302250000	-1.4700490000	-2.6279670000
C	1.2186000000	0.0000000000	-1.6181730000
H	1.8746660000	0.0000000000	-2.5166580000
H	1.9157540000	0.0000000000	-0.7554040000
C	-0.4017180000	-1.3014130000	0.8951110000
H	-1.3238210000	-1.4700520000	1.4986210000
H	0.2627820000	-2.1670990000	1.1204310000
B	-1.6724710000	0.0000000000	-0.8767340000
H	-2.2412140000	0.0000000000	-2.0962520000
C	-4.2655170000	-1.3176780000	-1.6892580000
H	-3.6922860000	-2.2531000000	-1.5095670000
C	-5.3547300000	0.0000000000	-3.6784360000
H	-6.4196280000	0.0000000000	-3.3679940000
H	-5.3805110000	0.0000000000	-4.7906550000
C	-5.4590900000	-1.3014140000	-0.6899410000
H	-6.1333080000	-2.1670970000	-0.8842720000
H	-5.0465260000	-1.4700520000	0.3319670000
C	-6.2953520000	0.0000000000	-0.6778210000
H	-6.9514130000	0.0000000000	0.2206670000
H	-6.9925100000	0.0000000000	-1.5405870000
C	-4.6750310000	-1.3014140000	-3.1911110000
H	-3.7529270000	-1.4700560000	-3.7946190000
H	-5.3395320000	-2.1670990000	-3.4164320000
B	-3.4042810000	0.0000000000	-1.4192660000
H	-2.8355390000	0.0000000000	-0.1997470000
C	-4.2655170000	1.3176780000	-1.6892580000
H	-3.6922860000	2.2531000000	-1.5095670000
C	-5.4590900000	1.3014140000	-0.6899410000
H	-6.1333080000	2.1670970000	-0.8842720000
H	-5.0465260000	1.4700520000	0.3319670000
C	-4.6750310000	1.3014140000	-3.1911110000
H	-3.7529270000	1.4700560000	-3.7946190000
H	-5.3395320000	2.1670990000	-3.4164320000
C	-0.8112350000	1.3176790000	-0.6067410000
H	-1.3844660000	2.2531000000	-0.7864320000
C	0.2779860000	1.3014130000	-1.6060590000
H	1.0565550000	2.1670970000	-1.4117290000
H	-0.0302250000	1.4700490000	-2.6279670000
C	-0.4017180000	1.3014130000	0.8951110000
H	-1.3238210000	1.4700520000	1.4986210000
H	0.2627820000	2.1670990000	1.1204310000

12.16. ClSiMe₂CH₂CH₂(9-BBN) (3)

Charge = 0 Multiplicity = 1

Si	-0.8165770000	-2.1082890000	1.2911930000
C	-0.7799610000	-1.8515180000	3.1619890000
C	-0.9418070000	-3.9426590000	0.8589410000
C	-2.1763620000	-1.0858020000	0.4544220000
H	-1.8862030000	-4.3784840000	1.2497210000
H	-0.0963380000	-4.5105870000	1.2994430000
H	-0.9197460000	-4.0954610000	-0.2399900000
H	-1.7180390000	-2.2172890000	3.6319700000
H	-0.6631560000	-0.7772960000	3.4145610000
H	0.0675760000	-2.4034590000	3.6185540000
H	-1.9687530000	-0.0138540000	0.6714230000
C	-3.6269020000	-1.4471360000	0.8501980000
H	-2.0373620000	-1.1878370000	-0.6455860000
H	-3.7739300000	-1.3607310000	1.9571400000
H	-3.8390180000	-2.5298510000	0.6664830000
B	-4.8257900000	-0.6364840000	0.2086860000
C	-6.3434440000	-0.9966480000	0.5028160000
H	-6.4513290000	-1.8520970000	1.2076740000
C	-7.0133900000	0.2451050000	1.1663890000
H	-8.0999110000	0.0519700000	1.3240340000
H	-6.5827950000	0.3560350000	2.1887560000
C	-6.8310450000	1.5781000000	0.4070190000
H	-7.1234900000	2.4188490000	1.0743110000
H	-7.5428980000	1.6250550000	-0.4420190000
C	-5.3933530000	1.8190770000	-0.1056890000
H	-5.3880570000	2.6877570000	-0.8041730000
H	-4.7551630000	2.1290410000	0.7541290000
C	-4.7109000000	0.5909030000	-0.7849000000
H	-3.6584310000	0.8742440000	-1.0059250000
C	-5.3645960000	0.1473970000	-2.1329450000
H	-5.3621390000	1.0006220000	-2.8502600000
H	-4.7057610000	-0.6252630000	-2.5930610000
C	-6.7944300000	-0.4268960000	-2.0166420000
H	-7.0646510000	-0.9248060000	-2.9740770000
H	-7.5222190000	0.4025300000	-1.9079250000
C	-6.9748030000	-1.4316140000	-0.8570910000
H	-6.5133290000	-2.4029980000	-1.1514740000
H	-8.0588370000	-1.6508860000	-0.7180010000
Cl	1.0313420000	-1.4097380000	0.5279080000

12.17. [ClSiMe₂CH₂CH₂F(9-BBN)]⁻

Charge = -1 Multiplicity = 1

Cl	-0.9163420000	-1.0911260000	1.0942890000
Si	1.0553650000	-0.7889770000	1.9034200000
C	2.3221540000	-0.6500040000	0.5293090000
C	1.3511630000	-2.2850370000	3.0304190000
C	0.9091130000	0.7827650000	2.9572330000
H	2.3157150000	-1.5947590000	-0.0608730000
C	3.7633930000	-0.3892210000	1.0458370000
H	2.0033070000	0.1461690000	-0.1815970000
H	0.6401790000	1.6548440000	2.3251810000
H	1.8811700000	1.0043080000	3.4469340000
H	0.1338380000	0.6728030000	3.7442500000
H	1.3711640000	-3.2208600000	2.4339340000
H	0.5562880000	-2.3772280000	3.7997840000

H	2.3316320000	-2.1899350000	3.5430740000
H	3.9984720000	-1.1066240000	1.8720940000
H	3.8155890000	0.6241110000	1.5096850000
C	6.4595910000	-0.5475610000	0.4578550000
H	6.5728800000	-1.2527040000	1.3194900000
C	6.5238530000	2.0220640000	-0.0151690000
H	7.3802030000	2.0783840000	-0.7211470000
H	6.5371080000	2.9978240000	0.5274990000
C	7.4255780000	-1.0358280000	-0.6493130000
H	8.4944510000	-1.0036030000	-0.3122350000
H	7.1915350000	-2.1082580000	-0.8328980000
C	7.3147500000	-0.2807800000	-1.9977600000
H	7.8485110000	-0.8620820000	-2.7876560000
H	7.8726030000	0.6793350000	-1.9309800000
C	6.7706700000	0.8712760000	0.9923010000
H	6.1313430000	1.0477000000	1.8889290000
H	7.8256560000	0.9510610000	1.3633720000
B	4.9151590000	-0.6189830000	-0.1306970000
F	4.6660230000	-1.9646440000	-0.6816180000
C	4.8931550000	0.4857070000	-1.3626370000
H	3.8794460000	0.5350130000	-1.8328250000
C	5.8635720000	-0.0056370000	-2.4657340000
H	5.9002650000	0.7048530000	-3.3320130000
H	5.4436490000	-0.9564880000	-2.8627450000
C	5.2073370000	1.9016570000	-0.8222810000
H	4.3638020000	2.2087800000	-0.1607570000
H	5.2296600000	2.6626830000	-1.6449530000

13. References

1. M. Cicač-Hudi, J. Bender, S. H. Schlindwein, M. Bispinghoff, M. Nieger, H. Grützmacher and D. Gudat, *Eur. J. Inorg. Chem.*, 2016, **2016**, 649–658.
2. G. M. Sheldrick, *Acta. Cryst.*, 2015, **A71**, 3–8.
3. O. V. Dolomanov, L. J. Bourhis, R. J. Gildea, J. A. K. Howard and H. Puschmann, *J. Appl. Cryst.*, 2009, **42**, 339–341.
4. W. Kohn and L. J. Sham, *Phys. Rev.*, 1965, **140**, A1133–6A1138.
5. P. Hohenberg and W. Kohn, *Phys. Rev.*, 1964, **136**, B864–6B871.
6. C. Peng, P. Y. Ayala, H. B. Schlegel and M. J. Frisch, *J. Comp. Chem.*, 1996, **17**, 49–656.
7. C. Peng and H. Bernhard Schlegel, *Isr. J. Chem.*, 1993, **33**, 449–6454.
8. R. A. Gaussian 09, M. J. Frisch, G. W. Trucks, H. B. Schlegel, G. E. Scuseria, M. A. Robb, J. R. Cheeseman, G. Scalmani, V. Barone, G. A. Petersson, H. Nakatsuji, X. Li, M. Caricato, A. Marenich, J. Bloino, B. G. Janesko, R. Gomperts, B. Mennucci, H. P. Hratchian, J. V. Ortiz, A. F. Izmaylov, J. L. Sonnenberg, D. Williams-Young, F. Ding, F. Lipparini, F. Egidi, J. Goings, B. Peng, A. Petrone, T. Henderson, D. Ranasinghe, V. G. Zakrzewski, J. Gao, N. Rega, G. Zheng, W. Liang, M. Hada, M. Ehara, K. Toyota, R. Fukuda, J. Hasegawa, M. Ishida, T. Nakajima, Y. Honda, O. Kitao, H. Nakai, T. Vreven, K. Throssell, J. A. Montgomery, Jr., J. E. Peralta, F. Ogliaro, M. Bearpark, J. J. Heyd, E. Brothers, K. N. Kudin, V. N. Staroverov, T. Keith, R. Kobayashi, J. Normand, K. Raghavachari, A. Rendell, J. C. Burant, S. S. Iyengar, J. Tomasi, M. Cossi, J. M. Millam, M. Klene, C. Adamo, R. Cammi, J. W. Ochterski, R. L. Martin, K. Morokuma, O. Farkas, J. B. Foresman, and D. J. Fox, Gaussian, Inc., Wallingford CT, 2016.
9. I. B. Sivaev and V. I. Bregadze, *Coord. Chem. Rev.*, 2014, **270–271**, 75–88.

10. K. Christe, D. Dixon, D. McLemore, W. Wilson, J. Sheehy and J. Boatz, *J. Fluor. Chem.*, 2000, **101**, 151–153.
11. P. Erdmann, J. Leitner, J. Schwarz and L. Greb, *ChemPhysChem*, 2020, **21**, 987–994.
12. A. Ramos, A. Antiñolo, F. Carrillo-Hermosilla, R. Fernández-Galán and D. García-Vivó, *Chem. Commun.*, 2019, **55**, 3073–3076.
13. M. Khononov, N. Fridman, M. Tamm and M. S. Eisen, *Eur. J. Org. Chem.*, 2020, **2020**, 3153–63160.
14. R. K. Sahoo, N. Sarkar and S. Nembenna, *Angew. Chem. Int. Ed.*, 2021, **60**, 11991–12000.
15. Y. Wu, C. Shan, J. Ying, J. Su, J. Zhu, L. L. Liu and Y. Zhao, *Green Chem.*, 2017, **19**, 4169–4175.
16. A. K. Jaladi, W. K. Shin and D. K. An, *RSC Adv.*, 2019, **9**, 26483–26486.
17. J. Bhattacharjee, A. Harinath, K. Bano and T. K. Panda, *ACS Omega*, 2020, **5**, 1595–1606.
18. W. Liu, Y. Ding, D. Jin, Q. Shen, B. Yan, X. Ma and Z. Yang, *Green Chem.*, 2019, **21**, 3812–3815.
19. X. Wang and X. Xu, *RSC Adv.*, 2021, **11**, 1128–1133.
20. B. van IJzendoorn, I. Vitorica-Yrezabal, G. Whitehead and M. Mehta, *Chem. Eur. J.*, 2021, **28**, e202103737.
21. C. R. Davis, I. K. Luvaga and J. M. Ready, *J. Am. Chem. Soc.*, 2021, **143**, 4921–4927.
22. T. Ohmura, Y. Yamamoto and N. Miyaoura, *J. Am. Chem. Soc.*, 2000, **122**, 4990–4991.
23. A. D. Bage, K. Nicholson, T. A. Hunt, T. Langer and S. P. Thomas, *ACS Catal.*, 2020, **10**, 13479–13486.